

# BULLETIN

OF THE POLISH HYDROGEN AND FUEL CELL ASSOCIATION

5<sup>TH</sup> POLISH FORUM

No. 9 (2015)

## SMART ENERGY CONVERSION & STORAGE

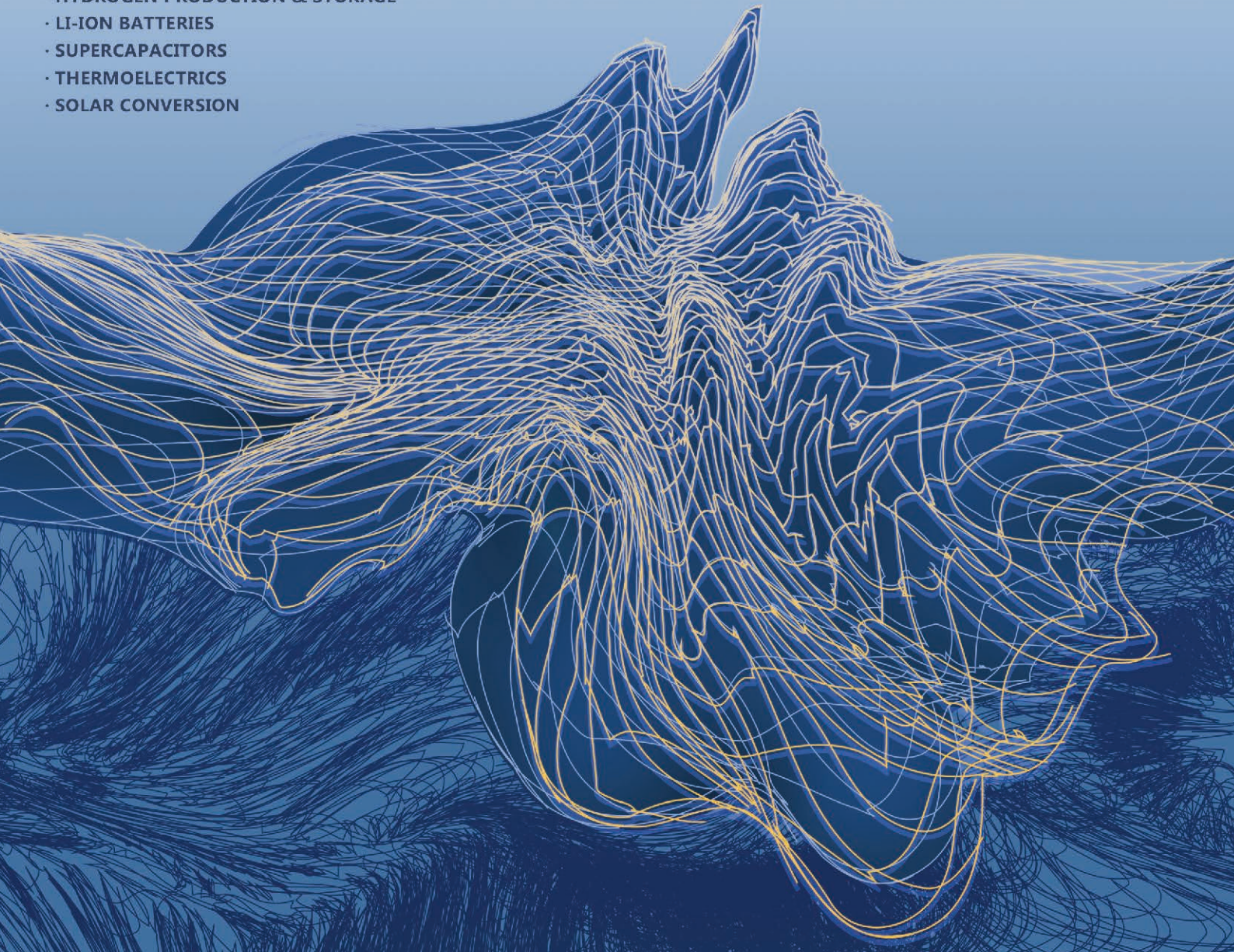
14<sup>th</sup> SYMPOSIUM ON FAST IONIC CONDUCTORS

22-25.09.2015 BIALKA TATRZANSKA

CHAIRMAN: PROF. JANINA MOLENDNA

### SCOPE:

- FUEL CELLS
- HYDROGEN PRODUCTION & STORAGE
- LI-ION BATTERIES
- SUPERCAPACITORS
- THERMOELECTRICS
- SOLAR CONVERSION



Ministry of Science  
and Higher Education  
Republic of Poland



SWISS  
CONTRIBUTION



<http://forum.hydrogen.edu.pl>



**SCIENTIFIC COMMITTEE:**

**PROF. ANDRZEJ CZERWIŃSKI**  
**PROF. HENRYK FIGIEL**  
**PROF. ELŻBIETA FRĄCKOWIAK**  
**PROF. PIOTR JASIŃSKI**  
**PROF. FRANCISZEK KROK**  
**PROF. PAWEŁ KULEZA**  
**PROF. ANNA LISOWSKA-OLEKSIAK**  
**PROF. GRZEGORZ PAŚCIAK**  
**PROF. CZESŁAW PAWLACZYK**  
**PROF. JANUSZ TOBOŁA**  
**PROF. WŁADYSŁAW WIECZOREK**

**BULLETIN OF THE POLISH HYDROGEN AND FUEL CELL ASSOCIATION NO. 9 (2015)**  
**EDITOR: JANINA MOLEND**

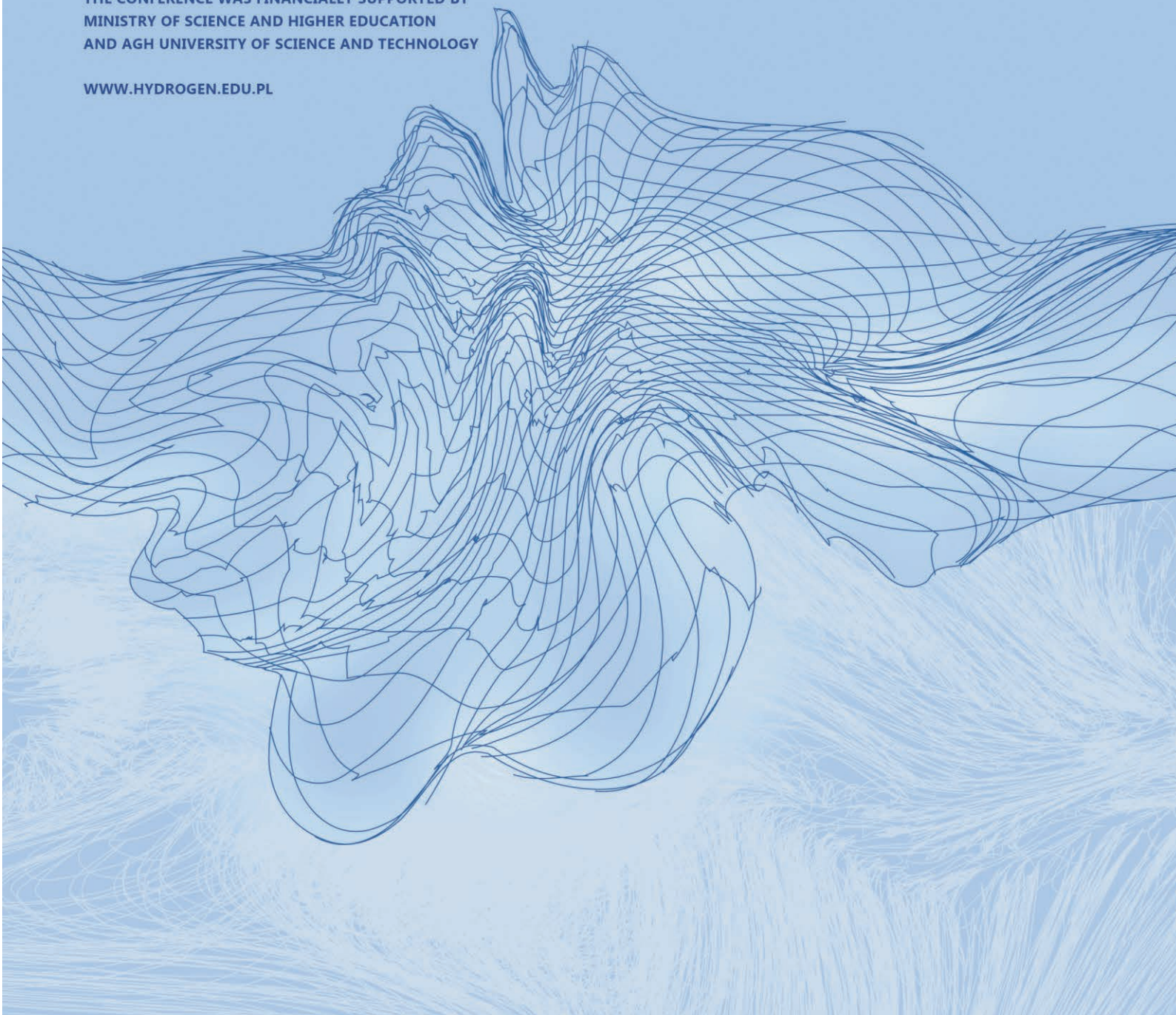
**ADDRESS OF THE REDACTION:**

**POLISH HYDROGEN AND FUEL CELL ASSOCIATION**  
**AGH AGH UNIVERSITY OF SCIENCE AND TECHNOLOGY**  
**FACULTY OF ENERGY AND FUELS,**  
**AL. MICKIEWICZA 30, 30-059 KRAKOW**

**ACKNOWLEDGEMENTS:**

**THE CONFERENCE WAS FINANCIALLY SUPPORTED BY**  
**MINISTRY OF SCIENCE AND HIGHER EDUCATION**  
**AND AGH UNIVERSITY OF SCIENCE AND TECHNOLOGY**

**[WWW.HYDROGEN.EDU.PL](http://WWW.HYDROGEN.EDU.PL)**





## Ladies and Gentlemen,

It is my great pleasure to welcome you to the 5<sup>th</sup> Polish Forum Smart Energy Conversion & Storage, held together with 14<sup>th</sup> Symposium on Fast Ionic Conductors in Białka Tatrzańska from September 22<sup>nd</sup> to 25<sup>th</sup> 2015. The conference is co-organized by Polish Hydrogen and Fuel Cells Association ([hydrogen.edu.pl](http://hydrogen.edu.pl)) and AGH University of Science and Technology. The first Forum in 2005 covered a relatively narrow issues of fuel cells and hydrogen technologies. After ten years of collecting experience of constantly expanding the formula of the Forums, this year's scope includes: fuel cells, hydrogen production and storage, ionic and electronic conductors, Li-ion and Na-ion batteries, supercapacitors, solar conversion and thermoelectrics. All these topics are highly important for modern energy conversion and storage. Albeit different, they are based on similar mass and charge transport mechanisms, related to ionic and electronic defect structure. This brought the idea of gathering of high-level specialists, including theoreticians, in this field.

Further progress in the field of modern energy technologies is conditioned by a development of the scientific basis of manufacturing of functional materials, which relies on comprehensive studies of their structural, transport, catalytic, thermal and mechanical properties, aiming to describe the relationship between crystal structure, chemical composition, electronic properties, and the catalytic efficiency of the electrochemical processes occurring in electrochemical devices.

An analysis of available technological solutions shows that there is still a gap

between current capabilities of fuel cells and practical needs of the hydrogen energy technology, in order to be competitive with the present ones based on coal, oil and natural gas. Failure of wide commercialization of fuel cells is associated with strenuous implementation of technology, which is based on technologically immature materials. Among many aspects of the hydrogen-based economy, which need to be considered, the key to its success is a solution of the fundamental issues of the used materials. Here, there is a particular place for technology of nanomaterials and studies of the catalytic processes. Understanding on the atomic-level of the fundamental processes involved in the catalysis, shall trigger correlated progress in all fields of modern energy technologies.

Understanding of microscopic, on atomic scale, transport phenomena in nanomaterials is still at an early stage. The grain size dependent defect formation energy and space charge effects are significantly influencing the transport properties. Elucidation of the grain boundaries impact on defects and transport properties will enable designing of materials with tailored properties. An extra difficulty, slowing down the progress in science and technology of the nanomaterials, is related to the stability of nanomaterials and reproducibility of their properties, because, as it was observed for example in thin films, unique microstructure may provide unique properties.

I put my big hope that this year's conference will be an excellent arena for interdisciplinary discussions in the field of materials and technologies for modern energy, and also a good school for Ph.D. students and young scientists, beginning their scientific carrier. I would like to thank all the participants who contribute to make this conference successful, wishing you an exciting and enjoyable time at the Forum.

A handwritten signature in cursive script, reading "Molenda".

Prof. Janina Molenda  
Chairman



# Contents

## Invited Lectures

Critical Behavior of Electronic Structure in Correlated Electronic Systems: Mott Localization and from Classical to Quantum Criticality <b><u>J. Spalek, M. Smoluchowski</u></b>	11
Structural and Electronic Stabilities of Oxide Cathodes for Lithium-Ion Batteries <b>A. Manthiram</b>	12
Calculation Of Electronic Band Structure Complexity and Electron Transport Properties In Disordered Systems <b><u>J. Tobola, K. Kutorasinski, B. Wiendlocha and S. Kaprzyk</u></b>	13
Electronic Structure “Engineering” in the $\text{Na}_x\text{CoO}_{2-y}$ Cathode System <b>J. Molenda</b>	14
Spinel-based cathode with extended capacity for high energy lithium-ion batteries <b>J. Lu, Y.-L. Chang, J. –R. Yang, K. S. Lee, L. Lu</b>	15
Operando Neutron Diffraction Studies of Li-Ion Battery Electrodes <b>M. Bianchini, E. Suard , L. Croguennec, C. Masquelier</b>	16
IV-VI Semiconductor Nanocomposites and Multilayers for Thermoelectricity and Infrared Optoelectronics <b><u>T. Story, M. Szot, K. Dybko, L. Kowalczyk, A. Mycielski, A. Szczerbakow</u></b>	17
Mechanism of electrode processes in SOFC <b><u>M.B. Mogensen, K. Kammer Hansen, C. Chatzichristodoulou, C. Graves</u></b>	18
Y-doped Barium Zirconate prepared by Flame Spray Synthesis as Electrolyte for Intermediate Temperature Proton Conducting Fuel Cells <b>F. Bozza, T. Graule,</b>	19
Thermoelectric Materials for Waste Heat Recovery <b>K. T. Wojciechowski</b>	20
Proton conducting fuel cells and the hydrogenation of $\text{CO}_2$ to hydrocarbons <b>Constantinos Vayenas</b>	21
Generation of Hydrogen by Solar Water Splitting of Photoelectrodes <b>Ru-Shi Liu</b>	22
Influence Of Temperature And Electrolyte Composition On Hydrogen Electrosorption in $\text{AB}_5$ Alloy <b>M. Karwowska, Z. Rogulski, A. Czerwiński</b>	24
Designing New Electrolytes For Ambient Temperature Batteries <b>M. Dranka, J. Zachara, M. Marcinek, L. Niedzicki, M. Kalita, A. Bitner, G, P. Jankowski, Z. Żukowska, M. Poterała and W. Wieczorek</b>	25
Nanostructured Hybrid Electrocatalytic and Photovoltaic Systems for Efficient Energy Conversion and Storage <b>P. J. Kulesza</b>	26
Advances in Supercapacitor Operating in Aqueous Medium <b><u>E. Frackowiak, J. Menzel, K. Fic</u></b>	27
Monitoring of a New Generation of High Pressure Vessels for Hydrogen Storage <b>P. Gašior, J. Kaleta, R. Rybczyński, F. Nony and S. Villalonga</b>	28
Universal features of conductivity spectra in superprotonic $(\text{NH}_4)_3\text{H}(\text{SO}_4)_2$ single crystals <b><u>Cz. Pawlaczyk, P. Ławniczak and A. Pawłowski</u></b>	29

## Young Scientists Forum

Semiconductor-Based Nanocomposites For Photocatalysis <b>A. Trenczek-Zajęc</b>	33
---	----



Degradation Mechanism of $\text{Li}_2\text{MnSiO}_4$ in Li-Ion Batteries	34
<b><u>M. Świątosławski, M. Molenda, M. Gajewska, R. Dziembaj</u></b>	
Multi-Component Thermoelectric Materials Fabricated by Novel Method of Reduction of Oxide Precursors	35
<b><u>B. Bochentyn, J. Karczewski, T. Miruszewski and B. Kusz</u></b>	
Transference Number Measurements In Bimevokes	36
<b><u>M. Malys, A. Kruk, M. Wójcik, W. Wróbel, J.R. Dygas, I. Abrahams and F. Krok</u></b>	
Ionic Associations in Glyme Based Electrolytes Doped with Salts Bearing Heteroaromatic Anion. Ionic Aggregation Modes in Solution And PEO Matrix	37
<b><u>G. Z. Żukowska, M. Dranka, P. Jankowski, W. Wiczorek</u></b>	
Factors Affecting Size and Location of Solid Electrolyte's Electrochemical Window. A Case of Inorganic Solid Lithium Conductors	38
<b><u>W. Zajac, T. Polczyk</u></b>	
Ab Initio Studies On Type-II $\text{Bi}_3\text{NbO}_7$	39
<b><u>M. Krzynski, W. Wrobel, J. Dygas, I. Abrahams, P. Spiewak, F. Krok</u></b>	

Posters - flash presentations indicated by \* symbol next to the poster number

P01	Effect Of Electrolyte Composition On Electrochemical Performance of $\text{LiMn}_2\text{O}_4$ -ySy Cathodes For Li-Ion Batteries	43
	<b><u>M. Bakierska, M. Molenda*, M. Świątosławski, D. Majda and R. Dziembaj</u></b>	
P02	Synergetic Substitution of Nickel and Sulphur in the $\text{LiMn}_2\text{O}_4$ Spinel Structure	44
*	<b><u>M. Bakierska, M. Molenda, M. Świątosławski and R. Dziembaj</u></b>	
P03	Multifunctional Carbon Aerogels Derived by Sol-Gel Process of Natural Polysaccharides of Different Botanical Origin	45
	<b><u>M. Bakierska, A. Chojnacka, M. Świątosławski, M. Molenda, P. Natkański, M. Gajewska and R. Dziembaj</u></b>	
P04	Comparison of Electrochemical Properties of Tin Nanoparticles Encapsulated in Different Origin Carbon Matrix	46
	<b><u>A. Chojnacka, M. Molenda and R. Dziembaj</u></b>	
P05	Preparation Of Prototype Carbon Lead-Acid Battery	47
	<b><u>K. Wróbel, J. Lach, J. Wróbel, Z. Rogulski, A. Czerwiński</u></b>	
P06	Electrochemical Properties of New Carbon Lead-Acid Battery	48
	<b><u>J. Lach, K. Wróbel, J. Wróbel, Z. Rogulski and A. Czerwiński</u></b>	
P07	$\text{Li}_{3.85}\text{Cu}_{0.15}\text{Ti}_5\text{O}_{12}$ - Anode for Li-Ion Batteries	49
	<b><u>A. Drobnik, D. Olszewska</u></b>	
P08	The Effect of Addition of 3% of Copper to the LTO Spinel on the Structural and Electrochemical Anode Material For Li-Batteries	50
	<b><u>D. Olszewska, A. Drobnik</u></b>	
P09	Transport And Electrochemical Properties Of $\text{Na}_{0.67}\text{Ni}_{0.33}\text{Mn}_{0.67-x}\text{Ti}_x\text{O}_2$ ( $x=0, 0.1, 0.2, 0.25, 0.33$ ) and Cu Substituted $\text{Na}_{0.67}\text{Ni}_{0.31}\text{Cu}_{0.02}\text{Mn}_{0.33}\text{Ti}_{0.33}\text{O}_2$ Cathode Materials	51
	<b><u>Anna Milewska, Wojciech Zajac, Konrad Świerczek, Łukasz Sawczuk, Janina Molenda</u></b>	
P10	Microwave Synthesis of $\text{LiVPO}_4\text{F}$ Cathode Material	52
	<b><u>K. Kwatek, J. L. Nowinski</u></b>	
P11	Electrochemical properties and <i>in-situ</i> XRD studies of $\text{LiFeO}_2$ based composites	53
*	<b><u>A. Kulka, K. Świerczek, J. Molenda</u></b>	
P12	Enhancing of electrochemical properties of crystalline nanometric $\text{LiFePO}_4$	54
	<b><u>K. Polak, K. Walczak, A. Kulka, W. Zajac, J. Molenda</u></b>	
P13	In-situ Structural Studies of Manganese Spinel-Based Cathode Materials	55
	<b><u>Ł. Kondracki, A. Kulka, A. Milewska, J. Molenda</u></b>	

P14	Towards Elucidation of the Unique Electrochemical Properties of $\text{Na}_x\text{CoO}_{2-y}$	56
*	<b><u>D. Baster, J. Molenda</u></b>	
P15	Effect of Conductive Carbon Layers on Structural and Electrochemical Properties of C/LiFePO <sub>4</sub> Nanocomposite Cathode Material	57
	<b><u>J. Świder, M. Molenda and R. Dziembaj</u></b>	
P16	Electronic System for Pulse Energy Storage	58
	<b><u>B. Tomasiak, Anna Plewa, J. Leszczynski</u></b>	
P17	Towards New SEI-Forming Additives for Lithium-ion Batteries	59
*	<b><u>P. Jankowski, P. Johansson, W. Wieczorek</u></b>	
P18	Generation of Methanol Through Photoelectrochemical Reduction of Carbon Dioxide	60
*	<b><u>E. Szaniawska, K. Bienkowski, R. Solarz, I. A. Rutkowska, P. J. Kulesza</u></b>	
P19	Nanoparticles–Sensitized TiO <sub>2</sub> for a Photo-Active Electrode in Photoelectrochemical Cell	61
	<b><u>J. Banaś and A. Trenczek-Zajac</u></b>	
P20	Oxidation/Reduction Behavior and Catalytic Activity of BaLnMn <sub>2</sub> O <sub>5+δ</sub> (Ln: Lanthanides, Y) Oxides	62
*	<b><u>A. Klimkowicz, T. Yamazaki, A. Takasaki, K. Świerczek</u></b>	
P21	Electrical Properties of Bi <sub>3</sub> Y <sub>0.9</sub> W <sub>0.1</sub> O <sub>6.15</sub> :LSM Composite Cathodes for SOFC	63
*	<b><u>M. Dudz, W. Wrobel, M. Malys, A. Borowska-Cenkowska, K-Z. Fung, F. Krok,</u></b>	
P22	Characterization of Novel Anode Catalytic Layers for Biogas Operating Solid Oxide Fuel Cells	64
	<b><u>B. Bochentyn, D. Szymczewska, M. Chlewińska, D. Niańkowski, P. Jasiński</u></b>	
P23	Composite Functional Cathode Layer Prepared by Infiltration for Proton Conducting SOFC	65
	<b><u>K. Gdula-Kasica, A. Chrzan, D. Szymczewska and P. Jasinski</u></b>	
P24	Degradation of Solid Oxide Electrolyzers	66
	<b><u>J. Karczewski, D. Szymczewska, A. Chrzan and P. Jasinski</u></b>	
P25	New Concept of Lightweight Short Stack of Anode Supported Solid Oxide Fuel Cells	67
	<b><u>R. Kluczowski, M. Krauz, M. Kawalec, A. Świeca</u></b>	
P26	Application of Graphene Oxide and Organically Modified Titanium/Silicon Dioxide Hybrid Particles for PEM Fuel Cells Electrodes Improvement	68
	<b><u>M. Malinowski, A. Iwan, A. Hreniak, G. Pasciak and Felipe Caballero-Briones</u></b>	
P27	Physicochemical Properties of Sr <sub>2-x</sub> Ba <sub>x</sub> MMoO <sub>6-δ</sub> (M: Mg, Mn, Fe) Oxides for SOFCs	69
	<b><u>K. Zheng, K. Świerczek</u></b>	
P28	Structure and Transport Properties of Ln <sub>2</sub> Ni <sub>0.5</sub> Cu <sub>0.5</sub> O <sub>4</sub> (Ln - La, Pr) Cathode Materials for IT-SOFCs	70
	<b><u>K. Zheng, K. Świerczek</u></b>	
P29	Synthesis and Structural Properties of (Y,Sr)(Ti,Fe,Nb)O <sub>3-δ</sub> Nanoparticles Prepared By The Low Temperature Calcining Method	71
	<b><u>T. Miruszewski, P. Gdaniec, J. Karczewski, P. Kupracz, M. Gazda, B. Kusz</u></b>	
P30	The Institute Of Power Engineering Novelty Developments In The Field Of Solid Oxide Fuel Cell Technology	72
	<b><u>J. Kupecki, M. Stepień, M. Blesznowski, M. Skrzypkiewicz, K. Wawryniuk, M. Krauz*, R. Kluczowski and T. Golec</u></b>	
P31	Influence of Anode Microstructure on Fuel Cell Performance	73
	<b><u>D. Szymczewska, J. Karczewski, A. Chrzan, P. Jasiński</u></b>	
P32	Graphite-Stainless Steel Composite for Bipolar Plates for PEM Fuel Cells	74
	<b><u>Włodarczyk Renata</u></b>	
P33	Synthesis of Tetragonal LaNbO <sub>4</sub> Nanopowders	75
	<b><u>K. Zagórski, M. Czarnowska, P. Czoska, K. Dzierzowski, S. Wachowski, A. Mielewczyk-Gryń, M. Gazda</u></b>	
P34	Optimized Thermoelectric Composite Structures Ag <sub>x</sub> Pb <sub>M</sub> SbYTe <sub>M-2</sub>	76
	<b><u>I. Horichok, T. Semko, L. Mezhylovska, V. Kotsyubynsky</u></b>	
P35	Composite Thermoelectric Materials on the Base of PbTe with Ag and ZnO Nano-inclusions	77
	<b><u>L. Nykyruy, D. Freik, R. Ahiska*, O. Matkivskiy, I. Lishchynskiy, I. Hryhoruk</u></b>	

P36	Theoretical Studies on Resonant Levels in Thermoelectric Materials <b>Bartłomiej Wiendlocha</b>	78
P37	Thin And Thick Film Lithium Conducting Garnet * <b>E. Hanc, L. Lu, B. Yan, M. Kotobuki, W. Zajac and J. Molenda</b>	79
P38	An X-RDF Study of Selected Ionic and Electronic Conductive Glasses <b>J. Kalabinski, S. Gierlotka, T.K. Pietrzak, P. Grabowski, J.L. Nowinski and J.E. Garbarczyk</b>	80
P39	Structural and Electrical Studies of $\text{Bi}_{2.8}\text{Pb}_{0.2}\text{YbO}_{5.9}$ <b>M. Leszczynska, M. Malys, A. Borowska-Centkowska, W. Wrobel, J.R. Dygas, I. Abrahams, F. Krok</b>	81
P40	Ionic and Electronic Conductivity in The $\text{Bi}_2\text{O}_3\text{-PbO-Y}_2\text{O}_3$ System <b>K. Lewandowski, W. Wrobel, A. Borowska-Centkowska, F. Krok, I. Abrahams, M. Malys, J. Dygas</b>	82
P41	Ionic and Electronic Conductivity of $\text{Bi}_{26}\text{Mo}_{10}\text{O}_{69}$ and $\text{Bi}_{26}\text{Mo}_9\text{W}_1\text{O}_{69}$ Compounds <b>M. Malys, K. Kosyl, M. Tyrakowska, M. Wójcik, A. Kruk, W. Wróbel, J.R.Dygas and F. Krok</b>	83
P42	Correlation Between Chemical Composition, Structure and Proton Conductivity in $\text{Ba}_{1-x}\text{La}_x(\text{Zr,In,Sn})\text{O}_{3-\delta}$ Perovskites <b>K. Świerczek, A. Olszewska, A. Niemczyk, A. Klimkowicz, B. Dabrowski</b>	84
P43	Structure and Transport Properties of Novel Ruddlesden-Popper-Related $\text{Ln}_{1+x}\text{Ba}_{1-x}\text{InO}_4$ (Ln: Pr, Nd, Sm) Oxides <b>M. Tarach, W. Zając, K. Świerczek</b>	85
P44	Impedance Spectroscopy Studies of Quasicrystal Anode Materials for Electrochemical Cells <b>K. Świerczek, M. Nowak, Y. Ariga, A. Klimkowicz, A. Takasaki</b>	86
P45	Physicochemical Properties Of Proton-Conducting $\text{Ba}_{1-x}\text{Ln}_x(\text{Zr,In,Sn})\text{O}_{3-\delta}$ (Ln: Selected Lanthanides) Oxides <b>W. Skubida, K. Zheng, K. Świerczek</b>	87
P46	Dependence of Glass Transition Temperature on the Heating Rate in DTA Experiments for Glasses Containing Transition Metal Oxides <b>P. P. Michalski, T. K. Pietrzak, J. L. Nowiński, M. WasiucioneK, J. E. Garbarczyk</b>	88
P47	Rare Earth Niobates – Doping and Properties <b>A. Mielewczyk-Gryń, S. Wachowski, J. Jamroz, M. Zalewska, K.Zagórski, A. Navrotsky, M. Gazda</b>	89
P48	Mössbauer Studies of $\text{Li}_2\text{O-FeO-V}_2\text{O}_5\text{-P}_2\text{O}_5$ Glasses and Nanomaterials <b>T. K. Pietrzak, K. Szlachta, J. Gałazka-Friedman, M. WasiucioneK, J. L. Nowiński,</b>	90
P49	Synthesis, and Electrical and Thermal Properties of $\text{Li}_2\text{O-Me}_2\text{O}_3\text{-P}_2\text{O}_5$ Glasses and Nasicon-like Nanomaterials <b>T. K. Pietrzak, P. P. Michalski, A. Starobrat, M. WasiucioneK, J. E. Garbarczyk</b>	91
P50	Ionic Conductivity and Lithium Transference Number of Poly(Ethylene Oxide)-Based Electrolytes <b>K. Pożyczka, M. Marzantowicz, J. R. Dygas, F. Krok</b>	92
P51	The High Capacity Effect in All – Conducting Electrons and Silver Ions <b>W. Ślubowska, J. L. Nowiński, J. E. Garbarczyk and M. WasiucioneK</b>	93
P52	Proton Conduction in $\text{LaNb}_{1-x}\text{Sb}_x\text{O}_4$ (x=0 to 0.3) <b>S. Wachowski, A. Mielewczyk-Gryń, M. Łapiński, P. Jasiński, M. Gazda</b>	94
P53	Synthesis and Electrical Properties of $\text{Ba}_x\text{Sr}_{1-x}\text{TiO}_3$ Ceramics <b>P. Gałat, M. Leszczynska, W. Wrobel, M. Struzik, J. R. Dygas, F. Krok</b>	95
P54	Kinetic Monte Carlo Modeling of $\text{Bi}_3\text{YO}_6$ * <b>B. JasiK, M. Krynski, W. Wrobel, J. Dygas and F. Krok</b>	96
P55	Imidazole-Malonic Acid Salt - Molecular Structure and Proton Conductivity <b>P. Ławniczak, A. Pietraszko, K. Pogorzelec-Glaser, B. Hilczer</b>	97
P56	Structural, Transport and Electrochemical Properties of $\text{Li}_x(\text{Li}_y\text{Fe}_z\text{V}_{1-y-z})\text{O}$ -Cathode Materials for Li-ion Batteries * <b>B. Gędziorowski, M. Fuksa, J. Molenda</b>	98



## INVITED LECTURES



# CRITICAL BEHAVIOR OF ELECTRONIC STRUCTURE IN CORRELATED ELECTRONIC SYSTEMS: MOTT LOCALIZATION AND FROM CLASSICAL TO QUANTUM CRITICALITY

***J. Spalek, M. Smoluchowski***

Institute of Physics, Jagiellonian University,  
Łojasiewicza 11, PL-30-048 Kraków,  
Academic Centre for Materials and Nanotechnology (ACMIN),  
AGH University of Science and Technology, Al. Mickiewicza 30,  
PL-30-059 Kraków  
e-mail: ufspalek@if.uj.edu.pl

Keywords: electronic structure, mott localization

In my talk I will overview briefly the current view on metal-insulator transitions of the Mott type, as well as introduce in an elementary manner the concept of quantum criticality in that case. In particular, the interplay of theoretical concepts with experiment will be emphasized, since the Mott transition marks the boundary of metallic state stability. The role of this kind of instability can be related to intriguing phenomena such as high temperature superconductivity or very large effective mass of the carriers. The effect of atomic disorder on the electronic properties will also be mentioned.

## **ACKNOWLEDGMENT**

This research was supported by the Grant MAESTRO, No. DEC 2012/04/AST3/00342 from the National Science Centre.



# STRUCTURAL AND ELECTRONIC STABILITIES OF OXIDE CATHODES FOR LITHIUM-ION BATTERIES

Arumugam Manthiram

Materials Science and Engineering Program & Texas Materials Institute  
The University of Texas at Austin  
Austin, TX 78712, U.S.A  
e-mail: manth@austin.utexas.edu

Keywords: energy storage, lithium-ion batteries, transition-metal oxides, electronic instability

## INTRODUCTION

The identification of oxide cathodes in the 1980s enabled the commercialization of lithium-ion battery technology in the 1990s that has revolutionized the portable electronics market during the past two decades. The lithium-ion technology is now intensively pursued for both electric vehicles and grid storage of electricity produced by renewable sources like solar and wind. Cost, cycle life, safety, energy, power, and environmental impact are the major criteria for these applications, which are in turn controlled by severe materials challenges. Solid-state chemistry and condensed-matter physics have been at the forefront of addressing these challenges for nearly four decades, and they will continue to do so for years to come. This presentation will provide an overview of the structural and electronic stabilities of the three major classes of oxide cathodes that are currently in play: layered, spinel, and olivine cathodes.

## EXPERIMENTAL

The layered and spinel oxide cathodes were synthesized by coprecipitation of the transition-metal hydroxides followed by firing with lithium hydroxide at elevated temperatures. The olivine phosphate cathodes were synthesized by a novel low-temperature microwave-assisted solvothermal process at  $< 300$  °C within a short reaction time of  $< 30$  min. Chemical lithium extraction was carried out by stirring the oxides thus synthesized with the oxidizing agent  $\text{NO}_2\text{BF}_4$  in an acetonitrile medium under argon atmosphere to mimic the electrochemical charge and obtain products free from binder and carbon for chemical analysis. The products were characterized by Rietveld structural refinement of X-ray diffraction data, compositional analysis by inductively coupled plasma analysis, oxidation-state analysis by redox titrations, scanning electron microscopy, transmission electron microscopy, infrared spectroscopy, charge-discharge measurements, and electrochemical impedance spectroscopy.

## RESULTS AND DISCUSSION

*Layered oxides:* Chemical and electrochemical delithiation reactions reveal that the layered  $\text{LiMO}_2$  ( $M = \text{Mn, Co, and Ni}$ ) oxides with the initial O3 structure exhibit rich, but complex, crystal chemistry during the charge-discharge process with phase transitions to O1 or P3 phases, depending on the M ion. The phases formed would be rationalized based on cation ordering between the layers and electrostatic repulsions. More importantly, the lithium content in  $\text{Li}_{1-x}\text{MO}_2$  at which

chemical instability begins to set in due to an overlap of the metal:3d band with the top of the oxygen:2p band increases from  $M = \text{Mn}$  to  $\text{Ni}$  to  $\text{Co}$ , which controls the reversible capacity achievable. Furthermore, the amount of oxygen loss during the first charge and the reversible capacity values of the recently identified lithium-rich layered oxides  $\text{Li}[\text{M}_{1-y-z}\text{Li}_y\text{M}'_z]\text{O}_2$  are sensitively influenced by the dopant  $\text{M}'$  due to the drastic changes in the  $\text{M}'\text{-O}$  bond covalence depending on the relative positions of the  $\text{M}'$ :3d band with respect to the top of the oxygen:2p band.

*Spinel oxides:* The 4 V spinel cathode  $\text{LiMn}_2\text{O}_4$  is plagued by the electronic/chemical instability associated with the high-spin  $\text{Mn}^{3+}:\text{t}_{2g}^3\text{e}_g^1$  ion to undergo Jahn-Teller distortion and, in presence of trace amounts of acid, to disproportionate into  $\text{Mn}^{4+}$  and  $\text{Mn}^{2+}$ , which leaches out into the electrolyte. The suppression of these instabilities with doping will be presented. On the other hand, with the 5 V spinel  $\text{LiMn}_{1.5}\text{Ni}_{0.5}\text{O}_4$ , the importance of surface planes and segregation of specific cations to the surface on the chemical reactivity with the electrolyte will be presented.

*Olivine phosphates:* The access to olivine samples with controlled particle size by the microwave-assisted synthesis process helps to demonstrate the importance of both electronic and lithium-ion conductivities for battery performance. The microwave-assisted process also helps to demonstrate the temperature dependence of aliovalent doping in olivines (doping decreases with temperature).

## CONCLUSIONS

The novel synthesis approaches coupled with in-depth characterization have enabled the establishment of a profound fundamental understanding of the structural, chemical, and electronic stabilities of the layered, spinel, and olivine cathode materials for lithium-ion batteries.

## ACKNOWLEDGMENT

This work was supported by the Welch Foundation grant F-1254 and the U.S. Department of Energy award numbers DEAC0205CH11231 and DE-SC0005397.

## REFERENCES

1. Z. Q. Deng and A. Manthiram, *Journal of Physical Chemistry C* **115** (2011) 7097.
2. A. Manthiram, K. Chemelewski, and E.-S. Lee, *Energy and Environmental Science* **7** (2014) 1339.
3. K. L. Harrison, C. Bridges, M. Paranthaman, C. U. Segre, J. Katsoudas, V. A. Maroni, J. C. Idrobo, J. B. Goodenough, and A. Manthiram, *Chemistry of Materials* **25** (2013) 768.

# CALCULATION OF ELECTRONIC BAND STRUCTURE COMPLEXITY AND ELECTRON TRANSPORT PROPERTIES IN DISORDERED SYSTEMS

*J. Tobola, K. Kutorasinski, B. Wiendlocha and S. Kaprzyk*

Faculty of Physics and Applied Computer Science,  
AGH University of Science and Technology,  
Al. Mickiewicza 30, 30-059 Krakow, Poland  
e-mail: tobola@ftj.agh.edu.pl

Keywords: electronic band structure, thermoelectricity, electron transport, disorder, ab initio calculations

## INTRODUCTION

Electron transport properties of crystalline systems belong to the most fascinating phenomena studied in materials science. Macroscopic quantities as electrical conductivity  $\sigma$ , thermopower  $S$ , Hall coefficient  $R_H$  or thermal conductivity  $\kappa$ , are traditionally used to probe and classify materials as metals, semimetals or semiconductors. The aforementioned quantities are also essential to determine usefulness of materials for thermoelectric (TE) applications, which is commonly expressed via dimensionless figure of merit  $ZT = T S^2 \sigma / \kappa$  at a given temperature  $T$ . The TE performance can be optimized by proper adjustment of carrier concentration  $n$  for a given temperature range. It should also be noted that theoretical description of electronic and transport properties of solid state materials has always been a difficult problem for condensed matter theory due to complexity of phenomena that should be taken into account. Electron transport behaviors are directly related to electronic states near the Fermi energy and searching for accurate information on  $k$ -space electron features appears to be the key factor for reliable modeling, or even predicting, of TE behaviors.

## THEORETICAL DETAILS

*Ab initio* electronic band structure calculations combined with the Boltzmann transport theory [1-4] were established to be a quite convenient way to study electron transport in materials. In practice, it is performed via highly accurate calculation of ground state properties ( $T=0$ ) of electrons near Fermi surface. Finite temperature effects, especially interesting in investigations of thermopower  $S(T)$  or electrical conductivity  $\sigma(T)$ , are not explicitly taken into account in such calculations, but modifications of ground state electronic properties with temperature can be incorporated through the Fermi–Dirac distribution function. The constant relaxation time approach is used as reference approximation in Boltzmann transport theory. We should also bear in mind that real TE materials habitually contain different types of imperfections (alloying, impurities, vacancy, antisite defects, etc.) that may strongly affect TE properties, in particular electron transport properties. The Korringa–Kohn–Rostoker (KKR) method based on Green function multiple scattering theory [3] was used to calculate electronic band structure and relevant kinetic parameters of electrons near the Fermi energy. Moreover, the coherent potential approximation (CPA) was employed

to account for chemical disorder effects on electronic structure. Complex energy electronic band structure and resulting velocities and life-times of electrons are calculated in disordered alloys to derive electron transport quantities depending on temperature and carrier concentration.

## RESULTS AND DISCUSSION

In this work recent results of KKR and KKR-CPA electronic structure calculations as well as modeling of electron transport properties of well-known TE bulk materials are discussed. We focus mostly on:

- (i) the effect of electronic band convergence achieved by alloy substitution in  $Mg_2(Si-Sn)$  on thermopower and  $ZT$  in function of carrier concentration and temperature [6];
- (ii) the effect of electronic band alignment in selected disordered half-Heusler alloys on thermopower [7],
- (iii) the role of the “pudding-mold-like” shape of the highest valence band (strongly nonparabolic dispersion relations) in remarkable anisotropy of electron transport properties in  $p$ -type orthorhombic SnSe [8].

Besides, in the case of  $p$ -type  $Mg_2X$  ( $X = Si, Ge$  and  $Sn$ ) series of compounds, we discuss the influence of spin–orbit interaction on TE properties, clearly evidencing that fully relativistic treatment in *ab initio* calculations may markedly affect electron transport properties [9].

## ACKNOWLEDGMENTS

This work is supported by the Polish National Science Center (NCN), under the grant Maestro DEC-2011/02/A/ST3/00124.

## REFERENCES

1. J. M. Ziman, *Electrons and Phonons*, Oxford University Press, London, 1960.
2. F. J. Blatt, *Physics of Electronic Conduction in Solids*, McGraw-Hill Book Co., New York, 1968.
3. J. Tobola, L. Chaput, in: *Thermoelectrics and Its Energy Harvesting*, CRC Press, Boca Raton (2012).
4. B. Wiendlocha, K. Kutorasinski, S. Kaprzyk, J. Tobola, *Scripta Materialia* (2015), in press.
5. A. Bansil, S. Kaprzyk, P. E. Mijnders, J. Tobola, *Phys. Rev. B* **60** (1999) 13396.
6. K. Kutorasinski, J. Tobola, S. Kaprzyk, *Phys. Rev. B* **87** (2013) 195205.
7. K. Kutorasinski, J. Tobola, S. Kaprzyk, *Phys. Stat. Sol. A* **211**, (2014) 1229.
8. K. Kutorasinski, B. Wiendlocha, S. Kaprzyk, J. Tobola, *Phys. Rev. B* **91** (2015) 205201.
9. K. Kutorasinski, B. Wiendlocha, S. Kaprzyk, J. Tobola, *Phys. Rev. B* **89**, 115205 (2014).

# ELECTRONIC STRUCTURE “ENGINEERING” IN THE $\text{Na}_x\text{CoO}_{2-y}$ CATHODE SYSTEM

J. Molenda

AGH University of Science and Technology, Faculty of Energy and Fuels  
al. Mickiewicza 30, 30-059 Krakow, Poland  
e-mail: molenda@agh.edu.pl

Keywords: Na-ion batteries, cathode material,  $\text{Na}_x\text{CoO}_{2-y}$

## INTRODUCTION

Recently,  $\text{Na}_x\text{CoO}_2$  has attracted much attention because of its unusual electronic and electrochemical properties. In hydrated form it exhibits superconductor properties below 4 K [1]. At high sodium concentration ( $x \approx 0.65-0.75$ ) it exhibits remarkable high values of thermoelectric power combined with metallic character of electrical conductivity, which was first reported in early 1980s [2]. Electrochemical studies on  $\text{Na}_x\text{CoO}_{2-y}$  ( $x \approx 0.65 - 0.85$ ) revealed unusual electrochemical behavior, establishing itself in a form of a step-like character of the discharge curve [2]. Moreover, previous examination of sodium intercalation into  $\text{Na}_x\text{CoO}_{2-y}$  indicated a strong dependence of EMF of cells on conditions of preparation of the cathode material (T,  $p\text{O}_2$ ), which affected structure of ionic and electronic defects in the compound [2, 3].

## RESULTS

Our comprehensive studies [4-6] of physicochemical properties of  $\text{Na}_x\text{CoO}_{2-y}$  cathode material (XRD, electrical conductivity, thermoelectric power, electronic specific heat, NEXAFS) supported by electronic structure calculations using KKR-CPA method [8] with account for chemical disorder, revealed that the observed step-like character of the discharge curve reflects the variation of the chemical potential of electrons (Fermi level) in the density of states of  $\text{Na}_x\text{CoO}_{2-y}$ , which is anomalously perturbed by the presence of the oxygen vacancy defects and sodium ordering. Fig. 1 presents correlation between proposed electronic structure of  $\text{Na}_x\text{CoO}_{2-y}$  and its electrochemical behavior in  $\text{Na}/\text{Na}^+/\text{Na}_x\text{CoO}_{2-y}$  cell.

In this work we undertaken attempt to improve electrochemical properties of  $\text{Na}_x\text{CoO}_{2-y}$  by partial substitution of Co with Mn in order to achieved continuous density of states, monotonic variation of the Fermi level and consequently monotonic character of charge/discharge curve. We would like to show a new approach to an explanation of the nature of the discharge-charge curve of  $\text{Na}/\text{Na}^+/\text{Na}_x\text{Co}_{1-z}\text{Mn}_z\text{O}_{2-y}$  ( $z = 0, 0.3$ ) batteries. This is still an open problem, which until now had no proper description in the literature.

## CONCLUSIONS

Electronic structure “engineering” is a excellent method of controlling properties of cathode material, changing their unfavorable character of the discharge curve, from step-like to monotonic, through modification and control density of states function of a cathode material.

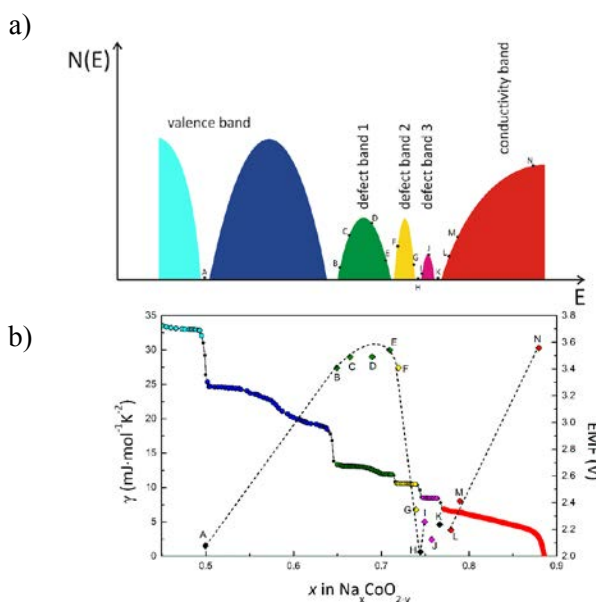


Fig.1. (a) Density of states of  $\text{Na}_x\text{CoO}_{2-y}$  from electronic structure calculations and measurements of electrical conductivity and thermoelectric power, (b) Sommerfeld coefficient illustrating density of states at the Fermi level in  $\text{Na}_x\text{CoO}_{2-y}$  plotted against discharge curve of  $\text{Na}/\text{Na}^+/\text{Na}_x\text{CoO}_{2-y}$  cell.

## ACKNOWLEDGMENTS

This work is supported by the Polish-Swiss Research Programme under grant no. 080/2010 LiBEV (Positive Electrode Materials for Li-ion Batteries for Electric Vehicles) and the financial support from the Polish Ministry of Science and Higher Education, under project AGH No. 11.11.210.911.

## REFERENCES

- [1] K. Takada, H. Sakurai, E. Takayama-Muromachi, F. Izumi, R.A. Dilanian and T. Sasaki, *Nature* 422 (2003) 53
- [2] J. Molenda, C. Delmas, P. Hagenmuller, *Solid State Ionics* 9 & 10 (1983) 431
- [3] A. Stoklosa, J. Molenda, Do Than, *Solid State Ionics* 15 (1985) 211
- [4] J. Molenda, D. Baster, M. Molenda, K. Świerczek, J. Tobola, *Phys. Chem. Chem. Phys.* 16 (2014) 14845
- [5] J. Molenda, D. Baster, A. Milewska, K. Świerczek, D. K. Bora, A. Braun, J. Tobola, *Solid State Ionics* 271 (2015) 15
- [6] J. Molenda, D. Baster, M. U. Gutowska, A. Szewczyk, R. Puźniak, J. Tobola, *Funct. Mater. Lett.* 7 (2014) 144000



# SPINEL-BASED CATHODE WITH EXTENDED CAPACITY FOR HIGH ENERGY LITHIUM-ION BATTERIES

J. Lu<sup>1</sup>, Y.-L. Chang<sup>2</sup>, J. -R. Yang<sup>2</sup>, K. S. Lee<sup>1</sup>, L. Lu<sup>1\*</sup>

<sup>1</sup>Department of Mechanical Engineering, National University of Singapore, Singapore 117575, Singapore

<sup>2</sup>Department of Materials Science and Engineering, National Taiwan University, Taiwan 10617, China  
e-mail: luli@nus.edu.sg

Keywords: structure, stabilized cathodes, cycle stability, high energy density, lithium-ion batteries

## INTRODUCTION

There are urgent needs to develop lithium-ion batteries with high energy density for applications in electric vehicle (EV) and hybrid-electric vehicle (HEV). Energy density is dependent on both capacity and voltage. However, the capacity of most current cathode materials is limited, which hinders their widespread adoption. [1] Recently, many efforts have been focused on new cathodes with high operating voltage and/or high capacity.  $\text{LiMn}_{1.5}\text{Ni}_{0.5}\text{O}_4$  spinel is a promising material because of its high operating voltage. Although it suffers from the limited capacity above 3 V, doubled capacity can be obtained by insertion of lithium ion into the structure below 3V. [2] However, in this case, Jahn-Teller distortion cannot be ignored and will result in a fast capacity fade. On the other hand, Mn-based layered oxides also become attractive recently as a result of their ability to deliver capacities of more than 250 mAh g<sup>-1</sup> with good cycle capability. Among them,  $\text{Li}_2\text{MnO}_3$  has already been successfully adopted to stabilize other layered materials. [3] Since the  $\text{Li}_2\text{MnO}_3$  component is inactive below 3V, it is possible to stabilize the structure of the spinel oxides and access good cycling stability. In result, high energy  $\text{Li}_2\text{MnO}_3$ -stabilized  $\text{LiMn}_{1.5}\text{Ni}_{0.5}\text{O}_4$  cathode was synthesized for the first time in present study and its electrochemical performance will be reported in detail.

## EXPERIMENTAL

A series of  $x\text{Li}_2\text{MnO}_3 \cdot (1-x)\text{LiMn}_{1.5}\text{Ni}_{0.5}\text{O}_4$  ( $x = 0, 0.1, 0.2, 0.3, 0.4, 0.5$  and 1) composites were prepared by co-precipitation using manganese sulfate and nickel sulfate. The aqueous metal sulfate solution was added dropwise into a mixed solution of sodium carbonate and ammonium bicarbonate. The obtained co-precipitated carbonate powders were filtered, washed, and dried in an air oven at 80°C. Thereafter, the dried carbonate powders were mixed with required amounts of lithium carbonate in a mortar. The mixtures were first heated at 600°C for 5h and then calcined at 900°C for 10h in air to obtain the final products.

The crystal structure of the as-prepared powders was characterized by X-ray diffraction (Shimadzu XRD-6000 Cu-K $\alpha$  radiation) in a 2 $\theta$  range of 10-80° with a scan rate of 2° min<sup>-1</sup>. Morphology and microstructure of different samples were investigated by a high resolution transmission electron microscope (FEI Tecnai G2 F20). The electrodes were prepared by mixing 80wt% active material, 10wt% Super P carbon conducting additive, and 10wt% polyvinylidene fluoride (PVDF) binder in a N-methyl-2-pyrrolidone (NMP) solution and the slurry

was finally casted on aluminum foils. Charge/discharge measurements were carried out at a current density of 20mA g<sup>-1</sup> between 2.0 and 4.8V by using Neware Battery Test Equipment.

## RESULTS AND DISCUSSION

According to the XRD and TEM results,  $x\text{Li}_2\text{MnO}_3 \cdot (1-x)\text{LiMn}_{1.5}\text{Ni}_{0.5}\text{O}_4$  composites have been synthesized with layered  $\text{Li}_2\text{MnO}_3$  nanodomains well embedded in the  $\text{LiMn}_{1.5}\text{Ni}_{0.5}\text{O}_4$  spinel matrix. From the cycling performance, the layered  $\text{Li}_2\text{MnO}_3$  structural unit substitution can greatly improve the structural stability of spinel structure when cycled between 2 and 4.8 V, leading to much increased reversible capacity (Figure 1). Ex-situ XRD results confirm that the cubic spinel phase in the composite with intermediate composition is very stable during cycling, which could be main reason for the superior cycle stability. Detailed studies that explain the effect of the domain structure on the electrochemical performance and stability of high energy spinel cathode will be presented.

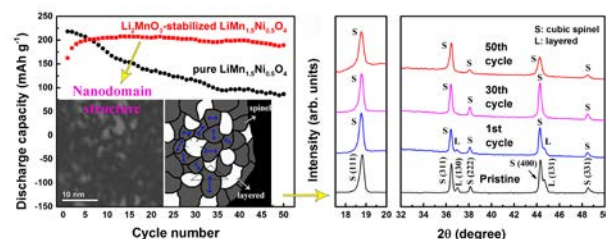


**Figure 1.** a schematic diagram showing the mechanisms behind the improved electrochemical performance

## CONCLUSIONS

Layered oxide  $\text{Li}_2\text{MnO}_3$  with good cycle stability has been successfully embedded into the spinel structure to extend its capacity by engineering the domain structure of the spinel and avoid the Jahn-Teller distortion. When it is used as a cathode material for lithium-ion batteries, it exhibits superior cycle stability after some conditioning cycles compared to pure spinel oxides and demonstrates a high energy density of about 700 Wh kg<sup>-1</sup>, showing great promise for advance high energy density lithium-ion batteries.

## REFERENCES

1. E.-S. Lee, K. -W. Nam, E. Hu, et al., *Chem. Mater.* **24**(2012)3610
2. S. Park, S. Kang, C. Johnson, et al., *Electrochem. Commun.* **9**(2007)262
3. M. M. Thackeray, S. -H. Kang, C. S. Johnson, et al., *J. Mater. Chem.* **17**(2007)3112

# OPERANDO NEUTRON DIFFRACTION STUDIES OF LI-ION BATTERY ELECTRODES

Matteo Bianchini <sup>a,b,c,d</sup>, Emmanuelle Suard <sup>c</sup>, Laurence Croguennec <sup>b,d</sup>, Christian Masquelier <sup>a,d</sup>

<sup>a</sup> Laboratoire de Réactivité et de Chimie des Solides, CNRS-UMR#7314, Université de Picardie Jules Vernes, F-80039 Amiens Cedex 1, France

<sup>b</sup> CNRS, Univ. Bordeaux, ICMCB, UPR 9048, F-33600 Pessac, France

<sup>c</sup> Institut Laue-Langevin, 71 Avenue des Martyrs, F-38000 Grenoble, France

<sup>d</sup> RS2E, Réseau Français sur le Stockage Electrochimique de l'Energie, FR CNRS#3459, F-80039 Amiens Cedex 1, France

Keywords: Lithium Batteries, Neutron diffraction, Operando

## INTRODUCTION

Despite the great interest generated by neutrons' sensitivity to lithium, *in-situ* neutron diffraction (ND) knew a slow development due to the intrinsic difficulties it held <sup>1</sup>. We recently designed an electrochemical cell manufactured with a completely neutron-transparent (Ti,Zr) alloy <sup>2</sup>, able to provide good electrochemical properties and ND patterns *operando*, with good statistics and no other Bragg peaks than those of the electrode material of interest. Importantly, this allows detailed structural determinations by Rietveld refinement during operation. The cell was validated using well-known battery materials such as LiFePO<sub>4</sub> and Li<sub>1.1</sub>Mn<sub>1.9</sub>O<sub>4</sub><sup>2</sup> for real *operando* experiments conducted on the D20 high flux neutron powder diffractometer at ILL Grenoble, France.

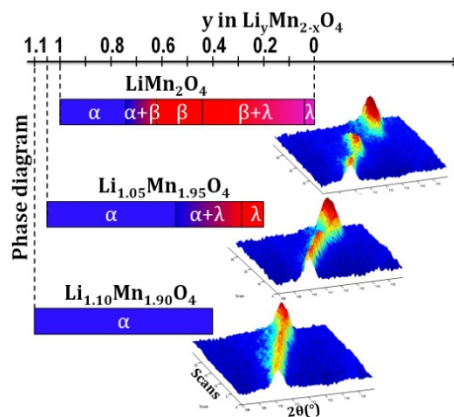
## RESULTS AND DISCUSSION

We report here in particular on a series of spinel materials Li<sub>1+x</sub>Mn<sub>2-x</sub>O<sub>4</sub> (x=0, 0.05, 0.1). The well-known difference in electrochemical performances (capacity fading) observed in this family of materials was thoroughly investigated using *operando* neutron diffraction. The study <sup>3</sup> showed that not only the volume change induced by the delithiation is reduced while going from LiMn<sub>2</sub>O<sub>4</sub> to Li<sub>1.10</sub>Mn<sub>1.90</sub>O<sub>4</sub>, but more importantly that the mechanism by which this happens is modified. In fact, while Li<sub>1.10</sub>Mn<sub>1.90</sub>O<sub>4</sub> reacts through a "simple" monophasic reaction (a solid solution), Li<sub>1.05</sub>Mn<sub>1.95</sub>O<sub>4</sub> shows the existence of a solid solution process followed by a biphasic reaction and LiMn<sub>2</sub>O<sub>4</sub> even shows a sequence of two biphasic reactions. Both the above mentioned features contribute to make over-lithiated Li<sub>1.10</sub>Mn<sub>1.90</sub>O<sub>4</sub> a much better candidate for use in Li-ion batteries than the standard stoichiometric LiMn<sub>2</sub>O<sub>4</sub>.

In more details, neutrons allow us to be sensitive to lithium's atomic parameters, such as atomic coordinates and even site occupancy factors (SOFs), and thus to include them in our analysis by the Rietveld method to increase the accuracy of our time-dependent structural model. In the specific case of Li<sub>1+x</sub>Mn<sub>2-x</sub>O<sub>4</sub> spinels, this meant the possibility to correlate, for the first time, the evolution of lithium's SOF with the electrochemical features of the materials, which is of key importance for

understanding and therefore improving Li-ion battery materials.

Moreover, we recently conducted similar investigations on high voltage LiNi<sub>1-y</sub>Mn<sub>y</sub>O<sub>4</sub> spinels and we'll present charge ordering phenomena within these spinels that occur for specific compositions during Li<sup>+</sup> extraction.



Contour plot of a selected 2θ range of neutron diffraction patterns recorded *operando* upon charge (Li<sup>+</sup> extraction at C/20 rate) for LiMn<sub>2</sub>O<sub>4</sub> (top), Li<sub>1.05</sub>Mn<sub>1.95</sub>O<sub>4</sub> (middle) and Li<sub>1.10</sub>Mn<sub>1.90</sub>O<sub>4</sub> (bottom). Phases in presence during Li<sup>+</sup> extraction are given <sup>3</sup>.

## ACKNOWLEDGMENT

The authors acknowledge Thomas Hansen (ILL) for scientific support on the D20 beamline at ILL, Philippe Dagault, Laetitia Etienne and Eric Lebraud (ICMCB) for technical help and discussion, Région Aquitaine for financial support and the Institut Laue-Langevin for the PhD thesis of MB.

## REFERENCES

1. M. Roberts, J. J. Biendicho, S. Hull, P. Beran, T. Gustafsson, G. Svensson and K. Edstrom, *Journal of Power Sources*, 226 (2013), 249.
2. M. Bianchini, J. B. Leriche, J.-L. Laborier, L. Gendrin, E. Suard, L. Croguennec and C. Masquelier, *Journal of The Electrochemical Society*, 160 (2013), A2176.
3. M. Bianchini, E. Suard, L. Croguennec and C. Masquelier, *Journal of Physical Chemistry C*, **118(45)**, 25947-25955 (2014)

# IV-VI SEMICONDUCTOR NANOCOMPOSITES AND MULTILAYERS FOR THERMOELECTRICITY AND INFRARED OPTOELECTRONICS

T. Story, M. Szot, K. Dybko, L. Kowalczyk, A. Mycielski, A. Szczerbakow  
Institute of Physics, Polish Academy of Sciences,  
al. Lotników 32/46, 02-668 Warsaw, Poland  
e-mail: story@ifpan.edu.pl

Keywords: thermoelectrics, IV-VI semiconductors, infrared optoelectronics

## INTRODUCTION

Application of thermoelectrics as autonomous power supplies (thermoelectric generators) or Peltier refrigerators requires new materials with thermoelectric figure of merit parameter  $ZT$  at least twice better than in currently used materials for which the  $p$ - $n$  couple effective parameter  $ZT=0.5$ -1. The concept of new thermoelectric material being an electron crystal but a phonon glass was recently successfully tested for various thermoelectric alloys, crystalline nanocomposites, and multilayers based on IV-VI narrow gap semiconductors. In heavily  $n$ - and  $p$ -type doped PbTe-PbS, PbTe-PbSe, PbTe-GeTe, PbTe-MnTe, PbTe-SrTe, PbTe-MgTe, and PbTe-CdTe materials systems the enhanced density of states at the Fermi level as well as the reduced thermal conductivity resulted in  $ZT$  parameter improved up to  $ZT=1.5$ -2 [1-6]. These materials and nanostructures are also of importance for optoelectronics as active elements in mid-infrared  $p$ - $n$  junction lasers and detectors.

Particularly important technological path involves spontaneous formation of nanoscale two-phase coherent crystalline structures, e.g. in PbTe-CdTe or PbTe-PbS semiconductor systems. It permits the growth of crystalline composite thermoelectrics with nanosize precipitates embedded in PbTe thermoelectric matrix [4,5,7,8]. The newest directions in this field are related to more environmentally friendly orthorhombic IV-VI materials, SnSe and SnS [9] as well as thermoelectric exploitation of newly discovered topological surface electronic states in  $Pb_{1-x}Sn_xSe$  and  $Pb_{1-x}Sn_xTe$  [10,11].

## EXPERIMENTAL

Using various technological methods (growth from the melt, vapor phase growth and molecular beam epitaxy) we prepared PbTe-CdTe materials as bulk  $Pb_{1-x}Cd_xTe$  ( $x=0$ -0.11) monocrystals, bulk  $Pb_{0.99}Cd_{0.01}Te$  (rock-salt) - CdTe (zinc-blende) two-phase nanocomposites as well as PbTe/CdTe multilayers deposited on GaAs substrate. We also developed molecular beam epitaxy regime and designed multilayer stack required to obtain, in a single technological step and in a single multilayer, a region consisting of PbTe thermoelectric matrix with epitaxially embedded CdTe quantum anti-dots (thermoelectric system) and an adjacent region consisting of CdTe insulating matrix with PbTe quantum dots (optoelectronic system) [7,8].

We experimentally studied electrical conductivity, Hall effect, thermoelectric power, thermal conductivity, and photoluminescence of PbTe-CdTe materials doped  $n$ -type with Bi or I and  $p$ -type with Na up to  $10^{19}$  cm<sup>-3</sup>. In agreement with theoretical predictions [6] we found

the band gap  $E_G$  of  $Pb_{1-x}Cd_xTe$  rapidly increasing with the increasing Cd content  $dE_G/dx=2.5$  eV. It results in a large increase of carriers effective mass and thermoelectric power as well as improved thermoelectric parameters of these materials [3-7]. Applying the Harman method we directly experimentally determined the parameter  $ZT=0.7$ -0.9 at  $T=700$  K for both  $n$ -type and  $p$ -type PbTe-CdTe. Good optical properties of PbTe-CdTe alloys and multilayers were confirmed by the observation of room temperature photoluminescence controlled in the mid-infrared spectral range of  $\lambda=2$  - 6 microns by chemical composition and dot size.

## CONCLUSIONS

The excellent lattice parameters match and immiscibility of rock-salt PbTe and zinc-blende CdTe crystals facilitate the growth of bulk  $Pb_{0.99}Cd_{0.01}Te$ -CdTe nanocomposites and PbTe-CdTe multilayers with high thermoelectric  $ZT$  parameter for both  $p$ -type and  $n$ -type materials. PbTe quantum wells and dots with CdTe electron barriers are also very efficient infrared emitters.

## ACKNOWLEDGMENT

This work is supported by the EU within the European Regional Development Fund, through the Innovative Economy grant (POIG.01.01.02-00-108/09).

## REFERENCES

1. W. Liu, X. Yan, G. Chen, Z. Ren, *Nano Energy* **1** (2012) 42.
2. H. Wang, Y. Pei, A.D. LaLonde, G.J. Snyder, *Adv. Mat.* **23** (2011) 1366.
3. Y. Pei, X. Shi, A.D. LaLonde et al., *Nature* **473** (2011) 66.
4. Y. Pei, A.D. LaLonde, N.A. Heinz, G.J. Snyder, *Adv. Energy Mat.* **2** (2012) 670.
5. M. Szot et al., *Cryst. Growth & Design* **11** (2011) 4794.
6. M. Bukała, P. Sankowski, R. Buczek, P. Kacman, *Phys. Rev. B* **86** (2012) 085205.
7. M. Szot, K. Dybko, P. Dziawa et al., *Funct. Mat. Lett.* **7** (2014) 1440007.
8. G. Karczewski, M. Szot, S. Kret et al., *Nanotechnology* **26** (2015) 135601.
9. K. Kutorasiński, B. Wiendlocha, S. Kaprzyk, J. Tobała, *Phys. Rev. B* **91** (2015) 205201.
10. P. Dziawa, B.J. Kowalski, K. Dybko et al, *Nat. Mat.* **11** (2012) 1023.
11. B.M.W. Wojek, P. Dziawa, B.J. Kowalski, *Phys. Rev. B* **90** (2014) 161202.



# MECHANISMS OF ELECTRODE PROCESSES IN SOFC

*M.B. Mogensen, K. Kammer Hansen, C. Chatzichristodoulou, C. Graves*

Department of Energy Conversion and Storage

Technical University of Denmark, DTU Risø Campus, Frederiksborgvej 399

DK-4000 Roskilde, Denmark

e-mail: momo@dtu.dk

Keywords: hydrogen and oxygen electrodes, Solid oxide fuel cells

## INTRODUCTION

Solid oxide cells (SOCs) are reversible high temperature (600 – 1000 °C) cells, that operate equally well in fuel cell (SOFC) and in electrolysis mode (SOEC)<sup>1-4</sup>. The cells consist mainly of ceramics and do not contain any noble metal<sup>5,6</sup>.

This presentation gives an analysis of the problems involved in defining and measuring electrocatalysis and electrocatalytic activity of metals and ceramics (metal oxides) that are deposited as electrodes on solid oxide electrolytes or as additives into solid oxide electrodes in order to improve their electrode kinetics. Besides the analysis of problems involved in determining the electrocatalytic activity of these electrodes, methods of measuring relative activity of SOC electrocatalysts in ways that makes it possible to compare different electrocatalysts at least semi-quantitatively are described.

## DEFINITION OF CONCEPTS

Many scientists in the area of electrocatalysis say that electrocatalysis at temperatures above ca. 300 °C is not an issue, because there are no problems with electron transfer, and bond breaking of H<sub>2</sub> and O<sub>2</sub> is fairly fast above this temperature. As a consequence electrocatalysts should not be necessary at all in an SOFC operating at temperatures above 600 °C. However, this actually depends on the definition of electrocatalysis, and as many workers in the area of SOFC use this term, it seems reasonable to consider if a suitable definition of the term can be given - a term which is not in conflict with IUPAC definitions of other catalysis terms.

Regrettably, the UPAC Gold Book does not mention the concept of electrocatalysis. Therefore, we take our starting point in the concept of heterogeneous catalysis. The IUPAC Gold Book<sup>7</sup> reads: "Catalyst: a substance that increases the rate of a reaction without modifying the overall standard Gibbs energy change in the reaction; the process is called catalysis. ... *text, which is not included here* ... heterogeneous catalysis, in which the reaction occurs at or near an interface between phases." Based on this we adopt the definition: an electrocatalyst is a catalyst that promotes electrochemical reactions in electrodes of electrochemical cells. In line with this, turnover frequency (TOF = number of chemical entities reacted per second per catalytic site, unit: s<sup>-1</sup>) is the quantity describing the electrocatalytic activity in a clear physical chemical meaningful way, i.e.: the electrocatalytic activity of an electrocatalyst is the TOF for the given electrochemical reaction at given conditions. Yet, today we are usually not able to determine TOF quantitatively for any of our practical electrocatalysts, because it is very difficult to determine the number of electrocatalytic active sites.

## METHODS

The difficulty of counting the number of active sites makes most workers look at the area specific electrocatalytic activity, i.e. the number of chemical entities reacted per second per unit area of electrocatalyst with unit: cm<sup>-2</sup> s<sup>-1</sup>. This is equivalent to current density for a given electrocatalytic reaction step in a given direction, and at equilibrium (open circuit voltage) it is equivalent to the exchange current density calculated using the area of active electrocatalyst.

We will show using examples of oxygen and hydrogen electrodes that it is not trivial to determine the area of the active electrocatalyst, but using impedance spectroscopy and cyclic potential sweep on model electrodes we may determine the relative order of electrocatalytic activity of different electrocatalytic active compounds<sup>8</sup> and figure out to which extent various parts of an electrode that are electrocatalytic active<sup>9</sup>. Finally, we will point out that electrocatalytic steps need not be rate limiting steps in electrode reactions. Proposals for electrode reaction mechanisms will be presented.

## ACKNOWLEDGMENT

This work was financially supported by Energinet.dk through the ForskEL program "Solid Oxide Fuel Cells for the Renewable Energy Transition" contract no 2014-1-12231.

## REFERENCES

1. E. Baur, H. Preis, *Zeitschrift für Elektrochemie* **43** (1937) 727.
2. J. Weissbart, W. Smart, T. Wydeven, *Aerospace Med.* **40** (1969) 136.
3. C.S. Tedmon, H.S. Spacil, and P. Mitoff, *J. Electrochem. Soc.* **116** (1969) 1170.
4. S. H. Jensen, P. H. Larsen, M. Mogensen, *Int. J. Hydrogen Energy* **32** (2007) 3253.
5. A. O. Isenberg, *Solid State Ionics* **3-4** (1981) 431.
6. M. Kertesz, I. Riess, D.S. Tanhauser, L. Langpape, F.J. Rohr, *J. Solid State Chemistry* **42** (1982) 125.
7. IUPAC. *Compendium of Chemical Terminology*, 2<sup>nd</sup> ed. (the "Gold Book"). Compiled by A. D. McNaught and A. Wilkinson. Blackwell Scientific Publications, Oxford (1997). XML on-line corrected version: <http://goldbook.iupac.org> (2006-2014) created by M. Nic, J. Jirat, B. Kosata; updates compiled by A. Jenkins.
8. K. Kammer Hansen, M. Mogensen, *ECSS Transactions*, **13(26)** (2008) 153-160
9. K. V. Hansen, K. Norrman, Torben Jacobsen, Y. Wu, M. B. Mogensen, *J. Electrochem. Soc.* **162** (2015) F1165

# Y-DOPED BARIUM ZIRCONATE PREPARED BY FLAME SPRAY SYNTHESIS AS ELECTROLYTE FOR INTERMEDIATE TEMPERATURE PROTON CONDUCTING FUEL CELLS

*Francesco Bozza, Thomas Graule*

Laboratory for High Performance Ceramics, EMPA, Dübendorf, Switzerland

BaZr<sub>0.8</sub>Y<sub>0.2</sub>O<sub>3-δ</sub> (BZY20) electrolyte nanoprecursors were prepared by Flame Spray Synthesis (FSS) technique. The nanoprecursors were composed of a perovskite phase, barium nitrate and doped zirconia. Pure BZY20 powder could be obtained after calcining the nanoprecursors at 1200°C. Both nanoprecursors and pure phase powder were sintered at 1600°C to obtain dense specimen. AC impedance spectroscopy performed on the sintered samples allowed correlation of the electrical properties of the samples to their microstructures. The sintered nanoprecursors compared with the sintered pure phase powders showed enhanced grain growth associated with an enhanced total proton conductivity of  $7.7 \times 10^{-3}$  S/cm at 450°C<sup>1</sup>.

The effect of Ni doping on the sintering and electronic behavior of the BZY20 nanoprecursors was also investigated. Microstructures and electrical properties of 1% and 2% mol. Ni doped BZY20 were analyzed after sintering at 1400°C and 1500°C. The inclusion of Ni into the BZY20 lattice, though allowed to strongly reduce the sintering temperature, resulted to have a negative effect on the electrical properties of the material. A total proton conductivity of  $4.1 \times 10^{-3}$  S/cm at 450°C was measured for the 2% mol. Ni doped sample sintered at 1400°C<sup>2</sup>.

1) F.Bozza, Y. Arroyo, T. Graule, Fuel Cells, 2015, DOI: 10.1002/fuce.201400179.

2) F.Bozza, K. Bator, W.W. Kubiak, T. Graule, submitted.

# THERMOELECTRIC MATERIALS FOR WASTE HEAT RECOVERY

*K. T. Wojciechowski*

Thermoelectric Research Laboratory,  
Faculty of Materials Science and Ceramics; Centre of Energetic  
AGH University of Science and Technology, Al. Mickiewicza 30  
30-059 Cracow, Poland  
e-mail: wojciech@agh.edu.pl

Keywords: thermoelectric materials, segmented TE modules, FGTM materials, energy conversion

## INTRODUCTION

Thermoelectric materials are used in power-generation devices that can be designed e.g. for direct conversion of waste heat into electrical energy or for cooling applications in solid-state refrigeration devices. Especially, the conversion of waste or renewable heat may play an important role in development of alternative energy technologies to lower fossil fuels consumption and reduce greenhouse gas emissions.

A number of different systems of potential TE materials are reviewed in the presentation. Research criteria for developing of new materials and devices are highlighted. These range from nanostructured materials [1], segmented TE elements [2] to functionally graded thermoelectric materials FGTM [3]. The possibilities of application of strong gravity engineering technique in development of new TE materials are discussed.

Potential applications of TE materials including conversion of waste heat energy of automotive exhausts gases into electricity [4,5] and for improvement of effectiveness of selected devices in power plants [6] are considered.

## EXPERIMENTAL DETAILS

High efficiency segmented thermoelectric unicouples STUs made of  $\text{Bi}_2\text{Te}_3$  and  $\text{CoSb}_3$ -based alloys doped with In and Te have been recently developed. The performance parameters of elements were tested on the constructed set-up for selected temperatures ranging from 288 to 673K. Characterizations of electrical resistances of contacts and materials were made by scanning thermoelectric microprobe (STM).

The results of investigations indicate that constructed thermoelectric elements exhibit very high experimental maximal efficiency  $\eta_{\max} = 9.3\%$  and power density of  $1.48 \text{ W}\cdot\text{cm}^{-2}$  for temperatures  $T_{\text{H}} = 673 \text{ K}$  at hot shoe and  $T_{\text{C}} = 288 \text{ K}$  at cold shoe. Measurements made by STM show very low electrical resistances of junctions from 16 to  $22 \mu\Omega\cdot\text{cm}^2$  which effect in excellent load parameters for STUs:  $I_{\max} = 60 \text{ A}$  (at  $U_{\text{out}} \rightarrow 0$ ) and  $I_{\text{opt}} = 26 \text{ A}$  for maximum power condition.

The new method of preparation of functionally graded thermoelectric materials FGTM in ultra-high centrifugal force of about  $10^6 \text{ G}$  is developed. For preliminary studies simple Bi-Sb and Bi-Sb-Te systems had been chosen. Sedimentation experiment using ultracentrifuge of special construction (Kumamoto

University, Japan) has been performed at different temperatures ( $265^\circ\text{C}$  and  $350^\circ\text{C}$ ) on alloys with 9:1, 8:2, 7:3 and 6:4 Bi:Sb ratio, respectively, for period of 60 h. Changes in microstructure and composition were analysed using SEM microscope with EDX/WDS analyser. The Seebeck coefficient profiles, following the differences in experimental conditions and Bi:Sb ratio, were obtained using Scanning Thermoelectric Microprobe (STM).

Theoretical calculations confirmed that a maximum value of figure of merit  $ZT_{\max}$ , as a function of carrier concentration, is attained just for one specific location of the Fermi level, with respect to the conduction band edge. The developed theoretical model allowed calculation of optimal dopant concentration profile especially in FGTM prepared by high-gravity sedimentation method. It was confirmed that for the optimal profile of carrier concentration the efficiency of TE elements can be improved by about 50%.

## CONCLUSIONS

New thermoelectric materials for construction of waste heat recovery devices have been developed. It is predicted that designed thermoelectric generators can have potential to reach maximum efficiency of 9%. The preliminary economic analysis made for large scale thermoelectric generator TEG with power 44 kW has shown that TE technologies can be competitive to photovoltaic.

## ACKNOWLEDGMENT

This work is supported by NCN under grant DEC-2013/09/B/ST8/02043.

## REFERENCES

1. K.T. Wojciechowski, J. Obłakowski, *Solid State Ionics*, 157 (2003)
2. K.T. Wojciechowski, et al, *AIP Conf. Proc. Series* 1449, Melville, New York, 2012
3. K. Januszko, A. Stabrawa, Y. Ogata, M. Tokuda, I. Jahirur, T. Mashimo, K. Wojciechowski, *Journal of Electronic Materials*, publishing
4. K.T. Wojciechowski, M.Schmidt, R. Zybala, J. Merkisz, P.Fuć, P. Lijewski, *Journal of Electronic Materials*, 39, (2010)
5. K. Wojciechowski, J. Merkisz, P. Fuć, J. Tomankiewicz, R. Zybala, J. Leszczyński, P. Lijewski, P. Nieroda, *Combustion engines*, 52, (2013)
6. K. T. Wojciechowski, W. Wieczorek, B. Sarapata, H. Kubiczek, *Journal of Electronic Materials*, publishing

# PROTON CERAMIC FUEL CELLS AND THE HYDROGENATION OF CO<sub>2</sub> TO HYDROCARBONS

Costas G. Vayenas

Department of Chemical Engineering, University of Patras, GR-26504 Patras, Greece

Academy of Athens, Panepistimiou 28 Ave., GR-10679 Athens, Greece

e-mail: cgvayenas@upatras.gr

Keywords: Hydrogenation of CO<sub>2</sub>, proton ceramic fuel cells, electrochemical promotion of catalysis (EPOC)

## INTRODUCTION

The hydrogenation of CO<sub>2</sub> to hydrocarbons is a reaction of great potential and technological importance since it can lead to the production of renewable fuels but might also serve in the future as a means for decreasing the overall CO<sub>2</sub> emissions. [1]. The hydrogenation of CO<sub>2</sub> on Ru, which is known to give only CH<sub>4</sub> and CO as products, has attracted considerable attention in recent years [2-4]. The electrochemical promotion of Catalysis (EPOC) or non-Faradaic electrochemical modification of catalysis (NEMCA effect) can be used to promote in situ the catalytic properties of metal catalyst films acting simultaneously as electrodes, which are deposited on solid electrolyte supports such as yttria-stabilized-zirconia (YSZ, an O<sup>2-</sup> conductor), BaZrO<sub>0.85</sub>Y<sub>0.15</sub>O<sub>3-α</sub> (BZY, a H<sup>+</sup> conductor), Na-β"-Al<sub>2</sub>O<sub>3</sub>, a Na<sup>+</sup> conductor or K-β"-Al<sub>2</sub>O<sub>3</sub>, a K<sup>+</sup> conductor.

In this work the kinetics and the electrochemical promotion the hydrogenation of CO<sub>2</sub> to CH<sub>4</sub> and CO is compared for Ru porous catalyst films deposited on Na<sup>+</sup>, K<sup>+</sup>, H<sup>+</sup> and O<sup>2-</sup> conducting solid electrolyte supports.

## EXPERIMENTAL

**Catalyst preparation:** The solid electrolytes were discs of 8 mol% Y<sub>2</sub>O<sub>3</sub>-stabilized ZrO<sub>2</sub> (YSZ) with 18 mm diameter and 2 mm thickness provided by Ceraflex, discs of β"-Al<sub>2</sub>O<sub>3</sub> with 20 mm diameter and 3 mm thickness provided by Ionotec and discs of BZY (BaZr<sub>0.85</sub>Y<sub>0.15</sub>O<sub>3</sub> + 1 w% NiO) with a diameter of 18 mm and a thickness of 2 mm provided by NorECs AS. Gold organometallic paste (Metalor, A1118) was used for the deposition of the Au counter and reference electrodes on one side of the discs, followed by calcination in air at 650°C for 1 hr. Blank experiments showed that gold was catalytically inactive both for the methanation and the RWGS reaction. The Ru catalyst films were deposited on the other side of the discs, via impregnation of a 150mM RuCl<sub>3</sub> solution in isopropanol at 50°C, followed by calcination in air at 500°C for 1 hr. The loading of the catalysts was ~1 mg for Ru/Na-β"-Al<sub>2</sub>O<sub>3</sub> and Ru/BZY, ~2 mg for Ru/K-β"-Al<sub>2</sub>O<sub>3</sub> and ~3 mg Ru/YSZ.

Prior to any hydrogenation activity measurements, a reduction pretreatment in 5% H<sub>2</sub>/He was performed at 300°C for 1 hr. The reaction was carried out in a continuous flow single pellet reactor analyzed in detail in previous papers [3, 4].

## RESULTS AND DISCUSSION

It was found that varying catalyst potential has a pronounced effect on the rates of CH<sub>4</sub> and CO formation and in product selectivity. An example is shown in Figure 1 which depicts the effect of the Ru catalyst

potential, U<sub>WR</sub>, on the product selectivity. The methanation selectivity, S<sub>CH<sub>4</sub></sub>, is generally enhanced with increasing potential for all four supports and this change in selectivity is very pronounced, particularly in the case of the K-β"-Al<sub>2</sub>O<sub>3</sub> supported catalyst where the selectivity to CH<sub>4</sub>, S<sub>CH<sub>4</sub></sub>, is enhanced from 4% to 97% upon increasing the catalyst potential by 0.5 V.

## CONCLUSIONS

The electrochemical promotion of the CO<sub>2</sub> hydrogenation on Ru affects the catalytic rates and product selectivity in a very pronounced manner. Regardless of the type of promoting ion (O<sup>2-</sup>, H<sup>+</sup>, K<sup>+</sup>, Na<sup>+</sup>) the same trends are observed, i.e. the selectivity to CH<sub>4</sub> is enhanced with positive potential (O<sup>2-</sup> supply to Ru, H<sup>+</sup>, Na<sup>+</sup>, K<sup>+</sup> renewal from Ru) and the selectivity to CO is enhanced with negative potential (O<sup>2-</sup> removal from Ru, H<sup>+</sup>, Na<sup>+</sup>, K<sup>+</sup> supply to Ru). The observed behaviour is in good agreement with the rules of chemical and electrochemical promotion [2].

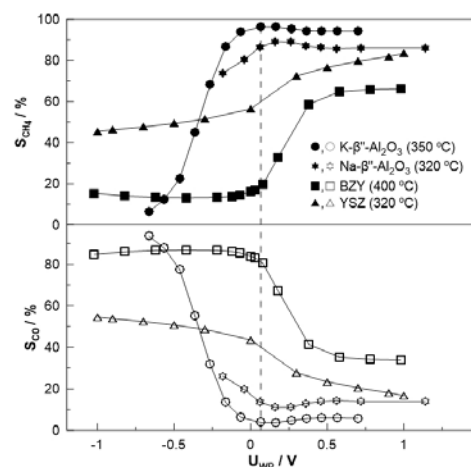


**Fig. 1.** Effect of catalyst potential, U<sub>WR</sub>, on the product selectivity of CO<sub>2</sub> hydrogenation on Ru deposited on four different solid electrolyte supports.

## ACKNOWLEDGMENT

Work supported under the ARISTEIA Programme.

## REFERENCES

1. S. Sharma, Z. Hu, P. Zhang, E.W. McFarland, H. Metiu, *J. Catal.*, **278** (2011) 297-309.
2. C.G. Vayenas, C.G. Koutsodontis, *J. Chem. Phys.*, **128** (2008) 182506.
3. D. Theleritis, M. Makri, S. Souentie, A. Caravaca, A. Katsaounis, C.G. Vayenas, *ChemElectroChem*, **1**(2014)254-262.
4. M. Makri, A. Katsaounis, C. Vayenas, *Electrochimica Acta*, in press (2015).



# QUANTUM DOTS AND NANO-SIZED GOLD SENSITIZED ZINC OXIDE NANOWIRES-ARRAY PHOTOELECTRODES FOR WATER SPLITTING

*Ru-Shi Liu*<sup>1,2,\*</sup>

<sup>1</sup>Department of Chemistry, National Taiwan University, Taipei 106, Taiwan

<sup>2</sup>Department of Mechanical Engineering and Graduate Institute of Manufacturing Technology, National Taipei University of Technology, Taipei 106, Taiwan  
e-mail: rslu@ntu.edu.tw

Keywords: quantum dots, nano-sized gold, zinc oxide wires, water splitting, photoelectrodes

## INTRODUCTION

Over the past decade, owing to the increasing need for clean energy production, significant effort has been made to exploit the properties of materials for applications in photovoltaic and related solar-harvesting devices [1]. Hydrogen generated by splitting of the water is one of the most potential forms of energy production, solar-harvesting devices can be an important source of sustainable energy and essential to decrease the consumption of fossil fuels. Metal oxides such as TiO<sub>2</sub>, ZnO, and WO<sub>3</sub> have been investigated for water splitting with various morphologies [2]. Nevertheless, most of the metal oxides have large bandgap, leading to limited light absorption in the visible region, which impose a fundamental limitation on overall efficiency. One of methods is the use of semiconductor nanocrystals, known as quantum dots (QDs). QDs provide the more matches the solar spectrum better due to their absorption spectrum can be tuned with particle size. Additionally, it has been recently shown that QDs can generate multiple electron-hole pairs per photon, which could enhance the efficiency of the device [3].

In order to address this fundamental issue, we examine the combination of CdTe and InP QDs with ZnO nanowires for photoelectrochemical water splitting. Employment of CdTe QDs in water splitting system could be exactly measured the efficiency for water splitting reaction in aqueous system.

The water splitting reaction was measured with the gold nanoparticles modified ZnO nanowires. Recently, the plasmon induced effects, such as “hot” electrons injection and the induced electromagnetic field, were demonstrated could improve the photovoltaic and the photoelectrochemical water splitting reaction [4]. Systematically investigation were designed for distinguishing the effects of the plasmon induced effects.

## EXPERIMENTAL

Zinc nitrate, absolute ethanol, zinc acetate, and Te powder were purchased from Sigma-Aldrich. Sodium borohydride and hexamethylenetetramine (HMT) was obtained from Acros Organics. Cadmium chlorite and mercaptopropionic acid (MPA) were purchased from Fluka. All chemicals were used as delivered without further purification. Fluorine-doped tin oxide substrates were purchased from Hartford Glass Company. The water used throughout this investigation was of reagent-grade, and was produced using a Milli-Q SP ultrapure-water purification system from Nihon Millipore Ltd., Tokyo. F:SnO<sub>2</sub> (FTO) was cleaned by ultrasonic agitation in acetone and ethanol bath individually. 100

mL of a 0.06 M solution of zinc acetate in absolute ethanol mixed with ultrasonic agitation. The FTO substrates were wet with zinc acetate solution for 10 s, and then blown dry with stream of argon. This coated step was repeated eight times. The substrates were annealed at 350°C for 30 minutes to yield a layer of ZnO seeds. The seeded substrates were suspended horizontally in a reagent solution containing 0.06 M zinc nitrate and 0.06 M HMT in the Teflon vessel, and then sealed in autoclave and heated to 110°C for nanowire growth. The nanowire substrate was removed from the autoclave and thoroughly washed with the distill water after 24 hours of growth, and then dried in air. NaBH<sub>4</sub> (0.08 g) was reacted with Te powder (0.127 g) in water (1.0 mL) to produce sodium hydrogen telluride (NaHTe, 0.99 M). The NaHTe solution (0.5 mL) was then added to a N<sub>2</sub>-saturated mixture (74.8 mL; pH 11.2) of MPA (38 mM) and CdCl<sub>2</sub> (16 mM) to give a final Cd<sup>2+</sup>/MPA/HTe-molar ratio of 1 : 2.4 : 0.5. This mixture was then heated under reflux at 90 °C for 6 hours. The color of the solution changed from dark red to orange-yellow. The CdTe QDs were purified by using centrifugation in absolute ethanol, which allowed removal of free ligands such as MPA and unreacted precursor ions from the CdTe QDs. A nanowire substrate was baked at 450°C for 30 minutes. After cooling in air the substrate placed nanowire-side up on the bottom of the vial containing the CdTe QD dispersion. After 24 hours the nanowire substrate was removed from the QD dispersion and thoroughly washed with the distill water, and then dried in the air. A module of three electrodes was used in an electrochemical test. A water splitting photoelectrode was used as the working electrode, a platinum plate served as the counter electrode and an Ag/AgCl was used as the reference electrode. All the PEC studies were operated in a 0.5M Na<sub>2</sub>SO<sub>4</sub> (pH = 6.8) solution as the supporting electrolyte medium. Water was used as the solvent in all reactions, in which sodium citrate acted as both the capping reagent and the reducing agent. In a typical preparation, the colloidal nanoparticles were prepared by adding 5 mL of sodium citrate (1%) to 50 mL of gold metal salt (HAuCl<sub>4</sub>, 0.4 mM) solution. The solution was heated at 95 °C in an oil bath for 15 min, and then allowed to cool before the subsequent experiment was carried out. The as-prepared ZnO nanorod array substrates were placed with their nanowire side up in a gold nanoparticle solution for the desired duration. Following deposition in a chemical bath, the substrate was removed from the solution and washed by D. I. water to remove any excess gold solution. Illuminating the water splitting

photoelectrode with light source was a Xenon lamp using PE300BF equipped filters to simulate the AM1.5 spectrum and ranged from 390 nm to 770 nm in visible region, in which light intensity fixed in 100 mW/cm<sup>2</sup>. Linear sweep voltammograms, collected at a scan rate of 20 mV/s at applied potential from -0.5 to +1.1V, Amperometric I-t curve of ZnO nanowires with decorating the CdTe QDs at an applied voltage of +0.5V at 100 mW/cm<sup>2</sup>. The UV/vis spectra of samples were obtained using a SHIMADZU UV-1700 spectrophotometer at room temperature. The nanowires were performed using a JEOL JSM-6700F field emission scanning electron microscope (FE-SEM) that was equipped with an EDS probe. Transmission electron microscopy (TEM) was used to characterize the surface morphology of the samples. The images of high-resolution transmission electron microscopy (HRTEM), electron diffraction patterns, and elemental mapping were collected on a JEOL JEM-2100F electron microscope. The specimens were obtained by placing many drops of the colloidal solution onto a Formvar-covered copper grid and evaporating it in air at room temperature. Prior to specimen preparation, the colloidal solution was sonicated for 1 min to improve the dispersion of particles on the copper grid.

## RESULTS AND DISCUSSION

To examine the photoresponse of this structure over time, I-t curve collected from the ZnO nanowires with loading of CdTe QDs (24 hrs) at +0.5 V. is shown in Fig 1 (a). These results further confirm that photogenerated electrons quickly transport from CdTe QDs to ZnO nanowires. In the long term, the chemical stability issue of this structure could be addressed by depositing a monolayer on the ZnO nanowires. Fig. 1(b) demonstrated that the photocurrent response was almost identical over 50 cycles, demonstrating the stability of this structure and used as photoanodes were relatively stable in the photo-oxidation process in aqueous solution. The achieved high efficiency and stability may be attributed to major improvement. Monolayer deposition of CdTe QDs allow a fast and efficient transfer of the photogenerated electrons from CdTe to the ZnO nanowires, which lead to a much reduced the anodic decomposition/corrosion and much improved the stability of photodevices.

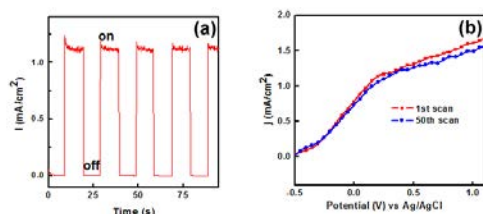


Fig. 1. (a) Amperometric I-t curves of ZnO nanowires with/without loading of CdTe QDs at 100 mW/cm<sup>2</sup> with on/off cycles. (b) Stability of PEC performance after 50 scans. [5]

Figure 2 presents a model mechanism of the enhancement by localized surface plasmon resonance on

an Au nanostructure. When the photoanode (Au-ZnO photoelectrode) captured solar illumination and ZnO simultaneously generated photoelectrons, the photogenerated electrons migrated to the conduction band of ZnO. Simultaneously, the Au nanostructure absorbed plasmon-induced irradiation, generating hot electrons and an electromagnetic field.

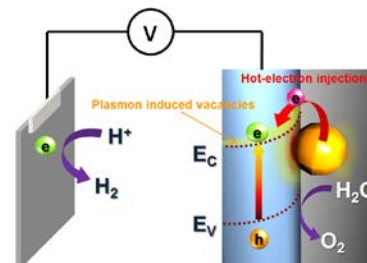


Fig. 2. Schematic illustration of the plasmon-induced effects on Au-ZnO photoelectrode.[6]

## CONCLUSIONS

We demonstrated the QDs and gold nanoparticles could enhance the photoelectrochemical water splitting. The QDs could absorb the visible light and generated photocurrent and thus enhance the water splitting reaction. The gold nanoparticles coupled the surface plasma resonance induced effects, explaining why the coupling of hot electrons that were formed by plasmons with the electromagnetic field effectively increases the probability of the photochemical reaction in the splitting of water [6-9].

## ACKNOWLEDGMENT

The authors would like thank the financial support of the Ministry of Science and Technology of Taiwan (Contract No. MOST 101-2113-M-002-014-MY3).

## REFERENCES

- W. U. Huynh, J. J. Dittmer and A. P. Alivisatos, *Science* **295**(2002) 2425.
- H. M. Chen, C. K. Chen, R. S. Liu, L. Zheng, J. Zhang and D. P. Wilkinson, *Chem. Soc. Rev.* **41**(2012)5654.
- S. U. M. Khan, M. Shahry and Jr. W. B. Ingler, *Science* **297**(2002)2243.
- S. Linic, P. Christopher and D. B. Ingram, *Nat. Mater.* **10**(2011)911.
- H. M. Chen, C. K. Chen, Y. C. Chang, C. W. Tsai, R. S. Liu, S. F. Hu, W. S. Chang and K. H. Chen, *Angew. Chem. Int. Edit.* **49**(2010)5966.
- H. M. Chen, C. K. Chen, C. J. Chen, L. C. Cheng, I. C. Wu, B. H. Cheng, Y. Z. Ho, M. L. Tseng, Y. Y. Hsu, T. S. Chan, J.-F. Lee, R. S. Liu, and D. P. Tsai, *ACS Nano* **6**(2012)7362.
- C. K. Chen, H. M. Chen, C. J. Chen and R. S. Liu, *Chem. Commun.* **49**(2013)7917.
- C. J. Chen, M. G. Chen, C. K. Chen, P. C. Wu, P. T. Chen, M. Basu, S. F. Hu, D. P. Tsai and R. S. Liu, *Chem. Commun.*, **51**(2015)549.
- M. Basu, Z. W. Zhang, C. J. Chen, P. T. Chen, K. C. Yang, C. G. Ma, S. F. Hu and R. S. Liu, *Angew. Chem. Int. Edit.* **54**(2015)6211.

# INFLUENCE OF TEMPERATURE AND ELECTROLYTE COMPOSITION ON HYDROGEN ELECTROSORPTION IN AB<sub>5</sub> ALLOY

M. Karwowska<sup>a</sup>, Z. Rogulski<sup>a,b</sup> and A. Czerwiński<sup>a,b</sup>

<sup>a</sup> University of Warsaw, Department of Chemistry, ul. Pasteura 1, 02-093 Warsaw, Poland

<sup>b</sup> Industrial Chemistry Research Institute, ul. Rydygiera 8, 01-793 Warsaw, Poland

e-mail: aczerw@chem.uw.edu.pl

Keywords: power sources, Ni-MH battery, AB<sub>5</sub> alloy, hydrogen absorption

## INTRODUCTION

Nickel-metal hydride batteries are still one of the most used electrochemical power sources. Ni-MH batteries are much less toxic than nickel-cadmium batteries and still much cheaper and safer than lithium-ion batteries. Although they are excellent for powering of many portable devices or Hybrid Electric Vehicles (HEV) [1, 2], the attainable current densities of Ni-MH batteries are not sufficient for their use in the devices demanding very high power densities or for usage at low temperatures. Preparation of new hydrogen storage alloys, used as the anode materials in Ni-MH batteries is one of the methods considered for the improvement of these batteries [3]

## EXPERIMENTAL

Limited Volume-Electrode (LVE) method has been used in the study of the LaMm-Ni<sub>4.1</sub>Al<sub>0.3</sub>Mn<sub>0.4</sub>Co<sub>0.45</sub>, - typical AB<sub>5</sub> alloy used in Ni-MH batteries which was deposited on gold matrix – neutral material to hydrogen sorption process. The electrode was placed in a specially designed PTFE holder [4]. We put the electrode between two pieces of separator (polyethylen) used in standard Ni-MH cells. Such experimental setup allows us to receive the electrochemical response from the pure alloy material, as no binder additives are necessary. All the measurements were performed in a three-electrode system in Teflon cell. MH-LVE electrode was used as a working electrode, Hg|HgO with 6M KOH and gold sheet were served as reference and counter electrodes.

## RESULTS AND DISCUSSION

A series of experiments using 1M solutions of alkali metal (Li, Na, K, Rb and Cs) bases: have been performed. One can observe that the activation process causes real surface increase (cracking of the grains). The capacity of the alloy obtained in CV technique is lower than in CA. These situation is due to non-equilibrium state during voltammetric measurements (with scanning rate  $v=2\text{mV/s}$ ). According to obtained results, the composition of the electrolyte significantly influences the electrochemical characteristics of the working electrode. The capacity value was obtained from charge of discharging electrode. The time required for full charge of electrode is dependent on the electrolyte composition.

Hydrogen diffusion coefficient ( $D_H$ ) has been determined by charging and discharging working electrode maintaining constant current. The model of a finite space diffusion inside spherical particles was

applied in the analysis of CA desorption curves [4],  $D_H$  value can be calculated from the slope of a linear part of  $\ln I$  vs. time plot.  $D_H$  changes non linearly in the function of state of charge (SOC) in a similar way for all the investigated electrolytes. At room temperature  $D_H$  value in different alkali metal hydroxide electrolytes changes in an order:  $\text{LiOH} < \text{NaOH} < \text{KOH} > \text{RbOH} > \text{CsOH}$ . The corrosion process takes place during measurements (hydroxides and oxides are formed) and this process depends on the electrolyte composition. The strongest corrosion was observed in RbOH and CsOH. The time required for hydrogen desorption from the electrode is longer in lower temperatures. It is due to slower diffusion of the hydrogen through the alloy grains at lower temperatures. We suggest that it can be also due to the higher viscosity of the electrolyte at lower temperatures. It can be also due to the higher viscosity of the electrolyte at lower temperatures.

## CONCLUSIONS

The alloy is stable in wide range of temperature (0–55°C) and its structure remains is unchanged after the electrochemical treatment. The highest capacity and  $D_H$  values have been observed in KOH solution. The decrease of the electrochemical capacity of the alloy was observed in other electrolytes LiOH, NaOH, RbOH and CsOH. It can be explained by strong interaction of the electrolyte with the surface of the alloy due to alkali metals intercalation and corrosion. Significant influence of temperature on capacity of the alloy has been observed. The decrease of temperature causes decrease of the capacity value. The capacity value is almost stable above 25°C. The results obtained suggest that the properties of the electrode made of the hydrogen storage alloy highly depend on the composition of the electrolyte. The presented electrochemical study is important in view of designing new electrolytes to be used in Ni-MH batteries.

## REFERENCES

- [1] D. Linden, T.B. Reddy, *Handbook of Batteries*, third ed., McGraw-Hill, New York, 2002.
- [2] M.A. Fetcenko, S.R. Ovshinsky, B. Reichman, K. Young, C. Fierro, J. Koch, A. Zallen, W. Mays, T. Ouchi, *J. Power Sources* 165 (2007) 544–551.
- [3] J. Kleperis, G. Wójcik, A. Czerwiński, J. Skowroński, M. Koczyk, M. Bełtowska-Brzezińska, *J Solid State Electrochem*, 5 (2001) 229.
- [4] M. Karwowska, T Jaron, K Fijalkowski, P.Leszczynski, Z. Rogulski, A.Czerwinski, *Journal of Power Sources*, **263**, (2014) 304–309

# DESIGNING NEW ELECTROLYTES FOR AMBIENT TEMPERATURE BATTERIES

*M. Dranka, J. Zachara, M. Marcinek, L. Niedzicki, M. Kalita, A. Bitner, G. P. Jankowski, Z. Żukowska, M. Poterala and W. Wiczorek*

Faculty of Chemistry, Warsaw University of Technology, ul. Noakowskiego 3, 00-664 Warszawa, Poland  
e-mail: wladek@ch.pw.edu.pl

Keywords: organic salts, batteries, polymeric electrolytes, ionic liquids

## ABSTRACT

Despite of the commercial success of lithium –ion batteries there is still need for energy storage systems with higher energy storage capacity longer cyclability and shorter charging time. To this end new positive and negative electrode materials are designed and studied in many university and industrial laboratories. Quite often these new electrodes do not work well with commercially available LiPF<sub>6</sub> based electrolytes. There is a need for the new systems which characterized by conductivities electrochemical stabilities and safety superior to currently commercially available electrolytes. Although most of the investigations are carried out on lithium electrolytes sodium analogues seems to be equally important. One of the ways to enhance properties of the studied electrolytes is to develop new salts having relatively large anions with delocalize charge which lead to the limitation in the formation of ionic associates and in turn to the improvement in the conductivity and cation transference numbers<sup>1-3</sup>. In the present work examples of newly developed lithium and sodium salts and their use in liquid as well as polymeric electrolytes based on low as well as high molecular weight systems will be presented.

The lecture will be illustrated by some examples of application of newly designed electrolytes in batteries with novel electrode materials (silicon anode) and discussion on possible extension of its use in novel post-lithium ion batteries assuming some unique properties of these electrolytes shown mainly on the bases of complementary electrochemical, X-ray and spectroscopic results<sup>4-5</sup>.

At the end formation of water hydrates in relation to possibility of application of these novel electrolytes in lithium-sulphur batteries will also be announced.

## REFERENCES

1. P. Johansson, S. Béranger, M. Armand, H. Nilsson, P. Jacobsson, **156** (2003) 129.
2. M. Dranka, L. Niedzicki, M. Kasprzyk, M. Marcinek, W. Wiczorek, J. Zachara, *Polyhedron* **51** (2013) 111.
3. L. Niedzicki, E. Karpierz, M. Zawadzki, M. Dranka, M. Kasprzyk, A. Zalewska, M. Marcinek, J. Zachara, U. Domanska, W. Wiczorek, *Phys. Chem. Chem. Phys.* **16** (2014) 11417.
4. P. Jankowski, M. Dranka, G. Z. Zukowska, and J. Zachara, *J. Phys. Chem. C* DOI: 10.1021/acs.jpcc.5b01352
5. P. Jankowski, M. Dranka and G. Z. Zukowska, *J. Phys. Chem. C* DOI: 10.1021/acs.jpcc.5b01826

# NANOSTRUCTURED HYBRID ELECTROCATALYTIC AND PHOTOVOLTAIC SYSTEMS FOR EFFICIENT ENERGY CONVERSION AND STORAGE

*Pawel J. Kulesza*

Faculty of Chemistry, University of Warsaw, Pasteura 1, PL-02-093 Warsaw, Poland.  
pkulesza@chem.uw.edu.pl

When it comes to electrocatalytic oxidations of importance to low temperature alcohol fuel cells, platinum nanoparticles are readily poisoned by the strongly adsorbed CO-type intermediate species requiring fairly high overpotentials for their removal. For example, to enhance activity of Pt-based catalysts toward the ethanol oxidation, additional metal or metal oxide nanostructures (rhodium, iridium, tin or molybdenum and tungsten oxides) will be intentionally introduced to the electrocatalytic interface. We are also going to demonstrate that catalytic activity of platinum-based nanoparticles can be significantly enhanced through their interfacial modification with ultra-thin monolayer-type films of mixed-metal-oxo-species of titanium, cerium, zirconium or molybdenum and tungsten in their simple and polyoxometallate forms. It is noteworthy that certain metal and mixed-metal oxides can generate –OH groups at low potentials: they induce oxidation of passivating CO adsorbates (e.g. on Pt) or breaking C-H bonds (e.g. during oxidation of methanol or dimethyl ether). When combined with dispersed Rh or Ir, immobilized in the organized manner in the vicinity Pt sites, they tend to weaken C-C bonds during ethanol oxidation.

Our research interests also concern development of electrocatalytic systems for reduction of carbon dioxide. For example, instead of conventional Pd nanoparticles, nano-sized Pd immobilized within tridentate Schiff-base ligands of the supramolecular complexes have been considered. Reduction of carbon dioxide begins now at less negative potentials and is accompanied by significant enhancement of the CO<sub>2</sub>-reduction current densities. Among important issues are specific interactions between nitrogen coordinating centers and metallic palladium sites at the electrocatalytic interface.

We will also show that nano-electrocatalytic systems are of importance to the development of the effectively operating iodine-based charge relays in dye sensitized solar cells and in molecular electronic (charge storage) devices. The ability of platinum to induce splitting of I-I bond in the iodine (triiodide) molecule is explored here to enhance electron transfers in iodine/iodide redox couple. Following incorporation of Pt nanoparticles, charge transport has been accelerated within the triiodide/iodide-containing 1,3-dialkylimidazolium room-temperature ionic liquid. When both Pt nanoparticles and multi-walled carbon nanotubes have been introduced to ionic liquid system, a solid-type (non-fluid) electrolyte has been obtained. The dye-sensitized solar cell with this electrolyte has yielded reasonably high power conversion efficiencies (up to 7.9% under standard reporting conditions).

Significant progress has recently been made in the development of n-type metal oxide semiconductors able to act as sunlight-driven photoanodes for oxygen generation (photoelectrochemical water splitting to oxygen and hydrogen). Among important issue for the semiconducting oxides characterized by indirect optical transition are the long absorption depths in visible part of the solar spectrum. We demonstrate here utility of gold nanoparticles (modified or stabilized with Keggin-type polyoxometallates, PMo<sub>12</sub>O<sub>40</sub><sup>3-</sup>, as capping agents) to enhance photocurrents generated by mesoporous tungsten trioxide, WO<sub>3</sub>, photoanodes irradiated with visible light in aqueous solutions. We also demonstrate generation of localized surface plasmons at the photoelectrocatalytic interface.



# ADVANCES IN SUPERCAPACITOR OPERATING IN AQUEOUS MEDIUM

*E. Frackowiak, J. Menzel, K. Fic.*

Institute of Chemistry and Technical Electrochemistry  
Poznan University of Technology, Sq. M. Skłodowskiej-Curie 5  
60-965 Poznan, Poland  
e-mail: elzbieta.frackowiak@put.poznan.pl

Keywords: supercapacitor, activated carbon, hybrid electrolyte

## INTRODUCTION

The electrochemical capacitors based on aqueous electrolytes start to be very attractive power sources. They present many benefits in comparison to capacitor operating with organic electrolytes even if the cell operating voltage is limited by the thermodynamic stability of water, i.e. 1.23V. Aqueous medium allows getting a higher charge propagation, better conductivity, construction out of glove box and low cost. However, they suffer from limited energy because of their lower operating voltage. The capacitance and voltage are the two main components of the formula of energy. The capacitance can be enhanced by applying nitrogen doped carbons, adding transition metal oxides and/or conducting polymers, hydrogen electrosorption etc.

The extension of capacitor voltage above the thermodynamic limit is another big challenge. Various methods will be presented for this target. Using redox active couples, it was possible to increase the capacitance values as well as to extend the operational voltage.

The application of neutral electrolytes and/or hybrid electrolytes is another interesting option to extend voltage. In this case, the specific energy of the system could be greatly improved.

## EXPERIMENTAL

Activated carbons from NORIT or Kuraray in the form of powder/tissue were used as electrode materials. Carbon tissue served as self-standing electrodes without using binder. All carbons were carefully characterized physico-chemically by nitrogen sorption, surface chemistry measurements. Most of experiments were performed in Swagelok system where electrodes have mass of 8-10 mg. Apart from detailed electrochemical characterization (cyclic voltammetry, galvanostatic cycling, impedance spectroscopy, floating), *in situ* Raman spectroscopy was used.

## RESULTS AND DISCUSSION

Most of electrochemical experiments were performed in neutral medium such as sulphates, nitrates, iodides of alkali metals. However, acidic ( $\text{H}_2\text{SO}_4$ ) and alkaline (KOH) solutions were used for comparison. Example of cyclic voltammograms in various electrolytes is shown in Fig. 1. Extension of operating voltage was possible in the case of neutral medium and constructing of capacitor where both electrodes are operating in different electrolyte [1].

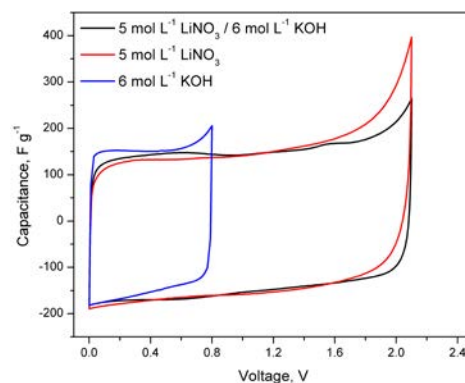


Fig. 1. Cyclic voltammograms ( $10 \text{ mV s}^{-1}$ ) for capacitors operating in different couples of electrolytes and single components

Combination of various electrolytes is especially beneficial to enhance energy of capacitor reaching almost values of organic medium (shown in Fig. 2 as Ragone plot).

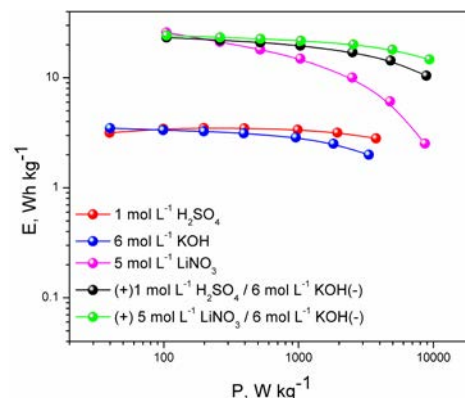


Fig. 1 Ragone plot for capacitor in pH combined electrolytes

## CONCLUSION

Capacitors operating in two well selected electrolytes of various pH is a next challenge to replace organic medium by more eco-friendly aqueous electrolytic solutions.

## ACKNOWLEDGMENT

Financial support by Swiss Contribution within the Polish Swiss Research Programme, Project PSPB 107/2010 INGEC is greatly acknowledged.

## REFERENCE

1. K. Fic, M. Meller, E. Frackowiak, *Journal of the Electrochemical Society* **162** (2015) A5140-5147.

# MONITORING OF A NEW GENERATION OF HIGH PRESSURE VESSELS FOR HYDROGEN STORAGE

*P. Gąsior, J. Kaleta, R. Rybczyński, F. Nony\* and S. Villalonga\**

Wrocław University of Technology, Wyb. Wyspiańskiego 27, 51-206 Wrocław, Poland

\*CEA, Commissariat à l'Énergie Atomique et aux Energies Alternatives, BP16 Monts, France

e-mail: pawel.gasior@pwr.edu.pl

Keywords: hydrogen storage, pressure vessels, SHM, optical fiber sensors

## INTRODUCTION

Composite overwrapped pressure vessels (COPV) for high-pressure gas fuels (CH<sub>2</sub>, CNG) storage, in order to increase safety of their usage, requires inspections of their technical condition. One of the methods for supporting preservation of technical objects from breakdowns is application of modern diagnostic tools (including measurement systems) that allow increase of reliability and safety of those objects during their operations.

The aim of this work is a development of Structural Health Monitoring (SHM) system for integrity monitoring of a high-pressure composite vessel, designated for storing pressurised hydrogen at 700 bar of nominal working pressure. It is expected that the SHM system should provide continuous and reliable monitoring of the structure during its manufacturing, proof testing and long operation and enable estimation of degradation level of the composite vessel load-carrying layer, and by that determination of its safe operation period.

## MONITORING OF HIGH PRESSURE VESSELS

Monitoring of COPV technical state is based on application of complex system to detect, localize, identify and predict development of a damage that can cause malfunction of the object now or in the future. This system performs constant measurement of various physical values (most often displacement, temperature) what allows determination of other parameters (for example distribution of stress/strain and temperature field, creep, initiation and propagation of delamination and fractures, detection and localization of leaks, etc.). It supports inspection of technical condition of COPVs and can increase safety of their use.

The SHM system is made of: sensors (eg. strain, temperature, pressure, gas detectors, etc.), data transmission systems (passive) as well as reading, computation and indication units. Sensors must be integrated with monitored object during its production or assembling. On-board availability of reading units depends on monitoring strategy which is developed for vessel monitoring.

## CRITICAL PHASES OF COPV LIFETIME

The most critical phases during COPV lifetime are:

- **Manufacturing:** non-visible defects during winding and curing process, technological errors, etc.
- **Refuelling:** temperature shock (-40 ÷ 85°C), overpressure, etc.

- **Accident:** impact loading (non-visible defects).
- **Handling:** installation, recertification/reinstallation.
- **Daily use:** degradation of composite material, unauthorized/authorized service operation, exceeding of temperature limits, etc.

## MONITORING STRATEGY

Strategy for monitoring of COPV may vary depending on the parameters that have to be controlled. Therefore following can be distinguished:

- **continuous or periodical monitoring** (at each refueling, during servicing, etc.),
- **hydrogen leak detection** (by hydrogen gas detectors),
- **damage evolution** (only in constant monitoring),
- **state or event approach** (strain, temperature, pressure or acoustic emission).

Application of SHM systems in form of so called “on-board monitoring systems” that are systems permanently integrated with an object and allow constant measurement of critical structure parameters. Nevertheless it is possible to use it periodically for example by diagnostic stations during periodical servicing (periodic inspection and admissibility of vessel operations). Advantage of solution based on continuous monitoring is possibility of early detection of defects critical for construction and constant monitoring of them. In case of periodical servicing, analysis of registered changes of parameters is possible (i.e. deformation field) only in specific periods of time. Sensors will register history of loading (sum from the last measurement) and during servicing their verification will be possible (i.e. comparative analysis of the signals recorded earlier). Periodical measurements significantly reduce number of registered data. However, at the same time critical information, that have crucial importance for vessels operation safety, can be lost.

## CONCLUSIONS

The most recommended solution for COPV monitoring is based on continuous measurements of parameters like: strain, temperature, hydrogen pressure and leaks, both during manufacturing process as well as normal operation and their analysis by on-board system. This approach is under development by COPERNIC project.

## ACKNOWLEDGMENT

This work is supported by FCH JU: COst & PERformaNces Improvement for Cgh2 composite tanks, Grant Agreement no.: 325330.

# UNIVERSAL FEATURES OF CONDUCTIVITY SPECTRA IN SUPERPROTONIC $(\text{NH}_4)_3\text{H}(\text{SO}_4)_2$ SINGLE CRYSTALS

Cz. Pawlaczyk, P. Ławniczak and A. Pawłowski

Institute of Molecular Physics, Polish Academy of Sciences, Smoluchowskiego 17, 60-179 Poznań

e-mail: czpawl@ifmpan.poznan.pl

Keywords: proton conductors, fuel cells, universal response

## INTRODUCTION

Frequency dependencies of conductivity  $\sigma'(\omega)$ , [ $\sigma^*(\omega) = \sigma'(\omega) - \sigma''(\omega)$ ,  $\sigma$  – conductivity,  $\omega$  – angular frequency of external electric field] of the most common disordered ion conductors show an universal frequency response, the so-called first and second universalities [1]. The first universality is a characteristic frequency dependence of the real part of electric conductivity. Using a proper scaling method, it is possible to rescale such dependencies measured for various temperatures to a single curve, called the master curve. The first universality refers to the thermally activated hopping mechanism of ionic migration through solid state in microscopic scale. The second universality is the effect which occurs in materials at sufficiently low temperatures or in a range of high frequencies, where translational movements of ions through solid state do not contribute to dielectric loss. Because of this, the second universality is often called Nearly Constant Loss (NCL) effect. The universal response was found to hold despite significant differences in structures and type of ionic charge carriers.

Recently [2,3] we have shown that similar universal conductivity response display also crystalline, hydrogen bonded proton conductors regardless of fact that the microscopic mechanism of proton migration through the network of hydrogen bonds is quite different from the hopping of the “normal” (not protons) ions.

This contribution aims to prove that similar universal conductivity response holds for crystalline proton conductors which undergo a phase transition from low (at lower temperatures) to high conductivity phase (at higher temperatures). The mechanism and dynamics of proton migration through the lattice changes significantly at the transition temperature  $T_s$  and our scientific objective is to find how it influences the conductivity frequency response.

## EXPERIMENTAL AND EXAMPLES OF RESULTS

As an example we show here some results of conductivity measurements for single crystalline  $(\text{NH}_4)_3\text{H}(\text{SO}_4)_2$  (AHS), which undergoes superprotonic phase transition at 413 K. The measurements were made using A.C. impedance spectroscopy (Broadband Dielectric Spectrometer, Novocontrol GmbH) in the frequency range 0.1Hz – 3GHz along the  $c^*$  direction ( $\perp$  (001) plane). Fig. 1 shows the temperature dependence of DC conductivity (Arrhenius plot) and Nyquist plots for three selected temperatures from different ranges. In Fig. 2 the master curve for the superionic phase is presented. Worth noting is a very good consistency of the results obtained in two frequency ranges (below and above 1 MHz), using two different sample cells.

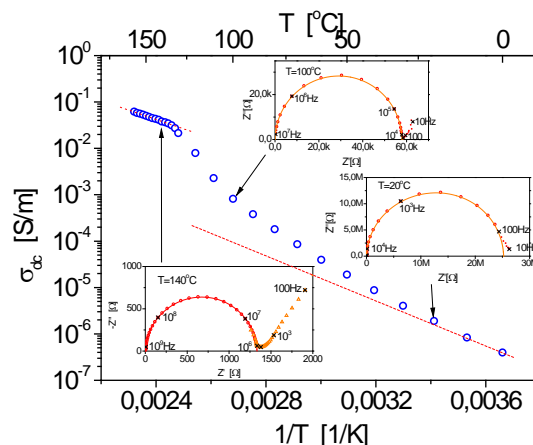


Fig. 1 Arrhenius plot and examples of Nyquist plots in various phases of AHS

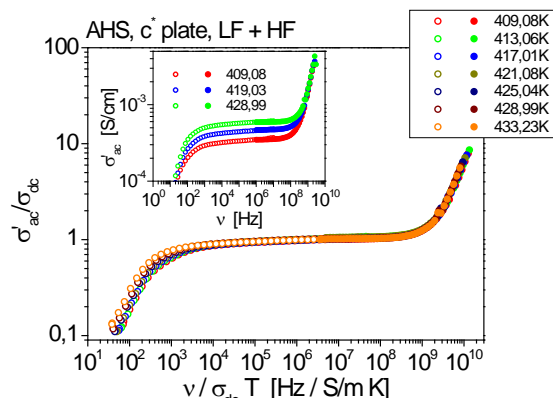


Fig. 2 Master curve and frequency dependencies of the real part of conductivity for a AHS sample in superionic phase (open points  $\nu < 1\text{MHz}$ , full points  $\nu > 1\text{MHz}$ )

## CONCLUSION

Conductivity spectra of  $(\text{NH}_4)_3\text{H}(\text{SO}_4)_2$  show in the superprotonic phase the same universal features as common disordered solid state ionic conductors.

## ACKNOWLEDGMENT

This work is supported by National Science Centre under grant No. 2014/15/D/ST3/03433.

## REFERENCES

1. K. Funke, R.D. Banhatti, D.M. Laughman, L.G. Badr, M. Mutke, A. Šantič, W. Wrobel, E. M. Fellberg and C. Biermann, *Z. Phys. Chem.* **224** (2010) 1891–1950
2. P. Ławniczak, M. Zdanowska-Frączek, Z.J. Frączek, K. Pogorzelec-Glaser, Cz. Pawlaczyk, *Solid State Ionics* **225** (2012) 268–271
3. Cz. Pawlaczyk, P. Ławniczak, M. Zdanowska-Frączek, *Biuletyn Polskiego Stowarzyszenia Wodoru i Ogniw Paliwowych* **No 7** (2013) 45



# YOUNG SCIENTISTS FORUM





# SEMICONDUCTOR-BASED NANOCOMPOSITES FOR PHOTOCATALYSIS

*A. Trenczek-Zajac, A. Kusior, and M. Radecka*

Faculty of Materials Science and Ceramics  
AGH University of Science and Technology, al. A. Mickiewicza 30  
30-059 Krakow, Poland  
e-mail: anita.trenczek-zajac@agh.edu.pl

Keywords: TiO<sub>2</sub>, CdS, nanoparticles, hydrogen generation

## INTRODUCTION

The main advantage of the narrow-band gap semiconductors such as CdS, CdSe, Ag<sub>2</sub>S or InSb, is their ability to absorb light from the visible range. Among them, cadmium sulfide draws a lot of attention, mainly when coupled with TiO<sub>2</sub>. Such a heterojunction composed of nanomaterials (2D, 1D, 0D) can be successfully applied in photocatalytic reactions, for example in the photoelectrochemical production of hydrogen [1,2]. The interesting feature of the nanomaterials is that their properties are determined not only by their chemical composition but also by morphology, surface properties and electronic structure.

The easiest and best repeatable way of CdS nanopowders preparation in the case of CdS is the precipitation method (solubility product is  $\sim 10^{-28}$ ). Thus, it was chosen as a starting point. The aim of the present study was to investigate the effect of preparation parameters of CdS on broadly-taken physico-chemical properties.

## EXPERIMENTAL

*Precipitation of CdS nanopowders.* Nanoparticles of CdS were prepared with the use of precipitation method by mixing Cd(NO<sub>3</sub>)<sub>2</sub> and Na<sub>2</sub>S water- or methanol-based solutions to obtain orange or yellowish precipitate.

*TiO<sub>2</sub> flower-like nanostructures preparation.* TiO<sub>2</sub> flower-like nanostructures (TiO<sub>2</sub>-NF) were prepared from Ti foils according to the procedure described in our previous work [2]. After preparatory procedure, Ti foil was immersed in 30% H<sub>2</sub>O<sub>2</sub> at elevated temperature for 15, 45 and 120 min and afterwards, rinsed, dried, and annealed in an Ar atmosphere at 450°C.

*Deposition of CdS.* TiO<sub>2</sub>-NF, Ti foils and TiO<sub>2</sub>-P25 were covered with CdS nanoparticles with the use of the successive ionic layer adsorption and reaction (SILAR) procedure using water- (*w-CdS*) and methanol-based solutions (*m-CdS*) as precursors (Cd(NO<sub>3</sub>)<sub>2</sub>, Na<sub>2</sub>S) and precipitation method.

*Measuring techniques.* In order to perform characterisation of nanopowders and nanoparticles deposited on Ti and TiO<sub>2</sub>-NF, the measurement techniques were used as follow: SEM, TEM, XRD, spectrophotometry and current-voltage measurements in the photoelectrochemical cell (PEC).

## RESULTS AND DISCUSSION

Based on the TEM analysis it was found that CdS nanopowders with the particles size  $\sim 4$  nm are partially agglomerated. XRD measurements revealed that *w-CdS* nanoparticles crystallize probably in the cubic structure

and *m-CdS* in hexagonal one, however, due to the large peak width at half-height a mixture of two phases cannot be excluded (Fig.1).

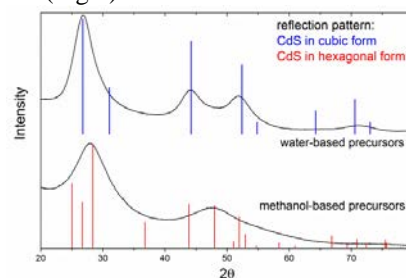


Figure 1. Diffraction pattern of CdS nanopowders prepared from water- and methanol-based solutions.

TiO<sub>2</sub>-NF were found to be a mixture of tetragonal phases of anatase and rutile wherein the ratio changes along with the H<sub>2</sub>O<sub>2</sub>-oxidation time. Measurements of I-V characteristics with/without white-light illumination revealed a significant incensement in the photocurrent for CdS-TiO<sub>2</sub>-NF in comparison to the TiO<sub>2</sub>-NF (Fig.2).

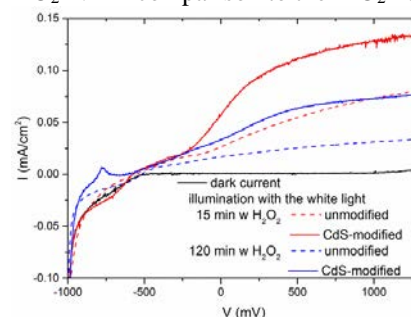


Figure 2. Current-voltage characteristics for TiO<sub>2</sub>-NF unmodified and CdS-modified.

## CONCLUSIONS

Based on the different ways of preparation of CdS nanoparticles and deposition on different substrates it was found that the physico-chemical properties are determined not only by the chemical composition of the material but also by varieties of attributes such as shapes and forms of the same substance.

## ACKNOWLEDGMENT

This project was financed by The National Science Centre (NCN), Poland based on the decision number DEC-2011/01/D/ST5/05859.

## REFERENCES

1. Y. Ma, X. Wang, Y. Jia, X. Chen, H. Han, C. Li, *Chem.Rev* **114**(2014)9987-10043
2. A. Trenczek-Zajac, A. Kusior, A. Lacz, M. Radecka, K. Zakrzewska, *Mat.Res.Bulletin* **60**(2014)28-37

# DEGRADATION MECHANISM OF $\text{Li}_2\text{MnSiO}_4$ IN LI-ION BATTERIES

M. Świątosławski<sup>1,\*</sup>, M. Molenda<sup>1</sup>, M. Gajewska<sup>2</sup>, R. Dziembaj<sup>1</sup>

<sup>1</sup>Jagiellonian University, Faculty of Chemistry, Ingardena 3, 30-060 Krakow, Poland

<sup>2</sup>AGH University of Science and Technology, Academic Centre for Materials and Nanotechnology, Mickiewicza 30, 30-059 Krakow, Poland

\*e-mail: m.swietoslowski@uj.edu.pl

Keywords: Li-Ion batteries, cathode materials,  $\text{Li}_2\text{MnSiO}_4$ , degradation mechanism, structural stability

## INTRODUCTION

$\text{Li}_2\text{MnSiO}_4$  is one of the most promising among all of polyanionic cathode materials for li-ion batteries [1–8]. Thanks to its unique composition the material is characterized by high theoretical capacity (333 mAh  $\text{g}^{-1}$ ) and potentially low production costs. On the other hand, the main disadvantage of  $\text{Li}_2\text{MnSiO}_4$  is its extremely low electrical conductivity [4]. According to Dominko et al. an electronic part of  $\text{Li}_2\text{MnSiO}_4$  conductivity is responsible for its poor electrochemistry [5]. The preparation of nanograined material and its modification by carbon coating is in this case essential to provide good electrochemical properties [1,4]. Another drawback of this material is its structural instability in charge/discharge process. There is a number of reports showing that  $\text{Li}_2\text{MnSiO}_4$  cathode material undergoes amorphization in the first few charging/discharging cycles [3,6]. The degradation of crystalline structure can be explained by Jahn–Teller distortion associated with changes in lattice parameters during  $\text{Mn}^{3+} \rightarrow \text{Mn}^{4+}$  transition [7]. Another explanation may be the occurrence of secondary reactions between electrolyte and delithated forms of lithium manganese silicate ( $\text{LiMnSiO}_4$  and  $\text{MnSiO}_4$ ). The aforementioned structural changes of the material entail variations in electrochemical properties of  $\text{Li}_2\text{MnSiO}_4$  [8].

The goal of this studies is to examine structural changes of  $\text{Li}_2\text{MnSiO}_4$  and  $\text{C}/\text{Li}_2\text{MnSiO}_4$  which occurs in first electrochemical charging/discharging cycle.

## EXPERIMENTAL

The  $\text{Li}_2\text{MnSiO}_4$  and  $\text{C}/\text{Li}_2\text{MnSiO}_4$  materials were prepared via Pechini's sol–gel reaction. Detailed description of synthesis procedure and structural characterization of the material can be found in our previous work [8–10]. Obtained materials were studied using in-situ XRD, TEM, SEM, AAS/AES, TGA, EIS, IS, CV techniques.

## RESULTS AND DISCUSSION

To determine degradation mechanism of  $\text{Li}_2\text{MnSiO}_4$  and  $\text{C}/\text{Li}_2\text{MnSiO}_4$  in working Li-ion cell two different aspects of LMS performance were analyzed. First was corrosive properties of liquid electrolytes. Solubility of manganese from LMS and  $\text{C}/\text{LMS}$  samples (occurring during electrochemical reaction) in  $\text{LiPF}_6$  solution in EC:DMC (1:1) was studied. On the other hand using in-situ XRD and TEM analysis in different SOC (in initial cycle in 1.5–4.8V potential range) the

process of amorphization of crystalline LMS was examined.

## REFERENCES

1. M.E. Arroyo-de Dompablo, M. Armand, J.M. Tarascon, U. Amator, *Electrochem. Commun.* 8 (2006) 1292–1298.
2. A. Nyten, A. Abouimrane, M. Armand, T. Gustafsson, J.O. Thomas, *Electrochem. Commun.* 7 (2005) 156–160.
3. Z.L. Gong, Y.X. Li, Y. Yang, *J. Power Sources* 174 (2007) 524–527.
4. A. Kokalj, R. Dominko, G. Mali, A. Meden, M. Gaberscek, J. Jamnik, *Chem. Mater.* 19 (2007) 3633–3640.
5. R. Dominko, M. Bele, M. Gaberscek, A. Meden, M. Remskar, J. Jamnik, *Electrochem. Commun.* 8 (2006) 217–222.
6. R. Dominko, M. Bele, A. Kokalj, M. Gaberscek, J. Jamnik, *J. Power Sources* 174 (2007) 457–461.
7. Y.-X. Li, Z.-L. Gong, Y. Yang, *J. Power Sources* 174 (2007) 528–532.
8. M. Świątosławski, M. Molenda, M. Grabowska, A. Wach, P. Kuśtrowski, R. Dziembaj, *Solid State Ionics* 263 (2014) 99–102.
9. M. Molenda, M. Świątosławski, A. Rafalska-Łasocha, R. Dziembaj, *Funct. Mater. Lett.* 4 (2011) 135–138.
10. M. Świątosławski, M. Molenda, K. Furczoń, R. Dziembaj, *J. Power Sources* 244 (2013) 510–514.

# MULTI-COMPONENT THERMOELECTRIC MATERIALS FABRICATED BY NOVEL METHOD OF REDUCTION OF OXIDE PRECURSORS

*B.Bochentyn, J.Karczewski, T.Miruszewski and B.Kusz*

Faculty of Electronics, Telecommunications and Informatics, Gdansk University of Technology, 80-233 Gdansk, ul. Narutowicza 11/12, Poland  
e-mail: bbochentyn@mif.pg.gda.pl

Keywords: thermoelectric, reduction, alloy, figure of merit

## INTRODUCTION

The figure of merit, determining their thermoelectric usage, strongly depends on temperature. The most popular thermoelectric materials at near-room temperature are BiTe-based compounds. Recently BiTe and BiSb materials experience a big revival due to unique properties of their surface electron states (topological insulators) [1-3]. Various scientific groups have reported that making a solid solution of Bi<sub>2</sub>Te<sub>3</sub> and isomorphous compounds such as Sb<sub>2</sub>Te<sub>3</sub>, PbTe or GeTe [4-6] leads to the controlled increase of carrier concentration and to the reduction of lattice thermal conductivity. Thermoelectric properties can be also controlled by suitable structural modifications. In order to reduce the lattice component of thermal conductivity, such modifications as nanostructuring, forming thin films or forming multilayer systems may be performed. However, these modifications also lead to a decrease of carrier mobility. One of the solutions can be a fabrication of composite material consisting of grains with different size, but an optimal ratio between fine and coarse grains should be maintained.

Basing on the literature reports and authors experience in the field of glasses an innovative method of thermoelectric material fabrication was suggested. Starting from oxide powders, melting at high temperature in air, quenching and reducing in hydrogen should lead to a formation of complex structure. Depending on the initial composition of reagents various products can be obtained. Moreover, the temperature of reduction will influence the final composition and structure of fabricated sample. The final product should present both structural and thermoelectrical properties sufficient for thermoelectric applications. For example, it seems to be possible to fabricate a layered structure with a controlled composition and thickness of every layer.

The aim of this work is to present a novel method of thermoelectric materials fabrication. Its potential and limitations will be considered with regard to the results obtained for Bi-Te, Bi-Sb-Te and Te-Ag-Ge-Sb (TAGS) alloys fabricated with this method.

## EXPERIMENTAL

Oxide samples of various compositions have been produced from appropriate reagent grade oxides. First, the reagents were pulverised in an agate mortar and melted in a ceramic crucible at 1000°C in air for 2 hours. Pouring them on a stainless steel plate quenched the melts. As a result, bulk samples of complex structure have been obtained. In the next step the samples were

ground in an agate mortar to obtain a powder. Then the powders were reduced at temperature above 340 °C in H<sub>2</sub> for at least 10 hours. After that it was put to the cylindrical matrix and shortly pressed uniaxially in a hydraulic press under elevated temperature (180°C) in a hydrogen atmosphere. In consequence, bulk cylindrical pellets (h≈5mm; Ø≈5mm) of a metallic colour have been obtained.

The X-Ray Diffraction method (XRD) and Scanning Electron Microscopy (SEM) have been used to analyze the morphology of fabricated samples. The electrical conductivity ( $\sigma$ ) using the four terminal DC method and Seebeck coefficient ( $\alpha$ ) of cylindrical samples were measured over temperature range from -196 to +127 °C in argon atmosphere. The values of Seebeck coefficient were calculated in reference to Pt. The total thermal conductivity was determined at 35 °C on the basis of the analysis of heat transfer between two copper blocks in vacuum conditions.

## CONCLUSIONS

The novel method of thermoelectric materials fabrication will be presented. Our investigations have shown that starting from oxide compounds, it is possible to fabricate multi-component materials, which are very promising for thermoelectric applications, such as Bi-Te, Bi-Sb-Te or Te-Ag-Ge-Sb (TAGS) alloys. The stoichiometry and structure of a final product can be controlled by methods described in this article. The suggested methodology is easy and enables to control a material structure.

## ACKNOWLEDGMENT

This work was supported by the National Science Center under the grant No. NCN 2012/05/B/ST3/02816.

## REFERENCES

1. H. Zhang, C.-X. Liu, X.-L. Qi, X. Dai, Z. Fang, S.-C. Zhang, *Nat. Phys.* 5 (2009) 438–442. doi:10.1038/nphys1270.
2. D. Hsieh, D. Qian, L. Wray, Y. Xia, Y.S. Hor, R.J. Cava, et al., *Nature.* 452 (2008) 970–4. doi:10.1038/nature06843.
3. D. Hsieh, Y. Xia, D. Qian, L. Wray, F. Meier, J.H. Dil, et al., *Phys. Rev. Lett.* 103 (2009) 146401. http://www.ncbi.nlm.nih.gov/pubmed/19905585.
4. G.J. Snyder, E.S. Toberer, *Nat. Mater.* 7 (2008) 105–114. doi:10.1038/nmat2090.
5. J.-C. Zheng, *Front. Phys. China.* 3 (2011) 12. doi:10.1007/s11467-008-0028-9.
6. C. Wood, *Reports Prog. Phys.* 51 (1988) 459–539. doi:10.1088/0034-4885/51/4/001.

# TRANSFERENCE NUMBER MEASUREMENTS IN BIMEVOXES

*M. Malys<sup>1</sup>, A. Kruk<sup>1</sup>, M. Wójcik<sup>1</sup>, W. Wróbel<sup>1</sup>, J.R.Dygas<sup>1</sup>, I.Abrahams<sup>2</sup> and F. Krok<sup>1</sup>*

<sup>1</sup> Faculty of Physics, Warsaw University of Technology, Warsaw, Poland.

<sup>2</sup> Centre for Materials Research, School of Biological and Chemical Sciences, Queen Mary, University of London, UK  
e-mail: malys@mech.pw.edu.pl

Keywords: transference number, solid electrolyte galvanic cell, bismuth oxides, BIMEVOX

## INTRODUCTION

Presence of electronic conductivity affects applicability of ionic conductors as solid electrolytes for fuel cells, potentiometric oxygen sensors, electrolytes or oxygen pumps and other electrochemical applications. Therefore determination of transference numbers of materials of potential applicability is one of the most important research tasks.

The BIMEVOXes are solid solutions based on substitution of V and/or Bi of other metals in the parent compound,  $\text{Bi}_4\text{V}_2\text{O}_{11-\delta}$ . High oxide ion conductivity at relatively low temperatures in the BIMEVOX family of solid electrolytes has made it of great interest and they are considered as the best oxide ion conductors in intermediate temperature range below 600°C.

Relation between ionic and electronic conductivity of BIMEVOXes are rather rarely discussed in literature [1, 2]. High temperature tetragonal  $\gamma$  phase is considered as mostly ionic conductor, while orthorhombic  $\alpha$  and  $\beta$  phases are expected to have noticeable electronic contribution of total conductivity.

One of the methods commonly used to determine transference numbers in ionic conductors is the EMF method, which gives oxygen ion transference number directly by comparing experimentally measured voltage in a concentration cell to the theoretical Nernst potential of the cell. However, applying this method directly to  $\text{Bi}_2\text{O}_3$ -based materials is difficult due to the existence of significant polarization resistance at the electrode-electrolyte interface. Recently developed approach, based on a modified EMF method under external load resistance conditions [3] or external voltage source [4], enable accuracy improvement in the determination of electronic contributions to the total conductivity.

The aim of the present work was to apply this method to investigate ionic and electronic transport properties of selected BIMEVOXes (ME = Cu, Cr, Nb, Ta, Mn). The experimental conditions were examined and discussed to evaluate validity of this method in comparison to theoretical aspects and problems presented in articles [4-5].

## EXPERIMENTAL

The transference numbers of the gas tight ceramics were measured using the concentration cell:  $\text{O}_2(\text{pO}_2 = 1.01 \times 10^5 \text{ Pa}); \text{Pt}|\text{Oxide}|\text{Pt}; \text{O}_2(\text{pO}_2 = 0,21 \times 10^5 \text{ Pa})$  by EMF method with external voltage source simulating the effect of enhanced electronic conductivity in range of 450°C-800°C. The total conductivity of the sample was examined by a.c. impedance spectroscopy. In both

cases (EMF method and a.c. impedance spectroscopy) four probe electrical setup was applied.

## RESULTS AND DISCUSSION

Ionic conductivity dominates in studied temperature range for all investigated materials. Example is shown in fig. 1 for parent material  $\text{Bi}_4\text{V}_2\text{O}_{11-\delta}$ . Electronic conductivity exhibits higher activation energy than in case of ionic contribution, therefore transference number decreases slightly as temperature increases. Oxygen transfer kinetics from gas phase to electrolyte on surface with platinum electrodes is relatively slow below 500°C. The measurements confirmed, that orthorhombic phases of BIMEVOXes have slightly lower ion transference numbers. Presented results confirm high ionic transference numbers for BIMEVOXes and their potential applicability as electrolytes in electrochemical applications.

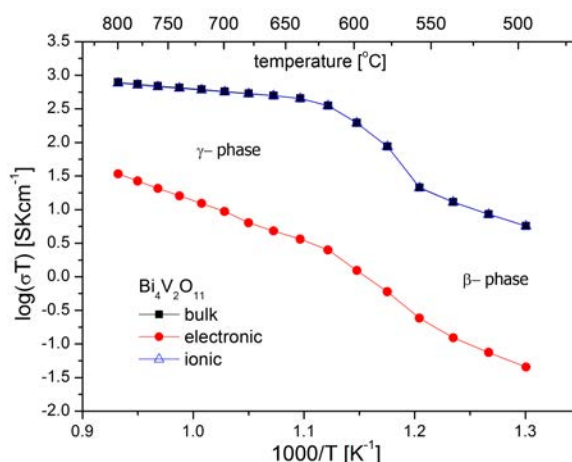


Fig. 1. Ionic and electronic conductivity of  $\text{Bi}_4\text{V}_2\text{O}_{11}$

## ACKNOWLEDGMENT

This work is supported by the National Science Centre, Poland under project grant number 2012/05/E/ST3/02767

## REFERENCES

- [1] A.A. Yaremchenko, V.V. Kharton, E.N. Naumovich, V. V. Samokhval, *Solid State Ionics* **111** (1998) 227.
- [2] A.A. Yaremchenko, V. V. Kharton, E.N. Naumovich, F.M.B. Marques, *J. Electroceramics* **4:1** (2000) 233.
- [3] V.V. Kharton, F.M.B. Marques *Solid State Ionics* **140** (2001) 381.
- [4] M. Malys, J.R. Dygas, M. Holdynski, A. Borowska-Centkowska, W. Wrobel, M. Marzantowicz, *Solid State Ionics* **225** (2012) 493.
- [5] J.R. Frade, V.V. Kharton, A.A. Yaremchenko, E.V. Tsipis, *J. Solid State Electrochem.* **10** (2006) 96.
- [6] I. Riess, *J. Phys. Chem.Solids* **47** (1986) 129.



# IONIC ASSOCIATIONS IN GLYME BASED ELECTROLYTES DOPED WITH SALTS BEARING HETEROAROMATIC ANION. IONIC AGGREGATION MODES IN SOLUTION AND PEO MATRIX

G. Z. Żukowska, M. Dranka, P. Jankowski, W. Wieczorek

Politechnika Warszawska, Wydział Chemiczny

00-664 Warszawa

Poland

e-mail: zosia@ch.pw.edu.pl

Keywords: electrolytes, crystal structures, Raman spectroscopy, Hückel anions, aggregation, lithium salts.

## INTRODUCTION

Lithium salts with so-called Hückel anions gained significant interest since the first attempt of their application in electrolytes dedicated to lithium batteries. Anions with the charge delocalized onto the whole structure offer possibility to obtain highly conducting systems in a wide salt concentration range. In particular properties of lithium and sodium 2-trifluoro-4,5-dicyanoimidazolates (TDI) doped electrolytes attracted major attention and have been intensively studied. Several others, such as tricyanodiazolates, tricyanoimidazolates and tetracyanopyrrolates have also been obtained.

Knowledge of anion- cation interactions, cation solvation and the structure of the electrolyte is necessary for effective development of materials for energy conversion and storage. This can be achieved with the use of theoretical modeling, crystal structure analysis or spectroscopy data. Particularly fruitful is combining of these methods, which brought in the last recent years a significant progress in the understanding of electrolyte systems. Comparing the XRD structures with Raman spectra we have identified spectral fingerprints of various structural motifs such as ionic pairs, dimers, "free ions" and higher aggregates. The coordination modes existing in the crystalline solvates repeat in the amorphous and liquid systems, serving as a tool to study the conductivity behavior. The comprehensive analysis of crystalline materials via XRD and spectroscopy studies reveal the coordination preferences of the studied anions and provide the basis for further developing a model for polymer and liquid electrolytes.

## CONCLUSIONS

The comprehensive analysis of Raman data performed for a series of crystalline solvates provided the basis for the correlation of spectral patterns with various types of structural motifs. On the basis of the results obtained we postulate a dissociation mechanism in the cyano substituted imidazolate and pyrrolate salts-oligoethers systems.

## REFERENCES

1. P. Jankowski, M. Dranka, G. Z. Żukowska, and J. Zachara, *J. Phys. Chem. C* DOI: 10.1021/acs.jpcc.5b01352
2. P. Jankowski, M. Dranka and G. Z. Żukowska, *J. Phys. Chem. C* DOI: 10.1021/acs.jpcc.5b01826

# FACTORS AFFECTING SIZE AND LOCATION OF SOLID ELECTROLYTE'S ELECTROCHEMICAL WINDOW. A CASE OF INORGANIC SOLID LITHIUM CONDUCTORS

*W. Zając, T. Polczyk*

Faculty of Energy and Fuels  
AGH University of Science and Technology, Al Mickiewicza 30  
30-059 Kraków, Poland  
e-mail: wojciech.zajac@agh.edu.pl

Keywords: all-solid state lithium batteries, solid electrolyte, electrochemical stability, reduction potential

## INTRODUCTION

State-of-the-art Li-ion batteries, despite their huge commercial success, suffer from lack of safety and not sufficient energy density. This results in either bulky and heavy or low capacity batteries. Safety issues arise from inflammability of standard liquid, non-aqueous electrolytes, whereas energy density is limited by voltage and charge accumulated in a battery. To overcome these limitations one may substitute liquid electrolyte with inorganic solid membrane exhibiting sufficient mobility of ions and lack of electronic conductivity [1]. Among various amorphous and crystalline materials titanium-based oxides show remarkably high ionic conductivity [2], albeit they are vulnerable to reduction, i.e. possesses relatively low upper edge of electrochemical window. It was demonstrated by Padhi et al. [3] that inductive effect can strongly affected location of redox couples therefore in this work we search for appropriate substituents to alter and tune position of  $Ti^{4+}/Ti^{3+}$  redox potential.

In this work we present comparative study of two kinds of promising lithium solid electrolytes. The first one is  $La_{2/3-x}Li_{3x}TiO_3$  (LLTO) perovskite and the second one is  $LiTi_2(PO_4)_3$  (LTP) nasicon. For comparison  $Li_7La_3Zr_2O_{12}$  garnet (LLZO) and  $Li_4Ti_5O_{12}$  spinel (LTO) were included. In order to examine the effect of chemical composition on location of redox potential the following series are studied:  $La_{2/3-x}Li_{3x}TiO_3$  ( $x=0.02, 0.05, 0.08, 0.11, 0.14, 0.167$ ) and  $Li_{1-y}Ti_{1.7}Me_{0.3}(PO_4)_3$  ( $Me=Al, Ga, In, Ti, Zr, Ge, Nb$ ).

## EXPERIMENTAL

Solid electrolyte samples were synthesized using conventional high-temperature solid-state reaction method. Crystal structure was confirmed using X-ray diffraction method. Ionic conductivity was measured using impedance spectroscopy technique. Cyclic voltammetry (CV) was applied to evaluate location of electrochemical window. CV scans were recorded on  $Li|Li^+|(WE)$  cells, where "Li<sup>+</sup>" denotes 1 M solution of  $LiPF_6$  in EC/DEC (1:1 vol.), "WE" denotes composite of solid electrolyte material (82 wt.%), carbon black (12 wt.%) and PVDF (6 wt.%).

## RESULTS AND DISCUSSION

Fig. 1 shows comparison of typical voltammetric profiles for the LLTO, LTP, LLZO and LTO in a 1 – 4 V range vs.  $Li^+/Li$ . During cathodic sweep clear current peak associated with reduction  $Ti^{4+} + e^- \rightarrow Ti^{3+}$  was observed defining edge of electrochemical window. For

the LTP phosphate maximum cathodic current was observed for 2.37 V vs.  $Li^+/Li$ . In the case of oxides reduction took place at 1.50 V (LTO) and at 1.48 and 1.14 V (LLTO). Upon reverse sweep all the peaks had their counterparts indicating reversibility of the redox processes. At the same conditions no redox process was observed for LLZO pointing to its high electrochemical stability due to lack of reducible ions. Present study points to possibility of further tuning location of this potential by variation of lithium content of LLTO structure and by partial substitution of titanium in LTP.

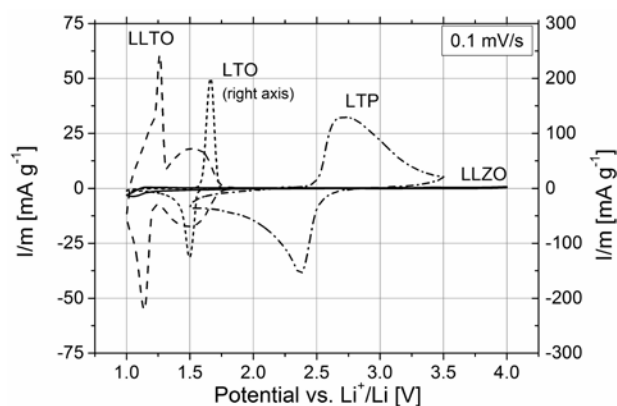


Fig. 1. Cyclic voltammograms measured for  $Li|Li^+|(tested\ sample)$  cell. Scan rate 0.1 mV/s.

## CONCLUSIONS

Cyclic voltammetry technique was successfully applied to evaluate electrochemical stability of lithium conducting inorganic solid electrolytes. Among the studied compositions only LLZO garnet proved to be stable in the studied potential range. Careful selection of anode materials has to be made for LLTO and LTP, in order to fit into their electrochemical window.

## ACKNOWLEDGMENT

This work was supported by National Science Centre Poland under grant 18.18.210.253. Comparative  $Li_4Ti_5O_{12}$  studies were carried out with support from Polish Ministry of Science and Higher Education under AGH project no. 11.11.210.911.

## REFERENCES

1. J.B. Goodenough., Y. Kim, *Chem. Mater.* **22**(2010) 587.
2. P. Knauth, *Solid State Ionics* **180**(2009)911.
3. A.K. Padhi, V. Manivannan, J.B. Goodenough, *J. Electrochem. Soc.* **145**(1998) 1518.

# AB INITIO STUDIES ON TYPE-II $\text{Bi}_3\text{NbO}_7$

*M. Krynski, W. Wrobel, J. Dygas, I. Abrahams\* and P. Spiewak\*\* and F. Krok*

Faculty of Physics, Warsaw University of Technology,  
ul. Koszykowa 75, 00-662 Warszawa, Poland

\* Centre for Materials Research, School of Biological and Chemical Sciences,  
Queen Mary University of London, Mile End Road, London E1 4NS, U.K

\*\* Faculty of Materials Engineering, Warsaw University of Technology,  
ul. Wołoska 141, 02-507 Warszawa, Poland  
e-mail: krynski.marcin@outlook.com

Keywords: bismuth oxide, ab initio, molecular dynamics

## INTRODUCTION

Fluorite like  $\delta$ -phase of  $\text{Bi}_2\text{O}_3$  is a compound characterized by highest known oxide ions conductivity of any solids what makes this material a promising solid electrolyte in the wide range of electrochemical devices, such as Low or Intermediate Temperature Solid Oxide Fuel Cells (LT-SOFC or IT-SOFC), oxygen detectors or oxygen pumps. Since the highly conductive  $\delta$ -polymorph is stable in narrow temperature range (ca  $730^\circ\text{C}$ - $825^\circ\text{C}$ ) [1], research effort is focused on stabilizing this phase to lower temperatures by partial substituting bismuth cations with cations of other metals like Nb, Y, Yb, Er.

In this study, *ab initio* DFT simulations are used in order to examine electron and crystal structure, oxide ions diffusion and vacancy ordering in the fluorite-like type-II  $\text{Bi}_3\text{NbO}_7$ .

## EXPERIMENTAL

Series of molecular dynamics density functional theory calculations were performed using the Vienna Ab-initio Simulation Package (VASP) for a range of elevated temperatures from 1223K to 1373K. The electron-ion interactions were described by the full potential projector augmented wave method. The sampling of the Brillouin zone was performed using the Monkhorst-Pack scheme with k-mesh of  $1 \times 1 \times 1$ . All calculations were performed under periodic boundary conditions.

Structural studies of  $\text{Bi}_3\text{NbO}_7$  reveal high structural disorder [2], therefore to model it, five parallel runs over 60ps, with different initial anion and cation distributions were performed in a  $2 \times 2 \times 2$  super-cell (88 atoms in total). Lattice parameters and initial atom positions were obtained from X-ray and neutron diffraction.

## RESULTS AND DISCUSSION

The preferred six-folded coordination of niobium cations was observed, that is in agreement with structural studies. This results in high concentration of oxide ion vacancies around  $\text{Nb}^{5+}$  cations (on average two vacancies per niobium cation) and consequently in a very low content of vacancies in bismuth rich areas. Oxide ion trajectories were examined in order to describe rotational movement of oxide ions around niobium cations (Fig. 1). In contrast the translational movements of  $\text{O}^{2-}$  in the bismuth rich areas are observed.

## CONCLUSIONS

*Ab initio* calculations for type-II  $\text{Bi}_3\text{NbO}_7$  show a strong preference for niobium ions to adopt octahedral coordination environments with oxide ions, which has the effect of decreasing the number of mobile vacancies and promoting short range, rotational-like movement of oxide ions around  $\text{Nb}^{5+}$  cations.

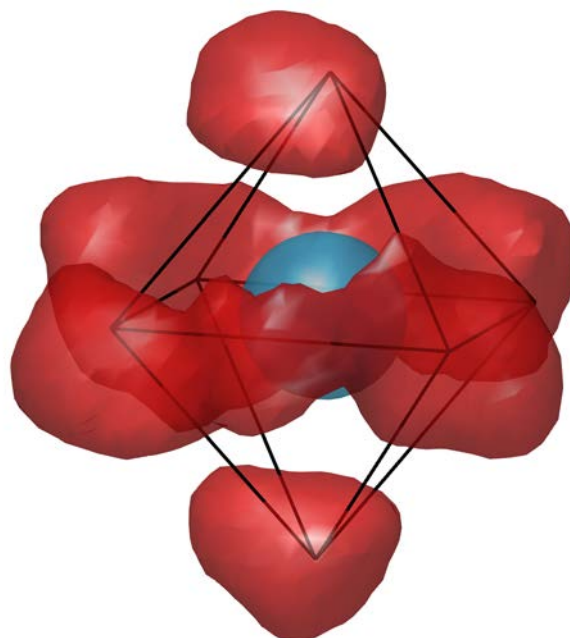


Fig. 1. Isosurface representation of oxide ion density around a typical niobium cation (blue sphere) in type-II  $\text{Bi}_3\text{NbO}_7$  at 1223 K. The octahedral coordination polyhedron around  $\text{Nb}^{5+}$  is indicated by black lines.

## ACKNOWLEDGMENT

We gratefully acknowledge the National Science Centre Poland for project grant numbers 2012/05/E/ST3/02767 and 2013/09/N/ST3/04326 and the National Center for Research and Development and Interdisciplinary Centre for Mathematical and Computational Modeling

## REFERENCES

1. T. Takahashi, H. Iwahara, Y. Nagai, *J. Appl. Electrochem.* **2**(1972)97
2. C.D. Ling, S. Schmid, et al., *J. Amer. Chem. Soc.*, **135**(2013)6477.



# POSTERS





# EFFECT OF ELECTROLYTE COMPOSITION ON ELECTROCHEMICAL PERFORMANCE OF $\text{LiMn}_2\text{O}_{4-y}\text{S}_y$ CATHODES FOR Li-ION BATTERIES

*M. Bakierska, M. Molenda\*, M. Świętosłowski, D. Majda and R. Dziembaj*

Faculty of Chemistry

Jagiellonian University, Ingardena 3  
30-060 Krakow, Poland

\*e-mail: molendam@chemia.uj.edu.pl

Keywords: Li-Ion batteries, cathode materials, electrolytes,  $\text{LiMn}_2\text{O}_4$ , sulphided spinels.

## INTRODUCTION

Due to the high energy density, the lithium-ion batteries (LIBs) have achieved a leading role in the consumer electronics market, where they are the key components of the portable equipment. Moreover, their applications are still expanding from small computing and telecommunication devices to large-scale appliances, such as hybrid electric vehicles (HEV), electric vehicles (EV) and stationary energy storage systems [1].

Lithium manganese oxide spinel ( $\text{LiMn}_2\text{O}_4$ , LMO) has been extensively studied as one of the most promising cathode materials for Li-ion batteries. Comparing with layered Ni or Co oxides, LMO spinel is inexpensive, more abundant, less toxic and exhibits good thermal stability as well as competitive practical capacity [2]. In spite of advantages, the stoichiometric spinel suffers from considerable capacity fading on cycling, which is originated from the instability of the spinel structure and the dissolution of manganese into the electrolyte [3]. Thus, the advancement in the electrochemical reversibility and chemical stability of  $\text{LiMn}_2\text{O}_4$  becomes more and more important.

This work evaluates the influence of different electrolyte compositions on stability of lithium manganese spinel materials, in which structural properties were improved by partial substitution with sulphur in the oxygen sublattice [4, 5].

## EXPERIMENTAL

A modified sol-gel method [4] was employed to synthesize nanostructured  $\text{LiMn}_2\text{O}_4$  and  $\text{LiMn}_2\text{O}_{3.99}\text{S}_{0.01}$  spinel materials. The syntheses were carried out with an argon flow to prevent oxidation of the  $\text{Mn}^{2+}$  ions. Condensation of the formed soles was performed at 90 °C for 3-4 days, and then the obtained xerogels were calcined in air at 300 °C and subsequently at 650 °C.

Different electrolyte solutions were prepared in an argon-filled glove box ( $\text{O}_2$  and  $\text{H}_2\text{O}$  levels less than 0.1 ppm), using three salts ( $\text{LiPF}_6$ ,  $\text{LiClO}_4$  and  $\text{LiTFSI}$ ) along with five various organic solvents (EC, DEC, DMC, TMS, EMC).

To characterize the physicochemical properties of the obtained Li-Mn-O-S spinel systems X-ray powder diffraction (XRD) and differential scanning calorimetry (DSC) were used. Atomic absorption/emission spectroscopy analysis (AAS/AES) was employed to determine the manganese dissolution from the spinel

materials. To examine the electrochemical behaviour of the electrolyte solution and cathode material compositions using  $\text{Li/Li}^+/\text{LiMn}_2\text{O}_{4-y}\text{S}_y$  cells, galvanostatic charge/discharge tests (CELL TEST) were performed on R2032 coin-type assembly. The electrochemical impedance spectroscopy (EIS) measurements were conducted as well.

## RESULTS AND DISCUSSION

X-ray diffraction confirmed that single phase nanomaterials of LMO spinel structure and  $Fd-3m$  symmetry were successfully obtained by the sol-gel method. Chemical stability of the synthesized spinel materials towards liquid electrolytes was verified on the basis of thermal analysis methods. The studies of cathode degradation upon electrochemical reactions, carried out with various electrolyte solutions, enabled identification of the most appropriate electrolyte composition.

## CONCLUSIONS

It can be pointed out that partial substitution of sulphur in the oxygen sublattice suppresses the Jahn-Teller distortion as well as enhances the electrochemical behavior. It was demonstrated that Li-Mn-O-S systems reveal higher capacity and improved cyclability (capacity retention) than stoichiometric spinel. Additionally, it was indicated that both, chemical stability and electrochemical reversibility of spinel materials highly depends on electrolyte composition.

## REFERENCES

1. W. Wen, S. Chen, Y. Fu, X. Wang, H. Shu, *Journal of Power Sources* **274**(2015)219.
2. J.W. Fergus, *Journal of Power Sources* **195**(2010) 939.
3. W. Xiao, W. Liu, X. Mao, H. Zhu, D. Wang, *Electrochimica Acta* **88**(2013)756.
4. M. Molenda, R. Dziembaj, D. Majda, M. Dudek, *Solid State Ionics* **176**(2005)1705.
5. M. Molenda, M. Bakierska, D. Majda, M. Świętosłowski, R. Dziembaj, *Solid State Ionics* **272**(2015)127.

# SYNERGETIC SUBSTITUTION OF NICKEL AND SULPHUR IN THE $\text{LiMn}_2\text{O}_4$ SPINEL STRUCTURE

*M. Bakierska, M. Molenda\*, M. Świętosławski and R. Dziembaj*

Faculty of Chemistry  
Jagiellonian University, Ingardena 3  
30-060 Krakow, Poland

\*e-mail: molendam@chemia.uj.edu.pl

Keywords: Li-Ion batteries, cathode materials,  $\text{LiMn}_2\text{O}_4$ , Li-Mn-Ni-O-S spinel systems, electrochemical behavior

## INTRODUCTION

The search for light weight, high energy and power density lithium-ion batteries (LIBs) has increased in the recent years due to growing demand for energy in the field of large scale applications (e.g., hybrid electric vehicles, electric vehicles and stationary energy storage systems) [1].

One of the most attractive cathode materials for rechargeable lithium-ion batteries is lithium manganese oxide spinel (LMO). The  $\text{LiMn}_2\text{O}_4$  reveals many intrinsic features such as low cost, wide abundance of resources, environmental benignity, high potential, excellent safety and sufficient practical capacity (about  $140 \text{ mAh}\cdot\text{g}^{-1}$ ) [2-4]. However, the poor cycling behavior of stoichiometric spinel is the main issue which hamper its broad application. The reasons responsible for the capacity fading are as follows: unstable crystal structure and manganese dissolution [5]. To circumvent these obstacles, many research efforts have been made so far. Synergetic substitution of nickel and sulphur in the  $\text{LiMn}_2\text{O}_4$  spinel structure is considered as a useful strategy which could improve the structural and chemical properties, leading to the promotion of cycling stability [6].

The aim of this work was to find the best compromise among chemical composition and physicochemical properties as well as electrochemical performance of  $\text{LiMn}_{2-x}\text{Ni}_x\text{O}_{4-y}\text{S}_y$  spinel materials.

## EXPERIMENTAL

A modified sol-gel method was carried out to synthesize Ni and S doped  $\text{LiMn}_{2-x}\text{Ni}_x\text{O}_{4-y}\text{S}_y$  spinel materials ( $0 \leq x \leq 0.5$  and  $y = 0.01$ ). All the syntheses were conducted under flow of argon to prevent oxidation of the  $\text{Mn}^{2+}$  ions. Condensation of the formed soles was performed at  $90^\circ\text{C}$  for 3-4 days. Finally, the obtained xerogels were calcined in air at  $300^\circ\text{C}$  and next at  $650^\circ\text{C}$  [7,8].

The dependence between chemical composition of the Li-Mn-Ni-O-S spinel systems and their physicochemical and electrochemical properties was extensively investigated by using X-ray powder diffraction (XRD), differential scanning calorimetry (DSC), low-temperature nitrogen adsorption/desorption measurements ( $\text{N}_2$ -BET), electrical conductivity studies (EC), galvanostatic charge-discharge tests (CELL TEST), cyclic voltammetry (CV) and electrochemical impedance spectroscopy (EIS).

## RESULTS AND DISCUSSION

Experimental results indicated that the applied method of the spinel synthesis allows obtaining of homogeneous nanostructures and enables the effective substitution of nickel and sulphur in the  $\text{LiMn}_2\text{O}_4$  spinel structure. The performed studies showed that as Mn or O are replaced by Ni or S respectively, the adverse phase transition close to room temperature diminishes and the cycling performance enhances due to stabilization of spinel structure. Compared to the pristine stoichiometric spinel, the Li-Mn-Ni-O-S materials exhibit higher capacities, increased cycling stability and better rate capability.

## CONCLUSIONS

On the whole, the presented investigation demonstrated the favourable characteristics of nickel and sulphur doped lithium manganese oxide spinels. The improved properties of modified spinel materials could be ascribed to the effect of synergetic substitution of Ni and S that resulted in stabilization of the spinel structure, enhancement of the chemical stability and advancement of electrochemical behaviour.

## REFERENCES

1. P.V. Braun, J. Cho, J.H. Pikul, W.P. King, H. Zhang, *Current Opinion in Solid State and Materials Science* **16**(2012)186.
2. T. Ohzuku, R.J. Brodd, *Journal of Power Sources* **174**(2007)449.
3. J.W. Fergus, *Journal of Power Sources* **195**(2010) 939.
4. K. Amine, J. Liu, I. Belharouak, S.H. Kang, I. Bloom, D. Vissers, G. Henriksen, *Journal of Power Sources* **146**(2005)111.
5. L. Yang, M. Takahashi, B. Wang, *Electrochimica Acta* **51**(2006)3228.
6. M.W. Raja, S. Mahanty, R.N. Basu, *Journal of Power Sources* **192**(2009)618.
7. M. Molenda, R. Dziembaj, D. Majda, M. Dudek, *Solid State Ionics* **176**(2005)1705.
8. M. Molenda, M. Bakierska, D. Majda, M. Świętosławski, R. Dziembaj, *Solid State Ionics* **272**(2015)127.

# MULTIFUNCTIONAL CARBON AEROGELS DERIVED BY SOL-GEL PROCESS OF NATURAL POLYSACCHARIDES OF DIFFERENT BOTANICAL ORIGIN

*M. Bakierska<sup>1</sup>, A. Chojnacka<sup>1</sup>, M. Świętosławska<sup>1</sup>, M. Molenda<sup>1,\*</sup>, P. Natkański<sup>1</sup>, M. Gajewska<sup>2</sup> and R. Dziembaj<sup>1</sup>*

<sup>1</sup> Faculty of Chemistry

Jagiellonian University, Ingardena 3  
30-060 Krakow, Poland

<sup>2</sup> Academic Centre for Materials and Nanotechnology  
AGH University of Science and Technology, Mickiewicza 30  
30-059 Krakow, Poland

\*e-mail: molendam@chemia.uj.edu.pl

Keywords: polysaccharide, starch, carbon aerogel, sol-gel, pyrolysis

## INTRODUCTION

Many people assume that aerogels are recent products of modern technology. In reality, the first aerogels were prepared in 1931 by Steven S. Kistler. After this discovery, new developments in aerogels science and technology occurred rapidly.

Carbon aerogels are a special class of nanostructured and highly porous aerogels that have been broadly studied in the last few years. These ultralight carbon materials exhibit extraordinary properties including well-defined and controlled porosity, large surface area, mechanical strength, chemical stability and low electrical resistance which make them desirable materials for a wide range of technological applications (eg. thermal insulation, heavy metal absorption, energy storage, catalyst supports and biomedicine) [1-3]. Generally, carbon aerogels are formed from the sol-gel polymerization of resorcinol and formaldehyde, followed by supercritical drying, and subsequent pyrolysis at an elevated temperature in an inert atmosphere [4]. Though, the use of natural polysaccharides and their derivatives is considered to be more appealing owing to their abundance, availability, renewability, stability, non-toxicity and low cost [5-8].

In this work, the impact of botanical origin of natural starches on thermal, structural, textural and electrical characteristics of carbon aerogels was determined.

## EXPERIMENTAL

To synthesize carbon aerogels, different types of starches (potato, maize and rice) were taken as the starting materials. In the first step the polycondensation of polysaccharides was carried out. The starch hydrogels were then kept immersed in ethanol for few days in order to replace water trapped inside the pores. In the third step, the new solvent (ethanol) was extracted by drying the alcogels. The last step in which the carbon aerogels were obtained involved the carbonization of organic aerogels.

The gelatinization temperature of starches was studied using differential scanning calorimetry (DSC). Decomposition of organic aerogels during pyrolysis was evaluated by thermal analysis methods

(TGA/DTG/SDTA/EGA-IR). The structure and the morphology of the prepared carbon materials were investigated using X-ray powder diffraction (XRD) and scanning electron microscopy (SEM). Electrical properties of the obtained aerogels were examined by electrical conductivity studies (EC) using 4-probe AC method within temperature range of -20 °C to +40 °C.

## RESULTS AND DISCUSSION

Carbon aerogels were successfully synthesized through the gelatinization process of natural starches (potato, maize and rice) followed by the carbonization of organic aerogels. This method enabled fabrication of carbon materials with tailored properties. In addition, it was examined that the thermal, structural, textural and electrical characteristics of the final products depend on the botanical origin of starches and can be easily controlled by different factors of the synthesis process.

## REFERENCES

1. D.A. Donatti, A. Ibanez Ruiz, D.B. Vollet, *Journal of Non-Crystalline Solids* 292 (2001) 44.
2. C. Moreno-Castilla, F.J. Maldonado-Hódar, *Carbon* 43 (2005) 455.
3. X. Wu, D. Wu, R. Fu, W. Zeng, *Dyes and Pigments* 95 (2012) 689.
4. R.W. Pekala, *Journal of Materials Science* 24 (1989) 3221.
5. O. Aaltonen, O. Jauhiainen, *Carbohydrate Polymers* 75 (2009) 125.
6. C. Tsiptsias, C. Michailof, G. Staurooulos, C. Panayiotou, *Carbohydrate Polymers* 76 (2009) 535.
7. X. Chang, D. Chen, X. Jiao, *Polymer* 51 (2010) 3801.
8. C.A. García-González, M. Alnaief, I. Smirnova, *Carbohydrate Polymers* 86 (2011) 1425.

# COMPARISON OF ELECTROCHEMICAL PROPERTIES OF TIN NANOPARTICLES ENCAPSULATED IN DIFFERENT ORIGIN CARBON MATRIX

A. Chojnacka, M. Molenda and R. Dziembaj

Faculty of Chemistry  
Jagiellonian University, Ingardena 3,  
30-060 Cracow, Poland  
e-mail: molendam@chemia.uj.edu.pl

Keywords: Li-ion batteries, anode materials, C/Sn nanocomposite, encapsulation, carbon matrix.

## INTRODUCTION

To improve the energy density of lithium-ion batteries, researches have been attempted to explore novel electrode materials [1-3]. Among the available anode materials, tin has been shown as one of the best alternatives due to its lithium uptake at low potential and high theoretical capacity ( $994 \text{ mAh}\cdot\text{g}^{-1}$  for  $\text{Li}_{4.4}\text{Sn}$  phase) [4]. However, the application of tin is limited by the poor cyclic performance due to the pulverization and subsequent electrical disconnection of the electrode caused by cyclic volume changes of elementary cell, during the insertion and extraction processes of lithium ions [5]. One of the ways to overcome this issue is development of tin-carbon nanocomposite, in which nanometric tin grains will be encapsulated in a flexible and conductive carbon layers [6-8]. Nevertheless, such nanocomposites are able to provide appropriate electrochemical properties, only if the formed carbon layer is leak-proof, flexible and porous, featuring local free space to compensate volume changes.

The goal of the present work was the development of two types of carbon-tin nanocomposite anode materials in which carbon matrix was derived from different origin sources of carbon and comparison of their electrochemical properties.

## EXPERIMENTAL

The precursor of active material ( $\text{SnO}_2$ ) was obtained using a modified reverse microemulsion method (w/o) and then coated by a source of carbon (potato starch or water soluble polymer) [7,8]. The carbon-tin precursors were afterwards pyrolyzed, affording formation of tin-based nanograins encapsulated in conductive carbon buffer matrix. Optimal conditions of the thermal treatment were determined by thermal analysis methods (EGA-TGA). The resulting materials with different carbon loading (20-60 wt.%) were investigated by powder X-ray diffraction (XRD), low-temperature nitrogen adsorption method ( $\text{N}_2$ -BET) and by transmission electron microscopy (TEM) as well. Comprehensive electrochemical characterization of obtained nanocomposites including the electrical conductivity (EC), cyclic voltammetry (CV) and impedance spectroscopy (IS) was carried out. Discharge-charge tests were performed in R2032-type coin cells within 0.01–1.5 V potential range.

## RESULTS AND DISCUSSION

The low-temperature nitrogen adsorption method as well as transmission electron microscopy images show that the sort of carbon precursor and temperature of pyrolysis have strong impact on morphology of the obtained carbon buffer matrix. Comparison of the electrochemical research for both series of obtained tin-based composites suggests that the relevant loading of carbon in the resulting composites, which depends on the type of applied carbon precursor, strictly affects the specific capacity and cell cyclability.

## CONCLUSIONS

Electrode materials consisted of tin-based nanograins encapsulated in a different origins carbon buffer matrix were successfully obtained in a simple and inexpensive green process. The electrochemical studies showed that columbic efficiency and capacity retention in discharge-charge tests for resulting nanocomposite anode materials strongly depend on the carbon loading and sort of carbon precursor.

## ACKNOWLEDGMENT

This work is supported by National Science Center of Poland under grant 2012/07/N/ST8/03725.

## REFERENCES

1. B. Guo, M. Chi, X.G. Sun, S. Dai, *Journal of Power Sources* **205**(2012)495.
2. P. Meduri, E. Clark, J.H. Kim, E. Dayalan, G.U. Sumanasekera, M.K. Sunkara, *Nano Letters* **12**(2012)1784.
3. C. Wang, Y. Zhou, M. Ge, X. Xu, Z. Zhang, J.Z. Jiang, *Journal of the American Chemical Society* **132**(2010)46.
4. M. Winter, J.O. Besenhard, *Electrochimica Acta* **45**(1999)31.
5. S. Ding, X.W. Lou, *Nanoscale* **3**(2011)3586.
6. M. Molenda, *Functional Materials Letters* **4**(2011)129.
7. M. Molenda, A. Chojnacka, M. Bakierska, R. Dziembaj, *Materials Technology* **29**(2014)A88.
8. A. Chojnacka, M. Molenda, M. Bakierska, R. Dziembaj, *Procedia Engineering* **98**(2014)2.

# PREPARATION OF PROTOTYPE CARBON LEAD-ACID BATTERY

*K. Wróbel<sup>a</sup>, J. Lach<sup>a</sup>, J. Wróbel<sup>b</sup>, Z. Rogulski<sup>a,b</sup> and A. Czerwiński<sup>a,b</sup>*

<sup>a</sup> Industrial Chemistry Research Institute, ul. Rydygiera 8, 01-793 Warsaw, Poland

<sup>b</sup> University of Warsaw, Department of Chemistry, ul. Pasteura 1, 02-093 Warsaw, Poland  
e-mail: aczerw@chem.uw.edu.pl

Keywords: power sources, lead-acid battery, carbon materials

## INTRODUCTION

The lead-acid battery still remains one of the most widely used electrochemical power sources. There are numerous applications of lead-acid batteries. They range from the extremely large battery systems used in load leveling by electrical utility companies to the relatively small batteries used in hand tools. A promising approach to increase the relatively low specific energy and capacity of lead-acid batteries is the use of lightweight porous carbon materials, coated with lead or lead alloys, as current collectors.<sup>1)</sup>

Carbon lead-acid battery (CLAB) is a new type of lead-acid battery, in which a carbon material with high specific surface area and conductivity is used as a current collector.

The aim of our work was to apply the carbon materials in a new carbon lead-acid battery. Carbon materials coated with lead has been used as a current collector in prototype batteries.

## EXPERIMENTAL

Two types of carbon materials were employed as substrates for grid manufacturing. The first of them was reticulated vitreous carbon (RVC) while the second conductive porous carbon (CPC). CPC is a new carbon material created and manufactured by the Faculty of Chemistry, University of Warsaw, which is characterized by increased conductivity and better mechanical properties than RVC. Then carbon slabs were galvanostatically coated with Pb or Pb-Sn alloy using a methanesulfonate bath.

We made two series of prototype 12-volt Carbon Lead-Acid Batteries. The nominal capacity of batteries were 6,5Ah in first series and 40Ah in second series. A battery cell consisted of two positive plates and two negative plates. The cured plates were separated with the SLI-type polyethylene separator. The plates were enclosed in a plastic battery case and then submersed in H<sub>2</sub>SO<sub>4</sub> electrolyte with density of 1,28g cm<sup>-3</sup>. In both cases the prototype batteries were made in the conventional casings for SLI batteries (40Ah) and UPS systems batteries (6,5Ah).

The carbon slab used in this study had dimensions of ca. 50mm x 38mm x 5mm (series I) and 118mm x 100mm x 5mm (series II) and pore size ca. 20 or 30 pores per inch. Typically a coating thickness of about 100µm was applied for the positive and 10-20 µm for the negative collector. Positive and negative collectors were pasted with industrial standard negative and positive pastes obtained directly from lead-acid battery manufacturer.

Formation was performed in a H<sub>2</sub>SO<sub>4</sub> electrolyte with density of 1,14g cm<sup>-3</sup>. After formation the

electrolyte was replaced with H<sub>2</sub>SO<sub>4</sub> with density of 1,28g cm<sup>-3</sup>.

In both cases the specific energy of prototype batteries were ca. 45Wh/kg.

## CONCLUSIONS

Two series of prototype Carbon Lead-Acid Batteries were made by the University of Warsaw. They display behavior similar to a typical lead-acid battery. The combination of high specific surface area and optimal use of lead leads to increase of the utilization efficiency of the positive active mass and the lead-acid battery weight reduction. Particularly the negative grids are 2 to 3 times lighter than the standard lead grids.

We are in the process of constructing further two types of 12V batteries: small battery for tools with capacity of 2Ah and SLI battery with capacity of 60Ah.

## ACKNOWLEDGMENT

This work was supported by The National Centre for Research and Development under grant INNOTECH, IN1/152819/U and by the Faculty of Chemistry, University of Warsaw through project 501/64-BST-169757.

## REFERENCES

1. A.Czerwiński, S.Obrębowski, Z. Rogulski, *Journal of Power Sources* **198** (2012) 378-382



# ELECTROCHEMICAL PROPERTIES OF NEW CARBON LEAD-ACID BATTERY

*J. Lach*<sup>a</sup>, *K. Wróbel*<sup>a</sup>, *J. Wróbel*<sup>b</sup>, *Z. Rogulski*<sup>a,b</sup> and *A. Czerwiński*<sup>a,b</sup>

<sup>a</sup> Industrial Chemistry Research Institute, ul. Rydygiera 8, 01-793 Warsaw, Poland

<sup>b</sup> University of Warsaw, Department of Chemistry, ul. Pasteura 1, 02-093 Warsaw, Poland

e-mail: aczerw@chem.uw.edu.pl

Keywords: power sources, lead-acid battery, reticulated current collector

## INTRODUCTION

In last years we have seen a dynamic growth of new types of power sources, like lithium-ion batteries. However, lead-acid batteries are still a large portion of the total battery sales. In 2010 this type of power source had over 60% share in the value of the worldwide rechargeable battery market [1]. Their main advantages are low cost and reliability. Despite being known for over 150 years their design can still be improved. One of the possible changes is the usage of a reticulated, carbon current collector in place of a standard, lead grid. Such solution improves the greatest disadvantage of lead-acid battery – its low specific energy. Using light, carbon collectors instead of heavy, lead grids lowers the overall mass of the battery, without lowering its capacity. A new type of Carbon Lead-Acid Battery (CLAB) with reticulated collectors can allow to increase its specific capacity by up to 50%.

## EXPERIMENTAL

Two different types of 12 V CLABs were constructed. Two types of cells were used: with the predicted capacity of 40 Ah or 6,5 Ah. Single 2 V cells of the same capacities were also tested in some experiments. Measurements were conducted on Atlas 1361 and 0461 potentiostats/galvanostats and Digatron UBT 50-18-6ME battery tester. For comparison commercial lead-acid batteries with similar capacity were tested in the same conditions.

## RESULTS AND DISCUSSION

CLABs, constructed by the University of Warsaw, were first discharged with C/20 current. The bigger 12 V batteries and 2 V cells reached the predicted capacity of about 40 Ah, smaller – about 7 Ah. In comparison to commercial cells specific energy improved by up to 50%.

Measurements with higher discharge currents showed that CLAB has a adequate discharge characteristic even for discharge currents of 3C.

The endurance test for vented lead-acid starter batteries was also conducted, with accordance to the EN 50342-1:2006 standard. Commercial batteries, depending on the type endured around discharge 125 cycles. Our improved CLABs endured about 275 cycles. The resistance to corrosion of CLAB during shallow discharge cycles seems to be vastly improved in comparison to a standard battery.

Discharge characteristics during deep discharge cycles were also measured for CLAB and a standard battery. The number of cycles completed in this experiment was comparable for both of them.

Additionally the test of a self-discharge of CLAB was conducted on a 2V cell. It retained 93% of its initial capacity after a six months storage period. Such result is competitive with batteries available on the market.

## CONCLUSIONS

Our tests shown that the new CLAB is a very exciting prospects for the future of lead-acid batteries. It has similar or even better discharge characteristics as the standard lead-acid batteries in various conditions. Simultaneously it has a higher specific energy. This allows it to be used as an alternative to more expensive battery types. Moreover, the carbon material manufactured by University of Warsaw and used for current collectors (Conductive Porous Carbon, CPC) is relatively inexpensive. The total cost of CLAB is very similar to the cost of standard lead-acid battery. Improvements such as described above can ensure continuous use of lead-acid batteries in the future.

## ACKNOWLEDGMENT

This work was supported by the National Centre for Research and Development under grant INNOTECH-K1/IN1/47/152819/NCBR/2012 and by the Faculty of Chemistry, University of Warsaw through project 501/64-BST-169757.

## REFERENCES

1. Avicenne Energy (April 2012). *The Worldwide rechargeable Battery Market 2011 – 2025*. Available from <http://www.avicenne.com/>

# Li<sub>3.85</sub>Cu<sub>0.15</sub>Ti<sub>5</sub>O<sub>12</sub> - ANODE FOR LI-ION BATTERIES

*A. Drobnik, D. Olszewska*

Faculty of Energy and Fuels

AGH University of Science and Technology, al. A. Mickiewicza 30

30-059 Cracow, Poland

e-mail: dolszew@agh.edu.pl

Keywords: Li-ion batteries, anode, Li<sub>4</sub>Ti<sub>5</sub>O<sub>12</sub>

## INTRODUCTION

The lithium-ion batteries have been considered as the best power sources for most of the electronic devices and the electric vehicles due to their advantages of high energy density, high work potential, good cycle life, and environmental friendliness.

The spinel Li<sub>4</sub>Ti<sub>5</sub>O<sub>12</sub> is the most attractive material to use as a anode material alternatives because of its advantages. The charge–discharge voltage plateau (1.6V) and its zero-strain feature during the charge/discharge process, safety and good cycling performance are the most important. However Li<sub>4</sub>Ti<sub>5</sub>O<sub>12</sub> material possesses so many advantages, it still exhibits a poor rate capability due to its lower electronic and ionic conductivity.

## EXPERIMENTAL

Li<sub>3.85</sub>Cu<sub>0.15</sub>Ti<sub>5</sub>O<sub>12</sub> material was obtained using solid state method. As the substrates lithium carbonate Li<sub>2</sub>CO<sub>3</sub>, titanium oxide TiO<sub>2</sub> and copper oxide CuO were used. Stoichiometric amounts of these substrates were taken to obtain and with 5% wt. excess of Li<sub>2</sub>CO<sub>3</sub> was used to compensate high temperature evaporation. Prepared material was characterized in terms of phase composition, crystal structure, grain size and surface morphology, as well as ionic and electronic conductivity. Phase composition and crystal structure parameters were determined using X-ray Panalytical Empyrean XRD diffractometer in the range of 10-110° with CuKα radiation. Obtained results were analyzed using Rietveld refinement implemented in GSAS computer software. Electrical conductivity measurements were carried out using impedance spectroscopy. Moreover, studies were carried out using scanning electron microscope – SEM - morphology studies.

## RESULTS

Electrochemical cycling performance of prepared sample at various C rates and result of voltammetry cyclic are presented as Fig. 1. and Fig. 2, respectively.

## CONCLUSIONS

Structural studies carried in the room temperature confirmed obtaining single-phased materials with Fd-3m space group. The studies shows that Li<sub>3.85</sub>Cu<sub>0.15</sub>Ti<sub>5</sub>O<sub>12</sub> material have good transport properties.

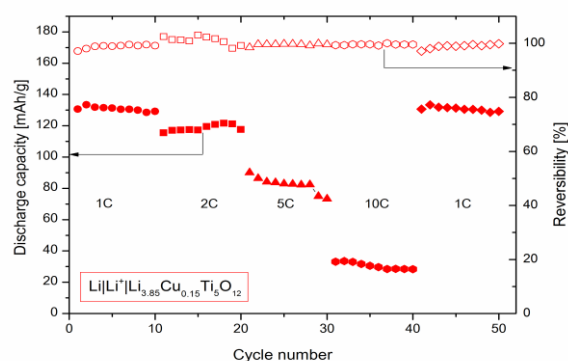


**Fig. 1** Discharge capacity and coulombic efficiency versus cycle number Li<sub>3.85</sub>Cu<sub>0.15</sub>Ti<sub>5</sub>O<sub>12</sub>.

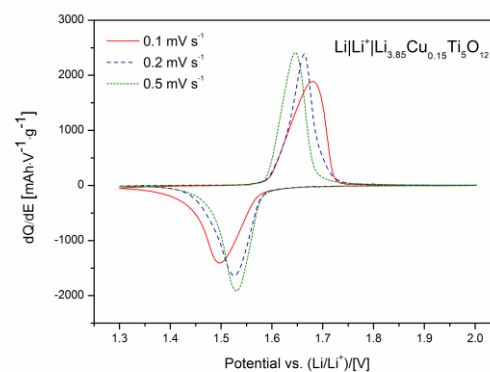


**Fig. 2** Result of voltammetry cyclic of Li<sub>3.85</sub>Cu<sub>0.15</sub>Ti<sub>5</sub>O<sub>12</sub> sample.

## ACKNOWLEDGMENT

Project supported by a grant from Switzerland through the Swiss Contribution to the enlarged European Union (grant no. 080/2010 LiBEV Positive Electrode Materials for Li-ion Batteries for Electric Vehicles).

## REFERENCES

1. E. Ferg, R.J. Gummow, A. de Kock, M.M. Thackeray, *J. Electrochem. Soc.* **141** (11) (1994) L147.
2. X. Li, L. Zhao, X. He, R. Xiao, L. Gu, Y-S. Hu, H. Li, Z. Wang, X. Duan, L. Chen, J. Maier, Y. Ikuhara, *Adv. Mater.* **24** (2012) 3233.
3. B. Yan, M. Li, X. Li, Z. Bai, J. Yang, D. Xiong, D. Li, *J. Mat. Chem. A* **3** (2015) 11773.

# THE EFFECT OF ADDITION OF 3% OF COPPER TO THE LTO SPINEL ON THE STRUCTURAL AND ELECTROCHEMICAL ANODE MATERIAL FOR LI-BATTERIES

*D. Olszewska, A. Drobnik*

Faculty of Energy and Fuels

AGH University of Science and Technology, al. Mickiewicza 30

30-059 Cracow, Poland

e-mail: dolszew@agh.edu.pl

Keywords: Li-ion batteries, anode, fuel cells

## INTRODUCTION

The authors of many papers described electrochemical properties of  $\text{Li}_4\text{Ti}_5\text{O}_{12}$  and their modifications by doping [1-2]. A spinel based on  $\text{Li}_4\text{Ti}_5\text{O}_{12}$  was used as model material for anode of Li-ion batteries for the first time in 1994 year by Ferg et al. [3].

## EXPERIMENTAL

The authors prepared anode materials by addition of 3% wt. of Cu from copper nitrates to  $\text{Li}_4\text{Ti}_5\text{O}_{12}$  spinel carried out by solid state reaction of  $\text{Li}_2\text{CO}_3$  (Aldrich 99.997%) and  $\text{TiO}_2$  (Aldrich 99.998%). Prepared material  $\text{Cu-Li}_4\text{Ti}_5\text{O}_{12}$  was characterized in terms of phase composition, crystal structure, grain size and surface morphology. Phase composition and crystal structure parameter were determined using X-ray PANalytical Empyrean MPD diffractometer. Obtained results were analysed using Rietveld refinement implemented in GSAS computer software.

The obtained powders were applied in  $\text{Li}|\text{Li}^+|\text{Cu-Li}_4\text{Ti}_5\text{O}_{12}$  - type cells. Cyclic voltammetry, specific capacity of the studied material, reversibility and stability during charge-discharge cycles measurements were carried out to characterize electrochemical properties of the cells. Additional Scanning Electron Microscopy (SEM) measurements were performed using FEI Nova NanoSEM 200 apparatus on prepared powders.

## RESULTS

Examples of results presented in the drawings below. Fig. 1 presents the scanning electron microscopy (SEM) image in magnification of 30 000 times.

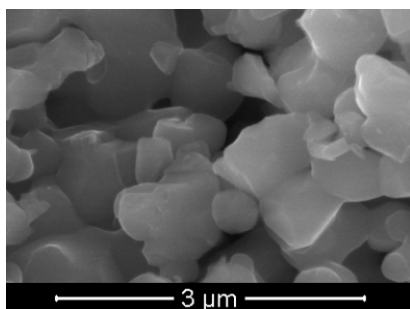


Fig. 1 SEM image of  $\text{Cu-Li}_4\text{Ti}_5\text{O}_{12}$  in magnification of 30 000 times.

Fig. 2 shows electrochemical cycling at various C rates for prepared sample.

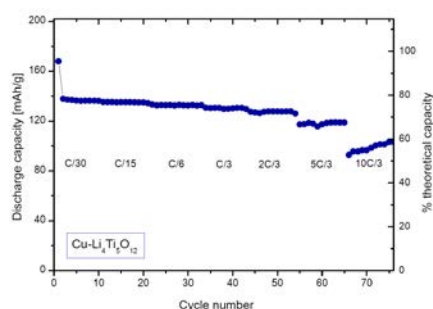


Fig. 2 Cycling performance of  $\text{Cu-Li}_4\text{Ti}_5\text{O}_{12}$  at different rates.

Lattice parameter  $a$  for sample doped Cu is the same like spinel  $\text{Li}_4\text{Ti}_5\text{O}_{12}$ . Gravimetric capacity of this material exceeds  $172 \text{ mAh}\cdot\text{g}^{-1}$ , which is lower than that for graphite ( $372 \text{ mAh}\cdot\text{g}^{-1}$ ). The specific charge capacities were 140, 120 and 80  $\text{mAh/g}$  at C/30, 2 C and 10 C rates, respectively. Reversibility during the measurement 100 cycles was almost 100%.

## CONCLUSIONS

In summary, the spinel material based on  $\text{Cu-Li}_4\text{Ti}_5\text{O}_{12}$ , prepared by the solid method have very good electrochemical and structural properties and may be used as anode material for Li-ion batteries.

## ACKNOWLEDGMENT

The authors gratefully acknowledge the financial support of this work by the Polish Ministry of Science and Information Society Technologies under the AGH University of Science and Technology statutory research No. 11.11.210.911.

## REFERENCES

1. S. Goriparti, E. Miele, F. De Angelis, E. Di Fabrizio, R. P. Zaccaria, C. Capiglia, *J. Powder Sources* **257** (2014) 421.
2. G. Zhou, F. Li, H.-M. Cheng, *Energy Environ. Sci.*, **7**, (2014) 1307.
3. E. Ferg, R.J. Gummow, A. de Kock, M.M. Thackeray, *J. Electrochem. Soc.* **141** (11) (1994) L147.

# TRANSPORT AND ELECTROCHEMICAL PROPERTIES OF $\text{Na}_{0.67}\text{Ni}_{0.33}\text{Mn}_{0.67-x}\text{Ti}_x\text{O}_2$ ( $x=0, 0.1, 0.2, 0.25, 0.33$ ) AND Cu SUBSTITUTED $\text{Na}_{0.67}\text{Ni}_{0.31}\text{Cu}_{0.02}\text{Mn}_{0.33}\text{Ti}_{0.33}\text{O}_2$ CATHODE MATERIALS

*Anna Milewska, Wojciech Zajęc, Konrad Świerczek, Łukasz Sawczuk, Janina Molenda*

AGH University of Science and Technology, Faculty of Energy and Fuels

al. A. Mickiewicza 30, 30-059 Krakow, Poland

e-mail: anna.milewska@agh.edu.pl

Keywords: Na-ion batteries, cathode materials, intercalation process, transport properties

## INTRODUCTION

Currently, the most popular power devices are Li-ion batteries. This is due to the fact that lithium cells have one of the highest volumetric and gravimetric energy. Because of the price and the limited resources of lithium, Li-ion batteries may soon be replaced by Na-ion batteries. This is because Na has similar physicochemical properties to Li.

In this presentation we present the results of transport and electrochemical properties of series of compounds:  $\text{Na}_{0.67}\text{Ni}_{0.33}\text{Mn}_{0.67-x}\text{Ti}_x\text{O}_2$  ( $x=0, 0.1, 0.2, 0.25, 0.33$ ) and  $\text{Na}_{0.67}\text{Ni}_{0.31}\text{Cu}_{0.02}\text{Mn}_{0.33}\text{Ti}_{0.33}\text{O}_2$ . Titanium was found to stabilize P2-type structure of  $\text{Na}_{0.67}\text{Ni}_{0.33}\text{Mn}_{0.33}\text{Ti}_{0.33}\text{O}_2$  and has beneficial effect on the transport properties of the analysed material. On the other hand doping with small amount of Cu in  $\text{Na}_{0.67}\text{Ni}_{0.31}\text{Cu}_{0.02}\text{Mn}_{0.33}\text{Ti}_{0.33}\text{O}_2$  completely deteriorates the transport properties of this compound.

## EXPERIMENTAL

$\text{Na}_{0.67}\text{Ni}_{0.33}\text{Mn}_{0.67-x}\text{Ti}_x\text{O}_2$  ( $x=0, 0.1, 0.2, 0.25, 0.33$ ) and  $\text{Na}_{0.67}\text{Ni}_{0.31}\text{Cu}_{0.02}\text{Mn}_{0.33}\text{Ti}_{0.33}\text{O}_2$  oxides were obtained using the high temperature solid state method from the following reactants:  $\text{Na}_2\text{CO}_3$ , NiO,  $\text{MnCO}_3$ ,  $\text{TiO}_2$  and CuO. Crystal structure of the synthesized materials was examined by X-ray diffraction method (XRD) in 10-110 deg range using Cu  $K_\alpha$  radiation. Studies were conducted on Panalytical Empyrean diffractometer equipped with PIXcel3D detector. The X-ray patterns were analysed by Rietveld method using GSAS/EXPGUI set of software [1, 2].

In order to measure total conductivity of the pristine samples, Electrochemical Impedance Spectroscopy method (EIS) was applied, with excitation voltage of 100 mV over 300 kHz to 0.01 Hz frequency range. DC Asymmetric Polarisation (AP) method was also used to establish the electronic component of the conductivity. Electrochemical tests were carried out for cells consisting of sodium metal anode, 1M  $\text{NaPF}_6$  in propylene carbonate (PC) electrolyte and composite cathode. The composite cathodes consisted of 80 wt.% of the studied material, 10 wt.% carbon black and 10 wt.% of poly(vinylidene fluoride). Coin-type R2032 cells were assembled in the glove-box with controlled  $\text{O}_2$  and  $\text{H}_2\text{O}$  partial pressure ( $< 0.1$  ppm).

## RESULTS AND DISCUSSION

All samples indicate hexagonal P2-type structure and  $P6_3/mmc$  space group. Also, a small amount of an

additional NiO phase was detected. The investigated  $\text{Na}_{0.67}\text{Ni}_{0.33}\text{Mn}_{0.67-x}\text{Ti}_x\text{O}_2$  ( $x=0, 0.1, 0.2, 0.25, 0.33$ ) and  $\text{Na}_{0.67}\text{Ni}_{0.31}\text{Cu}_{0.02}\text{Mn}_{0.33}\text{Ti}_{0.33}\text{O}_2$  materials exhibit mixed ionic-electronic conductivity with prevailing ionic component. High concentration of Ti facilitates the conductivity of  $\text{Na}_{0.67}\text{Ni}_{0.33}\text{Mn}_{0.33}\text{Ti}_{0.33}\text{O}_2$  sample. This might be related to the higher  $\text{Na}_f/\text{Na}_e$  occupation ratio, which likely favours self-diffusion of Na-ions. For samples with higher concentration of Ti the step like charge and discharge curves are turned to slope type profiles. Ti stabilizes initial P2-type structure of the  $\text{Na}_{0.67}\text{Ni}_{0.33}\text{Mn}_{0.33}\text{Ti}_{0.33}\text{O}_2$  in low  $\text{Na}^+$  region. Small substitution of nickel by copper worsens conductivity of the  $\text{Na}_{0.67}\text{Ni}_{0.31}\text{Cu}_{0.02}\text{Mn}_{0.33}\text{Ti}_{0.33}\text{O}_2$  oxide. This provides to drastic declination of the discharge capacity. This can be related with cation-mixing effect due to similar ionic radii of  $\text{Li}^+$  (0.76 Å) and  $\text{Cu}^{2+}$  (0.73 Å). However we didn't confirmed this phenomena on the base on Rietveld refinement. Deterioration of the properties of the  $\text{Na}_{0.67}\text{Ni}_{0.31}\text{Cu}_{0.02}\text{Mn}_{0.33}\text{Ti}_{0.33}\text{O}_2$  oxides might be also related with segregation of the  $\text{Cu}^{2+}$  in grain boundaries, which block the diffusion path of Na-ions between grains. The character of the charge-discharge curves correlates with the shapes of the obtained cycling voltammograms.

## CONCLUSIONS

High amount of Ti facilitates in-plane self-diffusion of Na-ions, and increase conductivity of the materials. The obtained results indicate that  $\text{Na}_{0.67}\text{Ni}_{0.33}\text{Mn}_{0.67-x}\text{Ti}_x\text{O}_2$  ( $0.2 \leq x \leq 0.33$ ) compounds can be consider as cathode materials in Na-ion batteries, but require new electrolytes with wider electrochemical window.

## ACKNOWLEDGMENT

Project supported by the Polish Ministry of Science and Higher Education, under project AGH No. 11.11.210.911.

## REFERENCES

1. A.C. Larson, R.B. Von Dreele, Los Alamos Natl. Lab. Rep. - LAUR 86-748, 2004.
2. B.H. Toby, J. Appl. Crystallogr., 34 (2001) 210.

# MICROWAVE SYNTHESIS OF $\text{LiVPO}_4\text{F}$ CATHODE MATERIAL

*K. Kwatek, J. L. Nowinski*

Faculty of Physics, Warsaw University of Technology, ul. Koszykowa 75, 00-662 Warszawa, Poland  
e-mail: nowin@if.pw.edu.pl

Keywords: lithium vanadium fluorophosphates, cathode material, microwave synthesis

## 1. INTRODUCTION

$\text{LiVPO}_4\text{F}$  is a cathode material, promising for the next generation of lithium-ion batteries. It shows a high operational potential of 4.19 V versus lithium metal and theoretical capacity of 155 mA/g [1]. Due to addition of a fluorine atom in the structure, and consequent presence of very stable V-F bonds, the fluorophosphate structure remains stable and resistant against repeated Li insertion and extraction.

Preparation of the  $\text{LiVPO}_4\text{F}$  was described first by Barker et al [1]. The two-step synthesis based on a carbothermal reduction (CTR) requires, at the beginning, preparation of a  $\text{VPO}_4$  precursor. The process is carried out for 4-6 hrs at 300-350 °C in presence of a neutral gas atmosphere flow. Then the product, after mixing with LiF, is annealed at 700-800 °C for 0.5-2 hr. Other routs employ hydrothermal method, in which starting materials are reacting in an autoclave under high pressure and elevated temperature for 3-5 days [2].

In our approach we employ also the CTR process but stimulated by a microwave radiation heating. Such processing shortens a synthesis duration to the order of tens of minutes. Additionally, a graphite-powder-wrap we apply, combined with a short-time radiation inhibit  $\text{V}^{3+}/\text{V}^{4+}$  oxidation, so there is no need to use a neutral gas protection. Also we demonstrate, that the whole, two-step synthesis, one can proceed by the means of a domestic appliance - a microwave oven. All mentioned characteristics indicate that the method we propose is simpler and cheaper in comparison to the other known routes. According to our best knowledge, the microwave supported synthesis of  $\text{LiVPO}_4\text{F}$  has not been described in the literature.

## 2. EXPERIMENTAL

The  $\text{VPO}_4$  precursor was prepared from  $\text{V}_2\text{O}_5$ ,  $\text{NH}_4\text{H}_2\text{PO}_4$  and one of the: graphite, citric or oxalic acids. Appropriate amounts of the reactants after grinding with a mortar a pestle were pressed to from a pellet. This was places in an alumina crucible and covered by the graphite-powder-wrap. A direct synthesis was carried out in a domestic microwave oven operating with the nominal output radiation power of 800 W. The process was conducted for various radiation times. The X-ray diffraction method, employing Philips X'Pert Pro ( $\text{CuK}\alpha$ ), was used for examination of the quality of both precursor and the final product. When the first-

step of the synthesis was successful in production of the  $\text{VPO}_4$ , then such material was selected for the second-step of the synthesis, even if it contained other unwanted by-products. During that stage, the fabricated precursor material was ground together with LiF and then pelletized. The final microwave heating was proceeded similarly like for the first-step reaction, although different radiation times were applied. Fig 1. presents, as an example, the X-ray pattern of the synthesized lithium vanadium fluorophosphate.

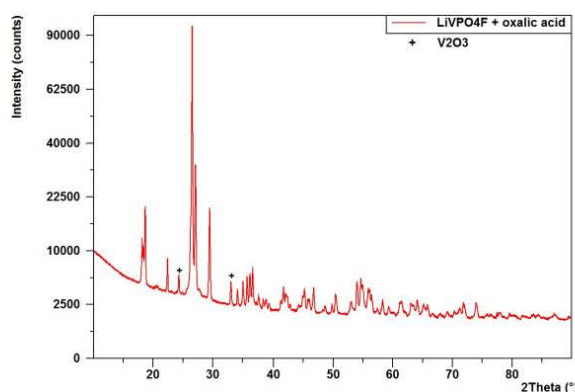


Fig. 1: The X-ray pattern for the product after 15 min. microwave irradiation.

## 3. CONCLUSIONS

In the work we demonstrate that the  $\text{LiVPO}_4\text{F}$  cathode material can be produce by the microwave radiation way. The method is simple and cheap, and competitive in comparison to other ones reported in the literature.

## REFERENCES

1. J. Barker, M.Y. Saidi and J.L. Swoyer, J. Electrochem. Soc. 150 (2003) A13,
2. B. Ellis, Thesis, Waterloo University, Ontario, Canada, 2013.



# Electrochemical properties and *in-situ* XRD studies of LiFeO<sub>2</sub> based composites.

*A. Kulka, K. Świerczek and J. Molenda*

AGH University of Science and Technology  
Faculty of Energy and Fuels, Department of Hydrogen Energy  
Al. Mickiewicza 30, 30-059 Krakow, Poland  
e-mail: molenda@agh.edu.pl

Keywords: Li-ion batteries, *in-situ* XRD, LiFeO<sub>2</sub>, phase transition

## INTRODUCTION

Iron based cathode materials for Li-ion batteries are especially interesting in terms of their non-toxicity and low fabrication costs. In past decade LiFeO<sub>2</sub> have attracted considerable research attention mainly due to its high theoretical capacity. This material however is metastable upon lithium insertion/deinsertion process what is regarded as a significant obstacle standing in the way for its wider commercialization. Here we present evaluation of electrochemical properties of stable LiFeO<sub>2</sub>/Mo glassy phase composites. We discuss *in-situ* XRD studies of phase transition occurring upon Li insertion/deinsertion during formation of LiFeO<sub>2</sub> based composites.

## EXPERIMENTAL

We manufactured lithium ion battery unit, which can be mounted on a sample stage in XRD apparatus, accustomed for simultaneous galvanostatic and XRD measurements. Gas-tight, *in-situ* XRD Li-ion battery unit is composed of metal and Teflon containers, sealed by gaskets and tighten by screws. Beryllium window acts as a current collector from the cathode material side, as well as is the X-rays transparent medium. *In-situ* accustomed Li/Li<sup>+</sup>/cathode material cells were assembled in MBraun glove box. The XRD measurements were performed using PANalytical Empyrean diffractometer equipped with Pixcell 3D detector and CuK<sub>α</sub> radiation tube.

LiFeO<sub>2</sub>/Mo glassy phase composites were synthesized by simple high-temperature method and subsequent charge/discharge in Li-ion cells. Li-ion coin cells were assembled in Mbraun glove box using lithium metal as a negative electrode, LiFeO<sub>2</sub>-based cathode and 1 M solution of LiPF<sub>6</sub> in ethylene carbonate/diethyl carbonate (EC/DEC) as the electrolyte. Electrochemical tests were performed using KEST galvanostat in 1.5-4.4 V voltage range.

## RESULTS AND DISCUSSION

Obtained composites show remarkably high and stable discharge capacity during charge/discharge process. It was found that Mo-glassy phases stabilize crystal structure of LiFeO<sub>2</sub> which is present after 60 charge/discharge cycles. *In-situ* XRD measurements were employed in order to investigate the evolution of crystal structure of LiFeO<sub>2</sub> during first and forth charge/discharge process. In order to discuss developed

*in-situ* XRD measurements technique exemplary results are also presented.

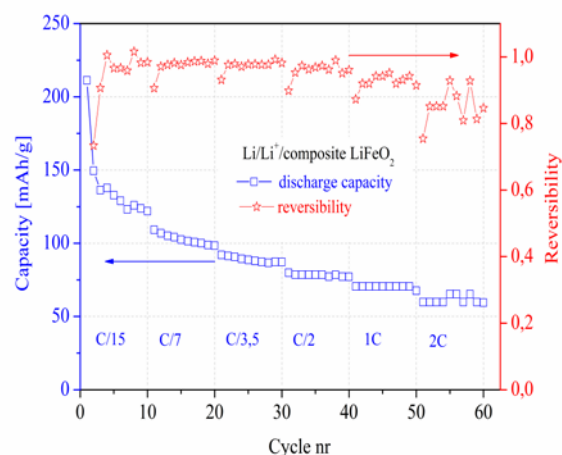


Fig. 1. Discharge capacity and reversibility of Li/Li<sup>+</sup>/LiFeO<sub>2</sub> cells as a function of cycle number and discharge rate.

## CONCLUSIONS

Our result indicate possibility of stabilization of LiFeO<sub>2</sub> metastable phase during lithium insertion/deinsertion process by introduction Mo-glassy phases. We also discuss *in-situ* XRD measurements technique in terms of its application in selected electrode materials.

## ACKNOWLEDGMENT

Work was supported by the Polish-Swiss Research Programme under grant no. 080/2010 LiBeV and the Polish Ministry of Science and Higher Education, under project AGH No. 11.11.210.911.



# Enhancing of electrochemical properties of crystalline nanometric LiFePO<sub>4</sub>

*K. Polak, K. Walczak, A. Kulka, W. Zajac and J. Molenda*

AGH University of Science and Technology  
Faculty of Energy and Fuels, Department of Hydrogen Energy  
Al. Mickiewicza 30, 30-059 Krakow, Poland  
e-mail: molenda@agh.edu.pl

Keywords: Li-ion batteries, LiFePO<sub>4</sub>, nano-materials,

## INTRODUCTION

Among iron-based cathode materials for Li-ion batteries LiFePO<sub>4</sub> is considered as the most promising one since it possesses high operational voltage (about 3.4 V versus lithium metal), high theoretical capacity (about 170 mAh/g) as well as high thermal and chemical stability. Moreover due to its' chemical formula LiFePO<sub>4</sub> is environmentally benign and cheap. Phospholivine possesses low ionic and electronic conductivity which severely limits its performance as a cathode material and is major obstacle in wider application in lithium ion batteries with high energy density. Transition to the nano-scale is an effective way of improvement of electrochemical properties due to decrease of the lithium-ion diffusion path length within LiFePO<sub>4</sub> particle. Here we present evaluation of low temperature synthesis conditions in order to obtain LiFePO<sub>4</sub> with reduced Fe<sup>3+</sup> content and LiFePO<sub>4</sub>/Fe<sub>2</sub>P composites.

## EXPERIMENTAL

We present low-cost synthesis method based on the co-precipitation reaction of nanometric LiFePO<sub>4</sub> from LiOH, FeSO<sub>4</sub> and H<sub>3</sub>PO<sub>4</sub> solutions composed of water and organic liquids. Influence of addition of reducing agents during one-step synthesis procedure such as potassium iodide, ammonium thiosulfate, glucose or reducing atmospheres on concentration of Fe<sup>3+</sup> cations in LiFePO<sub>4</sub> precipitates is evaluated. Method of fabrication of LiFePO<sub>4</sub>/Fe<sub>2</sub>P composites based on high-temperature annealing in reducing atmospheres of nanometric LiFePO<sub>4</sub> is presented.

Relationship between concentration of Fe<sup>3+</sup> ions and electrochemical properties of cathode materials based on obtained phospholivines is investigated by means of Moessbauer measurements, charge/discharge and cyclic voltammetry tests. Microstructure of obtained precipitates was verified by TEM and SEM techniques. Li/Li<sup>+</sup>/LiFePO<sub>4</sub> cells were electrochemically tested using KEST galvanostat in 2.5-4.4 V voltage range.

## RESULTS AND DISCUSSION

Synthesized powders were found to possess plate-like morphology. Li-ion cells with cathode materials based on obtained phospholivines showed discharge capacity equal to 95% of theoretical capacity of LiFePO<sub>4</sub> at C/5 discharge current rate. It was found that

use of reducing agents effectively reduces Fe<sup>3+</sup> to Fe<sup>2+</sup> ions during low-temperature fabrication process.

It was found that the morphology of obtained LiFePO<sub>4</sub>/Fe<sub>2</sub>P composites varies as a function of annealing time and temperature. Optimized LiFePO<sub>4</sub>/Fe<sub>2</sub>P composites showed discharge capacity equal to 95% of theoretical capacity of LiFePO<sub>4</sub> at C/5 discharge current rate.

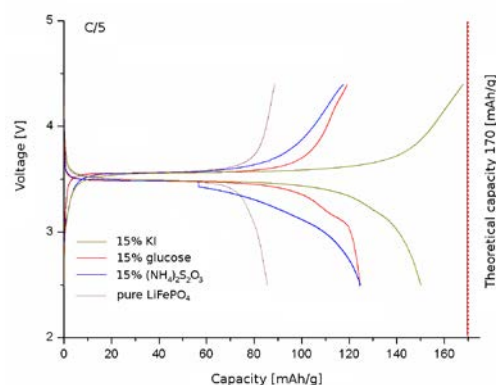


Fig. 1. Charge/discharge profiles of Li/Li<sup>+</sup>/LiFePO<sub>4</sub> cell based on nanometric phosphoolivines prepared with presence of reducing agents, compared with pure LiFePO<sub>4</sub> at C/5 discharge current rate.

## CONCLUSIONS

Our result eliminates necessity of heat treatment stage of phospholivine powders aiming to reduce Fe<sup>3+</sup> ions and enables fabrication of nanometric LiFePO<sub>4</sub> with enhanced electrochemical properties at temperatures as low as 105°C. We also discuss the structural and electrochemical properties of LiFePO<sub>4</sub>/Fe<sub>2</sub>P composites.

## ACKNOWLEDGMENT

Work was supported by the Polish-Swiss Research Programme under grant no. 080/2010 LiBeV and the Polish Ministry of Science and Higher Education, under project AGH No. 11.11.201.911.

# IN-SITU STRUCTURAL STUDIES OF MANGANESE SPINEL-BASED CATHODE MATERIALS

*L. Kondracki, A. Kulka, A. Milewska, J. Molenda*

Department of Hydrogen Energy, Faculty of Energy and Fuels,  
AGH University of Science and Technology, al. A Mickiewicza 30, 30-059 Kraków  
e-mail: molenda@agh.edu.pl

Keywords: Li-ion batteries, in-situ XRD,  $\text{LiMn}_{1.5}\text{Ni}_{0.5-y}\text{Cu}_y\text{O}_4$ , phase transition

## INTRODUCTION

One of the most interesting materials that is considered for application in technology of Li-ion batteries is  $\text{LiMn}_2\text{O}_4$ , more affordable and less toxic material than commonly used  $\text{LiCoO}_2$ . The nickel-doped spinels exhibit a 4.7V-plateau and therefore they are attractive candidates for high-voltage Li-ion batteries. This work focuses on crystal structure, namely *in-situ* studies of  $\text{LiMn}_{1.5}\text{Ni}_{0.5}\text{O}_4$ ,  $\text{LiMn}_{1.5}\text{Ni}_{0.45}\text{Cu}_{0.05}\text{O}_4$  spinels and  $\text{LiMn}_2\text{O}_4$  reference material.

## EXPERIMENTAL

To obtain all the materials a synthesis by sol-gel method was carried out. Soluble salts of relevant cations were dissolved in deionized water, that had been treated with argon. Small amount of ammonia solution was added into the solution until the pH of 9.1 was reached. Such obtained sol was dried at 90°C for 48hrs, then annealed at 350°C and 800°C, respectively for 24 and 6 hrs. Series of  $\text{LiMn}_2\text{O}_4$  (reference material),  $\text{LiMn}_{1.5}\text{Ni}_{0.5}\text{O}_4$ ,  $\text{LiMn}_{1.5}\text{Ni}_{0.45}\text{Cu}_{0.05}\text{O}_4$  were obtained.

Such obtained materials were mixed with carbon black and PVDF manufactured lithium ion battery unit, which can be mounted on a sample stage in XRD apparatus, accustomed for simultaneous galvanostatic and XRD measurements. Gas-tight, in-situ XRD Li-ion battery unit is composed of metal and Teflon containers, sealed by gaskets and tighten by screws. Beryllium window acts as a current collector from the cathode material side, as well as is the X-rays transparent medium. In-situ accustomed  $\text{Li}/\text{Li}^+/\text{Li}_x\text{Mn}_2\text{O}_4$   $\text{Li}/\text{Li}^+/\text{LiMn}_{1.5}\text{Ni}_{0.5-y}\text{Cu}_y\text{O}_4$  cells were assembled in MBraun glove box using lithium as a negative electrode,  $\text{LiMn}_2\text{O}_4$ - and  $\text{LiMn}_{1.5}\text{Ni}_{0.5-y}\text{Cu}_y\text{O}_4$ -based cathode and 1 M solution of  $\text{LiPF}_6$  in ethylene carbonate/diethyl carbonate (EC/DEC) as the electrolyte. The XRD measurements were performed using PANalytical Empyrean diffractometer equipped with Pixcel 3D detector and  $\text{CuK}\alpha$  radiation tube.

## RESULTS AND DISCUSSION

The evolution of [400] and [311] reflection is shown in Fig. 1. We did not observe any significant difference between change of lattice parameters for materials examined *in-situ* and after relaxation. The results obtained for reference materials are shown in Fig. 1.

## CONCLUSIONS

The studies revealed that the mechanism of intercalation of lithium into manganese spinel-based materials is single phased for both pristine  $\text{LiMn}_2\text{O}_4$  and doped spinels. Below the lithium content of 0.5 mole/mole of  $\text{Li}_x\text{Mn}_2\text{O}_4$  for pristine material the change of lattice cell parameter is more rapid. This is connected most

probably with the lithium ordering in the lattice occurring at  $x_{\text{Li}} \approx 0.5$ .

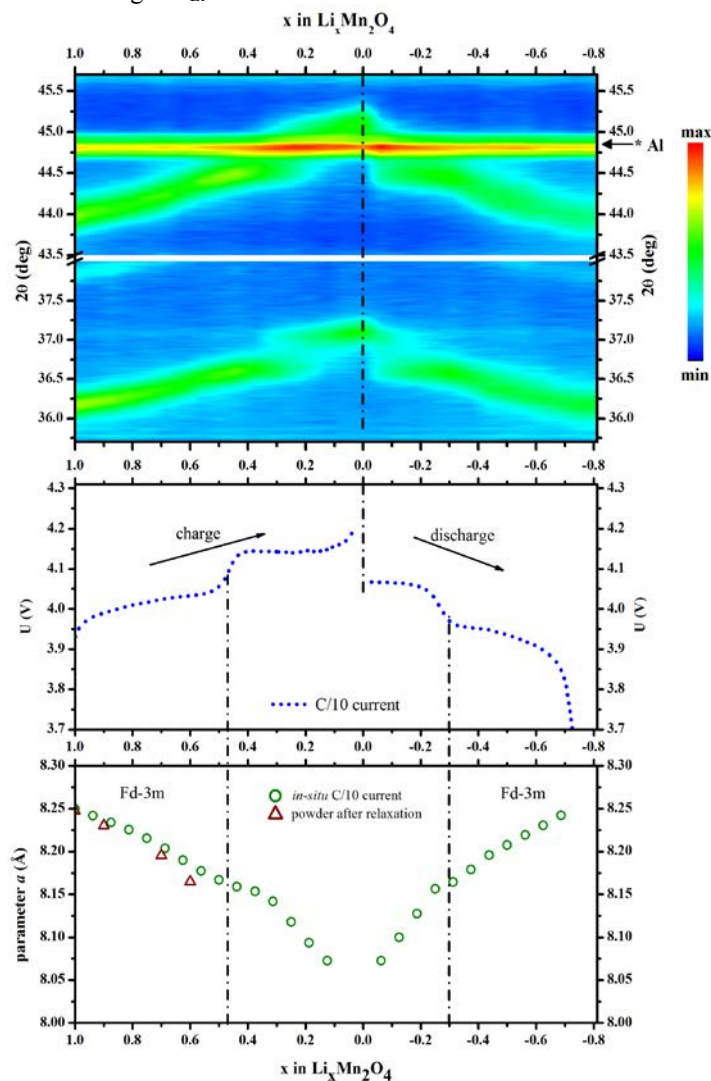


**Fig. 1.** Results of XRD *in-situ* measurements of electrochemically deintercalated/intercalated  $\text{Li}_x\text{Mn}_2\text{O}_4$  for 1 cycle of  $\text{Li}/\text{Li}^+/\text{Li}_x\text{Mn}_2\text{O}_4$  cell. Enlargement of XRD patterns showing position changes of [400] and [311] peaks of  $\text{Li}_x\text{Mn}_2\text{O}_4$  with corresponding change of voltage and change of  $a$  parameter of Fd-3m phase during charge and discharge. Reflection of [200] Al plane is also marked.

## ACKNOWLEDGMENT

Project supported by a grant from Switzerland through the Swiss Contribution to the enlarged European Union (grant no. 080/2010 LiBEV *Positive Electrode Materials for Li-ion Batteries for Electric Vehicles*)

## REFERENCES

L. Wang, H. Li, X. Huang, E. Baudrin, *Solid State Ionics*, 193 (2011) 32-38

# TOWARDS ELUCIDATION OF THE UNIQUE ELECTROCHEMICAL PROPERTIES OF $\text{Na}_x\text{CoO}_{2-y}$

*D. Baster, J. Molenda*

Faculty of Science and Technology  
AGH University of Science and Technology, Faculty of Energy and Fuels  
al. Mickiewicza 30, 30-059 Krakow, Poland  
e-mail: molenda@agh.edu.pl

Keywords: Na-ion batteries, cathode material,  $\text{Na}_x\text{CoO}_{2-y}$

## INTRODUCTION

$\text{P2-Na}_x\text{CoO}_2$  has attracted much attention due to its remarkable electronic features together with unusual electrochemical behavior [1], [2].  $\text{P2-Na}_x\text{CoO}_2$  system possesses astonishing phase diagram with many competing phenomena, such as strong electronic correlations and geometrical frustration of the antiferromagnetic interactions on triangular lattice. Electrochemical studies of  $\text{P2-type Na}_x\text{CoO}_{2-y}$  ( $x \approx 0.7$ ) as a cathode material for sodium batteries revealed step-like character of discharge curve, with several pseudo-plateaus [1].

The present work shows comprehensive studies on the crystal structure and microstructure, together with detailed electrochemical investigations, including cyclic voltammetry and charge/discharge curves.

## EXPERIMENTAL

$\text{Na}_{0.72}\text{CoO}_2$  was synthesized by a solid-state high-temperature reaction in air at  $850^\circ\text{C}$  for 24 h with an intermediate grinding. Crystal structure of the considered material was investigated in using X-ray diffraction (XRD) method on Panalytical Empyrean diffractometer with  $\text{Cu K}\alpha$  radiation. Electrochemical studies were carried out in electrochemical  $\text{Na}/\text{Na}^+/\text{Na}_x\text{CoO}_{2-y}$  cells. Low-temperature electrical conductivity and thermoelectric power were determined by a 4-probe AC method and dynamic method, respectively.

## RESULTS AND DISCUSSION

XRD diffractogram at room temperature of the synthesized sodium cobaltate was refined by Rietveld analysis using hexagonal crystal system with  $P6_3/mmc$  space group [1]. Fig. 1 shows results of current rate influence on the electrochemical behavior of  $\text{Na}/\text{Na}^+/\text{Na}_x\text{CoO}_2$  cells, as recorded during discharge for currents in  $C/50$  to  $C/5$  range. Apart from the expected decrease of the capacity for high currents, another interesting effect can be noticed: small voltage steps visible near 2.5 V disappear for higher current rates, making the voltage curve to appear more smooth. For higher currents, the deintercalation/intercalation process proceeds far from the equilibrium state. Additional voltammetry studies performed for low scanning rates are shown in Fig. 2. The observed behavior with several characteristic anodic and cathodic peaks corresponds very well with discharge curves (Fig. 1).

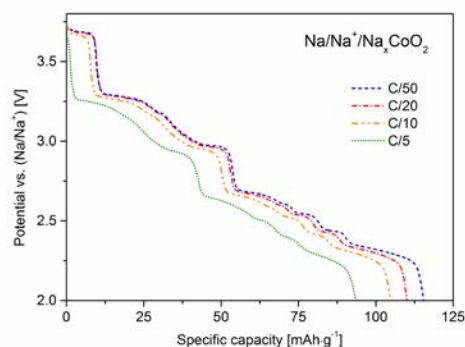


Fig. 1. Discharge curves of  $\text{Na}/\text{Na}^+/\text{Na}_x\text{CoO}_2$  cells measured for  $C/50$  to  $C/5$  current range.

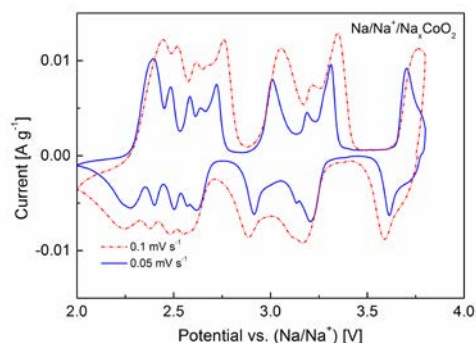


Fig. 2. Voltammetry studies of  $\text{Na}/\text{Na}^+/\text{Na}_x\text{CoO}_2$  cell with scan rates 0.05 and  $0.1\text{ mV}\cdot\text{s}^{-1}$ .

## CONCLUSIONS

Electrochemical studies confirmed presence of several pseudo-plateaus on discharge curves of  $\text{Na}/\text{Na}^+/\text{Na}_x\text{CoO}_2$  cells, which can be related to characteristic anodic and cathodic peaks on voltammograms.

## ACKNOWLEDGMENTS

This work is supported by the Polish-Swiss Research Programme under grant no. 080/2010 LiBEV (Positive Electrode Materials for Li-ion Batteries for Electric Vehicles) and the financial support from the Polish Ministry of Science and Higher Education, under project AGH No. 11.11.210.911.

## REFERENCES

- [1] "R. Berthelot, D. Carlier, C. Delmas, Nature Materials 10 (2011) 74."
- [2] "M. L. Foo, Y. Wang, S. Watauchi, H. W. Zandbergen, T. He, R. J. Cava, N. P. Ong, Phys. Rev. Lett. 92 (2004) 247001-1."

# EFFECT OF CONDUCTIVE CARBON LAYERS ON STRUCTURAL AND ELECTROCHEMICAL PROPERTIES OF C/LiFePO<sub>4</sub> NANOCOMPOSITE CATHODE MATERIAL

*J. Świder, M. Molenda\* and R. Dziembaj*

Faculty of Chemistry  
Jagiellonian University, ul. Ingardena 3  
30-060 Cracow, Poland  
e-mail: : molendam@chemia.uj.edu.pl

Keywords: Li-ion batteries, lithium iron phosphate, LiFePO<sub>4</sub>, carbon nanocoatings, carbon conductive layers, CCL

## INTRODUCTION

There is currently a strong drive towards the improvement of LiFePO<sub>4</sub> (LFP) properties in order to fully exploit its potential as cathode material in large scale Li-ion batteries [1]. It is possible to overcome limitation related with the poor electronic and ionic conductivities by minimizing the particles size [2] and coating the material grains by carbon [3]. The C/LiFePO<sub>4</sub> composite was confirmed as an effective solution for the enhancement of electrochemical properties of LiFePO<sub>4</sub> cathode material. Attempts have been made to find optimal parameters of preparation conductive carbon layers (CCL) onto electrode materials, with different morphology, for lithium ion batteries [4,5].

In the present study, the effects of carbon content in CCL/LFP composites were investigated in terms of their morphological and electrochemical properties.

## EXPERIMENTAL

Technological process of coating active material by CCL consists of two main stages [6]:

- preparation of carbon precursor - as polymer carbon precursors were used poly-N-vinylformamide (PNVF) modified by pyromellitic acid (5% content);
- wet impregnation of LFP material and pyrolysis of composite precursor under controlled condition.

## RESULTS AND DISCUSSION

The crystal structures and morphology of all the composites were characterized by X-ray powder diffraction (XRD), nitrogen adsorption/desorption measurements (N<sub>2</sub>-BET), Transmission Electronic Microscopy (TEM) and Raman spectroscopy.

Electrical properties of C/LiFePO<sub>4</sub> materials were investigated using an electrical conductivity measurements (EC) (4-probe AC method within temperature range of -20°C to +40°C). The electrochemical performance was carried out in galvanostatic mode with stable charge-discharge current and performed in Li/Li<sup>+</sup>/(CCL/LFP) type cells. As an electrolyte was used solution of 1M lithium

hexafluorophosphate (LiPF<sub>6</sub>) dissolved in mixture of EC:DMC = 1:1.

## CONCLUSIONS

Carbon coated LiFePO<sub>4</sub> powder products with the olivine-type structure has been successfully obtained using wet impregnation method. The C/LiFePO<sub>4</sub> nanocomposites on account of homogeneous carbon dispersion effectively enhances its electrochemical performance.

Presented technology is very valuable and process of producing carbon coated LiFePO<sub>4</sub> cathode materials according to described method requires optimization and scaling up for industrial production.

## ACKNOWLEDGMENT

This work is supported by National Science Centre, Poland under research grant no. 2014/13/B/ST5/04531.

## REFERENCES

1. A.K. Padhi, K.S. Nanjundaswamy, J.B. Goodenough, *J. Electrochem. Soc.* **144** (1997) 1188–1194
2. T. Liu, L. Zhao, D. Wang, J. Zhu, B. Wang, C. Guo, *RSC Adv.* **4** (2014) 10067-10075
3. K. Zaghbi, J. Dubé, A. Dallaire, K. Galoustov, A. Guerfi, M. Ramanathan, A. Benmayza, J. Prakash, A. Mauger, C.M. Julien, *J. Power Sources* **219** (2012) 36-44
4. M. Molenda, R. Dziembaj, Z. Piwowarska, M. Drozdek, A new method of coating of powdered supports with conductive carbon films, *J. Therm. Anal. Cal.* **88(2)** (2007) 503-506
5. M. Molenda, M. Świątosławski, M. Drozdek, B. Dudek, R. Dziembaj, Morphology and electrical conductivity of carbon nanocoatings prepared from pyrolysed polymers, *J. Nanomaterials* **2014** (2014) 1-7
6. M. Molenda, R. Dziembaj, A. Kochanowski, E. Bortel, M. Drozdek, Z. Piwowarska, PAT.216549; US 8,846,135 B2; JP 5476383 B2



# ELECTRONIC SYSTEM FOR PULSE ENERGY STORAGE

*Bartłomiej Tomasiak, Anna Plewa and Jacek Leszczyński*

AGH University of Science and Technology  
Faculty of Energy and Fuels, Department of Hydrogen Energy  
Al. Mickiewicza 30, 30-059 Krakow, Poland  
e-mail: {luisbartek, annaplewa09}@gmail.com, jale@agh.edu.pl

Keywords: pulse power energy, storage, capacitor, battery, microcontroller

## INTRODUCTION

Pulses of energies reveal in many cases in nature [1]. The pulse means as a rapid jump of energy generated randomly over time, having random time width, and having random amplitudes. Such pulses may observe in energy harvesting devices, renewable sources of energy, weapons, accidents, etc. In previous decade, the energy pulses, due to their disadvantages as random behaviour, low energy levels, were determined as energy losses. Today, pulses of energy are a great of industrial interest [2,3] because there is a chance to increase energy efficiency in any system or to build autonomous systems. One of possible way transfers arbitrary form of energy to the electrical one. The electrical energy is easy to storage in batteries.

In this study we focus on the electronic system which is convenient to manage and storage the pulses of electrical energy in batteries.

## EXPERIMENTAL

During the work there were used two energy storage devices. There were batteries and supercapacitors. Batteries had a large energy density but a small power density. At the opposite, supercapacitors had a very low energy density but a large power density, so energy could be transferred very quickly but not much energy can be stored. Thus the cooperation of these two elements can be very effective.

As shown in Figure 1, the system for energy storage consists of generator, resistance, battery pack and supercapacitors, which are connected with charging/discharging control system.

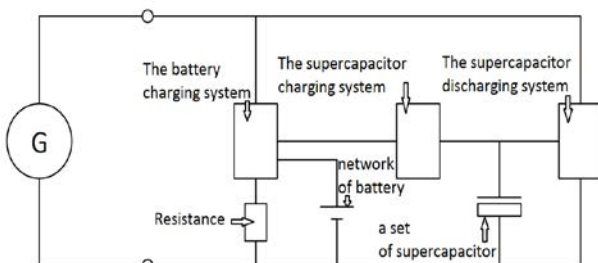


Figure 1. Scheme of system for pulse energy storage.

The range of voltage for the generation is 0-20V and the maximum current equals to 5A. The generator provides a pulse of energy. At the beginning the battery pack is charged. The charging current is 0,9A. Once the level of voltage is too high and the battery pack cannot be charged the system transfers energy current to the supercapacitors. When supercapacitors are fully charged (up to  $U_c=16V$ ) the current flows to resistance. In case of turning off the generator, batteries take energy stored in supercapacitors.

## RESULTS AND DISCUSSION

The voltage on generator, batteries and supercapacitors were measured over time. The width and the frequency of impulses were manually changed and effects were observed. Thus it was possible to define some charging and discharging phases for both batteries and supercapacitors. It may observe a correlation between picks provided by generator and the voltage on storage devices.

## CONCLUSIONS

In conclusion the test results show that there were developed a system that is able to storage pulses of energies. It is working in different conditions and it does not relay on width of the impulse. In the future the project will adapt to storage the pulses of energies from renewable energy sources.

## ACKNOWLEDGMENT

This work is supported the Polish Ministry of Science and Higher Education, under contact AGH No. 11.11.210.911.

## REFERENCES

1. Luo X., Wang J., Dooner M., Clarke J., Overview of current development in electrical energy storage technologies and the application potential in power system operation, *Applied Energy* **137** (2015) 511–536
2. Senthil K., Mitra S., Roy A. *et al*, Compact inductive energy storage pulse power system, *Review of Scientific Instruments* **83** (2012) 054703
3. Crider J., Sudhoff S., Reducing Impact of Pulsed Power Loads on Microgrid Power Systems, *IEEE Transactions on Smart Grid* **1(3)** (2010) 270-277

# TOWARDS NEW SEI-FORMING ADDITIVES FOR LITHIUM-ION BATTERIES

*P. Jankowski*<sup>1,2</sup>, *P. Johansson*<sup>2</sup> and *W. Wieczorek*<sup>1</sup>

<sup>1</sup>Faculty of Chemistry, Warsaw University of Technology, Noakowskiego 3, 00-664 Warsaw, Poland

<sup>2</sup>Department of Applied Physics, Chalmers University of Technology, SE-412 96 Gothenburg, Sweden

Keywords: lithium-ion batteries, passivation layer, computations

## INTRODUCTION

Lithium-ion batteries (LIBs), despite almost quarter of a Century of commercialization, are still an area of intense studies. Their improvement is aimed at two main cases: expansion of the energy density of the cell; increasing lifetime and stability of battery during operation. The first is performed primarily by applying novel electrode materials with higher voltages of intercalation [1] and also requires development of electrolytes with broader electrochemical stability windows [2]. The latter is usually accomplished by special additives; compounds to reduce adverse processes occurring at the interface between electrode and electrolyte [3].

Currently the most used electrolyte – solution of LiPF<sub>6</sub> in a mixture of organic carbonates – is thermodynamically unstable against low potentials of anode. The reduction of carbonates occur at approximately 1 V vs. Li, while the intercalation of lithium cations between the graphene layers of graphite occurs below 0.2 V vs. Li [4]. Hence, this leads to electrolyte decomposition products, which deposit on the electrode surface during cycling and form a layer – the Solid Electrolyte Interphase (SEI). The SEI mainly consists of inorganic Li<sub>2</sub>CO<sub>3</sub> and oligomer-like compounds. Its task is to protect electrolyte against contact with negative electrode and not to hinder the transport of lithium cations between the electrolyte and the electrode. Therefore, the properties of this layer affect many important parameters such as cycle life, coulombic efficiency, irreversible capacity, power density and safety. The attempts to control the SEI creation process, instead of the spontaneous formation, may lead to improvement of these key battery properties.

Applying functional electrolytes is postulated as the best way to control the SEI [5]. Such an electrolyte contains additive compounds, responsible for the formation of SEI. The additive has a higher reduction potential, whereby its decomposition occurs before the carbonate reduction. This approach makes the process of forming the SEI more controlled, which can be managed by selecting appropriate compounds as the additives. The emerged SEI-layer must have a high lithium cation conductivity and hinder electrons. The desired SEI is thin, well adherent to the electrode layer, containing oligo- or even polymeric compounds, similar to polymer electrolytes. Controlled and rapid formation of a protective layer also prevents cointercalation of solvent molecules.

## RESULTS AND DISCUSSION

During presentation, there will be showed the line of thought that leads from the quantum modeling to the tests of new additives in real systems. Proper designed model and conducted analysis allow for well prediction such significant data as reduction potential and reduction path with determination of the decomposition products. The use of these computational techniques for screening, significantly facilitates the search for new, better compounds, which could act as SEI-forming additives. The confrontation of our predictions with experimental data allows us to validate used method and test their effectiveness in real battery systems.

## ACKNOWLEDGMENT

Calculations have been carried out at the Wrocław Centre for Networking and Supercomputing (<http://www.wcss.pl>), grant No. 346. The support by Chalmers Area of Advance Energy for a travel scholarship is gratefully acknowledged

## REFERENCES

1. V. Etacheri; R. Marom; R. Elazari; G. Salitra; D. Aurbach, *Energy Environ. Sci.*, **4** (2011) 3243.
2. L. Niedzicki; S. Grugeon; S. Laruelle; P. Judeinstein; M. Bukowska; J. Prejzner; P. Szczeniński; W. Wieczorek; M. Armand, *J. Power Sources*, **196** (2011) 8696.
3. K. Xu, *Chem. Rev.*, **114** (2014) 11503.
4. J. O. Besenhard, M. Winter, J. Yang, W. Biberacher, *J. Power Sources* **54** (1993) 228
5. T. R. Jow; K. Xu; O. Borodin; M. Ue, “*Electrolytes for Lithium and Lithium-Ion Batteries*”, Springer, New York 2014



# GENERATION OF METHANOL THROUGH PHOTOELECTROCHEMICAL REDUCTION OF CARBON DIOXIDE

*Ewelina Szaniawska, Krzysztof Bienkowski, Renata Solarska, Iwona A. Rutkowska, Pawel J. Kulesza*

Faculty of Chemistry, University of Warsaw, Pasteura 1, PL-02-093 Warsaw, Poland

Due to gradual decline of energy resources, there has been growing interest in new energy systems that include direct transformation of solar energy to chemical energy using oxide semiconductor materials. Furthermore, carbon dioxide (CO<sub>2</sub>), as the primary greenhouse gas also emitted through human activities, could be converted using sunlight to organic compounds. The approach permits simultaneous generation of alternative fuels and environmental remediation of carbon emissions from the continued use of conventional fuels.

The aim of this work has been to develop hybrid materials by utilizing combination of metal oxide semiconductors thus capable of effective photoelectrochemical reduction of carbon dioxide. The combination of titanium (IV) oxide (TiO<sub>2</sub>) and copper (I) oxide (Cu<sub>2</sub>O) has been explored toward the reduction of carbon (IV) oxide (CO<sub>2</sub>) before and after sunlight illumination. Application of the hybrid system composed of both above-mentioned oxides resulted in high current densities originating from photoelectrochemical reduction of carbon dioxide mostly to methanol (CH<sub>3</sub>OH) as demonstrated upon identification of final products.

In particular, fabrication of the hybrid system (heterojunction photocathode) of TiO<sub>2</sub> and Cu<sub>2</sub>O (on the conducting glass) has required first the cathodic electrodeposition copper (I) oxide (at -0.64V vs. Hg/Hg<sub>2</sub>SO<sub>4</sub> from a basic solution of 3 mol/dm<sup>3</sup> lactate-stabilized 0.4 mol/dm<sup>3</sup> copper (I) sulfate). The latter step has been followed by sputtering n-type titanium (IV) oxide. The spectral responses of the Cu<sub>2</sub>O/TiO<sub>2</sub> electrode is comparable to that of simple Cu<sub>2</sub>O, and the photoresponse is enhanced at relatively short wavelengths. It is reasonable to expect that the light absorbed by the inner Cu<sub>2</sub>O film produces energetic electron (e<sup>-</sup>) – hole (h<sup>+</sup>) pairs. The excited electrons are driven through the conduction band to the external TiO<sub>2</sub>/electrolyte interface. The role of TiO<sub>2</sub> is not stabilizing; the oxide is also expected to prevent the recombination of charge carriers (e<sup>-</sup> - h<sup>+</sup> pairs). By using gas chromatography with the flame ionization detector, it was confirmed that methanol predominates as a final product.

# NANOPARTICLES-SENSITIZED TiO<sub>2</sub> FOR A PHOTO-ACTIVE ELECTRODE IN PHOTOELECTROCHEMICAL CELL

*J. Banaś and A. Trenczek-Zajac*

Faculty of Materials Science and Ceramics  
AGH University of Science and Technology, ul. Mickiewicza 30  
30-059 Cracow, Poland  
e-mail: banasjk@gmail.com

Keywords: TiO<sub>2</sub>, CdS, Ag<sub>2</sub>S, photoelectrochemical cell, hydrogen generation

## INTRODUCTION

Materials considered as a photoelectrodes in Photo-Electrochemical Cells (PECs) used to produce hydrogen should meet two fundamental requirements: the first one is optical features allowing to maximize absorption of the solar energy, and the second one is exhibiting catalytic properties enabling decomposition of water. It is also of particular importance for a candidate to possess both corrosion resistance in the water-based electrolytes as well as an appropriate microstructure. Among materials which fulfill these demands there is a certain group of semiconducting oxides with the titanium dioxide at the forefront [1]. The only drawback of TiO<sub>2</sub> is the limited absorption in the visible range of light. Therefore, from the designing point of view it is essential to choose a preparation method that allows to produce TiO<sub>2</sub> with an extended absorption in the visible range of light.

Several approaches were concerned both with methods and materials utilized as photo-electrode sensitizers [2,3]. One of the methods that deserves a special attention due to substantial effect on microstructure and of which have not yet been given a deep insight is oxidation of the titanium foil that leads to formation of TiO<sub>2</sub> layer. Additionally, deposition of the metal-oxides nanoparticles (e.g. CdS, Ag<sub>2</sub>S), can provide beneficial impact on photoresponse of TiO<sub>2</sub>.

## EXPERIMENTAL

The first step in the samples preparation process was etching of titanium foil in HCl at 55 or 80°C for 5-60 min. Etched samples were thermally annealed at the temperatures between 500-900°C for 7h. CdS and Ag<sub>2</sub>S nanoparticles were deposited onto TiO<sub>2</sub> by the subsequent ionic layers adsorption and reaction SILAR procedure. In order to obtain information concerning transformation of Ti→TiO<sub>2</sub> layer, the variety of research methods were used: XRD, SEM, spectrophotometry, and I-V measurements in the PEC.

## RESULTS AND DISCUSSION

SEM analysis of HCl-etched Ti foils shows that in the case of both 55 and 80°C the increase in time causes a significant changes in the titanium surface. This is confirmed by XRD results – etching in hot HCl gradually removes lower titanium oxides, e.g. TiO, Ti<sub>3</sub>O, Ti<sub>6</sub>O, furthermore, it also leads to some incorporation of hydrogen into the structure of titanium. This is demonstrated by the presence of TiH<sub>x</sub> (x=1-2) reflections in the diffraction pattern.

Comparison between SEM images of oxidized samples reveals that samples oxidized at the same tempera-

ture but etched at 80°C have larger grains. XRD analysis have shown that 700°C is the temperature for entire transformation of titanium into TiO<sub>2</sub> rutile. It was also observed that changes in the crystal structure are accompanied by changes in the spectral dependence of the total reflectance of oxidized samples. According to I-V characteristics, annealing at 600/700°C allows to obtain the highest PEC performance (Fig.1). Additionally, Ag<sub>2</sub>S and CdS nanoparticles sensitization results in increasing of photocurrent.

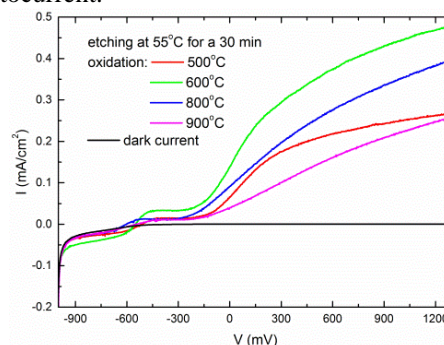


Figure 1. Current–voltage characteristics for Ti foils oxidized at different temperatures.

## CONCLUSIONS

Photoanodes based on TiO<sub>2</sub> were prepared by etching in HCl and annealing titanium foils at the temperatures between 500-900°C. According to XRD analysis annealing at 700°C leads to obtain TiO<sub>2</sub> with rutile structure. I-V characteristics confirmed that temperature ~700°C allows to obtain the best PEC performance, and the sensitization with nanoparticles leads to furthered enhancement.

## ACKNOWLEDGMENT

This work was supported by the National Science Centre (NCN) based on decision no. DEC-2011/01/D/ST5/05859. The authors would like to thank gratefully Ph.D. Magdalena Ziabka from AGH University of Science and Technology, Krakow, Poland for performing SEM analysis.

## REFERENCES

1. M. Radecka, A. Trenczek-Zajac, K. Zakrzewska, M. Rekas, *Journal of Power Sources* **173**(2007)816-821
2. M. Radecka, *Thin Solid Films* **451-452**(2004)98-104
3. A. Trenczek-Zajac, A. Kusior, A. Lacz, M. Radecka, K. Zakrzewska, *Materials Research Bulletin* **60**(2014)28–37

# OXIDATION/REDUCTION BEHAVIOR AND CATALYTIC ACTIVITY OF BaLnMn<sub>2</sub>O<sub>5+δ</sub> (Ln: LANTHANIDES, Y) OXIDES

A. Klimkiewicz<sup>1,2,\*</sup>, T. Yamazaki<sup>2</sup>, A. Takasaki<sup>2</sup>, K. Świerczek<sup>1</sup>

<sup>1</sup>AGH University of Science and Technology, Faculty of Energy and Fuels  
Department of Hydrogen Energy, al. A. Mickiewicza 30, 30-059 Krakow, Poland

<sup>2</sup>Shibaura Institute of Technology, Faculty of Engineering  
3-7-5 Toyosu, Koto-ku, 135-8548 Tokyo, Japan

\*e-mail: aklim@agh.edu.pl

Keywords: cation-ordered perovskites; crystal structure; oxygen storage; catalytic activity

## INTRODUCTION

Ceramic materials having ability to reversibly incorporate oxygen into their structure at elevated-temperatures, so called oxygen storage materials (OSM), have been recently increasingly researched.

OSMs may find potential application in many developing technologies and industrial processes, which require precise control of the oxygen partial pressure. For instance, OSMs could be used for separation of air components in a modified Pressure Swing Adsorption (PSA) or Temperature Swing Adsorption (TSA) methods, as well as in another variation of these techniques, called Vacuum Swing Adsorption (VSA), which is pursued at lowered pressure (vacuum) and near ambient temperature conditions [1]. It seems to be possible to modify the described above methods by using oxygen absorbing OSMs, instead of commonly utilized adsorbing materials, like zeolites. Furthermore, OSMs may be possibly applied in so called Ionic Transport Membranes (ITM), which allow for effective production of the oxygen [1, 2].

Here we report on structural properties, oxidation/reduction behavior and catalytic activity of perovskite-type oxides from BaLnMn<sub>2</sub>O<sub>5+δ</sub> group, having layered type of Ba-Ln arrangement. The presented studies were conducted from a point of view of oxygen storage in the considered materials.

## EXPERIMENTAL

Synthesis of BaLnMn<sub>2</sub>O<sub>5+δ</sub> materials was performed at 1100 °C for 8 h in 1 vol.% of H<sub>2</sub> in Ar atmosphere, with flow of gas of about 100 cm<sup>3</sup>min<sup>-1</sup>. Structural studies were carried out in 10-110 deg range with CuKα radiation. For high temperature measurements, Anton Paar HTK 1200N oven-chamber was installed on the diffractometer. Data for selected samples were collected in air, and in Ar and in low vacuum (~ 100 Pa).

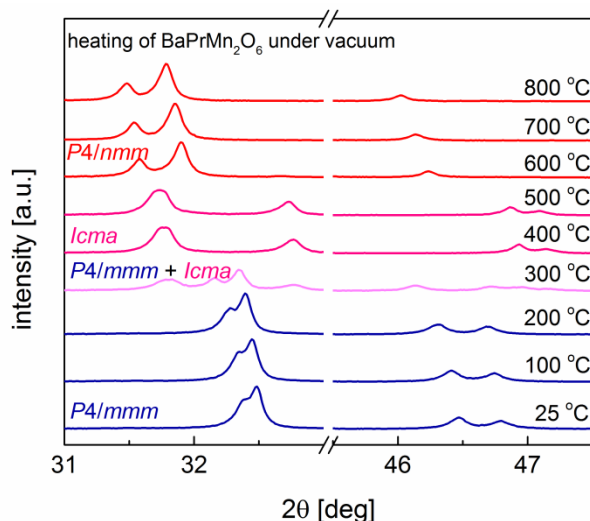
Oxygen storage-related properties were evaluated using thermogravimetric method on powdered samples. For reduction (at 400-600 °C), 5 vol.% H<sub>2</sub> in Ar mixture was used, while the oxidation process was studied in air.

Complementary catalytic activity studies of selected BaLnMn<sub>2</sub>O<sub>5+δ</sub> were conducted on a custom-made setup.

## RESULTS AND DISCUSSION

Among studied BaLnMn<sub>2</sub>O<sub>5+δ</sub> (Ln: Pr, Nd, Gd and Y) compounds, the best performance in terms of the oxygen release speed (reduction of the material) during

isothermal studies at 500 °C was measured for gadolinium-containing sample. However, during *in situ* structural studies under vacuum condition, only about 0.5 mol of oxygen was released from this material up to 800 °C. The most promising results were obtained for BaPrMn<sub>2</sub>O<sub>5+δ</sub> sample, for which release of 1 mol of oxygen per mol of the compound was documented during heating in vacuum up to 600 °C. As can be seen in the Fig. below, such investigations allowed for unique observations of the structural changes occurring in the process of reduction.



Furthermore, investigations of catalytic activity [3] of the materials point out to their ability for the effective oxidation of CO and CH<sub>x</sub>, as well as reduction of NO<sub>x</sub>.

## CONCLUSIONS

The presented here oxide materials exhibit very interesting properties considering the oxygen storage ability and catalytic activity. It seems that their usage in technological applications is possible.

## ACKNOWLEDGMENT

The project was funded by the National Science Centre Poland (NCN) on the basis of the decision number DEC-2011/01/B/ST8/04046.

## REFERENCES

1. J. da Costa, et al., *State of Art (SOTA) Report on Dense Ceramic Membranes for Oxygen Separation from Air*
2. J. Sunarso, et al., *J. Membrane Sci.* **320**(2008)13
3. T. Motohashi, et al., *Chem. Mater.* **22**(2010)3192

# ELECTRICAL PROPERTIES OF $\text{Bi}_3\text{Y}_{0.9}\text{W}_{0.1}\text{O}_{6.15}$ :LSM COMPOSITE CATHODES FOR SOFC

*M.Dudz<sup>a</sup>, W. Wrobel<sup>a</sup>, M. Malys<sup>a</sup>, A. Borowska-Cenkowska<sup>a</sup>, K-Z. Fung<sup>b</sup>, F. Krok<sup>a</sup>*

a) Faculty of Physics, Warsaw University of Technology, Koszykowa 75, 00-662 Warszawa, Poland  
b) Material Science and Engineering, National Cheng Kung University, 1# University Road, Tainan, Taiwan  
e-mail: wrobel@if.pw.edu.pl

Keywords: SOFC, cathode, composite, ionic conductivity, electronic conductivity

## INTRODUCTION

Solid oxide fuel cells (SOFC) with yttria or ceria based electrolytes require high operating temperatures. Bismuth based electrolytes exhibit highest oxide ion conductivity at high and intermediate temperatures and are widely studied for its potential applications in the intermediate solid oxide fuel cells (IT-SOFC). However, lower operating temperature results in a higher interfacial polarization resistances. These polarization effects are especially important for the commonly used perovskite cathodes, like  $(\text{La},\text{Sr})\text{MnO}_3$ , which are poor ionic conductors. Improvement of performance of cathode based on LSM can be obtained by forming a composite cathode with a second component characterized by high oxide ion conductivity. Recently much work was carried out on development of LSM/YSZ or LSM/GDC composite cathodes suitable for SOFC systems [1,2].

In this paper composite cathode, build of LSM and bismuth based oxide material ( $\text{Bi}_3\text{Y}_{0.9}\text{W}_{0.1}\text{O}_{6.15}$ ) was studied. Selected oxide ion conductor was shown to provide high conductivity, but also good long term stability. Additionally both components of composite cathode, LSM and  $\text{Bi}_3\text{Y}_{0.9}\text{W}_{0.1}\text{O}_{6.15}$ , exhibit similar thermal expansion coefficients. Significant decrease of interfacial resistance of the composite system is expected in comparison to that of LSM material.

## EXPERIMENTAL

Powders of component materials were mixed in different molar ratios ( $\text{Bi}_3\text{Y}_{0.9}\text{W}_{0.1}\text{O}_{6.15}$  : LSM) from 10:1 to 1:1, then formed into disc membranes, pressed and sintered. Prepared samples were investigated by HT-XRD, SEM and DTA methods. Electrical conductivity of composites was examined by a.c. impedance spectroscopy, while ionic and electronic contribution to the total conductivity (transference numbers) were measured using modified EMF method with oxygen concentration cell.

## RESULTS AND DISCUSSION

XRD and DTA measurements indicate, that there was no chemical reaction between component phases of composite in the temperature range from room temperature to 850°C. It has been shown, that total conductivity of composite systems decreases with the increasing  $\text{Bi}_3\text{Y}_{0.9}\text{W}_{0.1}\text{O}_{6.15}$  content, in particular in the systems with dominant share of the ionic component.

Applicability of the classical percolation model was examined. The results of transference number studies show, that for the systems with molar ratio equal 1:1, the electronic conductivity is dominating total conductivity, whereas ionic conductivity is dominating for the systems with molar ratio above 2:1. Arrhenius plot of electronic and ionic conductivity obtained for  $\text{Bi}_3\text{Y}_{0.9}\text{W}_{0.1}\text{O}_{6.15}$  : LSM composite at molar ratio 1:1 is presented at Fig. 1.

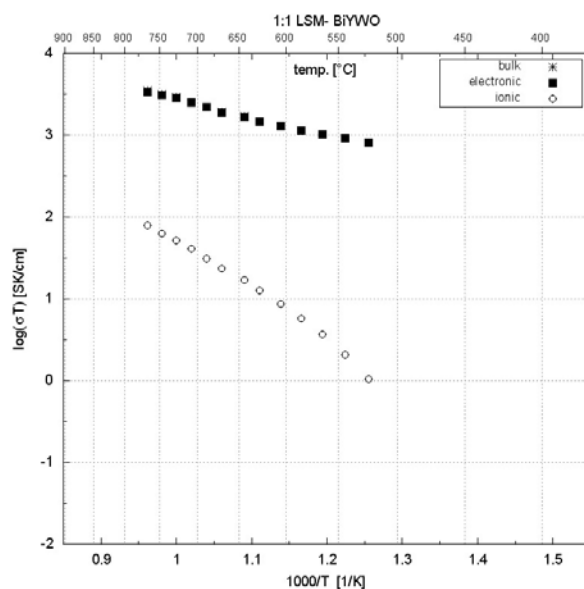


Fig. 1. Ionic and electronic components of total conductivity for  $\text{Bi}_3\text{Y}_{0.9}\text{W}_{0.1}\text{O}_{6.15}$  : LSM composite at molar ratio 1:1

## ACKNOWLEDGMENT

This work is supported by the National Centre for Research and Development Poland under grant number DKO/PL-TW1/6/2013.

## REFERENCES

- Nielsen J., Hjelm J. *Electrochimica Acta* 115 (2014) 31–45
- Dusastre V., Kilner J.A. *Solid State Ionics* 126 (1999) 163–174

# CHARACTERIZATION OF NOVEL ANODE CATALYTIC LAYERS FOR BIOGAS OPERATING SOLID OXIDE FUEL CELLS

*B.Bochentyn<sup>a</sup>, D.Szymczewska<sup>b</sup>, M.Chlewińska<sup>a</sup>, D.Niańkowski<sup>a</sup> and P.Jasiński<sup>b</sup>*

<sup>a</sup> Faculty of Electronics, Telecommunications and Informatics, Gdansk University of Technology, 80-233 Gdansk, ul. Narutowicza 11/12, Poland

<sup>b</sup> Faculty of Applied Physics and Mathematics, Gdansk University of Technology, 80-233 Gdansk, ul. Narutowicza 11/12, Poland

e-mail: bbochentyn@mif.pg.gda.pl

Keywords: solid oxide fuel cells, biogas, catalysts

## INTRODUCTION

A solid oxide fuel cell (SOFC) is a device that can directly convert the chemical energy of various gaseous fuels into electrical energy and heat. One of the possible fuels for SOFCs is biogas, which consists mainly of methane (CH<sub>4</sub>) and carbon dioxide (CO<sub>2</sub>), with some traces of other gases, e.g. hydrogen sulfide (H<sub>2</sub>S), ammonia (NH<sub>3</sub>), hydrogen (H<sub>2</sub>), nitrogen (N<sub>2</sub>), oxygen (O<sub>2</sub>) and vapor water (H<sub>2</sub>O) [1]. Due to relatively high operation temperature (up to 800 °C) of the solid oxide fuel cell an internal reforming of biogas is possible directly on the SOFC anode, without the external reformer. However, in practice the commercially used solid oxide fuel cells with Ni-YSZ anode suffer from carbon deposition and sulfur poisoning during the internal reforming process [2].

Carbon deposition on the anode takes place via methane cracking on nickel and/or Boudouard reaction [1]. Mainly crystalline graphite, amorphous carbon or carbon fibers are formed [3]. This process can be minimized by a proper anode modification (composition/structure [4]) as well as by operating parameters, e.g. current density or in a way of biogas pre-mixing with steam, carbon dioxide, hydrogen or oxygen [5,6].

The aim of this work is to present properties of various catalytic materials such as Sm<sub>0.2</sub>Ce<sub>0.8</sub>O<sub>1.9</sub>, Sm<sub>0.2</sub>Ce<sub>0.8</sub>O<sub>1.9</sub>-YSZ, CuO-CeO<sub>2</sub>, NiO-Al<sub>2</sub>O<sub>3</sub> and LiLaNi-Al<sub>2</sub>O<sub>3</sub> as active components for biogas reforming.

## EXPERIMENTAL

All catalytic materials were synthesized using a Pechini method. As a result powders of suitable compositions have been obtained. In order to form pastes the obtained powders were grinded in a mortar for about 1 hour together with ESL 403 organic binder (ElectroScience Laboratory, USA). Then the obtained pastes were applied on the anode surface forming catalytic layers (16 mm in diameter). Finally, the modified fuel cells with deposited catalytic layers were fired for 2 hours.

The phase composition of the investigated materials was analyzed by the X-ray Diffraction method using an X'Pert Pro MPD Philips diffractometer with Cu K<sub>α</sub> (1.542Å) radiation at room temperature. The morphology of fuel cells cross sections was observed using the FEI Quanta FEG 250 Scanning Electron Microscope (SEM). To recognize the elements and their distribution in the fuel cell, the energy-dispersive X-ray (EDX) spectroscopy was performed on the fuel cells

cross sections using the EDAX Genesis APEX 2i with Apollo X SDD spectrometer at 10 kV.

The electrical properties of the reported four sets of fuel cells were measured using a measuring cell build and dedicated for this experiment. Two types of measurement data were collected using computer software: a current density versus voltage plot and a current density versus time plot at a loading condition of 0.65 V for the time over 168h (7 days). In order to initially reduce anodes, the pure hydrogen was delivered as a fuel for 24h. After this time hydrogen was replaced by dry synthetic biogas consisting of methane and carbon dioxide mixed at a volume ratio of 60/40. The total flow rate of the gas mixture was 40 cm<sup>3</sup>min<sup>-1</sup>. The current-voltage measurements were collected every 24 hours. The measurements were performed at 750 °C.

## RESULTS AND DISCUSSION

It has been found that using a Pechini method it is possible to obtain a desirable, single phase material with an average grain size equal tens of nanometers. Then these materials have been applied as potential catalytic layers for Solid Oxide Fuel Cells. The fuel cells with cerium containing layers are stable in time in both hydrogen and biogas atmospheres, whereas the fuel cells with nickel containing layers deteriorate in a similar way as the reference cell without a catalytic layer. The SEM analysis indicated that on the surface of investigated layers carbon nanofibres are formed after running in biogas. However, for ceria containing catalysts the anode area remains clear from carbon deposition.

## REFERENCES

- [1] A. Fuerte, R.X. Valenzuela, M.J. Escudero, L. Daza, International Journal of Hydrogen Energy 39 (2014) 4060-4066
- [2] H. Takahashi, T. Takegichi, N. Yamamoto, M. Matsuda, E. Kobayashi, W. Ueda, J. Mol. Catal. A Chem. 350 (2011) 69-74
- [3] G. Bonura, C. Cannilla, F. Frusteri, Applied Catalysis B: Environmental 121-122 (2012) 135-147
- [4] Atkinson A, Barnett S, Gorte RJ, Irvine JTS, McEvoy AJ, Mogensen M, et al. Nature 2004;3:17e27.
- [5] Mermelstein J, Millan M, Brandon N., J Power Sources 2010;195:1657e66.
- [6] A. Galvagno, V. Chiodo, F. Urbani, F. Freni, International Journal of Hydrogen Energy 38 (2013) 3913-3920

# COMPOSITE FUNCTIONAL CATHODE LAYER PREPARED BY INFILTRATION FOR PROTON CONDUCTING SOFC

*K. Gdula-Kasica, A. Chrzan, D. Szymczewska and P. Jasinski*  
Faculty of Electronics, Telecommunications and Informatics  
Gdańsk University of Technology, ul. Narutowicza 11/12,  
80-233 Gdańsk, Poland  
e-mail: kgdula@eti.pg.gda.pl

Keywords: solid oxide fuel cells, proton conduction, BCYZ, LSCF

## INTRODUCTION

In the face of climate change caused by progressive destruction of the environment and progressive depletion of natural resources, mankind is forced to seek alternative energy sources. Driven by economic pressure alternative energy technologies become a dominant area of research and innovation all over the world [1-2]. It has become a necessity to develop new, efficient and environmentally friendly sources of energy. From this perspective, fuel cells seem to be one of the most promising new technologies of energy production [3].

Solid oxide fuel cells (SOFCs) are defined as electrochemical devices that directly convert chemical energy into electricity. One of the most promising devices are SOFCs based on proton-conducting electrolytes (PC-SOFCs). Compared to SOFCs based on oxygen ion-conducting electrolytes, in this case there is no fuel dilution at the anode side, because water vapor as a product is generated at the cathode. Additionally, PC-SOFCs may have higher power output than oxygen ion-conducting SOFCs at temperatures below 600 °C [3]. Unfortunately, in typical fuel gas compositions proton-conducting materials exhibit rather low chemical stability, which limits the applicability of these materials in SOFCs technology.

In this work we attempt to build and testing anode-supported planar cell with configuration NiO-BCYZ/BCYZ/LSCF-BCYZ/LSCF, where: BCYZ –  $\text{BaCe}_{0.8}\text{Y}_{0.1}\text{Zr}_{0.1}\text{O}_{3-\delta}$ , LSCF –  $\text{La}_{0.6}\text{Sr}_{0.4}\text{Co}_{0.2}\text{Fe}_{0.8}\text{O}_{3-\delta}$ .

## EXPERIMENTAL

The BCYZ nanopowder was prepared by a self-combustion synthesis [4], where ethylene glycol, citrate acid, metal nitrates ( $\text{Ce}(\text{NO}_3)_3 \times 6\text{H}_2\text{O}$ ,  $\text{Y}(\text{NO}_3)_3 \times 6\text{H}_2\text{O}$ ,  $\text{ZrOCl}_2 \times 8\text{H}_2\text{O}$ ) and  $\text{BaCO}_3$  were used as substrates. The LSCF precursor was synthesized by a modified Pechini method [5] by mixing ethylene glycol, citrate acid, and appropriate metal nitrates ( $\text{La}(\text{NO}_3)_3 \times 6\text{H}_2\text{O}$ ,  $\text{Fe}(\text{NO}_3)_3 \times 9\text{H}_2\text{O}$ ,  $\text{Sr}(\text{NO}_3)_2$ ,  $\text{Co}(\text{NO}_3)_2 \times 6\text{H}_2\text{O}$ ).

The anode material in this system is a NiO-BCYZ composite. NiO and BCYZ powders were mixed with 10 wt% activated carbon as a pore former (NiO:BCYZ=6:4) by the ball-milling method. The anode powder was dried at 100 °C for 24 h. Next, the mixture was pressed into a pellet and calcinated at 1100 °C.

The thin layer of BCYZ electrolyte material was applied by spray pyrolysis method. All of the spray pyrolysis parameters were strictly controlled. After that the structure was sintered at 1500 °C in air. The BCYZ

porous structure was deposited on this electrolyte layer. Then thin LSCF layer was deposited on the surface by infiltration of polymer precursors. This thin layer was directly infiltrated by BCYZ and sintered in air at 1000 °C. After sintering the cathode layer of LSCF was applied by spin coating method.

## RESULTS AND DISCUSSION

The structural properties of precursors (BCYZ and LSCF) were studied with use of X-ray diffraction (XRD). Both precursor materials were single-phase. The planned cell configuration is shown in Fig. 1. In order to examine sample morphology scanning electron microscopy (SEM) was used. The electrical properties of BCYZ cells were measured by means of electrochemical impedance spectroscopy.



Fig. 1. The planar BCYZ cell configuration.

## CONCLUSIONS

In this study, the BCYZ material with thin layer of LSCF-BCYZ was applied to a planar-type cell. The cell with configuration of NiO-BCYZ/BCYZ/LSCF-BCYZ/LSCF was analyzed.

## ACKNOWLEDGMENT

This work is partially supported by National Science Centre Poland based on decision DEC-2012/05/B/ST7/02153 and Statutory Funds of the Gdańsk University of Technology.

## REFERENCES

1. N. Brandon, D. Thompsett (Editors), Fuel Cells Compendium, Elsevier, 2005.
2. P. Corbo, F. Migliardini, O. Veneri, Hydrogen Fuel Cells for Road Vehicles, Springer, 2011.
3. D. Medvedev, A. Murashkina, E. Pikalova, A. Demin, A. Podias, P. Tsiakaras, Progress in Materials Science **60** (2014) 72.
4. K. Gdula-Kasica, A. Mielewczyk-Gryn, S. Molin, P. Jasinski, A. Krupa, B. Kusz, M. Gazda, Solid State Ionics **255** (2012) 245.
5. P. Jasinski, S. Molin, M. Gazda, V. Petrovsky, H.U. Anderson, J. Power Sources **194** (2009) 10.



# DEGRADATION OF SOLID OXIDE ELECTROLYZERS

*J. Karczewski, D. Szymczewska\*, A. Chrzan\* and P. Jasinski\**

Faculty of Applied Physics and Mathematics, Gdansk University of Technology

\*Faculty of Electronics, Telecommunications and Informatics, Gdansk University of Technology

ul. Narutowicza 11/12, 80-233 Gdansk, Poland

e-mail: jkarczew@mif.pg.gda.pl

Keywords: hydrogen, solid oxide electrolyzers

Solid oxide electrolyzers (SOEC) are the most efficient electrolyzers of steam to hydrogen and oxygen. In the future energy system, where large amounts of energy will be created by fluctuating sources (wind, solar), there will be a need to store this energy and use it when there is a demand. Generation and usage profiles of energy coming from renewable sources are not overlapping. Electrolyzers will therefore be an inevitable part of the modern energy system based on fluctuating sources. Technologies for generating renewable energy are already available but now the biggest concern is to store this energy. Before successful commercialisation of SOEC several aspects have to be solved: primarily obtaining high current densities with low degradation rates. Current state-of the art in solid oxide electrolysis is based primarily on the use of state-of the art solid oxide fuel cells. These cells can work with power densities reaching  $1 \text{ A cm}^{-2}$  at thermoneutral voltage ( $\sim 1.3 \text{ V}$ ) at  $800^\circ\text{C}$ . It has been shown that in comparison to solid oxide fuel cells, different polarization of electrodes lead to rise of the electrochemical potential drop across the electrode/electrolyte/electrode system and this can lead to new degradation mechanisms [1-3]. To be able to solve the degradation problems of solid oxide electrolyzers a thorough knowledge of the phenomena occurring during operation is needed.

The aim of the study is to investigate the degradation processes on electrolyte/air electrode interface in a typical configuration with the porous electrode, as well as with additional, dense thin perovskite buffer layer.

In order to evaluate degradation process symmetrical cells with two LSCF electrodes were prepared on yttria stabilized zirconia (YSZ) substrate. Thin ( $\sim 200\text{nm}$ ) perovskite layers were fabricated using spin coating of a metallo-organic precursor. Sample morphology was determined by scanning electron microscopy (SEM, Quanta 250 FEI). Symmetrical cells were characterized by the electrochemical impedance spectroscopy (EIS) using Solartron SI 1260 impedance analyzer coupled with SI 1287 electrochemical interface.

## ACKNOWLEDGMENT

This work is supported by NCBiR under Polish-Taiwanese/Taiwanese-Polish Joint Research project "Innovative Solid Oxide Electrolyzers for Storage of Renewable Energy" based on decision DZP/PL-TW2/6/2015.

## REFERENCES

1. Y. Zhang, K. Chen, C. Xia, S. P. Jiang, M. Ni. *International Journal of Hydrogen Energy* **37** (2012) 13914 -13920.
2. J.Kim, H.I.Ji, H.P.Dasari, D.Shin, H.Song, J.H.Lee, B.K.Kim, H.J.Je, H.W Lee, K.J.Yoon, *International Journal of Hydrogen Energy* **38** (2013) 1225 -1235
3. K.Chen, S.P.Jiang, *International Journal of Hydrogen Energy* **36** (2011) 10541-10549

# NEW CONCEPT OF LIGHTWEIGHT SHORT STACK OF ANODE SUPPORTED SOLID OXIDE FUEL CELLS

*R. Kluczowski, M. Krauz, M. Kawalec, A. Świeca*

Institute of Power Engineering Ceramic Department CEREL,

1 Techniczna St., 36-040 Boguchwała, Poland

e-mail: kluczowski@cerel.pl

Keywords: hydrogen, fuel cells

## INTRODUCTION

The world's state of knowledge of application of fuel cells in aviation has shown particular trend in recent years towards the search for a new alternative source of power on boards of helicopter and airplane [1]. One of the kind of fuel cell which can be used in aviation are solid oxide fuel cells (SOFC). One of the application where this kind of fuel cell will be used is Solid Oxide Fuel Cell - Gas Turbine Hybrid Auxiliary Power Unit (SOFC-GT APU) [2-3]. The main aim of this work is to demonstrate stack of Anode Supported Solid Oxide Fuel Cells (AS-SOFC) as the auxiliary power supply integrated with ignition system of ASZ-62IR engine. Taking into account the requirements for the power density of the fuel cell system, defined as the ratio of power output of fuel cell stack per mass of this stack, which value should be as high as possible, in the construction of the fuel cell stack will be used lighter and cheaper ceramic materials instead of currently used metal materials. Additionally stack configuration will be changed in way which will enable reduction of weight and size of stack.

## EXPERIMENTAL

Direct housing of the fuel cell is made from light modular ceramic material made of alumina (C799) (fig. 1). Membranes of fuel cells (AS-SOFC made in CEREL) are placed inside of ceramic housing elements with serially – parallel way: the pair of membranes will be alternately faced each other of anode and cathode sides what. Instead of expensive, complex and time-consuming metal interconnectors, structured alumina elements are used which distribute fuel (hydrogen) on the anode side and oxidant (air) on the cathode side. Between structured alumina element and given electrode a perforated flat current collector made of heat resistant alloy is set. The current collector will collect electrical charge comes from anode surface and conduct it to cathode surface or to electric current receiver. Both ceramic structured elements designed for gases distribution and housing elements of fuel cells membranes are made by means of cheap and highly efficient methods of low and high pressure ceramic injection moulding. The insulation elements of the stack will be made of flat seals made of a refractory ceramic paper based on  $\text{SiO}_2\text{-Al}_2\text{O}_3$  fibers. This seals prevent from fuel leakage to the outside or to oxidant part during operation of cell at high temperatures. Thermal insulation of inside part of stack will be made of ultra-light mats of refractory fibers with very low heat transfer coefficient which will allow to minimize of heat losses and prevent from increasing of weight of whole construction. This system of construction will

allow to make external cover of stack by using thin protective covering what additionally will reduce weight of whole stack. The use in the stack of high power density (max. power density  $1,25 \text{ W/cm}^2$  at  $800^\circ\text{C}$ ) AS-SOFC membranes produced in CEREL will allow obtain high power density of the fuel cell system.



Fig. 1. AS-SOFC lightweight short stack.

## CONCLUSIONS

Concept of SOFC stack made of lightweight elements like alumina housing, interconnect structured alumina elements with thin perforated current collectors, is able to significantly reduce the whole mass of Solid Oxide Fuel Cell Stack. This will allow to use SOFC stack as the auxiliary power supply integrated with ignition system of ASZ-62IR engine. The success of this system also allows for future development of this kind of fuel cells not limited to stationary application.

## ACKNOWLEDGMENT

This work is supported by National Center of Research and Development, as a Sector Program INNOLOT, project EPOCA „Device for power supplying and controlling on-board and ground equipment”, um. nr INNOLOT/I/1/NCBR/2013

## REFERENCES

1. D. Dagget, “Commercial Airplanes – Fuel Cell APU – overview” SECA Annual Meeting (Seattle, WA) 15.04.2003
2. K. Rajashekara, J. Grieve, D. Daggett, D. “Solid Oxide Fuel Cell/Gas Turbine Hybrid APU System for Aerospace Applications” Industry Applications Conference, 2006. 41st IAS Annual Meeting. Conference Record of the 2006 IEEE 5 (2006) 2185 – 2192
3. C. J. Steffen, Jr., J. E. Freeh, and L. M. Larosiliere “Solid Oxide Fuel Cell/Gas Turbine Hybrid Cycle Technology For Auxiliary Aerospace Power”, Turbo Expo 2005, American Society of Mechanical Engineers Reno, Nevada, 6–9.06.2005

# APPLICATION OF GRAPHENE OXIDE AND ORGANICALLY MODIFIED TITANIUM/SILICON DIOXIDE HYBRID PARTICLES FOR PEM FUEL CELLS ELECTRODES IMPROVEMENT

*M. Malinowski<sup>1\*</sup>, A. Iwan<sup>1</sup>, A. Hreniak<sup>1</sup>, G. Pasciak<sup>1</sup> and Felipe Caballero-Briones<sup>2</sup>*

Division of Electrotechnology and Materials Science

<sup>1</sup>Electrotechnical Institute, M. Skłodowskiej-Curie 55/61 50-369 Wrocław, Poland, \*e-mail: m.mal@iel.wroc.pl

<sup>2</sup>Laboratorio de Materiales Fotovoltaicos, Instituto Politécnico Nacional, CICATA Altamira.

Km 14.5 Carretera Tampico-Puerto Industrial Altamira, 89600 Altamira, México

Keywords: PEMFC, GDE, graphene oxide, TiO<sub>2</sub>-SiO<sub>2</sub>, surface area and porosity, maximum power density

## INTRODUCTION

Commercialization phase of polymer electrolyte fuel cells (PEMFCs) has significantly accelerated since several recent years. However, there are still two major issues that PEMFCs suffer from i.e. life time and production costs. The former one is mainly connected with limited durability of basic fuel cell components – typically PFSA-based electrolytes and Pt/carbon electrodes. Major production costs are due to platinum catalyst and graphite bipolar plates. This work aims to mitigate some drawbacks by incorporation of new materials to fuel cell catalyst layer in order to enhance the electrode durability and decrease the amount of platinum used. The fundamental approach is to apply graphene oxide (GO) and organically modified TiO<sub>2</sub>-SiO<sub>2</sub> hybrid material (obtained by sol-gel method) as catalyst support. High surface area (SA) and microporosity ( $\mu$ P) and chemical durability of above additives in connection with potential catalytic activity of TiO<sub>2</sub>-SiO<sub>2</sub> suggests that such a novel electrode material may operate sufficiently in PEMFCs. Investigations of physical and electrochemical parameters of prepared catalyst mixtures and single fuel cells are key objectives of this work.

## EXPERIMENTAL

Catalyst mixtures were fabricated in the following way. Pt black powder was first mixed with small amount of deionized water (to protect against catalyst burning) and Vulcan XC72 carbon black to establish a Pt-on-carbon mass fraction of 30%. Then, ethanol was added in the amount of 15% of mixture volume ratio. The mixture was stirred by applying ultrasonication and mixed simultaneously for about 40 minutes. At this stage various additives such as graphene oxide or synthesized TiO<sub>2</sub>-SiO<sub>2</sub> were added in required amounts. Finally, 20 wt.% Nafion solution was put into the beaker in the amount of 30 wt.% following by cooling down the mixture temperature to about 0 °C. As a result, 4 catalyst pastes were prepared i.e. Pt/Carbon/GO, Pt/Carbon/TiO<sub>2</sub>-SiO<sub>2</sub>, Pt/Carbon/GO/TiO<sub>2</sub>-SiO<sub>2</sub> and reference one. GDL papers with hydrophobic treatment were chosen to make gas diffusion electrodes (GDE). These electrodes acting as anodes, activated Nafion-115 films as electrolytes and 2 mg Pt/cm<sup>2</sup> commercial GDE as cathodes were taken to carry out MEA procedure (hot pressing for 5 min. at 110 °C and 30 bar), resulting in 1 cm<sup>2</sup> single PEMFCs. Surface area and porosity measurements were performed for catalyst mixtures and

its particular components prior to electrochemical properties evaluation of PEMFCs.

## RESULTS AND DISCUSSION

Commonly-used carbon support i.e. Vulcan XC72R is characterized by SA of 249.2 m<sup>2</sup>/g and  $\mu$ P surface area of 82.5 m<sup>2</sup>/g, according to the measurements. Any addition of chemical compounds such as Nafion decreases this area, therefore its initial value should be as high as possible. The investigation of reference catalyst material reveals a decrease of SA to 69.7 m<sup>2</sup>/g and absolute filling of microporosity structure. At the same time, the average pore width increased from 11.6 nm to 40.6 nm. However, the experiments showed that the addition of only 1:22 weight ratio of graphene oxide can mitigate this negative effect. According to the investigation, for Pt/carbon/GO paste, SA of 85.6 m<sup>2</sup>/g and average pore width of 34.7 nm were recorded. Further scaling up the graphene content may bring even better results.

Some promising data were found for organically modified TiO<sub>2</sub>-SiO<sub>2</sub> hybrid material. Total SA of 370.2 m<sup>2</sup>/g, pore size of 3.7 nm and microporosity structure (126 m<sup>2</sup>/g, 0.61 nm) in connection with potential catalytic properties indicate that this additive may have superior influence on GDE characteristics. Moreover, preliminary performance measurements of single fuel cells revealed that the addition of 30% GO/Carbon increased the maximum power density from 105 mW/cm<sup>2</sup> to 120 mW/cm<sup>2</sup> despite Pt catalyst amount was scaled down from 0.54 mg/cm<sup>2</sup> to 0.39 mg/cm<sup>2</sup>.

## CONCLUSIONS

Modification of catalyst mixture structure is important for reducing of expensive platinum used in PEMFCs. It can be done by incorporation of new support materials with high surface area and microporosity structure and by application of new material that reveal catalytic activity. In this work GO and organically modified TiO<sub>2</sub>-SiO<sub>2</sub> materials were taken into account. Some positive feedbacks were found in terms of surface area and porosity and electrical performance. Further experiments are required to confirm the usefulness of such approach for PEMFCs.

## REFERENCES

1. S. Martin et al. Journal of Power Sources **272** (2014) 559.
2. C-Y. Jung, S-C. Yi, Electrochimica Acta **113** (2013) 37.
3. S. Litster, G. McLean, Journal of Power Sources **130** (2004) 61.

# PHYSICOCHEMICAL PROPERTIES OF $\text{Sr}_{2-x}\text{Ba}_x\text{MMoO}_{6-\delta}$ (M: Mg, Mn, Fe) OXIDES FOR SOFCS

*K. Zheng\**, *K. Świerczek*

AGH University of Science and Technology, Faculty of Energy and Fuels  
Department of Hydrogen Energy, al. A. Mickiewicza 30, 30-059 Krakow, Poland  
\*e-mail: zheng@agh.edu.pl

Keywords: anode material; SOFCs; crystal structure; transport properties; chemical stability;

## INTRODUCTION

Fuel flexibility of Solid Oxide Fuel Cells (SOFC), with possibility of utilization of non-hydrogen fuels, can be an essential factor for the commercial adoption of SOFC technology in power generation, as the future of hydrogen economy is still to be realized, due to some of the major barriers related to costs, technological uncertainty, and infrastructure set-up [1, 2]. One of the main problems with SOFCs directly running on non-hydrogen fuels, such as natural gas, methane or syngas is carbon deposition on the anode, which can cause significant or even detrimental decrease of the cell's performance [1, 2, 4]. The considered non-hydrogen fuels usually contain sulfur (in a form of  $\text{H}_2\text{S}$ ), which can irreversibly poison Ni-YSZ cermet anodes [1, 2]. Therefore, development of novel materials with improved tolerance towards carbon deposition and sulfur poisoning is essential for the construction of robust SOFCs with fuel versatility.

Application of mixed ionic-electronic conductors (MIEC) in the SOFC anode is considered to be highly beneficial, as it allows for the electrode reaction to occur on the whole surface on the electrode material, improving electrochemical properties [1, 2, 4]. Among the new anode material candidates, perovskite-type oxides from  $\text{AMMoO}_{6-\delta}$  (A - Sr, Ba; M - Mg, Mn, Fe, Co, Ni) families, either B-site cation ordered or disordered, seem to be particularly attractive [1-4]. In this study, A-site doped with barium  $\text{Sr}_{2-x}\text{Ba}_x\text{MMoO}_{6-\delta}$  (M: Mg, Mn, Fe) oxides were studied and evaluated as anode materials for SOFCs.

## RESULTS AND DISCUSSION

Mo-containing  $\text{Sr}_{2-x}\text{Ba}_x\text{MMoO}_{6-\delta}$  (M: Mg, Mn, Fe) perovskite-related oxides have been evaluated in terms of their possible application as anode materials in Solid Oxide Fuel Cells.

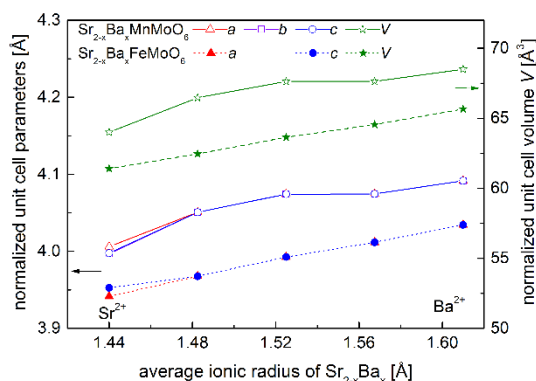


Fig. 1. Normalized unit cell volume and parameters of  $\text{Sr}_{2-x}\text{Ba}_x\text{MMoO}_{6-\delta}$  (M = Mn, Fe) oxides.

Crystal structure, transport properties, oxygen content, chemical stability have been studied. The doping with different amount of barium at A-site, and the B-site metals M (M: Mg, Mn, Fe) significantly affect the physicochemical properties of considered materials. It shows that double perovskites with Fe at B-site have highest conductivity in reducing condition, among  $\text{Sr}_{2-x}\text{Ba}_x\text{MMoO}_{6-\delta}$  materials. While those materials are only stable in reduction conditions.

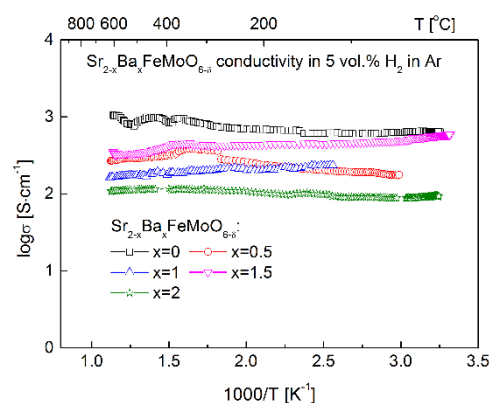


Fig. 2. Electrical conductivity for  $\text{Sr}_{2-x}\text{Ba}_x\text{FeMoO}_{6-\delta}$  materials as a function of temperature.

## CONCLUSIONS

Physicochemical properties of  $\text{Sr}_{2-x}\text{Ba}_x\text{MMoO}_{6-\delta}$  (M: Mg, Mn, Fe) anode materials were investigated, and the effect of A-site doping with barium and B-site metals M (M: Mg, Mn, Fe) on physicochemical properties of the considered oxides was evaluated.

## ACKNOWLEDGMENT

The project was funded by the National Science Centre Poland (NCN) on the basis of the decision number DEC-2011/03/N/ST5/04785, and the Polish Ministry of Science and Higher Education under project AGH No. 11.11.210.911.

K. Zheng acknowledges financial support from NCN under the ETIUDA doctoral scholarship DEC-2013/08/T/ST5/00100

## REFERENCES

1. X. Ge, S. Chan, Q. Liu, Q. Sun, Adv. Energy Mater. 2 (2012) 1156-1181.
2. Y. Huang, R.I. Dass, Z. Xing, J.B. Goodenough, Science 312 (2006) 254-257.
3. K. Zheng, K. Świerczek, J. Eur. Ceram. Soc. 34 (2014) 4273-4284.
4. K. Zheng, K. Świerczek, J.M. Polfus, M.F. Sunding, M. Pishahang, T. Norby, J. Electrochem. Soc. 162(9) (2015) F1078-F1087.

# STRUCTURE AND TRANSPORT PROPERTIES OF $\text{Ln}_2\text{Ni}_{0.5}\text{Cu}_{0.5}\text{O}_4$ (Ln - La, Pr) CATHODE MATERIALS FOR IT-SOFCs

K. Zheng\*, K. Świerczek

AGH University of Science and Technology, Faculty of Energy and Fuels  
Department of Hydrogen Energy, al. A. Mickiewicza 30, 30-059 Krakow, Poland  
\*e-mail: zheng@agh.edu.pl

Keywords: Layered perovskites; Crystal structure; Transport properties; Cathode materials, IT-SOFC

## INTRODUCTION

Layered type  $\text{Ln}_2\text{MO}_{4\pm\delta}$  and  $(\text{Ln}_{1-x}\text{Sr}_x)_2\text{MO}_{4\pm\delta}$  oxides (Ln: lanthanides, M: 3d metals) are studied as candidate cathode materials for Intermediate Temperature Solid Oxide Fuel Cells (IT-SOFC), due to their good mixed ionic-electronic transport properties and moderate values of thermal expansion coefficient. In these materials, especially if  $M = \text{Ni}$ , significant amount of interstitial oxygen is present, which diffusion may enhance oxygen reduction reaction occurring on the cathode in the intermediate temperature range [1-4].

The structural aristotype for  $\text{Ln}_2\text{MO}_{4\pm\delta}$ , realized in case of  $\text{K}_2\text{NiF}_4$ , is characterized by tetragonal structure with  $I4/mmm$  space group. It can be described as layered sequence of perovskite-like  $\text{ABO}_3$  and NaCl-like AO units along c axis, with Ni cations having octahedral coordination [1-4].

There are literature reports showing good electrochemical properties of  $\text{Ln}_2\text{NiO}_{4\pm\delta}$  nickelates, which were used as cathode materials in IT-SOFCs [3]. Also some works show possibility of application of  $\text{Ln}_2\text{CuO}_{4\pm\delta}$  cuprates [4], as well as materials, in which Ni and Cu cations are present together at the M-site [2].

## RESULTS AND DISCUSSION

In this work, physicochemical properties in terms of crystal structure, oxygen nonstoichiometry, electrical conductivity, Seebeck coefficient, for  $\text{La}_2\text{Ni}_{0.5}\text{Cu}_{0.5}\text{O}_4$  and  $\text{Pr}_2\text{Ni}_{0.5}\text{Cu}_{0.5}\text{O}_4$  oxides are reported.

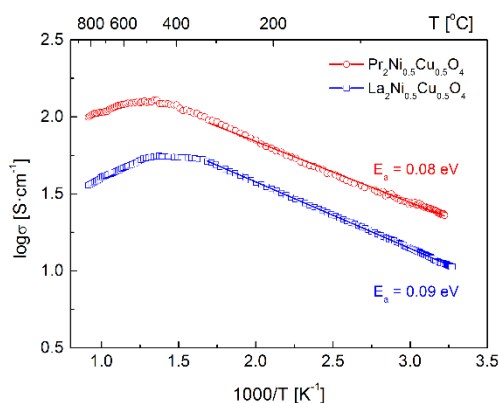


Fig. 1. Electrical conductivity of the studied materials as a function of the temperature.

$\text{Pr}_2\text{Ni}_{0.5}\text{Cu}_{0.5}\text{O}_4$  compound was selected as the candidate cathode material, and electrochemical properties of  $\text{Pr}_2\text{Ni}_{0.5}\text{Cu}_{0.5}\text{O}_4$ -based IT-SOFC are given. The results are supplemented by chemical stability data of the considered materials at high temperature and in relation to  $\text{Ce}_{0.8}\text{Gd}_{0.2}\text{O}_{1.9}$  and  $\text{Zr}_{0.84}\text{Y}_{0.16}\text{O}_{1.92}$

electrolytes.

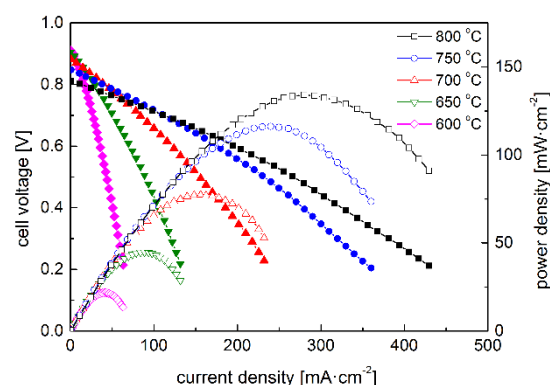


Fig. 2. Voltage and power density of button-type  $\text{H}_2$  |  $\text{Pr}_2\text{Ni}_{0.5}\text{Cu}_{0.5}\text{O}_4$  |  $\text{Ce}_{0.8}\text{Gd}_{0.2}\text{O}_{1.9}$  | 8YSZ-Ni | air cell as a function of current density.

## CONCLUSIONS

Structural properties, oxygen nonstoichiometry, electrical conductivity and Seebeck coefficient data were measured for  $\text{La}_2\text{Ni}_{0.5}\text{Cu}_{0.5}\text{O}_4$  and  $\text{Pr}_2\text{Ni}_{0.5}\text{Cu}_{0.5}\text{O}_4$  oxides synthesized by a soft chemistry method.  $\text{Pr}_2\text{Ni}_{0.5}\text{Cu}_{0.5}\text{O}_4$  was selected as candidate cathode material for electrolyte-supported IT-SOFC having power densities exceeding  $0.13 \text{ W}\cdot\text{cm}^{-2}$  at  $800 \text{ }^\circ\text{C}$ . Despite promising performance, the main issue considering possible application of the compounds arises from their low chemical stability at high temperatures. This instability is driven by a tendency to separation into Cu-rich  $T'$ -type and Ni-rich T-type phases.

## ACKNOWLEDGMENT

The project was funded by the National Science Centre Poland (NCN) on the basis of the decision number DEC-2011/03/N/ST5/04785, and the Polish Ministry of Science and Higher Education under project AGH No. 11.11.210.911.

K. Zheng acknowledges financial support from NCN under the ETIUDA doctoral scholarship DEC-2013/08/T/ST5/00100.

## REFERENCES

1. S. Takahashi, S. Nishimoto, M. Matsuda, M. Miyake, J. Am. Ceram. Soc. 93 (2010) 2329-2333.
2. V.V. Kharton, E.V. Tsipis, A.A. Yaremchenko, J.R. Frade, Solid State Ionics 166 (2004) 327-337.
3. J. Han, K. Zheng, K. Świerczek, Funct. Mater. Lett. 4 (2011) 151-155.
4. K. Zheng, A. Gorzkowska-Sobaś, K. Świerczek, Mater. Research Bull. 47 (2012) 4089-4095.



# Synthesis and structural properties of (Y,Sr)(Ti,Fe,Nb)O<sub>3-δ</sub> nanoparticles prepared by the low temperature calcining method

*T.Miruszewski<sup>1</sup>, P.Gdaniec<sup>1</sup>, J.Karczewski<sup>1</sup>, P.Kupracz<sup>1</sup>, M.Gazda<sup>1</sup>, B.Kusz<sup>1</sup>*

<sup>1</sup>Faculty of Mathematics and Applied Physics, G.Narutowicza 11/12, 80-233 Gdansk

e-mail: tmiruszewski@mif.pg.gda.pl

Keywords: perovskite, doped-SrTiO<sub>3</sub>, nanoceramics.

## INTRODUCTION

In recent years, the nanoceramics have become the very important and promising materials of applied research. In this group of materials, modified perovskite-related structures are very promising materials *i.a.* for SOFC anodes. One of the most important process in this device is fuel oxidation. Performance of this process is determined, *i.a.* by oxygen vacancies concentration [1]. It was shown [1], that electrical and structural properties of perovskite-type oxide structures depends on fabrication method. Moreover, the amount of grain boundaries and the surface defects are also responsible for oxygen diffusion performance. This process can be more efficient in nanostructures.

For many of applications microcrystalline doped strontium titanate has been prepared by the conventional solid-state reaction method. On the other hand, chemical synthesis, like a sol-gel or self-combustion methods have been proved to be more suitable for the preparation of nanocrystalline SrTiO<sub>3</sub> particles [2-4]. However, these methods need high sintering temperature, and due to a series of disadvantages, they have not been able to achieve industrial production.

In this work, the nano-particles of Y, Fe and Nb-doped SrTiO<sub>3</sub> mixed ionic-electronic conductor material synthesized by novel low-temperature method were analyzed. The Y, Fe and Nb dopant contents were selected according to results of previous own measurements and certain literature report [5]. The obtained products were fully characterized *i.a.* by XRD, SEM, FT-IR, BET and TG-DSC methods.

## EXPERIMENTAL

Two different powders: Y<sub>0.07</sub>Sr<sub>0.93</sub>Ti<sub>1-x</sub>Fe<sub>x</sub>O<sub>3-δ</sub> for x=0; 0.2 and SrTi<sub>0.98</sub>Nb<sub>0.02</sub>O<sub>3-δ</sub> were prepared by modified polymer precursor method (assigned as MPPM in this work) from the following precursors: Y(NO<sub>3</sub>)<sub>3</sub>·6H<sub>2</sub>O, non-dried Sr(OH)<sub>2</sub>·8H<sub>2</sub>O, Ti(OCH<sub>2</sub>CH<sub>2</sub>CH<sub>2</sub>CH<sub>3</sub>)<sub>4</sub>, Fe(NO<sub>3</sub>)<sub>3</sub>·9H<sub>2</sub>O and Nb(OCH<sub>2</sub>CH<sub>3</sub>)<sub>5</sub>. The different temperatures of calcinations (400-600 °C) have been used. Then, the phase composition of samples was analyzed by the X-ray diffraction technique (XRD). The structure and morphology of obtained nanoparticles was observed by a scanning electron microscopy (SEM). The thermal decomposition of the initial precursor was tested by thermogravimetry and differential scanning calorimetry (TG-DSC). The bond structure and impurity in the product was analyzed using a FT-IR spectrometer.

The specific surface area of particles was studied using a BET method.

## RESULTS AND DISCUSSION

The pure cubic-phase strontium titanate nanoarticles were successfully synthesized at 400-600 °C temperature range. The average crystallite sizes, calculated by using Scherrer's formula, were to be in range of 30-80 nm and their size strongly depends on calcination temperature and composition. The SEM images shown the nanoparticles with a uniform morphology, a non-uniform agglomerates of grains and particle sizes of about 30-70 nm. This is consistent results with estimation of grains size from Scherrer's equation from XRD data. The BET analysis showed a large specific surface area (S<sub>BET</sub>>30 m<sup>2</sup>/g) and small BET particle size d<sub>BET</sub> for all obtained powders. The results of TG-DSC showed the different regimes of decomposition of initial precursor. In the stage between 250-700 °C the decomposition of complex polycondensate may take place and some exo- and endothermic peaks which may refer to crystallization process can be observed. The FT-IR analysis will be also done for obtain an information about the impurity of powders and their bond structures.

## CONCLUSIONS

The Y, Fe and Nb-doped SrTiO<sub>3</sub> powders successfully synthesized at very low temperature of calcination. The 30-80 nm nanoparticles can be observed in obtained powder. According to shown structural properties, it can stated, that MPPM method allows obtaining a pure perovskite phase. Moreover, the crystallization process can occur in temperature which is 600-700 °C lower than that from the traditional solid state synthesis method.

## REFERENCES

1. J.S.Yoon, Y.H.Kim, E.J.Lee, H.J.Hwang, *Electronic Material Letters* **3** (2011) 209-213.
2. V.V.Srdic, R.R. Djenadic, *Journal of Optoelectronics and Advanced Materials* **7** (2005) 3005-3013
3. R.M.Piticescu, P.Vilarnho, L.M.Popescu, R.R.Piticescu., *Journal of Optoelectronics and Advanced Materials* **8** (2006) 543-547
4. Q.A.Zhu, J.G.Xu, S.Xiang, L.X.Chen, Z.G.Tan, *Material Letters* **65** (2011) 873-875
5. P. Blennow, A. Hagen, K. Hansen, L. Wallenberg, M. Mogensen, *Solid State Ionics* **179** (2008) 2047-2058

# THE INSTITUTE OF POWER ENGINEERING NOVELTY DEVELOPMENTS IN THE FIELD OF SOLID OXIDE FUEL CELL TECHNOLOGY

J. Kupecki, M. Stępień, M. Blesznowski, M. Skrzypkiewicz, K. Wawryniuk, M. Krauz\*, R. Kluczowski\* and T. Golec

Thermal Processes Department, Institute of Power Engineering, ul. Mory 8  
01-330 Warsaw, Poland

\*Ceramic Department CEREL, Institute of Power Engineering, ul. Techniczna 1  
36-040 Boguchwała, Poland  
e-mail: [michal.stepien@ien.com.pl](mailto:michal.stepien@ien.com.pl)

Keywords: SOFC, DC-SOFC, fuel cells, fuel cell stack, micro-CHP, hydrogen, modeling

## ABSTRACT

Institute of Power Engineering (IEN) has conducted extensive research related to solid oxide fuel cells (SOFC) since year 2004. The scope of IEN activities includes works devoted to design, modeling and operation of single cells, stack of fuel cells and complex micro-CHP systems, utilization of alternative fuels (natural gas, biogas, carbonaceous fuels), and sensitivity study. IEN designed, constructed and tested the first Polish micro-CHP unit based on solid oxide fuel cells. These works were preceded by tests

of auxiliary system units such as hot water tank, steam reformer, water vapor generator and burner. The range of activities includes online operation of SOFC stack with biomass gasifier [2] with simultaneous removal of chlorine and sulphur compounds to the required levels [3]. With a view to a comprehensive approach to the subject, the set of mathematical models and numerical simulators for detailed analysis aspects mentioned above were developed [4]. Studies of direct carbon solid oxide fuel cell (DC-SOFC) were also conducted [5]. IEN Fuel Cell Group has analyzed a set of commercial single SOFCs (different suppliers) and own production SOFCs which were prepared in the Ceramic Department (CEREL) of IEN. The cell components were characterized by microstructure investigations (using scanning electron microscopy), direct current operation (I-V measurements) and electrochemical impedance spectroscopy examinations (EIS). Currently high-temperature SOFCs, based on yttria-stabilized zirconia (YSZ) electrolyte, lanthanum-strontium manganite (LSM) cathode, and a nickel-YSZ cermet anode, operate at 750 – 850°C for the electrolyte supported cells. Reduction in the operating temperature of SOFCs is desirable to lower the costs, improve durability, and overcome the technological disadvantages associated with elevated temperatures. This is actually the key challenge on the way to commercialization of the SOFCs. The reduction in the operating temperature can be achieved in different ways, primarily by development of new materials and novel design concepts for the single cells and stacks. The design of cell, stack, and system was supported by the CFD and system-level modeling [6,7].

Commercialization of the micro-CHP systems based on SOFC as a main goal of IEN is realized by several

steps: organization of laboratory for SOFC development and testing; electrolyte supported SOFC (850 °C) – development and testing; anode supported SOFC (750°C) – development and testing; fuel testing (including biofuels and carbonaceous fuels); short SOFC stack – preparing and testing; demo SOFC stack (2.5 – 10 kW); 2.5 – 10 kW process module based on SOFC stacks, afterburner, heat exchanger, and other peripheries [8].

Presently, IEN is taking a leading role as a national developer of energy generation solutions based on solid oxide fuel cells for clean, sustainable, cheap and reliable energy delivery for residential and industrial applications.

## REFERENCES

1. T. Golec, R. Antunes, J. Jewulski, M. Miller, R. Kluczowski, M. Krauz, K. Krząstek, M. Blesznowski „The Institute of Power Engineering Activity in the Solid Oxide Fuel Cell Technology”, *Journal of Fuel Cell Science and Technology*, February 2010, vol. 7
2. Jewulski J., Zieleniak A., Stępień M. et al. Testing of SOFC fuel cell stack fuelled by gas from biomass gasification reactor [in] *Energy production from biomass - combustion & gasification*, T.Golec (ed), 2014;1:311-333.
3. M Blesznowski, J Jewulski, A Zieleniak, Determination of H<sub>2</sub>S and HCl concentration limits in the fuel for anode supported SOFC operation, *Central European Journal of Chemistry* 2013;11(6):960-967
4. Kupecki J., Milewski J., Badyda K., Jewulski J. Evaluation of Sensitivity of a Micro-CHP Unit Performance to SOFC Parameters, *ECS Transactions* 2013;51(1):107-116
5. Jewulski J, Skrzypkiewicz M, Struzik M, Lubarska-Radziejewska I. Lignite as a fuel for direct carbon fuel cell system, *Int J Hydrogen Energy* 2014;39:21778-21785
6. Kupecki J., Jewulski J., Milewski J., Multi-Level Mathematical Modeling of Solid Oxide Fuel Cells [in] *Clean Energy for Better Environment*, ISBN: 978-953-51-0822-1, pp. 53-85, Intech, Rijeka, 2012
7. Kupecki J., Skrzypkiewicz M., Wierzbicki M., Stępień M., Analysis of a micro-CHP unit with in-series SOFC stacks fed by biogas, *Energy Procedia*, in print
8. Jewulski J., Kupecki K., Blesznowski M. Progress in development of micro-CHP systems with fuel cells, *Instal* 2014;1:11-15



# INFLUENCE OF ANODE MICROSTRUCTURE ON FUEL CELL PERFORMANCE

*D. Szymczewska, J. Karczewski,\* A. Chrzan and P. Jasiński*

Faculty of Electronics, Telecommunications and Informatics, Gdańsk University of Technology

\* Faculty of Applied Mathematics and Physics, Gdańsk University of Technology

ul. Narutowicza 11/12, 80-233 Gdańsk, Poland

e-mail: dagmara.szymczewska@pg.gda.pl

Keywords: hydrogen, fuel cells, anode, porosity.

## INTRODUCTION

Fuel cells are electrochemical devices which convert chemical energy to the electrical one. Solid Oxide Fuel Cells (SOFCs) consist of a cathode, a solid state electrolyte and an anode. From cathode site oxygen from air is supplied and from anode site fuel, e.g. hydrogen, methane, is delivered. An electrolyte conduct only ions thus the electrons created on one electrode during chemical reaction must cross to another electrode by external circuit.

A layer, on which SOFC is supported, must be the thickest and mechanically strong. In case of anode support it should be chemically stable, highly active and porous [1]. Right porosity is needed in order to allow fuel permeability [2].

As pore formers organic materials can be used, because they form voids during sintering. Such materials are, for example, graphite, PMMA, sucrose, polystyrene etc. [3]. Important is optimize anode structure that after final heat treatment in anode structure maintain proper porosity.

## EXPERIMENTAL

To prepare anode substrate, powders of NiO (J.T.Baker) and YSZ (TOSOH) (60:40 wt%) were used. The powders were mixed and ball milled (400 rpm). To obtain porous structure two sets of anodes were prepared. One set contained pore former of poly(methyl methacrylate-co-ethylene glycol dimethacrylate) (PMMA-EGDM) with 8 $\mu$ m particle size. A second set contained a PMMA-EGDM with particle size of 50 $\mu$ m. In case of the both sets, an anode powder and a pore former ratios of 50:50, 60:40, 70:30, 80:20, 90:10 and 100:0 (vol.%) were prepared and investigated. To mix uniformly all powders they were ball milled (200rpm). The anode pellets was pressed (hydraulic press Carver) using 1g powders. For the every set and for the every volume ratio three sintering temperatures, i.e. 900°C, 1000°C and 1400°C, were used for samples fabrication. Density of each sample was investigated using Archimedes methods.

In order to investigate performance of different anode supports, fuel cells were prepared and investigated. Yttria stabilized zirconia was sprayed from the suspension as an electrolyte. Suspension was made from 8YSZ powder (TOSOH) dispersed in mixture of ethanol and toluene in 80:20 vol.%. The anode supports with electrolyte were sintered at 1400°C. A cathode was deposited by brushing the LSCF paste and sintering at 850°C.

Electrical measurements were made using an impedance analyzer Solartron SI 1260 combined with a

potentiostat / galvanostat Solartron SI 1287. Measurements were performed in the frequency range from 1 MHz to 0.1 Hz with a voltage excitation of 20 mV in the temperature range 600 – 800°C.

## RESULTS

Different ratios of PMMA-EGDM from both sets gives resulted in different porosity of anode structure (see Fig. 1).

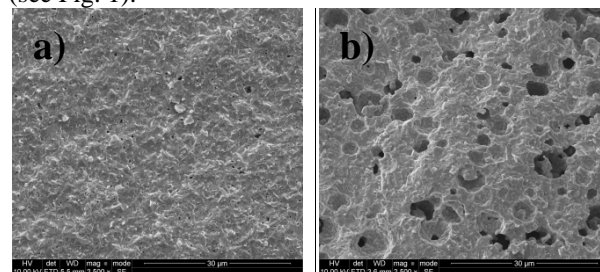


Fig. 1. SEM cross section micrographs of anode supports with PMMA-EGDM 8 $\mu$ m for anode powder : PMMA-EGDM of 100:0 vol.% (a) and 70:30 vol.% (b) ratio sintered at 1400°C.

## CONCLUSIONS

Anode supported solid oxide fuel cells with various porosities of anodes were prepared and investigated. The cell performances were electrically measured. Porosity has impact on SOFC efficiency.

## ACKNOWLEDGMENT

This work is partially supported by project founded by National Science Centre Poland based on decision DEC-2012/05/B/ST7/02153 and Statutory Funds for Research of Gdansk University of Technology.

## REFERENCES

1. A.J. Appleby, F.R. Foulkes, Fuel Cell Handbook, EG&G Technical Services, November 2004, 7-3
2. D. Simwonis, H. Thülen, F.J. Dias, A. Naoumidis, D. Stöver, *Journal of Materials Processing Technology* 92-93 (1999) 107-111
3. A. Sarikaya, V. Petrovsky, F. Dogan, *International Journal of Hydrogen Energy* 38 (2013) 10081-10091

# GRAPHITE-STAINLESS STEEL COMPOSITE FOR BIPOLAR PLATES FOR PEM FUEL CELLS

*Włodarczyk Renata*

*Department of Energy Engineering, Faculty of Environmental Engineering and Biotechnology,  
Czestochowa University of Technology,  
ul. Brzeznicka 60a, 42-200 Czestochowa,  
rwlodarczyk@is.pcz.czest.pl*

Keywords: Powder metallurgy, sintering, graphite, bipolar plates, fuel cells, PEMFC

The use of a graphite- stainless steel composite as bipolar plates (BP) in a polymer electrolyte membrane fuel cells (PEMFCs) has been evaluated. The study covers measurements of mechanical properties, microstructural examination, analysis of surface profile, wettability, porosity, and corrosion resistance of composite. The corrosion properties of composite were examined in  $0.1 \text{ mol dm}^{-3} \text{ H}_2\text{SO}_4 + 2 \text{ ppm F}^-$  saturated with  $\text{H}_2$  or with  $\text{O}_2$  and compared with 316L stainless steel.

# Synthesis of tetragonal $\text{LaNbO}_4$ nanopowders.

*K. Zagórski<sup>1</sup>, M. Czarnowska<sup>1</sup>, P. Czoska<sup>1</sup>, K. Dziergowski<sup>1</sup>, S. Wachowski<sup>1</sup>, A. Mielewczyk-Gryn<sup>1</sup>, M. Gazda<sup>1</sup>*

<sup>1</sup>Gdańsk University of Technology, Faculty of Applied Physics and Mathematics, Department of Solid State Physics, Narutowicza 11/12 80-233 Gdańsk, Poland  
e-mail: kzagorski@mif.pg.gda.pl

Keywords: nanocrystalline powders,

## INTRODUCTION

Acceptor doped lanthanum orthoniobate is a proton conducting oxide with relatively high proton conductivity and chemical stability. For example, its total conductivity is of the order of  $10^{-3}$  S/cm at 900°C [1]. This material could be successfully applied in such devices as fuel cells and gas sensors provided that it does not exhibit the structural phase transition in temperature range between room temperature and a device working temperature. Typical acceptor doped lanthanum niobates, e.g.  $\text{La}_{0.98}\text{Ca}_{0.02}\text{NbO}_4$ ,  $\text{La}_{0.98}\text{Sr}_{0.02}\text{NbO}_4$ , or  $\text{La}_{0.98}\text{Mg}_{0.02}\text{NbO}_4$  crystallize in the tetragonal Scheelite structure and at temperature between 500°C and 450°C transit into the monoclinic Fergusonite structure [2]. In order to avoid the phase transition, several strategies can be applied. For example, substitution of niobium with antimony [3] or vanadium [4] leads to a decrease of the transition temperature. On the other hand substitution of niobium with tantalum increases the transition temperature [5]. Another strategy leading to the stabilization of the tetragonal structure in room temperature is to decrease the crystallite sizes.

## EXPERIMENTAL

In this work nanocrystalline  $\text{La}_{0.98}\text{Ca}_{0.02}\text{NbO}_4$  powders were prepared by two methods: mechanosynthesis and molten salt synthesis. In both cases stoichiometric amounts of  $\text{CaCO}_3$ ,  $\text{Nb}_2\text{O}_5$  and  $\text{La}_2\text{O}_3$  (preheated at 900°C for 3 h) were used as reagents. The mechanosynthesis of  $\text{La}_{0.98}\text{Ca}_{0.02}\text{NbO}_4$  included several ball milling steps with the total duration time of 11 hours. It was followed by the calcination at 800°C for 2h. The molten salt synthesis was carried out in the eutectic mixture of KCl and NaCl flux heated in a covered crucible. Heating temperature was between 665°C and 710°C. Then, the salt residues were washed by deionised water and the powder was dried at 80°C for 24 h.

Obtained powders were characterized by X-ray diffraction and their grain morphologies were analysed and compared by scanning electron microscopy.

## RESULTS AND DISCUSSION

Figure 1 shows examples of the XRD patterns of the  $\text{La}_{0.98}\text{Ca}_{0.02}\text{NbO}_4$  powders obtained with molten salt synthesis, mechanosynthesis, and for comparison, with a

conventional solid state synthesis. It can be seen that the lowering of crystallite sizes leads to the stabilization of tetragonal Scheelite structure.

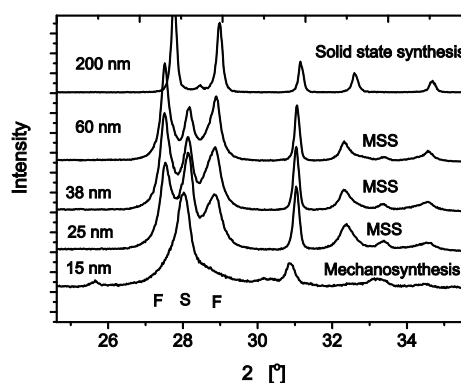


Fig. 1. XRD patterns of the  $\text{La}_{0.98}\text{Ca}_{0.02}\text{NbO}_4$  powders obtained with MSS, mechano- and solid state synthesis. F and S denote the strongest reflections of Fergusonite and Scheelite phases, respectively.

## CONCLUSIONS

Molten salt synthesis allowed to obtain the powders with a wide distribution of the crystallite sizes. These powders consisted of both tetragonal and monoclinic phases. On the other hand powders made by mechanosynthesis were tetragonal.

## ACKNOWLEDGMENT

This work is supported by the project POKL.04.01.01-00-368/09: “InterPhD: The development of interdisciplinary doctoral studies at the Gdansk University of Technology in modern technologies”.

## REFERENCES

- [1] R. Haugrud, T. Norby, *Solid State Ionics* 177 (2006) 1129.
- [2] A. Mielewczyk-Gryn, K. Gdula, T. Lendze, B. Kusz, M. Gazda, *Cryst. Res. Technol.* 45 (2010) 1225.
- [3] S. Wachowski, A. Mielewczyk-Gryn, M. Gazda, *J. Solid State Chem.* 219 (2014) 201.
- [4] A.D.Brandão, I.Antunes, J.R.Frade, J.Torre, V.V.Kharton, D.P.Fagg, *Chem. Mater.* 22 (2010) 6673–6683.
- [5] F.Vullum, F.Nitsche, S.M.Selbach, T.Grande, *J. Solid State Chem.* 181(2008) 2580–2585.

# OPTIMIZED THERMOELECTRIC COMPOSITE STRUCTURES

## $\text{Ag}_x\text{Pb}_m\text{Sb}_y\text{Te}_{m+2}$

*L. Horichok, T. Semko, L. Mezhylovska, V. Kotsyubynsky and V. Potyak*

Physical-Technical Faculty,

Vasyl Stefanyk Precarpathian National University, ul. Shevchenka 57, Iwano-Frankivsk, 76018, Ukraine

e-mail: [horichokihor@gmail.com](mailto:horichokihor@gmail.com)

Keywords: thermoelectric, composite materials, LAST

### INTRODUCTION

Thermoelectric power generators are solid state devices which can directly convert heat into electricity. Despite their clean and environmentally friendly operation, their current commercial applications are limited because of their low efficiency. A thermoelectric power generator device consists of heavily doped semiconductor legs which are connected electrically in series and thermally in parallel. Fundamental understanding of heat and charge carrier transport inside the thermoelectric legs can lead to new strategies to design and fabricate high efficiency thermoelectric materials.

With the optimal in terms of use in thermoelectric devices, complex physical and chemical properties of lead telluride is one of the most promising materials for making based on it thermoelectric generators for medium temperature range (500-800) K. In addition, the basic parameters of PbTe can be effectively changed by doping and solid solutions creation. In recent years, a significant increase in the efficiency of thermoelectric materials based Lead Telluride achieved through the creation of new class of compounds  $\text{Ag}_x\text{Pb}_m\text{Sb}_y\text{Te}_{m+2}$  (LAST) [1]. In paper was performed X-ray research and measurement of thermoelectric parameters (Seebeck coefficient, electrical conductivity, and thermal conductivity) of the  $\text{Ag}_x\text{Pb}_m\text{Sb}_y\text{Te}_{m+2}$  (with different value of x and y parameters), PbTe:Sb, and PbTe-Sb<sub>2</sub>Te<sub>3</sub>.

### EXPERIMENTAL

Synthesis of materials was carried out in quartz ampoules evacuated to residual pressure of  $10^{-4}$  Pa. Ampoules previously subjected to detailed cleaning. The resulting ingots were isolated and crushed to receive size fractions of (0.05-0.5) mm. Then they compressed under pressure (0.25-0.75) GPa. The resulting cylindrical sample with  $d = 5$  mm and  $h \approx 8$  mm subjected to annealing at  $T = (400-700)$  K by (5-20) hours.

### RESULTS AND DISCUSSION

It was found high values of dimensionless thermoelectric figure of merit:  $ZT \approx 1$  for PbTe:Sb (0,3 at.%), and Pb<sub>18</sub>Ag<sub>2</sub>Te<sub>20</sub> in the temperature range (450-550) K, and values  $ZT \approx (1.5-2.0)$  for Pb<sub>18</sub>Ag<sub>1</sub>Sb<sub>1</sub>Te<sub>20</sub> in the temperature range (500-600) K. Thermoelectric efficiency of other materials in the studied temperature range is significantly lower. The high values of thermoelectric figure of merit explained significant increase conductivity of the material, due to

the action of the donor atoms of antimony for PbTe:Sb. And, the high values of ZT explained by reduction of thermal conductivity, resulting in the creation of a significant number of phonon scattering centers for Pb<sub>18</sub>Ag<sub>1</sub>Sb<sub>1</sub>Te<sub>20</sub> and Pb<sub>18</sub>Ag<sub>2</sub>Te<sub>20</sub>.

### CONCLUSIONS

Was received high value of the thermoelectric figure of merit for PbTe:Sb (0,3 at.%) and Pb<sub>18</sub>Ag<sub>1</sub>Sb<sub>1</sub>Te<sub>20</sub>: ( $ZT \approx 1$  at the (450-550) K) and for Pb<sub>18</sub>Ag<sub>2</sub>Te<sub>20</sub> ( $ZT \approx 2$  at the temperature region (500-600) K).

These values caused increasing of electrical conductivity after donor action of the atoms of Sb for PbTe:Sb.

The efficient of heat conductivity was decreasing in the case of Pb<sub>18</sub>Ag<sub>1</sub>Sb<sub>1</sub>Te<sub>20</sub> and Pb<sub>18</sub>Ag<sub>2</sub>Te<sub>20</sub> after increase role of phonon scattering.

### ACKNOWLEDGMENT

This work is sponsored by NATO's Public Diplomacy Division in the framework of "Science for Peace" (NATO.NUKR.SFPP 984536).

### REFERENCES

1. J. Dadda, E. Muller, B. Klobes, P. Bauer Pereira, R. Hermann., *Journal of Electronic Materials*, **41**(2012)2065.

# COMPOSITE THERMOELECTRIC MATERIALS ON THE BASE OF PbTe WITH Ag AND ZnO NANOINCLUSIONS

*L. Nykyruy, D. Freik, R. Ahiska\*, O. Matkivskiy, I. Lishchynskiy and I. Hryhoruk*

Physical-Technical Faculty,

Vasyl Stefanyk Precarpathian National University, ul. Shevchenka 57, Iwano-Frankivsk, 76018, Ukraine

\*Faculty of Science, Gazi University, Teknikokullar 06500 Ankara, Turkey

e-mail: [lyubomyr.nykyruy@gmail.com](mailto:lyubomyr.nykyruy@gmail.com)

Keywords: thermoelectric, composite materials, nanoinclusions, lead telluride

## INTRODUCTION

Recent studies identify two possible ways to further improve the efficiency of thermoelectric materials: transition to using of materials with lower dimensionality (2D-, 1D- and 0D-structures) or create of new composite materials through modification the size of grain in bulk materials [1].

The quantum-size effects use for increasing of the Seebeck coefficient ( $S$ ) and for further changes of specific electrical conductivity ( $\sigma$ ) in the first case. In the second case, the creation the numerical limits leads to scattering of phonons more effectively than scattering of electrons. Another important factor is the increase of Seebeck coefficient ( $S$ ) to the field of strong degeneracy after selection of carriers through the creation of an energy barrier at the boundaries of crystallites or grains. It is particularly effective for the composite material [2].

In work the research for thermoelectric semiconductor composite materials based on PbTe with inclusion of nanoparticles of Ag and nanoparticles of ZnO was explored.

## EXPERIMENTAL

The purified Pb and Te used as initial components. Synthesis and growing of alloys was carried out in highly pure quartz ampoules. Ampoule was pumped to  $2 \cdot 10^{-4}$  Pa on the next stage with soldering, and placed in oven whose temperature is slowly increases to 40-60 degrees above the temperature of the solidus of PbTe (1220-1240 K) for prevent of the explosion of Tellurium.

Formation of thermocouples by pressing powder of thermoelectric material with micro- and nano- size range creates large internal borders for additional phonon scattering [2]. However, it need not only reduce the thermal conductivity, but also increase the Seebeck coefficient to improve the thermoelectric properties of material. For this case, around thermoelectric grain PbTe of the size of (0.5-1.0) micrometers prompted to create nano-channels for the stream of an electric current. In this work was development technology for create of the conductive nano-channels on the base of colloidal Silver and ZnO nanoparticles.

## RESULTS AND DISCUSSION

*Silver nanoparticles.* It was finding that the introduction of Ag nanoparticles (size is  $\sim 50$  nm), not only reduces the thermal conductivity, but also increases the Seebeck coefficient after additional throttling of electrons on the barriers of Silver nanoparticles. Thermal conductivity of (0.06-0.2) W/(m·K) has been achieved in

the case of the scattering of medium-wave phonons (MWP). The absolute value of Seebeck coefficient in these conditions increases up to 340  $\mu\text{V/K}$ .

*ZnO nanoparticles.* The introduction of nanodisperse ZnO leads to the increase of Seebeck coefficient in 2-3 times and leads to monotonic decrease of thermal conductivity. The result figure of merit of this thermoelectric material  $ZT \approx 1.38$  at 0.5 at.% ZnO. For PbTe (ZnO) were obtained the significantly higher values of Seebeck coefficient (430-500  $\mu\text{V/K}$ ) in compare to PbTe(Ag).

## CONCLUSIONS

1. The compaction technology of thermoelectric composite materials based on PbTe with the inclusion of colloidal silver nanoparticles has been shown.
2. The increase of Seebeck coefficient is explained throttling of high energy carriers through the barriers on the grain boundaries.

## ACKNOWLEDGMENT

This work is sponsored by NATO's Public Diplomacy Division in the framework of "Science for Peace" (NATO.NUKR.SFPP 984536).

## REFERENCES

1. Y. Ma, R. Heijl, A.E. Palmqvist. *J. Mater. Sci.* **48**(2013)2767.
2. J. He, M.G. Kanatzidis, and V.P. Dravid, *Materials Today* **16**(2013)166.

# THEORETICAL STUDIES ON RESONANT LEVELS IN THERMOELECTRIC MATERIALS

*Bartłomiej Wiendlocha*

AGH University of Science and Technology,  
Faculty of Physics and Applied Computer Science, Al. Mickiewicza 30,  
30-059 Krakow, Poland  
e-mail: wiendlocha@fis.agh.edu.pl

Keywords: thermoelectrics, resonant levels

## INTRODUCTION

One of the ways of improving the efficiency of thermoelectric materials is via doping with so called resonant impurities [1]. Resonant levels (RL) are formed by specific impurity atoms in semiconductors or metals, at energies, where in the absence of neighboring atoms a real bound state would be formed. One of the manifestations of the resonant level is a presence of a sharp peak of the density of electronic states on impurity atom at the resonance energy, thus resonant impurities may significantly modify the host material's band structure. As was experimentally shown e.g. for PbTe:TI [2], RL may lead to the large increase in the thermopower ( $S$ ) of the system, although idea of positive role of RL in thermoelectrics (TE) is sometimes questioned.

## RESULTS AND DISCUSSION

In this work we show some of the recent theoretical results concerning resonant impurities in thermoelectric materials, giving a comprehensive picture of the “resonant” systems, and propose an intuitive understanding for the thermopower enhancement. Using the Korringa-Kohn-Rostoker method and the coherent potential approximation, quantities like the electronic densities of states, Bloch spectral functions (describing electronic band structure in the case of disordered systems) and energy dependent residual electronic conductivity (calculated within the Kubo-Greenwood formalism) are obtained from first principles and provide understanding of different RL systems. We start by recalling the example of constantan (Cu-Ni), one of the highest thermopower metallic alloys, where the RL on Ni is responsible for the large and negative value of thermopower ( $S$ ). Next, the cases of PbTe:TI [3], SnTe:In, Bi<sub>2</sub>Te<sub>3</sub>:Sn [4] show the common features of RL working in TE materials. The modifications of the electronic bands and Fermi surface in PbTe, caused by the TI resonant impurity, shows that the positive effect of the resonant level on the thermopower may be understood as similar the increase in band degeneracy, as the resonant impurity forms a “cloud” of electronic states around the PbTe valence band. Next, the contrasting example of PbTe doped with titanium (Ti), where RL does not lead to the increase of  $S$  [5] provides a further insight on the issue of localization of resonant states in host semiconductor and shows the critical role of hybridization. Further, the case of Mg<sub>2</sub>Sn:Ag [6]

proves that the resonant-or-classic character of impurity depends not only on the doping element, but also on the crystal site, where dopant is located. Finally, the comparison of Cu-Ni with PbTe:TI shows the fundamental differences between mechanisms of thermopower enhancement by the RL in metals and semiconductors, resulting in different sign of  $S$  in spite of the similar location of the Fermi level (decreasing slope of DOS).

## ACKNOWLEDGMENT

This work is partly supported by the Polish National Science Center (NCN) (Project No. DEC-2011/02/A/ST3/00124).

## REFERENCES

1. J.P. Heremans, B. Wiendlocha and A.M. Chamoire, *Energy Environ. Sci.*, **5**, (2012) 5510
2. J.P. Heremans, V. Jovovic, E.S. Toberer, A. Saramat, K. Kurosaki, A. Charoenphakdee, S. Yamanaka, and G. J. Snyder, *Science* **321** (2008) 554
3. B. Wiendlocha, *Physical Review B* **88** (2013) 205205
4. B. Wiendlocha, K. Kutorasinski, S. Kaprzyk, J. Tobola, *Scripta Materialia*,  
*doi:10.1016/j.scriptamat.2015.04.014*
5. B. Wiendlocha, *Applied Physics Letters* **105** (2014) 133901
6. S Kim, B Wiendlocha, H Jin, J Tobola, JP Heremans, *J.Appl. Phys.* **116** (2014) 153706



# THIN AND THICK FILM LITHIUM CONDUCTING GARNET

*E. Hanc<sup>1</sup>, L. Lu<sup>2</sup>, B. Yan<sup>2</sup>, M. Kotobuki<sup>2</sup>, W. Zajac<sup>1</sup> and J. Molenda<sup>1</sup>*

<sup>1</sup>AGH University of Science and Technology, Faculty of Energy and Fuels, al. Mickiewicza 30, 30-059 Krakow, Poland

<sup>2</sup>Materials Science Group, Department of Mechanical Engineering, National University of Singapore, Singapore  
e-mail: wojciech.zajac@agh.edu.pl

Keywords: lithium-ion batteries, Li-electrolyte, tape-casting, pulsed laser deposition

## INTRODUCTION

One of the basic requirements of the materials for Li-ion batteries is the safety of their use. Recently, due to chemical instability and flammability of liquid organic electrolytes, lithium conducting ceramic oxides attract much attention as electrolytes for Li-cells. Garnet-structured materials from  $\text{Li}_7\text{La}_3\text{Zr}_2\text{O}_{12}$ -group (LLZO) seems to be especially attractive, which is caused by their extraordinarily wide electrochemical window ranging from 0 up to 10 volts vs.  $\text{Li}^+/\text{Li}$  and high ionic conductivity. The standard synthesis process of LLZO is 2-step high-temperature solid state method. Using this procedure, temperature as high as  $1200^\circ\text{C}$  is required to obtain dense pellets of LLZO. However, annealing at as high temperature leads to intensified evaporation of  $\text{Li}_2\text{O}$ , which causes difficulty in controlling the stoichiometry of material. For further reduction of resistance of an electrolyte layer one may wish to use LLZO in a form of thin films. This is of particular importance for nano-scale All-Solid-State batteries to be unified in integrated circuits. Those problems causes necessity of development of different methods of synthesis LLZO electrolytes.

LLZO materials were prepared by high temperature solid state synthesis, tape-casting method and pulsed laser deposition. Effect of ZnO-doping on sinterability of LLZO material during standard solid state synthesis was studied. Influence of additives such as binders, plasticizers and solvents was investigated for tape-casting method. Influence of oxygen pressure, type of substrate and its temperature were investigated during pulsed laser depositing.

## EXPERIMENTAL

LLZO-films were deposited on silica, Au coated silica, Pt coated silicon, Au/Pt coated silicon, MgO substrates. Crystal structure of the obtained materials was investigated at ambient and high temperature using X-ray diffraction (XRD) method. Crystal structure parameters were determined using the Rietveld method with GSAS/EXPGUI software package. Electrical conductivity was measured by means of impedance spectroscopy and potentiostatic polarization. Sinterability of materials was investigated using dilatometric method.

## CONCLUSIONS

The large effect of the Zn addition on the sinterability of LLZO-garnet was observed. The optimal amount of the zinc oxide additive was defined as 0.1 mol per mol of LLZO. Electronic conductivity was determined to be as low as  $10^{-9}$  S/cm at room

temperature indicating purely ionic conductivity. LLZO thick films, produced by tape-casting method, showed high ionic conductivity about 0.08 mS/cm at room temperature and density close to theoretical value. Optimal composition of slurry and annealing process of tapes were found. Most of substrates used for PLD coating technique, such as MgO, silica and Pt coated silicon, showed high reactivity towards LLZO. Among studied candidate for substrates deposition of LLZO was possible only on Au coated silica substrate. Optimal annealing process leading to the garnet phase was described. However, density of films was very low, which causes unmeasurably low ionic conductivity.

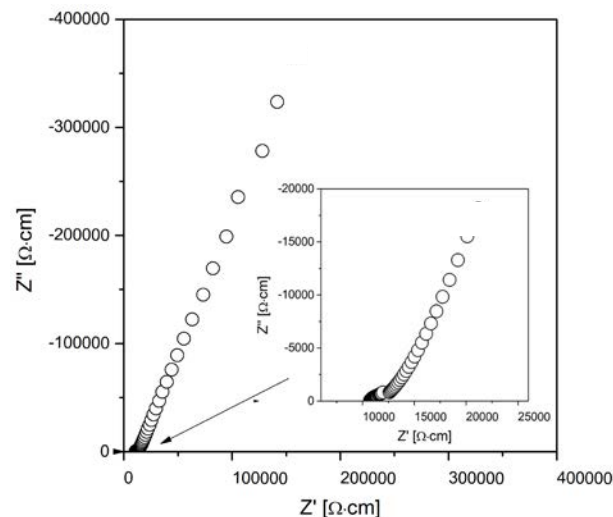


Fig. 1. Impedance spectra of LLZO-sample obtained by tape-casting method, measured at room temperature.

## ACKNOWLEDGMENT

This work was funded by the National Research Foundation, Prime Minister's Office, Singapore under its Competitive Research Program (CRP Award No. NRF-CRP 10-2012-06), by National Science Centre Poland under grant no. 2012/05/D/ST5/00472 and. by a grant from Switzerland through the Swiss Contribution to the enlarged European Union (grant no. 080/2010).

One of the authors (E.H.) would like to express his gratitude to National Science Centre Poland for doctoral scholarship under grant no. 2014/12/T/ST5/00267

# AN X-RDF STUDY OF SELECTED IONIC AND ELECTRONIC CONDUCTIVE GLASSES

*J. Kalabinski, S. Gierlotka\*, T.K. Pietrzak, P. Grabowski, J.L. Nowinski and J.E. Garbarczyk*

Faculty of Physics, Warsaw University of Technology, Koszykowa 75, 00-662 Warsaw, Poland

\*Institute of High Pressure Physics, PAS, al. Prymasa Tysiąclecia 98, 01-424 Warsaw, Poland

e-mail: kalabinski@if.pw.edu.pl

Keywords: radial distribution function, mechanosynthesis, glasses, X-ray diffraction

## INTRODUCTION

An X-RDF (radial distribution function) study has been carried out on silver ion conductive glasses  $\text{AgI-Ag}_2\text{O-MoO}_3$  and lithium ion conductive glasses  $\text{Li}_2\text{O-FeO-V}_2\text{O}_5\text{-P}_2\text{O}_5$ . The former glass system was studied in detail by Minami [1] and other researchers, however some issues still have remained open. In particular, it concerns to the mechanism of glass formation during mechanosynthesis. Aim of the presented study was to investigate evolution of the local structure arrangement with milling time. The glasses of the second system are capable to electro-intercalate/deintercalate  $\text{Li}^+$  ions and are considered as cathode materials in batteries. Their electrical properties depend on  $\text{V}_2\text{O}_5$  doping and are significantly changed after nanocrystallization [2]. The work focuses on changes of the local arrangement in the glass structure caused by nanocrystallization and  $\text{V}_2\text{O}_5$  doping.

## EXPERIMENTAL

$50\text{AgI}\cdot 25\text{Ag}_2\text{O}\cdot 25\text{MoO}_3$  glass samples were prepared by mechanosynthesis performed by Fritsch Pulverisette P7 planetary ball mill operating at a constant speed of 600rpm. Milling time varied from 1h up to 18h.

$\text{Li}_2\text{O-FeO-V}_2\text{O}_5\text{-P}_2\text{O}_5$  glass samples were prepared as follows. Starting powders in appropriate amounts were homogenized and annealed under 5N nitrogen flow in two subsequent steps: (i) at  $300^\circ\text{C}$  for 2h and (ii) at  $570^\circ\text{C}$  for 2h. The batch was then melted at  $1200^\circ\text{C}$  in alumina crucibles placed in a chamber furnace, using a double-crucible technique. After 15 minutes of annealing, the melt was quenched between two stainless steel plates at room temperature.

X-ray diffraction measurements of prepared samples were carried out using a modified Bruker D8 diffractometer. To achieve best RDF resolution, Ag-anode with mean  $K_\alpha$  radiation wavelength of  $0.5609 \text{ \AA}$  was used as X-ray source. Diffraction data were collected within the angle range of  $0\text{-}145^\circ$ .

Radial distribution functions were calculated using GudrunX software package [3]

## RESULTS

Samples of nominal composition of  $50\text{AgI}\cdot 25\text{Ag}_2\text{O}\cdot 25\text{MoO}_3$  were mechanosynthesized for four different milling times: 0h (crystalline substrates were mixed manually), 3h, 6h and 18h. The 0h-sample, (fully crystalline), was investigated and treated as a reference for further analysis. Milling for 3h and 6h resulted in formation of a glass-crystalline material,

whereas longer, 18h lasting, led to formation of a fully amorphous one.

Calculated RDF for the 3h, 6h and 18h milled samples exhibit no major differences (Fig. 1). Atomic interaction up to  $6\text{ \AA}$  are easily identifiable and yield information on average bond lengths in and coordination numbers of those atom pairs.

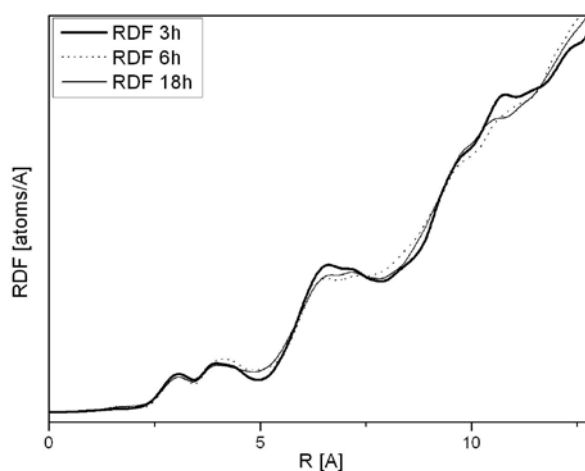


Fig. 1. RDF of  $50\text{AgI}\cdot 25\text{Ag}_2\text{O}\cdot 25\text{MoO}_3$  samples for different milling times

## CONCLUSIONS

During mechanosynthesis of a mixture of  $50\text{AgI}$ ,  $25\text{Ag}_2\text{O}$  and  $25\text{MoO}_3$  crystalline compounds, an amorphous phase is formed, but the process is incomplete if milling time is shorter than 18h. The local ordering of that glassy phase is different than that observed for the starting components or intermediate crystalline products. The interatomic distances for identifiable atom pairs and coordination numbers were calculated. The study shed some light on our understanding of mechanosynthesis process and its nature.

## ACKNOWLEDGMENT

This work has been financed by National Science Centre: project OPUS-4 no. DEC-2012/07/B/ST5/03184 (2013-2016).

## REFERENCES

1. T Minami, H Nambu, M Tanaka, *J. Am. Ceram. Soc.* **60** (1977), p. 467.
2. P. Michalski, J. Nowinski, T. Pietrzak, M. Wasiuconek, J. Garbarczyk, A. Zalewska, *Procedia Engineering* **98**(2014), p.78.
3. A.K. Soper, E.R. Barney, *J. Appl. Cryst.* **44** (2011), p. 714.

# STRUCTURAL AND ELECTRICAL STUDIES OF $\text{Bi}_{2.8}\text{Pb}_{0.2}\text{YbO}_{5.9}$

*M. Leszczynska, M. Malys, A. Borowska-Centkowska, W. Wrobel, J.R. Dygas, I. Abrahams\* and F. Krok*

Faculty of Physics, Warsaw University of Technology, ul. Koszykowa 75, 00-662 Warszawa, Poland

\* Centre for Materials Research, School of Biological and Chemical Sciences,

Queen Mary University of London, Mile End Road, London E1 4NS, U.K

e-mail: leszczynska@if.pw.edu.pl

Keywords: bismuth oxide, bismuth lead ytterbium oxide

## INTRODUCTION

Bismuth oxide based solid electrolytes have been studied for many years because of their exceptional oxide ion conductivities at temperatures significantly lower than traditional electrolytes, such as the stabilised zirconias. Much research on these systems has been carried out on stabilisation of the highly conducting  $\delta$ -phase of  $\text{Bi}_2\text{O}_3$ , which is only stable at temperatures above *ca.* 730°C [1]. This is typically achieved by solid solution formation with other metal oxides, in particular the lanthanide oxides  $\text{Ln}_2\text{O}_3$  ( $\text{Ln} = \text{Y}, \text{Yb}, \text{Er}$ ), some of which show high oxide ion conductivity. The  $\text{Bi}_2\text{O}_3$ - $\text{Yb}_2\text{O}_3$  binary system has been extensively investigated. At 25% of  $\text{Yb}_2\text{O}_3$ , the *fcc* phase is readily obtained at room temperature [2]. Partial substitution of  $\text{Bi}^{3+}$  by aliovalent cations, such as  $\text{Pb}^{2+}$  can lead to increase of the nominal vacancy concentration per metal atom beyond that in pure  $\delta$ - $\text{Bi}_2\text{O}_3$ .  $\text{Pb}^{2+}$  ions show also many similarities to  $\text{Bi}^{3+}$ , e.g. both ions exhibit stereochemical activity of the  $6s^2$  electron pairs. But in the  $\text{Bi}_2\text{O}_3$  –  $\text{PbO}$  binary system, the cubic  $\delta$ -phase is only observed at elevated temperatures [3]. However, in ternary systems of  $\text{Bi}_2\text{O}_3$ - $\text{MO}_x$ - $\text{PbO}$  ( $\text{M} = \text{Y}, \text{Er}$ ) it has been shown that  $\delta$ -type phases can be preserved to room temperature [4, 5]. Here we present a study of the ternary system  $\text{Bi}_2\text{O}_3$ - $\text{Yb}_2\text{O}_3$ - $\text{PbO}$  of chemical formula  $\text{Bi}_{2.8}\text{Pb}_{0.2}\text{YbO}_{5.9}$ .

## EXPERIMENTAL

Sample of composition  $\text{Bi}_{2.8}\text{Pb}_{0.2}\text{YbO}_{5.9}$  was prepared by standard solid state methods from stoichiometric amounts of the parent oxides. Structural characterisation was carried out by X-ray and neutron powder diffraction at various temperatures. Total scattering analysis involving Reverse Monte Carlo (RMC) modelling, was used to analyze the short-range ion pair correlations. Electrical conductivity was characterised by a.c. impedance spectroscopy. Ionic transference numbers were measured using a modified EMF method.

## RESULTS AND DISCUSSION

X-ray and neutron powder diffraction results were consistent with a simple cubic phase and could be satisfactorily indexed in space group *Fm-3m*. Structure refinements were proceeded using a cubic-subcell model. Cations were located on the ideal  $4a$  site (0,0,0) with oxide ions distributed over three sites;  $8c$  at (0.25, 0.25, 0.25),  $32f$  at approximately (0.3, 0.3, 0.3) and  $48i$  at around (0.5, 0.2, 0.2).

At high temperature range (480 - 850 °C), the total conductivity of  $\text{Bi}_{2.8}\text{Pb}_{0.2}\text{YbO}_{5.9}$  is slightly higher than

in  $\text{Bi}_3\text{YbO}_6$ . However, at temperatures below 400 °C the conductivity values for  $\text{Bi}_{2.8}\text{Pb}_{0.2}\text{YbO}_{5.9}$  are significantly lower than those for the lead free analogue  $\text{Bi}_3\text{YbO}_6$  (fig. 1). The measurement of the oxide ion transference numbers showed that the ionic conductivity has predominant share in the total conductivity.

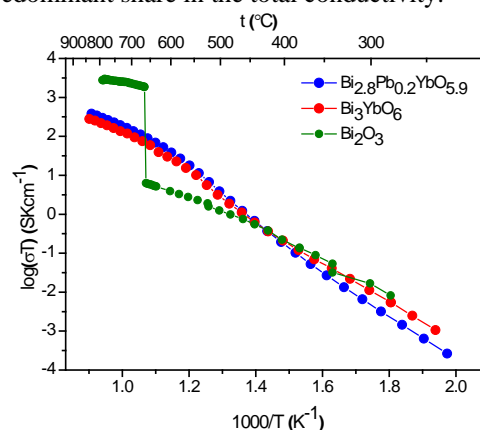


Fig. 1. Arrhenius plots of total conductivity for  $\text{Bi}_{2.8}\text{Pb}_{0.2}\text{YbO}_{5.9}$ . For comparison the data for  $\text{Bi}_3\text{YbO}_6$  and  $\text{Bi}_2\text{O}_3$  are included.

## CONCLUSIONS

Di-substitution of lead and ytterbium for bismuth in  $\text{Bi}_2\text{O}_3$  leads to formation of  $\delta$ -type phase, with nominally higher vacancy concentration than in pure  $\delta$ - $\text{Bi}_2\text{O}_3$ . Although the  $\text{Bi}_{2.8}\text{Pb}_{0.2}\text{YbO}_{5.9}$  compound exhibits higher vacancy concentration, the conductivity values at high temperature range are comparable to the mono-substituted bismuth ytterbium system.

## ACKNOWLEDGMENT

This work is supported by grant from National Science Centre, grant number 2012/05/E/ST3/02767.

## REFERENCES

- [1] T. Takahashi, H. Iwahara, Y. Nagai, *J. Appl. Electrochem.* 2 (1972) 97
- [2] M. Leszczynska, X. Liu, W. Wrobel, M. Malys, S.T. Norberg, S. Hull, F. Krok, I. Abrahams, *J. Phys.: Condens. Matter* 25 (2013) 454207
- [3] N.M. Sammes, G. Tompsett, R. Phillips, C. Carson, A.M. Cartner, M.G. Fee, *Solid State Ionics* 86–88 (1996) 125
- [4] M. Omari, M. Drache, P. Conflant, J.C. Boivin, *Solid State Ionics* 40 (41) (1990) 929.
- [5] N.A.S. Webster, C.D. Ling, C.L. Raston, F.J. Lincoln, *Solid State Ionics* 178 (2007) 1451

# IONIC AND ELECTRONIC CONDUCTIVITY IN THE $\text{Bi}_2\text{O}_3\text{-PbO-Y}_2\text{O}_3$ SYSTEM

*K. Lewandowski<sup>1</sup>, W. Wrobel<sup>1</sup>, A. Borowska-Centkowska<sup>1</sup>, F. Krok<sup>1</sup>, I. Abrahams<sup>2</sup>, M. Matys<sup>1</sup>, J. Dygas<sup>1</sup>*

<sup>1</sup>Faculty of Physics, Warsaw University of Technology, Koszykowa 75, 00-662 Warsaw, Poland

<sup>2</sup>Materials Research Institute, School of Biological and Chemical Sciences, Queen Mary University of London, Mile End Road, London E1 4NS, United Kingdom  
e-mail: christopher.lewan@gmail.com

Keywords: bismuth oxide, bismuth lead yttrium oxide; fluorite structure, X-ray diffraction, ac. impedance spectroscopy, oxygen partial pressure, cation reduction

## INTRODUCTION

Bismuth oxide based compounds are promising materials for application in SOFC, due to its high oxide ion conductivity at high and intermediate temperatures. Subvalent substitution of bismuth by  $\text{Pb}^{2+}$  in bismuth oxide offers the possibility of increasing the nominal vacancy concentration per metal atom beyond that in pure  $\delta\text{-Bi}_2\text{O}_3$ . Bismuth and lead cations exhibit similar stereochemical activity of the  $6s^2$  electron pairs, comparable polarizabilities and adoption of similar distorted coordination environments in oxide systems. Despite these apparent similarities the cubic  $\delta$ -phase in the  $\text{Bi}_2\text{O}_3\text{-PbO}$  binary system is only observed at elevated temperatures [1]. However, in ternary systems of the type  $\text{Bi}_2\text{O}_3\text{-MO}_x\text{-PbO}$  ( $M = \text{Ca}, \text{Y}, \text{Er}$  and  $\text{La}$ ) it has been shown that  $\delta$ -type phases can be preserved to room temperature [2].

In this study influence of oxidizing / reducing atmospheres on structural and electrical properties of compounds in  $\text{Bi}_2\text{O}_3\text{-PbO-Y}_2\text{O}_3$  ternary system is presented.

## EXPERIMENTAL

Samples of general formula  $\text{Bi}_{2+x}\text{Pb}_{0.5}\text{Y}_{1-x}\text{O}_{5.5}$  and  $\text{Bi}_{2+x}\text{Pb}_{0.5}\text{YO}_{5.75+3x/2}$  were prepared using proper molar ratios of bismuth oxide (Aldrich >99,9%), lead oxide (Aldrich >99,9%) and yttrium oxide (Aldrich >99,9%). Powders were ball milled with ethanol and synthesised in temperature range from 650-800°C, depending on composition. Prepared samples were characterised using X-ray diffraction and differential thermal analysis methods under controlled atmospheres of air and nitrogen. In order to examine electrical conductivity and ionic transference numbers, impedance spectroscopy measurements in controlled oxygen partial pressure atmospheres and modified EMF method were performed.

## RESULTS AND DISCUSSION

All of the studied compositions show small degree of reduction at high temperatures. Such a reduced state can be preserved to room temperature by rapid quenching of the sample or by slow cooling under atmosphere of reducing gas. Re-oxidation, which can appear on cooling under oxidizing atmospheres, at intermediate temperatures, is reflected in the unit cell

parameter variation (Fig.1) and the Arrhenius plot of conductivity. Reduction / oxidation processes affect conduction mechanism in studied compounds. The electronic component of total conductivity was studied using modified EMF method in the oxygen concentration cell. In both studied systems electronic transference number was found to be almost zero at high temperatures and increasing below ca. 550°C. Measurements of impedance spectroscopy under different oxygen partial pressure atmospheres were done to determine mechanism of electronic conductivity in studied systems. Redox reactions similar to those observed in the present system are likely to be a common feature in bismuth oxide based materials and may well be associated with the commonly observed instability of these materials at intermediate temperatures.

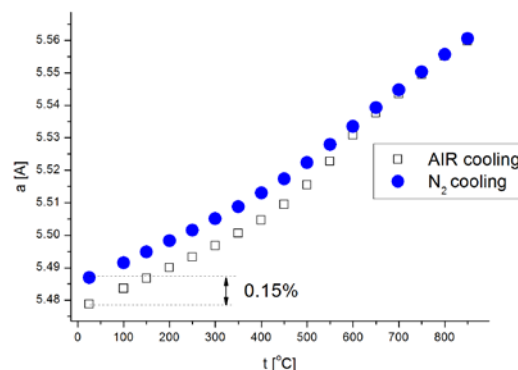


Figure 1. Structural dependence on oxidizing/reductive atmospheres of  $\text{Bi}_{2.5}\text{Pb}_{0.5}\text{YO}_{5.75}$ .

## ACKNOWLEDGMENT

This work is supported by the National Science Centre, Poland under project grant number 2012/05/E/ST3/02767

## REFERENCES

1. R.M. Biefeld, S.S. White, *J. Am. Ceram. Soc.*, 64 (1981) 182.
2. M. Omari, M. Drache, P. Conflant, J.C. Boivin, *Solid. State Ionics*, 40/41 (1990) 929.

# IONIC AND ELECTRONIC CONDUCTIVITY OF $\text{Bi}_{26}\text{Mo}_{10}\text{O}_{69}$ AND $\text{Bi}_{26}\text{Mo}_9\text{W}_1\text{O}_{69}$ COMPOUNDS

*M. Malys<sup>1</sup>, K. Kosyl<sup>1</sup>, M. Tyrakowska<sup>1</sup>, M. Wójcik<sup>1</sup>, A. Kruk<sup>1</sup>, W. Wróbel<sup>1</sup>, J.R.Dygas<sup>1</sup> and F. Krok<sup>1</sup>*

<sup>1</sup> Faculty of Physics, Warsaw University of Technology, Warsaw, Poland.

e-mail: malys@mech.pw.edu.pl

Keywords: bismuth oxides, transference number, ac impedance spectroscopy

## INTRODUCTION

$\text{Bi}_{26}\text{Mo}_{10}\text{O}_{69}$  belongs to family of oxide ion conductors with specific columnar structure based on  $[\text{Bi}_{12}\text{O}_{14}]_{\infty}$  columns [1,2]. Depending on the temperature, this compound exhibits two polymorphs: a triclinic form, stable from room temperature to 310°C, and a monoclinic one, stable above 310°C up to the melting point (975°C). Partial substitution of molybdenum by tungsten ( $\text{Bi}_{26}\text{Mo}_{10-x}\text{W}_x\text{O}_{69}$  for  $0 < x < 2$ ) results in significant increase of conductivity. The best results are obtained for  $x = 1$  composition, where electrical conductivity values are over one order of magnitude higher than that for parent compound (Fig.1). Tungsten substitution does not create additional oxygen vacancies in the parent material, therefore increase of conductivity may be caused by change of mobility of vacancies or increase of electronic contribution to total conductivity.

The aim of the present work was to apply modified EMF method to investigate ionic and electronic transport properties of  $\text{Bi}_{26}\text{Mo}_{10}\text{O}_{69}$ -related materials.

## EXPERIMENTAL

Polycrystalline samples were prepared by solid state reaction in air, from stoichiometric amounts of pure oxides:  $\text{Bi}_2\text{O}_3$  (99.9% Aldrich),  $\text{MoO}_3$  (Merck 99.5%), and  $\text{WO}_3$  (Aldrich 99.6%). The weighed amount of reagents, mixed and ground in an agate mortar, were first progressively preheated at 500°C and then reground and calcinated at 800°C for 12 hours, reground and pelletised. Pellets were then sintered at 850°C for 5 hours in air.

The total conductivity of the sample was examined by a.c. impedance spectroscopy in frequency range 1-10<sup>6</sup>Hz using Solatron SI 1260 frequency analyzer. The transference numbers of the gas tight ceramics were measured using the concentration cell:  $\text{O}_2(\text{pO}_2 = 1.01 \times 10^5 \text{ Pa}); \text{Pt}|\text{Oxide}|\text{Pt}; \text{O}_2(\text{pO}_2 = 0,21 \times 10^5 \text{ Pa})$  by EMF method with external voltage source simulating the effect of enhanced electronic conductivity in range of 450°C-820°C. In both cases (EMF method and a.c. impedance spectroscopy) four probe electrical setup was applied with platinum porous electrodes.

## RESULTS AND DISCUSSION

Electrical conductivity values of  $\text{Bi}_{26}\text{Mo}_9\text{WO}_{69}$  are approximately one order of magnitude higher than for parent material  $\text{Bi}_{26}\text{Mo}_{10}\text{O}_{69}$ . Parent material exhibits improved stability, while tungsten doped compound decompose in temperature range 600-700°C, during annealing for several days in oxygen or air. This decomposition is reversible at higher temperatures. Preliminary measurements suggest that transference numbers are close to 1 for both materials in studied temperature range, when experiment is performed fast to avoid decomposition of  $\text{Bi}_{26}\text{Mo}_9\text{WO}_{69}$ .

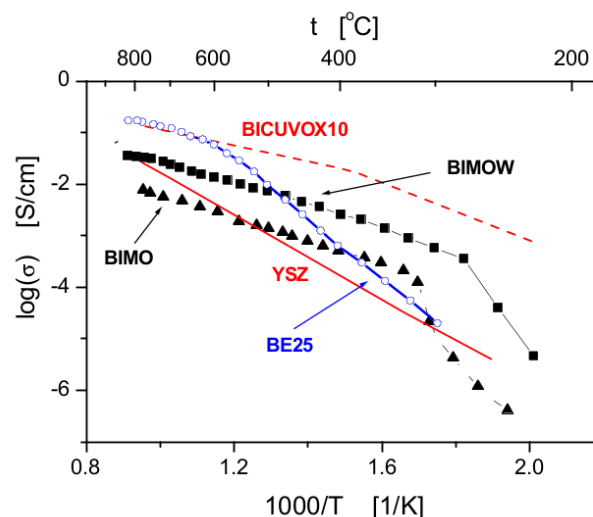


Fig. 1. Total conductivity of  $\text{Bi}_{26}\text{Mo}_9\text{WO}_{69}$  (BIMO),  $\text{Bi}_{26}\text{Mo}_9\text{WO}_{69}$  (BIMOW), compared to other oxide ion conductors.

## REFERENCES

- [1] F.C. Fonseca, M.C. Steil, R.N. Vannier, G. Mairesse, R. Muccillo, *Solid State Ionics* **140** (2001) 161.
- [2] R.N. Vannier, G. Mairesse, F. Abraham, G. Nowogrocki, *Solid State Ionics* **406** (1996) 394.



# CORRELATION BETWEEN CHEMICAL COMPOSITION, STRUCTURE AND PROTON CONDUCTIVITY IN $\text{Ba}_{1-x}\text{La}_x(\text{Zr,In,Sn})\text{O}_{3-\delta}$ PEROVSKITES

*K. Świerczek<sup>1,\*</sup>, A. Olszewska<sup>1</sup>, A. Niemczyk<sup>1</sup>, A. Klimkowicz<sup>1,2</sup>, B. Dabrowski<sup>3</sup>*

<sup>1</sup>AGH University of Science and Technology, Faculty of Energy and Fuels

Department of Hydrogen Energy, al. A. Mickiewicza 30, 30-059 Krakow, Poland

<sup>2</sup>Shibaura Institute of Technology, Faculty of Engineering

3-7-5 Toyosu, Koto-ku, 135-8548 Tokyo, Japan

<sup>3</sup>Northern Illinois University, Department of Physics, DeKalb, IL 60115, USA

\*e-mail: xi@agh.edu.pl

Keywords: perovskite-type oxides; crystal structure; thermogravimetry; proton conductivity

## INTRODUCTION

One of the considered ways to improve operating parameters of Solid Oxide Fuel Cells is to replace the commonly used oxygen ion-conducting electrolytes with the proton-conducting ones, which should allow to decrease the operating temperature [1]. In addition, materials exhibiting high proton conductivity may be applied in high-temperature electrolyzes, gas sensors or hydrogen separation membranes [1-3].

Nonstoichiometric perovskite-type oxides with a general formula of  $\text{Ba}_{1-x}\text{La}_x(\text{Zr,In,Sn})\text{O}_{3-\delta}$  are among candidate solid electrolyte materials, due to their enhanced proton conductivity at elevated temperatures in  $\text{H}_2\text{O}$ -containing atmospheres. This work presents data on correlation between chemical composition, crystal structure and transport properties of two series of oxides:  $\text{Ba}(\text{Zr,In,Sn})\text{O}_{3-\delta}$  and  $\text{Ba}_{0.9}\text{La}_{0.1}(\text{Zr,In,Sn})\text{O}_{3-\delta}$ .

## EXPERIMENTAL

Selection of the chemical composition of the considered materials was based on the Goldschmidt's tolerance factor  $t$ , electronegativity of elements and the expected level of the oxygen nonstoichiometry  $\delta$ .

Considered oxides with two elements at the B-site:  $\text{BaZr}_{0.75}\text{In}_{0.25}\text{O}_{2.875}$ ,  $\text{BaZr}_{0.5}\text{In}_{0.5}\text{O}_{2.75}$ ,  $\text{BaSn}_{0.75}\text{In}_{0.25}\text{O}_{2.875}$ ,  $\text{BaSn}_{0.5}\text{In}_{0.5}\text{O}_{2.75}$ , as well as ones with three elements present:  $\text{BaZr}_{0.5}\text{Sn}_{0.25}\text{In}_{0.25}\text{O}_{2.875}$ ,  $\text{BaZr}_{0.25}\text{Sn}_{0.5}\text{In}_{0.25}\text{O}_{2.875}$  and  $\text{BaZr}_{0.25}\text{Sn}_{0.25}\text{In}_{0.5}\text{O}_{2.75}$ , with the respective series of the materials doped with 0.1 mol of La at the A-site, were prepared by a high-temperature solid state route. After milling in a high-efficiency mill, the respective mixtures were pressed into pellets, and annealed in 1000-1450 °C temperature range.

Structural studies of the synthesized samples were carried out at room temperature in 10-110 deg range using  $\text{CuK}\alpha$  radiation on Panalytical Empyrean diffractometer. Gathered data were analyzed using Rietveld method.

Thermogravimetric data measured for the hydrated samples allowed to establish the remaining proton content in the oxides as a function of temperature. The studies were conducted on TA 5000IR thermobalance.

Electrical conductivity was measured on sinters of the selected compounds by electrochemical impedance spectroscopy in dry,  $\text{H}_2\text{O}$ - and  $\text{D}_2\text{O}$ -containing synthetic air, in order to establish the isotope effect [4]. The obtained results allowed to calculate the respective proton and deuterium conductivities, as well as transference numbers.

## RESULTS AND DISCUSSION

In accordance to the relatively high tolerance factor values ( $0.966 \leq t \leq 0.983$ ), all the synthesized single-phase materials show cubic structure. La-containing materials exhibit smaller unit cell volume, comparing to the corresponding  $\text{Ba}(\text{Zr,In,Sn})\text{O}_{3-\delta}$  series. However, dependence between the chemical composition, value of the parameter  $t$ , relative free volume  $V_f$  and the electronegativity difference  $\Delta\chi_{\text{B-A}}$  in the studied oxides was found to be complicated.

Thermogravimetric experiments performed on the previously hydrated samples allowed to establish the initial proton concentration, which was found to be proportional to the oxygen nonstoichiometry  $\delta$ . The oxides heated in synthetic air up to about 600 °C lose weight, corresponding to the release of protons (water).

Impedance spectroscopy measurements showed a decrease of the high frequency arc upon change of the atmosphere from dry air to  $\text{D}_2\text{O}$ - and  $\text{H}_2\text{O}$ -containing air, which is a strong evidence for the proton (deuterium) conductivity in the samples. Similarly to the previously published data, proton conductivity was found to increase with temperature, while proton transference number was found to be relatively high in 300-500 °C and decreased to small values at 850 °C.

## CONCLUSIONS

The reported structural and transport properties of  $\text{Ba}(\text{Zr,In,Sn})\text{O}_{3-\delta}$  and  $\text{Ba}_{0.9}\text{La}_{0.1}(\text{Zr,In,Sn})\text{O}_{3-\delta}$  oxides can be correlated with their chemical composition. The studied materials exhibit proton conductivity in wet atmospheres, and seem attractive as candidate solid electrolytes.

## ACKNOWLEDGMENT

The project was funded by the National Science Centre Poland (NCN) on the basis of the decision number DEC-2012/05/E/ST5/03772.

## REFERENCES

1. N. Ito, M. Iijima, K. Kimura, S. Iguchi, *J. Power Sources* **152**(2005)200
2. E. Wachsman, T. Ishihara, J. Kilner, *MRS Bulletin* **39**(2014)773
3. E. Fabbri, D. Pergolesi, E. Traversa, *Chem. Soc. Rev.* **39**(2010)4355
4. A.S. Nowick, A.V. Vaysleyb, *Solid State Ionics* **97**(1997)17



# STRUCTURE AND TRANSPORT PROPERTIES OF NOVEL RUDDLESDEN-POPPER-RELATED $\text{Ln}_{1+x}\text{Ba}_{1-x}\text{InO}_4$ (Ln: Pr, Nd, Sm) OXIDES

*M. Tarach, W. Zając, K. Świerczek\**

AGH University of Science and Technology, Faculty of Energy and Fuels  
Department of Hydrogen Energy, al. A. Mickiewicza 30, 30-059 Krakow, Poland  
\*e-mail: xi@agh.edu.pl

Keywords: crystal structure; Ruddlesden-Popper oxides; interstitial oxygen; electrical conductivity

## INTRODUCTION

Crystal structure of the Ruddlesden-Popper series of oxides ( $\text{A}_{n+1}\text{B}_n\text{O}_{3n+1}$ ,  $n \geq 1$ ) can be described as formed by  $n$  perovskite-related layers, which are separated by rock salt-type layer, with the well-known end members:  $\text{A}_2\text{BO}_4$ ,  $n = 1$ ;  $\text{ABO}_3$ ,  $n = \infty$ . Among many different examples, Ni-containing  $\text{Ln}_{n+1}\text{Ni}_n\text{O}_{3n+1\pm\delta}$  oxides are of special interest, due to their mixed ionic-electronic transport properties and possible presence of significant amount of interstitial oxygen ( $\delta > 0$ ).

Surprisingly, only recently initial reports have been published considering In-containing oxides, which structure may be linked to that of the Ruddlesden-Popper ones. Interestingly, with determination of the crystal structure, data showing high ionic conductivity was published for  $\text{NdBaInO}_4$  [1],  $\text{Nd}_{1-x}\text{Sr}_x\text{BaInO}_4$  [2] and  $\text{LnBaInO}_4$  (Ln: La, Nd) [3]. The materials were found to show transition from  $n$ - to  $p$ -type conductivity, occurring over a wide range of the oxygen partial pressures, as well as a region of solid electrolyte-type behavior.

In this work we show data on the synthesis procedure, determination of the phase composition, structural parameters, together with thermogravimetric studies, as well as results of the impedance spectroscopy measurements of transport properties in dry,  $\text{H}_2\text{O}$ - and  $\text{D}_2\text{O}$ -containing artificial air for series of  $\text{Ln}_{1+x}\text{Ba}_{1-x}\text{InO}_4$  (Ln: Pr, Nd, Sm) oxides.

## EXPERIMENTAL

Considered samples were prepared by a typical, high-temperature solid state route. Alternatively, soft chemistry method was also utilized, with respective nitrates and ammonia salt of the EDTA acid used.

Structural studies of the samples were carried out in 10-110 deg range using  $\text{CuK}\alpha$  radiation on Panalytical Empyrean diffractometer. Recorded data were refined using Rietveld method.

Thermogravimetric measurements of the samples were conducted on TA 5000IR thermobalance in different atmospheres.

Electrical conductivity of the synthesized single-phase materials was measured by the AC impedance technique, using Solartron 1260 Frequency Response Analyzer. Measurements were conducted in dry and wet air (ca. 3 vol.%  $\text{H}_2\text{O}$  or  $\text{D}_2\text{O}$ ). The conducted studies allowed to calculate oxygen ion, proton and deuterium conductivities.

## RESULTS AND DISCUSSION

Synthesis of the single-phase materials was found to be difficult, with a required high temperature on the order of 1400 °C and significant issues related to evaporation of barium. It seems that the excess of Ln helps with the synthesis, which may be linked to the changing oxygen content.

The obtained results of the impedance spectroscopy measurements indicate relatively high oxygen ion conductivity at elevated temperatures. In the case of  $\text{Nd}_{1.1}\text{Ba}_{0.9}\text{InO}_4$  oxide, the activation energy of the electrical conduction was found to be 0.99 eV in 300-500 °C range and 1.30 eV in 600-800 °C range. It seems possible that transport properties can be linked with the interstitial mechanism of the oxygen ions movement. Interestingly, the mentioned sample showed enhanced conductivity in  $\text{D}_2\text{O}$ - and  $\text{H}_2\text{O}$ -containing atmospheres, suggesting that protons (deuterium ions) can be also mobile in such materials. We speculate about nature of the possible proton transfer mechanism, with the vehicular transfer via interstitial oxygens (i.e. mobile  $\text{OH}_{\text{O}(i)}^*$  groups) not being excluded.

## CONCLUSIONS

Details about phase composition, crystal structure and transport properties of selected  $\text{Ln}_{1+x}\text{Ba}_{1-x}\text{InO}_4$  oxides indicate their unique physicochemical properties. The materials can be considered as a novel group of ionic conductors.

## ACKNOWLEDGMENT

This work was supported by the Polish Ministry of Science and Higher Education research grant 'Diamantowy Grant' No. D12013 003243.

## REFERENCES

1. K. Fujii et al., *Chem. Mater.* **26**(2014)2488
2. K. Fujii et al., *J. Mater. Chem. A* **3**(2015)11985
3. T. Ishihara et al., Oral presentation at 20<sup>th</sup> International Conference on Solid State Ionics, Colorado USA (2015)

# IMPEDANCE SPECTROSCOPY STUDIES OF QUASICRYSTAL ANODE MATERIALS FOR ELECTROCHEMICAL CELLS

*K. Świerczek<sup>1,\*</sup>, M. Nowak<sup>1</sup>, Y. Ariga<sup>2</sup>, A. Klimkowicz<sup>1,2</sup>, A. Takasaki<sup>2</sup>*

<sup>1</sup>AGH University of Science and Technology, Faculty of Energy and Fuels  
Department of Hydrogen Energy, al. A. Mickiewicza 30, 30-059 Krakow, Poland

<sup>2</sup>Shibaura Institute of Technology, Faculty of Engineering  
3-7-5 Toyosu, Koto-ku, 135-8548 Tokyo, Japan

\* e-mail: xi@agh.edu.pl

Keywords: impedance spectroscopy; electrode materials; quasicrystals; electrochemical hydrogenation

## INTRODUCTION

Electrochemical Impedance Spectroscopy (EIS) is a commonly used, yet powerful tool, which can be utilized to characterize various electrochemical system, including studies of behavior of electrode materials during the charge/discharge processes in batteries.

In this work we present results of EIS studies, as well as structural characterization concerning quasicrystal-type  $\text{Ti}_{45}\text{Zr}_{38}\text{Ni}_{17}$  and  $\text{Ti}_{49}\text{Zr}_{26}\text{Ni}_{25}$  electrode materials electrochemically hydrogenated in 6 M KOH solution.

## EXPERIMENTAL

$\text{Ti}_{45}\text{Zr}_{38}\text{Ni}_{17}$  and  $\text{Ti}_{49}\text{Zr}_{26}\text{Ni}_{25}$  were prepared by mechanochemical alloying technique, as described elsewhere [1].

Structural studies (XRD) of the samples before and after hydrogenation were carried out in 10-110 deg range using  $\text{CuK}\alpha$  radiation on Panalytical Empyrean diffractometer.

The electrochemical measurements were performed using a two-electrode cell at room temperature with Solartron SI 1287 electrochemical interface and Solartron 1252A frequency response analyzer. The working electrode consisted of 25 wt.% of the active material and 75 wt.% of nickel, while the counter electrode was made from mixture of  $\text{Ni}(\text{OH})_2$  and  $\text{NiOOH}$  [1].

## RESULTS AND DISCUSSION

Fig. 1 shows exemplary XRD data for  $\text{Ti}_{45}\text{Zr}_{38}\text{Ni}_{17}$  material before and after charge (hydrogenation), corresponding to 440  $\text{mAh g}^{-1}$  capacity. It can be noticed that quasicrystal-related peaks shift to the right after the hydrogenation, which is related to an increase of the quasi-lattice parameter. Also, a significant broadening of the peaks can be observed.

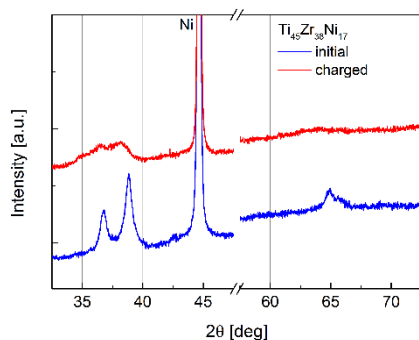


Fig. 1. XRD data for  $\text{Ti}_{45}\text{Zr}_{38}\text{Ni}_{17}$  before and after charge.

Fig. 2 shows charge curves and the recorded Open Circuit Voltage (OCV) of the  $\text{Ti}_{45}\text{Zr}_{38}\text{Ni}_{17}(\text{H})|\text{KOH}|\text{Ni}(\text{OH})_2/\text{NiOOH}$  cell. The measured EIS data for the considered cell are gathered in Fig. 3 below. A significant decrease of the resistance with initial charge can be noticed, however, much smaller changes occur up to 440  $\text{mAh g}^{-1}$  capacity.

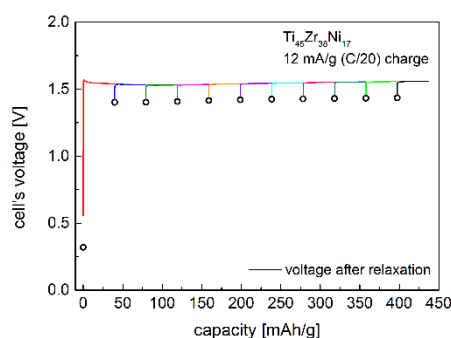


Fig. 2. Exemplary OCV and charge curves for the  $\text{Ti}_{45}\text{Zr}_{38}\text{Ni}_{17}$ -based cell.

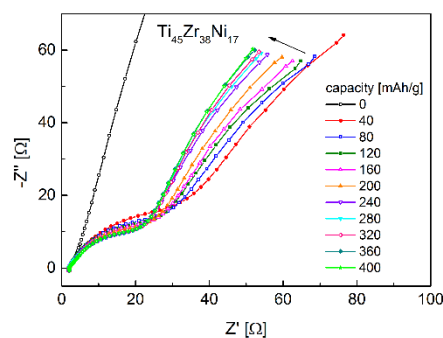


Fig. 3. EIS data for the  $\text{Ti}_{45}\text{Zr}_{38}\text{Ni}_{17}$ -based cell

## CONCLUSIONS

$\text{Ti}_{45}\text{Zr}_{38}\text{Ni}_{17}$  and  $\text{Ti}_{49}\text{Zr}_{26}\text{Ni}_{25}$  quasicrystals were successfully characterized in terms of their properties upon hydrogenation using EIS technique.

## ACKNOWLEDGMENT

K.Ś. and A.K. thank for the financial support from the Polish Ministry of Science and Higher Education, under project AGH No. 11.11.210.911.

## REFERENCES

1. Y. Ariga, A. Takasaki, T. Kimijima, K. Świerczek, J. Alloy. Compd. 645(S1) (2015) S152-S154

# PHYSICOCHEMICAL PROPERTIES OF PROTON-CONDUCTING $Ba_{1-x}Ln_x(Zr,In,Sn)O_{3-\delta}$ (Ln: SELECTED LANTHANIDES) OXIDES

*W. Skubida, K. Zheng, K. Świerczek\**

AGH University of Science and Technology, Faculty of Energy and Fuels  
Department of Hydrogen Energy, al. A. Mickiewicza 30, 30-059 Krakow, Poland  
\*e-mail: xi@agh.edu.pl

Keywords: crystal structure; thermogravimetry; proton conductivity; relaxation methods

## INTRODUCTION

Importance of proton-conducting oxides stems from their possible application in electrochemical devices like gas sensors, fuel cells, high-temperature electrolyzers or usage as membranes for hydrogen separation [1-4]. Among considered materials with enhanced proton conductivity,  $AB_{1-x}Ln_xO_{3-\delta/2}$  (A: Sr, Ba; B: Zr, Ce, Sn, In) perovskite-type oxides are of particular interest, with lanthanide  $Ln^{3+}$  cations being introduced in order to induce an appearance of the oxygen nonstoichiometry  $\delta$ . The oxygen vacancies are required for incorporation of hydrogen into the oxide lattice, with  $OH'_O$  defects being reversibly formed.

Chemical substitution on the B-site is commonly used to modify properties of such oxides, however, introduction of +3 cations at the A-site is relatively less studied. In this work, results of evaluation of physicochemical properties of  $Ba_{1-x}Ln_x(Zr,In,Sn)O_{3-\delta}$  (Ln: selected lanthanides) oxides are reported. The measured data concern crystal structure at room at high temperatures, proton content in wet atmospheres, as well as transport properties of the materials in dry,  $H_2O$ - and  $D_2O$ -containing atmospheres, together with evaluation of transport coefficients (diffusion coefficient  $D$  and surface exchange coefficient  $K$ ).

## EXPERIMENTAL

Considered samples were prepared by a typical, high-temperature solid state route, with respective oxides and carbonates used as the starting materials. After milling in a high-efficiency mill, the mixtures were pressed into pellets, and annealed in 1000-1450 °C temperature range.

Structural studies of the samples were carried out in 10-110 deg range using  $CuK\alpha$  radiation on Panalytical Empyrean diffractometer. For high-temperature studies, Anton Paar HTK 1200N oven-chamber was used.

Thermogravimetric measurements were conducted on TA 5000IR and Linseis STA PT 1600 thermobalance in different atmospheres.

Electrical conductivity of the studied samples was measured by the AC impedance technique, using Solartron 1260 Frequency Response Analyzer. Measurements were conducted in 300-850 °C range in dry and wet air (ca. 3 vol.%  $H_2O$  or  $D_2O$ ). The conducted studies allowed to calculate proton conductivity and transference numbers.

Chemical diffusion coefficient  $D$  and surface exchange coefficient  $K$  of the charge carriers were evaluated on a basis of relaxation-type experiments. The obtained data were fitted using custom made Matlab code.

## RESULTS AND DISCUSSION

It was found that choice of the optimal sintering temperature of  $Ba_{1-x}Ln_x(Zr,In,Sn)O_{3-\delta}$  oxides is strongly dependent on the relative ratio of B-site elements. In addition, at the highest temperatures (1400-1450 °C) the samples suffer from a significant evaporation of Ba. Most of the single phase materials exhibit cubic structure at room and at elevated temperatures, with the refined unit cell volume being proportional to the Zr:In:Sn ratio and ionic radius of Ln.

Calculated from the thermogravimetric experiments proton content in the samples annealed in wet atmosphere is proportional to the initial oxygen nonstoichiometry  $\delta$ , but smaller than the theoretical one. During heating in synthetic air, the materials release protons (water) up to about 600 °C, depending on the chemical composition.

Proton conductivity in the studied single phase  $Ba_{1-x}Ln_x(Zr,In,Sn)O_{3-\delta}$  samples was found to increase with temperature, with proton transference number being relatively high in 300-500 °C temperature range. The corresponding deuterium conductivity was found to be lower, and with higher activation energy, as can be expected considering higher mass of  $D^+$  in comparison to  $H^+$ , resulting in the lowered charge carrier mobility. Impedance data indicated also an appearance of the electronic component of the conductivity at the highest (~ 850 °C) temperatures. Additional, relaxation-type experiments allowed to calculate chemical diffusion coefficient  $D$  and surface exchange coefficient  $K$ .

## CONCLUSIONS

Substituted  $Ba_{1-x}Ln_x(Zr,In,Sn)O_{3-\delta}$  oxides were characterized in terms of their crystal structure, proton content in wet atmospheres and transport properties. The measured physicochemical properties were found to be correlated with chemical composition of the samples.

## ACKNOWLEDGMENT

The project was funded by the National Science Centre Poland (NCN) on the basis of the decision number DEC-2012/05/E/ST5/03772.

## REFERENCES

1. E. Wachsman, T. Ishihara, J. Kilner, *MRS Bulletin* **39**(2014)773
2. E. Fabbri, D. Pergolesi, E. Traversa, *Chem. Soc. Rev.* **39**(2010)4355
3. W. Zając, D. Rusinek, K. Zheng, J. Molenda, *Cent. Eur. J. Chem.* **11**(2013)471
4. N. Ito, M. Iijima, K. Kimura, S. Iguchi, *J. Power Sources* **152**(2005)200

# DEPENDENCE OF GLASS TRANSITION TEMPERATURE ON THE HEATING RATE IN DTA EXPERIMENTS FOR GLASSES CONTAINING TRANSITION METAL OXIDES

*Przemysław P. Michalski, Tomasz K. Pietrzak, Jan L. Nowiński, Marek Wasiucionek and Jerzy E. Garbarczyk*

Faculty of Physics  
Warsaw University of Technology, ul. Koszykowa 75  
00-662 Warsaw, Poland  
e-mail: michalski@if.pw.edu.pl

Keywords: transition metal oxide glasses, thermal analysis, glass transition, Kissinger's formula, Lasocka's formula

## INTRODUCTION

Thermal analysis (TA) is an interesting method to observe thermal events taking place in samples upon heating/cooling. In case of glasses, it is crucial to accurately determine the glass transition temperature ( $T_g$ ), because the parameters of a material usually drastically change after this point.

In 1950s H. E. Kissinger studied properties of materials by differential thermal analysis (DTA) performed at various heating rates and proposed an expression, which may be rewritten as follows [1]:

$$\ln\left(\frac{\theta}{T_m^2}\right) = -\frac{Q}{k_B T_m} + C \quad (1)$$

where:  $\theta$  – heating rate in  $^{\circ}\text{Cmin}^{-1}$ ,  $T_m$  – temperature of thermal event,  $k_B$  – Boltzmann constant,  $Q$  – activation energy of the thermal process and  $C$  – a constant.

Two decades later, M. Lasocka studied thermal properties of splat-cooled  $\text{Te}_{85}\text{Ge}_{15}$  metallic glasses and proposed a much simpler formula for  $T_g$  [2]:

$$T_g = A + B \ln \theta \quad (2)$$

where:  $A$ ,  $B$  – empirical constants,  $\theta$  – heating rate in  $^{\circ}\text{Cmin}^{-1}$ . A practical advantage of this expression, except its simplicity, is that fitting parameter  $A$  equals to the glass transition temperature upon heating with  $\theta = 1$   $^{\circ}\text{Cmin}^{-1}$ .

We wanted to take a closer look at both Kissinger's and Lasocka's formulas and check i) their applicability in case of various glasses containing transition metal oxides and ii) how well  $T_g(\theta = 1$   $^{\circ}\text{Cmin}^{-1})$  can be extrapolated from these expressions.

## EXPERIMENTAL

Several systems/compositions of glasses have been investigated: a)  $90\text{V}_2\text{O}_5 \cdot 10\text{P}_2\text{O}_5$  (VP) [3],  $\text{Li}_2\text{O} \cdot \text{FeO} \cdot \text{V}_2\text{O}_5 \cdot \text{P}_2\text{O}_5$  (LFVP) [4], c)  $\text{LiF} \cdot \text{M}_2\text{O}_3 \cdot \text{P}_2\text{O}_5$ , where  $M = \text{V}$ ,  $\text{Fe}$ ,  $\text{Ti}$ . All the compositions have been prepared by melt-quenching method.

Thermal events occurring in VP glasses were observed with a TA DSC Q200. DSC scans were carried in non-isothermal mode from ca.  $40$   $^{\circ}\text{C}$  to  $550$   $^{\circ}\text{C}$  at a series of heating rates ( $1$ – $40$   $^{\circ}\text{Cmin}^{-1}$ ) in nitrogen flow. Thermal events in LFVP and LMPF glasses were observed with TA SDT Q600 instrument, usually up to  $750$   $^{\circ}\text{C}$  at a series of heating rates ( $1$ – $40$   $^{\circ}\text{Cmin}^{-1}$ ) in argon flow. The temperatures of glass transitions were determined by TA Universal Analysis Software.

## RESULTS AND DISCUSSION

Eq. (2) was fitted to every batch in two ways. Firstly, the fits were performed in the full range of data.

Secondly, we used only fast heating rates data (i.e.  $\theta \geq 10$   $^{\circ}\text{Cmin}^{-1}$ ) and extrapolated the lines down to  $1$   $^{\circ}\text{Cmin}^{-1}$ .

All of investigated glasses exhibited linear dependence of glass transition temperature, when plotted in Lasocka's coordinates ( $T_g$  vs.  $\ln(\theta)$ ). The difference between the extrapolated  $T_g$  for  $\theta = 1$   $^{\circ}\text{Cmin}^{-1}$  and the measured ones was no higher than several  $^{\circ}\text{C}$ .

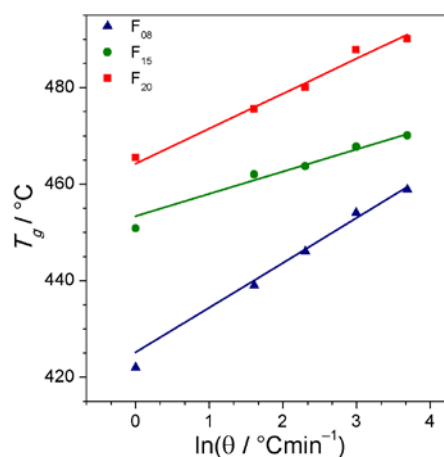


Fig. 1 Lasocka plot for different LFVP glasses fitted in  $10$ – $40$   $^{\circ}\text{Cmin}^{-1}$  range.

## CONCLUSIONS

It was shown that both Lasocka's and Kissinger's formulas can describe the dependence of  $T_g$  on the heating rate also in case of oxide glasses containing transition metals. Apart from formula's simplicity, Lasocka's plots are more comprehensive to the reader. The experiments have shown that the value of  $T_g$  at  $1$   $^{\circ}\text{Cmin}^{-1}$  can be satisfactorily extrapolated from measurements taken at high heating rates (e.g.  $\geq 10$   $^{\circ}\text{Cmin}^{-1}$ ).

## ACKNOWLEDGMENT

Part of this work has been financed by National Science Centre: project OPUS-4 no. DEC-2012/07/B/ST5/03184 (2012–2016).

## REFERENCES

1. H. E. Kissinger, *Analytical Chemistry* **29**(1957) 1702
2. M. Lasocka, *Materials Science and Engineering* **23**(1976) 173
3. T. K. Pietrzak, Ł. Pawliszak, P. P. Michalski *et al.*, *Procedia Engineering* **98**(2014) 28
4. J. E. Garbarczyk, T. K. Pietrzak, M. Wasiucionek *et al.*, *Solid State Ionics* **272**(2015) 53

# RARE EARTH NIOBATES – DOPING AND PROPERTIES

*Aleksandra Mielewczyk-Gryń<sup>1</sup>, Sebastian Wachowski<sup>1</sup>, Jan Jamroz<sup>1</sup>, Magdalena Zalewska<sup>1</sup>, Krzysztof Zagórski<sup>1</sup>, Alexandra Navrotsky<sup>2</sup>, Maria Gazda<sup>1</sup>*

<sup>1</sup>Gdańsk University of Technology, Faculty of Applied Physics and Mathematics, Department of Solid State Physics, Narutowicza 11/12 80-233 Gdańsk, Poland

<sup>2</sup>University of California, Davis, Peter A. Rock Thermochemistry Laboratory, One Shields Ave, 95616 Davis, CA  
e-mail: amielewczyk@mif.pg.gda.pl

Keywords: rare earth elements, ionic conductors

## INTRODUCTION

Rare earth niobates ( $RE_3NbO_7$ ) are materials with interesting both structural and electrical properties [1]. Several properties strongly depend on the rare earth element radius. This includes electrical, structural and thermochemical properties [2]. In this work further research is presented, including investigation of possible doping of rare earth niobates on niobium site by titanium. Results achieved by X-ray diffraction, scanning electron microscopy, high temperature drop solution calorimetry and electrochemical impedance spectroscopy will be shown and analysed.

## EXPERIMENTAL

Polycrystalline samples of  $RE_3NbO_7$  were synthesized by the solid-state reaction method. The hygroscopic sesquioxides were preheated overnight at 900°C prior to the synthesis. The stoichiometric amounts of  $RE_2O_3$  oxides and  $Nb_2O_5$  were mixed in the agate mortar in ethanol. The powders were pressed into pellets and calcined two times at 1400°C for 8h between which they were crushed and re-grinded. The phase purity of the samples was checked by powder X-ray diffraction method (XRD) using a Bruker diffractometer.

The enthalpies of formation from binary oxides of the investigated compounds were measured by the high temperature oxide melt drop solution calorimetry in a Tian-Calvet type twin calorimeter Setaram AlexSYS. System architecture is presented in Fig. 1.

In order to measure electrical conductivity an impedance data were obtained by using a Solartron 1260 analyzer in standalone mode. Impedance spectra have been collected in the frequency range of 1 Hz – 10 MHz.

## RESULTS AND DISCUSSION

The drop solution calorimetry results have shown that the stability of rare earth niobates rises with the rare earth cation ionic radius which is consistent with findings for other rare earth containing materials like e.g. rare earth pyrochlores [3]. The electrical measurements proved the ionic nature of conduction in investigated doped rare earth niobates.

## CONCLUSIONS

The energetics of rare-earth niobates ascribed by three different space groups has been investigated. The influence of size of a rare-earth cation on compound stability has been analyzed. The electrical properties of doped and undoped rare earth niobates has been investigated.

## ACKNOWLEDGMENT

Part of this work was supported by U.S. National Science Foundation, grant EAR-1321410.

## REFERENCES

1. López-Conesa, L., Rebled, J.M., Chambrier, M.H., Boulahya, K., González-Calbet, J.M., Braida, M.D., Dezanneau, G., Estradé, S., and Peiró, F. (2013). Fuel Cells, 13(1), 29-33.
2. A. Mielewczyk-Gryń, A. Navrotsky American Mineralogist in print  
<http://dx.doi.org/10.2138/am-2015-5210>

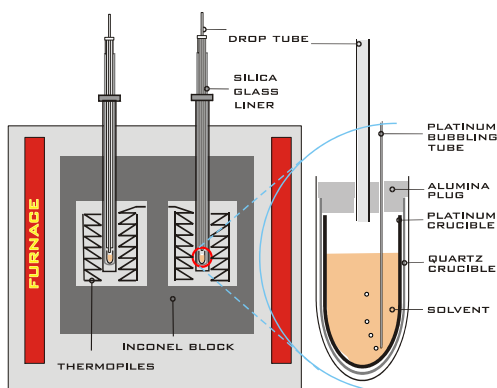


Fig. 1 Twin Tian-Calvet high temperature microcalorimeter. (courtesy of dr. S. Ushakov)

# MÖSSBAUER STUDIES OF $\text{Li}_2\text{O}-\text{FeO}-\text{V}_2\text{O}_5-\text{P}_2\text{O}_5$ GLASSES AND NANOMATERIALS

*Tomasz K. Pietrzak, Karol Szlachta, Jolanta Gałazka-Friedman, Marek Wasiucioneck, Jan L. Nowiński, and Jerzy E. Garbarczyk*

Faculty of Physics  
Warsaw University of Technology, Koszykowa 75  
00-662 Warszawa, Poland  
e-mail: topie@if.pw.edu.pl

Keywords: nanomaterials, olivines, Mössbauer, electron hopping

## INTRODUCTION

Poor electric conductivity is a major drawback of many potential cathode materials for lithium and sodium ion batteries. This has usually been circumvented by addition of various forms of carbon. It is however possible to achieve the acceptable level of the electrical conductivity without use of any carbon additive. We have shown that thermal nanocrystallization of glassy analogs of selected cathode materials results in a significant increase in their electric conductivity [1,2].

The electronic conductivity in glasses containing transition metal oxides (e.g.  $\text{V}_2\text{O}_5$  and  $\text{FeO}$ ) can be described by Mott's theory of electron hopping [3]:

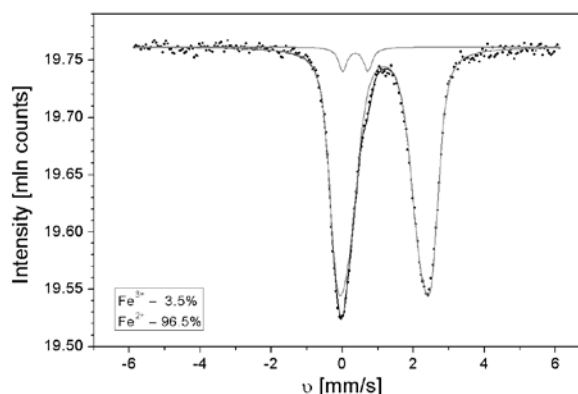
$$\sigma = \frac{e^2}{kTR} c(1-c)v_e \exp(-2\alpha R) \exp(-E_a/kT),$$

where  $R$  is the average distance between hopping centers,  $v_e = \hbar/m_e R^2$ ,  $\alpha$  is the inverse localization length of the electron wave function,  $c$  is the fraction of occupied hopping sites for electrons and  $E_e$  is the activation energy of electronic conduction.

In this research, we have investigated glasses and nanomaterials of  $\text{Li}_2\text{O}-\text{FeO}-\text{V}_2\text{O}_5-\text{P}_2\text{O}_5$  system. These compositions correspond to that of  $\text{LiFePO}_4$  with a small fraction of iron replaced by vanadium, according to a general formula  $\text{LiFe}_{1-5x/2}\text{V}_x\text{PO}_4$  with  $0.08 \leq x \leq 0.20$ . In this approach the relative content of  $\text{Fe}^{2+}$  and  $\text{Fe}^{3+}$  ions plays major role in electronic conductivity. Therefore Mössbauer studies of glassy and nanocrystalline samples would give a valuable insight in electronic conductivity processes in materials under study.

## EXPERIMENTAL

Starting reagents:  $\text{Li}_2\text{CO}_3$ , (Aldrich, 99.9%),  $\text{FeC}_2\text{O}_4 \cdot 2\text{H}_2\text{O}$  (Aldrich, 99.9%) and  $\text{V}_2\text{O}_5$  (ABCR, 99.5%) were homogenized and annealed under flow of nitrogen (purity 99.999%) in two steps: (i) at 300 °C for 2 h and (ii) at 570 °C for next 2 h. Subsequent stages of the synthesis of the glassy materials (second homogenization, melting at 1300 °C and quenching) followed the procedure described in detail in our previous paper [2]. The amorphousness of the as-quenched materials was confirmed by X-ray diffractometry (XRD). Diffraction studies were carried out on a Philips X'Pert Pro apparatus using the  $\text{CuK}\alpha$  line ( $\lambda = 1.542 \text{ \AA}$ ). Glass transition and crystallization temperatures were determined from DTA measurements using a SDT Q600 setup (TA Instruments). Samples were crystallized during temperature-dependent



impedance measurements with upper temperature in 450–510 °C range.

Fig. 1. Mössbauer spectrum of glassy sample with  $x = 0.08$ .

## RESULTS AND DISCUSSION

As it was expected, most of iron in as-received glassy samples is present in a  $\text{Fe}^{3+}$  oxidation state (Fig. 1). However, preliminary measurements showed that in samples with lower vanadium content (e.g.  $x = 0.08$ ) the  $\text{Fe}^{2+}/\text{Fe}^{3+}$  ratio is lower than in samples with higher vanadium content. This should result in lower electronic conductivity of the former. As expected, the conductivity of glassy sample with  $x = 0.08$  was  $10^{-9}$  S/cm, whereas the conductivity of glassy sample with  $x = 0.20$  was  $3 \cdot 10^{-9}$  S/cm. On the other hand, after nanocrystallization the situation was reversed: the conductivity of the former was significantly higher than that of the latter. The analyses of the Mössbauer spectra of these samples are to provide us with information, how important is the  $\text{Fe}^{2+}/\text{Fe}^{3+}$  ratio for the electronic conductivity in the system under study.

## ACKNOWLEDGMENT

This work has been financed by National Science Centre: project OPUS-4 no. DEC-2012/07/B/ST5/03184 (2013–2016).

## REFERENCES

1. T.K. Pietrzak, J.E. Garbarczyk, I. Gorzkowska, M. Wasiucioneck, J.L. Nowiński, S. Gierlotka, P. Joźwiak, *Journal of Power Sources* **194** (2009) 73–80.
2. J.E. Garbarczyk, T.K. Pietrzak, M. Wasiucioneck, A. Kaleta, A. Dorau, J.L. Nowiński, *Solid State Ionics* **272** (2015) 53–59.
3. I. G. Austin, N. F. Mott, *Advances in Physics* **50** (2001) 757–812.



# SYNTHESIS, AND ELECTRICAL AND THERMAL PROPERTIES OF $\text{Li}_2\text{O-Me}_2\text{O}_3\text{-P}_2\text{O}_5$ GLASSES AND NASICON-LIKE NANOMATERIALS

*Tomasz K. Pietrzak, Przemysław P. Michalski, Agnieszka Starobrat, Marek Wasiucioneck, and Jerzy E. Garbarczyk*  
Faculty of Physics

Warsaw University of Technology, Koszykowa 75  
00-662 Warszawa, Poland  
e-mail: topie@if.pw.edu.pl

Keywords: nanocrystallization, electric conductivity, phosphate glasses, NASICON

## INTRODUCTION

Search for new polyanionic Li-ion battery cathode materials with high capacities, exchanging more than one Li atom per transition metal, is currently a major issue in the battery research [1]. Lithium/sodium transition metal phosphates, including  $\text{Li}_3\text{V}_2(\text{PO}_4)_3$  and  $\text{Na}_3\text{V}_2(\text{PO}_4)_2\text{F}_3$ , belong to interesting cathode materials for lithium/sodium ion batteries, mainly due to their high theoretical capacity ( $\sim 190$  mAh/g) and cyclability. In our research (e.g. [2,3]) we have shown that glassy analogs of some cathode materials exhibit significantly enhanced —electric conductivity when subject to appropriate thermal treatment. This phenomenon was ascribed to the appearance of densely packed nanograins (sub-100 nm). In this research, we have attempted to synthesize amorphous analogs of  $\text{Li}_3\text{Me}_2(\text{PO}_4)_2\text{F}_3$  (Me = V, Fe, Ti), such as e.g.  $\text{Li}_3\text{V}_2(\text{PO}_4)_2\text{F}_3$ ,  $\text{Li}_3\text{FeV}(\text{PO}_4)_2\text{F}_3$  etc.

## EXPERIMENTAL

After pre-heating at  $200^\circ\text{C}$ , the initial powders were melted at  $1300^\circ\text{C}$  for ca. 30 minutes using a double crucible technique. Then they were poured onto a stainless steel plate and pressed with another plate (melt quenching technique). The structure of as-received materials was investigated by X-ray diffractometry (XRD). Thermal events taking place in samples upon heating (e.g. glass transition and crystallization) were observed by differential thermal analysis (DTA) at different heating rates (from 1 to  $40^\circ\text{C}/\text{min}$ ). Activation energies of glass transition and crystallization (in amorphous batches) were calculated from the Kissinger formula. Electric conductivity was measured by impedance spectroscopy (IS) during heating and subsequent cooling ramps.

## RESULTS AND DISCUSSION

Most of the synthesized batches were amorphous. However, batches with higher iron content ( $> 1$  Fe per nominal formula) at least partly crystallized during solidification. This is due to poor glass forming properties of iron oxides. The glass transition temperature for the amorphous samples was observed within the  $367\text{--}433^\circ\text{C}$  range, depending of the composition. Temperature XRD studies showed that heating the glasses up to  $500^\circ\text{C}$  resulted in formation of grains with average size of  $60\text{--}75$  nm. The predominant crystalline component was a NASICON-like phase, of other phases were also detected. SEM micrographs showed that microstructure of  $\text{Li}_3\text{V}_2(\text{PO}_4)_2\text{F}_3$  sample

heated to  $500^\circ\text{C}$  consisted in nanorods uniformly distributed in the whole sample (Fig. 1).

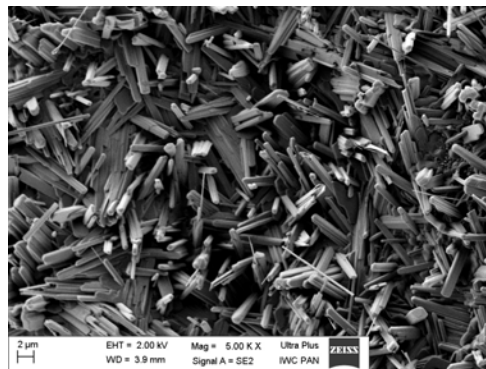


Fig. 1. SEM image of  $\text{Li}_3\text{V}_2(\text{PO}_4)_2\text{F}_3$  sample after heating to  $500^\circ\text{C}$ .

An irreversible and significant change in the conductivity due to heat-treatment was correlated with a crystallization peak observed in DTA traces. The conductivity of the best-conducting sample was as high as  $2 \cdot 10^{-3}$  S/cm at room temperature. The influence of the heat-treatment on electric conductivity was dependent not only on the transition metal present in a glass composition, but also on LiF excess and synthesis conditions.

## CONCLUSIONS

It was shown that  $\text{Li}_2\text{O-Me}_2\text{O}_3\text{-P}_2\text{O}_5$  is one more system of glasses whose heat-treatment leads to formation of highly-conducting nanomaterials. At least two crystalline phases were detected in synthesised samples. It was observed that synthesis conditions have significant effect on the phase composition of the final material. Therefore one may expect that further research will result in synthesis of pure NASICON-like highly-conducting nanomaterials, which should exhibit good electrochemical properties for cathodes in Li-ion batteries.

## REFERENCES

1. G. Hautier, A. Jain, T. Mueller, Ch. Moore, Sh. Ping Ong, G. Ceder, *Chemistry of Materials* **25** (2013) 2064–2074.
2. T.K. Pietrzak, J.E. Garbarczyk, I. Gorzkowska, M. Wasiucioneck, J.L. Nowiński, S. Gierlotka, P. Joźwiak, *Journal of Power Sources* **194** (2009) 73–80.
3. J.T.K. Pietrzak, M. Wasiucioneck, I. Gorzkowska, J.L. Nowiński, J.E. Garbarczyk, *Solid State Ionics* **251** (2013) 40–46.

# IONIC CONDUCTIVITY AND LITHIUM TRANSFERENCE NUMBER OF POLY(ETHYLENE OXIDE) – BASED ELECTROLYTES

*K. Pożyczka, M. Marzantowicz, J.R. Dygas, F. Krok*

Faculty of Physics

Warsaw University of Technology, Koszykowa 75

00-662 Warszawa, Poland

e-mail: pozyczka@if.pw.edu.pl

Keywords: lithium transference number, ionic conductivity, polymer electrolytes

## INTRODUCTION

Polymer electrolytes have been proven as an effective and safe material for solid electrolyte in Li-ion rechargeable batteries. Among all polymers which have been proposed for that application, poly(ethylene oxide) known since early years of research in this field, is still considered one of the best solid solvents for Li salts. Traditionally, polymer electrolytes are obtained by dissolution of a small amount of salt in polymer. However, despite high ionic conductivity, in such a system only a fraction of charge is transported by cations, which is not favorable for application in rechargeable cell.

It is generally accepted that increasing amount of lithium salt in the system is accompanied by increasing role of ion-ion interactions in ion transport process. Therefore, one could expect also decrease of lithium transference number. Since the value of ionic conductivity of electrolytes rich in salt is also lower than that of electrolytes with moderate amount of salt, at first glance increasing amount of salt does not seem to be an appropriate direction in search for improvement of properties of polymer electrolyte.

Our poster will show that, by application of an appropriate combination of experimental methods, interesting and unexpected phenomena can still be observed even for such a well known system as PEO with LiTFSI salt.

## EXPERIMENTAL

Linear PEO of high molecular weight PEO ( $M_w=5 \times 10^6$  g/mol) was obtained from Aldrich. Polymer electrolytes with addition of  $\text{LiN}(\text{CF}_3\text{SO}_2)_2$  (LiTFSI) salt have been obtained by mixing polymer and salt in an acetonitrile solution. After casting, the electrolytes were placed in a vacuum chamber for at least one week to remove solvent.

Samples of electrolytes were characterized by Differential Scanning Calorimetry and impedance spectroscopy performed between blocking gold-plated electrodes. Measurement of lithium transference number was performed by electrochemical method employing a modified version of Bruce–Vincent procedure [1]. This recently developed method allows to obtain more repeatable and reliable values than standard approach.

## RESULTS AND DISCUSSION

Measurement of electrolytes based on linear PEO with different amount of lithium salt indicate that, in contradiction to some earlier reports, the values of lithium transference number do not exhibit a continuous decrease upon increasing concentration of salt. Instead,

it seems that electrolytes with the highest ionic conductivity (representing EO:Li of 10:1) are characterized by the lowest lithium transference number. In electrolytes with higher content of salt, lithium transference number increases significantly. This can be possibly explained by “binding” of anions in stoichiometric complexes with polymer. The structure of such complexes can be partially preserved in amorphous state, thus impeding anion mobility. Our findings indicate possibility to obtain efficient lithium ion transport in “polymer in salt” systems – which, as described in our earlier publication [2] can exhibit metastable states of high ionic conductivity.

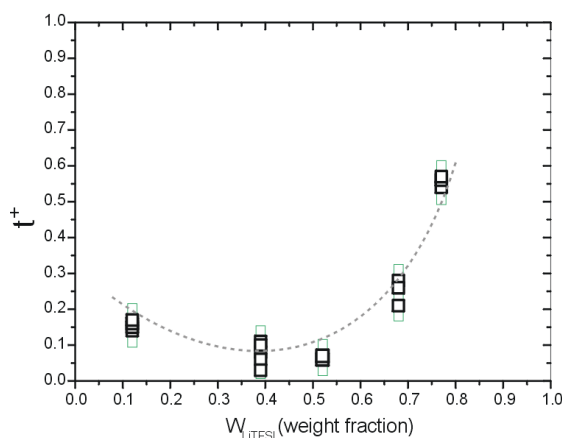


Fig. 1. Lithium transference number  $t^+$  of electrolytes based on PEO and LiTFSI.

## CONCLUSIONS

Measurement of lithium transference number allows new interpretation of data obtained by other methods. In case of electrolytes based on linear PEO, it seems that despite increasing amount of salt and increasing decoupling of ion transport from motions of polymer chains, the lithium transference number of electrolytes rich in salt are considerably higher, than that of electrolytes with moderate salt concentration.

## ACKNOWLEDGMENT

This work is supported by grant of Dean of Faculty of Physics, WUT.

## REFERENCES

1. P.G. Bruce, J. Evans, C.A. Vincent, *Solid State Ionics*, **28–30** (1988) 918.
2. M. Marzantowicz, F. Krok, J.R. Dygas, Z. Florjańczyk, E. Zygadło-Monikowska, *Solid State Ionics* **179** (2008) 1670.

# THE HIGH CAPACITY EFFECT IN ALL – GLASS COMPOSITES CONDUCTING ELECTRONS AND SILVER IONS.

*W. Ślubowska, J. L. Nowiński, J. E. Garbarczyk and M. Wasiucionek*

Faculty of Physics Warsaw University of Technology

Faculty of Physics WUT, ul. Koszykowa 75

00-662 Warsaw, Poland

e-mail: slubowska@if.pw.edu.pl

Keywords: solid state ionics, all – glass composites, supercapacitors

## INTRODUCTION

All – glass composites conducting electrons and silver ions are a new class of heterogeneous materials. Their mixed electric conductivity depends on: electric conductivity of components, their content in a mixture, and its microstructure (e.g. grain size, shape, spatial distribution).

In the work we show that these systems can exhibit some interesting synergy effect resulting from interactions between components.

## EXPERIMENTAL

The all – glass composites were fabricated from two components:  $30\text{AgI}\cdot 35\text{Ag}_2\text{O}\cdot 35\text{P}_2\text{O}_5$  (ion – conducting glass, denoted as I) and  $90\text{V}_2\text{O}_5\cdot 10\text{P}_2\text{O}_5$  (electron – conducting glass, denoted as E).

The powdered glasses containing grains of selected size, after mixing in several volume ratios, were pressed to form pellets – the final composites.

Both, the components and composites were investigated by means of X – ray diffraction (XRD), differential scanning calorimetry (DSC), impedance spectroscopy (IS), whereas Hebb – Wagner polarization method (H – W) for the composites only.

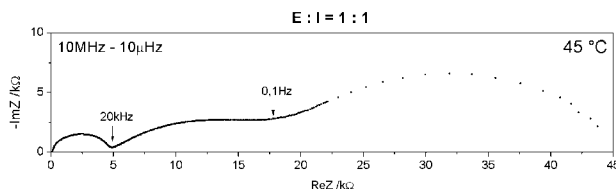


Figure 1. Impedance spectrum of electric – ionic composite 1 : 1 in a frequency range 10MHz – 10µHz at 45°C.

## RESULTS AND DISCUSSION

The AC (fig. 1) and DC (fig. 2) investigations as well, revealed existence of some processes responsible for a very high electric capacity of 0,1 F rank of order.

There was suggested that this synergy effect was due to some interactions taking place among the grains. The observed effect can be used for storing high electric charges and seem to be perspective for supercapacitor technology.

## CONCLUSIONS

High capacity effect was observed in all – glass  $30\text{AgI}\cdot 35\text{Ag}_2\text{O}\cdot 35\text{P}_2\text{O}_5$  (I) +  $90\text{V}_2\text{O}_5\cdot 10\text{P}_2\text{O}_5$  (E) system. It has been shown that this synergy effect is due to interactions between the component grains. The future work should be done to investigate possible applicability of these class of composites in energy

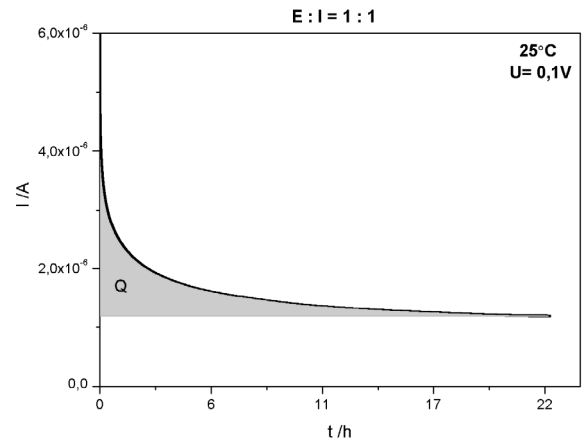


Figure 2. Current – time dependency plot for 1 : 1 composite (grey – coloured area correspond to electric charge stored in the system,  $Q = 2,6 \cdot 10^{-2}$  C). storage devices.

# PROTON CONDUCTION IN $\text{LaNb}_{1-x}\text{Sb}_x\text{O}_4$ ( $x=0$ to $0.3$ )

*S. Wachowski, A. Mielewczyk-Gryn, M. Lapiński, P. Jasiński\*, M. Gazda*

Faculty of Applied Physics and Mathematics

\*Faculty of Electronics, Telecommunications and Informatics

Gdańsk University of Technology

80-233 Gdańsk, Poland

e-mail: swachowski@mif.pg.gda.pl

Keywords: hydrogen in solids, proton conduction, ionic conduction, solid state electrolytes

## INTRODUCTION

High temperature proton conductors (HTPCs) are important materials for hydrogen energy conversion and storage [1]. Among HTPCs acceptor doped lanthanum niobates with total conductivity of  $10^{-3}$  S/cm at 900 °C are considered to be promising group of materials [2]. In our previous works we have shown that by substituting niobium with antimony structure and stability of the material can be altered [3,4]. In this work electrical properties of these compounds are studied by the electrochemical impedance spectroscopy. In particular, electrical conductivity has been studied as a function of temperature and oxygen partial pressure.

## EXPERIMENTAL

In order to measure electrical conductivity an impedance data were obtained by using a Solartron 1260 analyzer in standalone mode. Impedance spectra have been collected in the frequency range of 1 Hz – 10 MHz. In the cases where it was possible grain interior and grain boundary conductivities have been obtained by the deconvolution of impedance complex plots in EqC software. In other cases only total conductivity values have been determined. Data have been collected in temperature range of 250 – 900 °C in dry,  $\text{H}_2\text{O}$ - and  $\text{D}_2\text{O}$ -wet air. For selected temperature values conductivity has been measured as a function of  $p\text{O}_2$  within the range  $\sim 10^{-6}$  to 0.2 Bar.

Additionally, X-ray photoelectron spectroscopy measurements have been performed in order to determine valence states of substituent and native ions.

## RESULTS AND DISCUSSION

Measurements of the conductivity have shown a difference of total conductivity of approximately one order of magnitude higher in wet than in dry air. Moreover, H-D isotope exchange experiment has shown that ratio of total conductivity in wet  $\text{H}_2\text{O}$  and  $\text{D}_2\text{O}$  is close to the value of  $1/\sqrt{2}$  within the temperature range between 400 and 800 °C.

Application of the Brick Layer Model for the analysis of impedance complex plots has led to the separation of the conductivity data into grain bulk and grain boundary specific conductivities. It has been shown that Sb-substitution on Nb sites has a higher impact on the grain boundary rather than bulk conductivity.

In general a higher value of antimony concentration in the compound led to a higher value of conductivity.

## CONCLUSIONS

It has been shown that in wet oxidizing atmospheres, in the temperature range of 400 – 800 °C, protons are dominating charge carriers in  $\text{LaNb}_{1-x}\text{Sb}_x\text{O}_4$ . Therefore,  $\text{LaNb}_{1-x}\text{Sb}_x\text{O}_4$  is a high temperature proton conductor in this temperature range. Furthermore, the total conductivity depends on the Sb concentration in the compound mostly due to the impact of the substitution on the grain boundary conductivity levels. The highest measured conductivity value was about  $10^{-4}$  S/cm at 900 °C in wet air.

## ACKNOWLEDGMENT

Authors of this work would like to acknowledge prof. Truls Norby, prof. Reidar Haugrud and SMN research group at University of Oslo in Norway for their help, support and guidance in the early stage of this research.

## REFERENCES

- [1] T. Norby, *Solid State Ionics* 125 (1999) 1.
- [2] R. Haugrud, T. Norby, *Solid State Ionics* 177 (2006) 1129.
- [3] S. Wachowski, A. Mielewczyk-Gryn, M. Gazda, J. *Solid State Chem.* 219 (2014) 201.
- [4] A. Mielewczyk-Gryn, S. Wachowski, K.I. Lilova, X. Guo, M. Gazda, A. Navrotsky, *Ceram. Int.* 41 (2015) 2128.

# SYNTHESIS AND ELECTRICAL PROPERTIES OF $\text{Ba}_x\text{Sr}_{1-x}\text{TiO}_3$ CERAMICS

P.Galat<sup>1</sup>, M. Leszczynska<sup>1</sup>, W.Wrobel<sup>1</sup>, M. Struzik<sup>1,2</sup>, J.R. Dygas<sup>1</sup>, F.Krok<sup>1</sup>

<sup>1</sup>Faculty of Physics, Warsaw University of Technology, Koszykowa 75, 00-662 Warsaw, Poland

<sup>2</sup>Department of Materials, Federal Institute of Technology in Zurich, Schafmattstr. 30, 8093 Zürich, Switzerland  
e-mail: pawel.galat@wp.pl

Keywords: strontium barium titanate; perovskite structure, X-ray diffraction, density, ac. impedance spectroscopy, dielectric constants

## INTRODUCTION

In the barium titanate ( $\text{BaTiO}_3$ ; BT) and strontium titanate ( $\text{SrTiO}_3$ ; ST) pseudo-binary system ( $\text{Sr}_x\text{Ba}_{1-x}\text{TiO}_3$ , BST) perovskite type structure ceramic compounds are obtained in the whole substitution range. BST compounds show interesting dielectric and ferroelectric properties with dielectric constant and Curie temperature being dependent on substitution level  $x$ . Thus, these materials are considered for dynamic random access memories, dielectric capacitors, microwave phase shifters, transducers, positive temperature coefficient resistors and energy storage ceramics [1]. Recently permanent photoelectric effect for BST compounds was reported [2]. Many efforts have been put to improve the microstructure and electrical properties of BST ceramics synthesized by different chemical processes.

The aim of presented work was to obtain high density BST by the use of solid state reaction and to characterise physical properties of obtained materials.

## EXPERIMENTAL

Samples of general formula  $\text{SrTiO}_3$ ,  $\text{Sr}_{0.75}\text{Ba}_{0.25}\text{TiO}_3$ ,  $\text{Sr}_{0.5}\text{Ba}_{0.5}\text{TiO}_3$ ,  $\text{Sr}_{0.25}\text{Ba}_{0.75}\text{TiO}_3$  and  $\text{BaTiO}_3$  were prepared from titanium dioxide (Aldrich > 98%), strontium carbonate (Aldrich > 99,9%) and barium carbonate (Aldrich > 99%). Reagents at proper molar ratios were milled in planetary ball mill for 24h and calcined for 4h at 1150 °C. Prepared pellets (approx. 10mm diameter and 3mm thickness) were sintered in air for 2, 4 and 6h at temperature 1350 °C, to obtain high density samples. Prepared samples were characterized using X-ray diffraction, Archimedes method, SEM and differential thermal analysis. Impedance spectroscopy and the polarization–electric field (P–E) hysteresis loops were measured to study electrical properties of studied samples.

## RESULTS AND DISCUSSION

XRD patterns collected for all of prepared samples show patterns characteristic for single phase perovskite type structure (Fig. 1). Prepared samples show high density values measured by the Archimedes method. Typically the highest density values were obtained for 6h sintering time as presented at Fig. 2 for  $\text{SrTiO}_3$

compound. SEM micrograph pictures show uniform distribution of grain sizes of ca. 4  $\mu\text{m}$ .

Impedance spectroscopy results as well as P-E hysteresis loops will be presented.

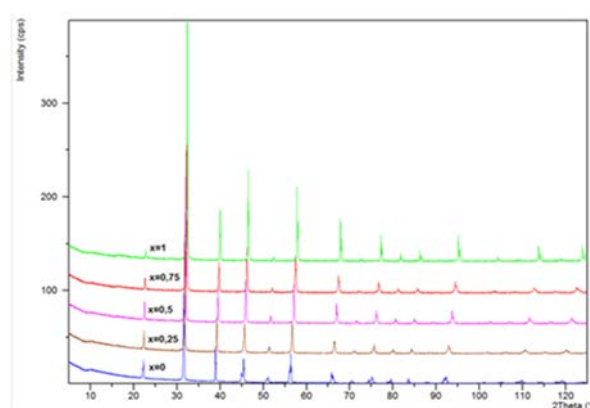


Fig. 1. X-ray diffraction patterns for  $\text{Sr}_x\text{Ba}_{1-x}\text{TiO}_3$  compounds

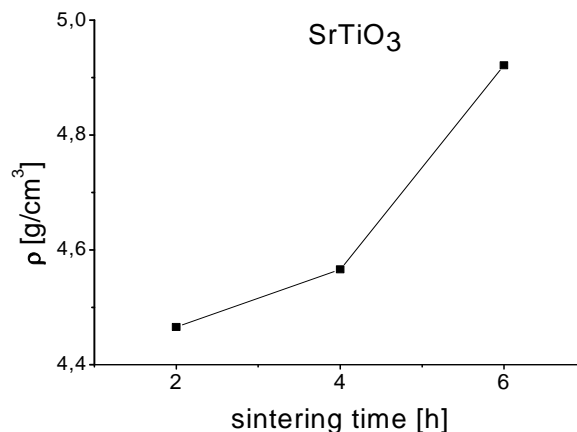


Fig. 2. Density measurements results for  $\text{SrTiO}_3$  compound

## REFERENCES

1. Wu, T, Pu, Y, Gao, P, Liu, D, *Journal of Materials Science: Materials in Electronics*, 24(10) (2013) 4105-4112.
2. TARUN, M.C., SELIM, F.A. MCCLUSKEY, M.D., *Physical Review Letters*, 111(18) (2013) 187403.



# KINETIC MONTE CARLO MODELING OF $\text{Bi}_3\text{YO}_6$

*B. Jasik, M. Krynski, W. Wrobel, J. Dygas and F. Krok*

Faculty of Physics, Warsaw University of Technology,  
Koszykowa 75, 00-662 Warszawa, Poland

e-mail: barjas02@gmail.com

Keywords: bismuth yttrium oxide, ionic conductivity, kinetic monte carlo, ab initio

## INTRODUCTION

The highest known oxide ion conductivity of any solid, with a value of *ca.*  $1 \text{ S cm}^{-1}$  at *ca.* 1000K, is observed for the  $\delta\text{-Bi}_2\text{O}_3$  phase of the cubic fluorite type structure [1]. Below 1000K bismuth oxide undergoes series of phase transitions into lower symmetry polymorphs, which is correlated with three orders of magnitude drop of conductivity. The cubic fluorite  $\delta\text{-Bi}_2\text{O}_3$  phase can be preserved to lower temperatures by partial substitution of bismuth cations with different metal cations. For the yttrium doped system, the  $\delta\text{-Bi}_2\text{O}_3$  type phase was stabilized to room temperature and high ionic conductivity was preserved to intermediate and low temperatures, for the  $\text{Bi}_3\text{YO}_6$  compound [2] (acronym  $\delta\text{-Bi}_3\text{YO}_6$  will be used).

The *ab initio* molecular dynamics simulations for  $\delta\text{-Bi}_3\text{YO}_6$  compound revealed information on site residence time or site occupancy but also trapping mechanism of oxide ions in the yttrium cation neighborhood was determined [3]. However, the *ab initio* modeling is limited only to small systems containing only tens of atoms and is very time consuming with a 60ps molecular dynamics calculation for 80 atoms taking over a month.

In this project the Kinetic Monte Carlo modeling was used to extend both the size of the studied system and the simulation time scale. Results of *ab initio* calculations were used as a input parameters for Kinetic Monte Carlo calculations. Similar approach was previously applied by Pornprasertsuk et al. for yttria stabilized zirconia [4].

## EXPERIMENTAL

Series of Kinetic Monte Carlo calculations were performed for  $\delta\text{-Bi}_3\text{YO}_6$  at 1073K for the  $7 \times 7 \times 7$  supercell containing 2058 oxide ions. Initial oxide ion distribution in the system, including oxide ion site occupancy and cation coordination numbers, was based on results of *ab initio* calculations [3]. The probability of oxide ions jumps between different sites was calculated from the site residence time [3]. All calculations were done using a self-written C++ software and performed on personal class computer. The computer calculation time of 10ms was equal *ca.* 10 minutes.

## RESULTS AND DISCUSSION

Performed Kinetic Monte Carlo calculations allowed to model  $\delta\text{-Bi}_3\text{YO}_6$  system in time scale of six

orders of magnitude longer than achieved in the *ab initio* cautions and for *ca.* 30 times bigger number of oxide ions. Within such a scale it is possible to study the influence of cation dopant clustering on oxide ion diffusion. It was observed, that yttrium cation clusters significantly blocks the diffusion process in these areas creating visible pathways of diffusing oxide ions in bismuth rich areas.

The Kinetic Monte Carlo calculations were done under the external electric field (Fig. 1). The ionic current was calculated for ac voltage with electrostatic field varying in a wide frequency range, to reconstruct impedance spectroscopy data.

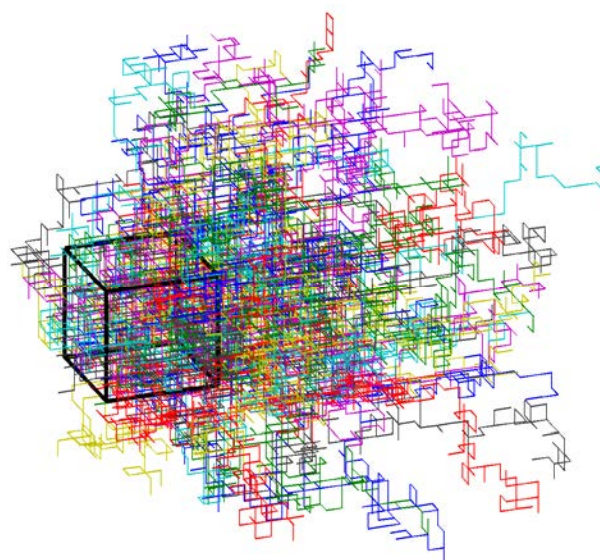


Fig. 1. Oxide ions trajectories calculated during Kinetic Monte Carlo modeling under external electrostatic field. Black box represents initial oxide ions positions.

## REFERENCES

1. T. Takahashi, H. Iwahara, Y. Nagai, *J. Appl. Electrochem.* **2**(1972)97
2. I. Abrahams, F. Krok, A. Kozanecka-Szmigiel, W. Wrobel, S.C.M. Chan, J.R. Dygas, *J. Power Sources* **173**(2007)788.
3. M. Krynski, W. Wrobel, C.E. Mohn, J.R. Dygas, M. Malys, F. Krok, I. Abrahams, *Solid State Ionics* **264**(2014)49.
4. R. Pornprasertsuk, J. Cheng, H. Huang, F. B. Prinz, *Solid State Ionics* **178**(2007)195



# IMIDAZOLE-MALONIC ACID SALT - MOLECULAR STRUCTURE AND PROTON CONDUCTIVITY

*P. Ławniczak, A. Pietraszko\*, K. Pogorzelec-Glaser, B. Hilczer*

Institute of Molecular Physics PAS, ul. M. Smoluchowskiego 17, 60-195 Poznań, Poland

\*Institute of Low Temperature and Structure Research PAS, ul. Okólna 2,  
50-422 Wrocław, Poland

e-mail: lawniczak@ifmpan.poznan.pl

Keywords: proton conductors, hydrogen bonds

## INTRODUCTION

For a long time we are interested in crystal engineering and hydrogen bond formation in salts of dicarboxylic acid with heterocyclic bases, which are known to form similar to water hydrogen bond network [1,2]. Among the compounds worthy noticing is imidazole-malonic acid (Im-MAL) salt due to a disorder apparent in one of the imidazole rings. The disorder has been reported by us at RT [3] and later at 120K [4]. Here we report the structure of Im-MAL at 14K, 120K, 295K and 330K and the relationship with proton conductivity in the temperature range 273K - 378K.

## EXPERIMENTAL

Imidazole and malonic acid were dissolved in distilled water at RT. The crystallization of imidazole-malonic acid salts was carried out by slow evaporation of the solvent at RT and plate-like crystallites ~5 mm in length and ~0.3 mm thick were obtained.

Molecular structure was determined at 14K, 120K, 295K and 320K (X-ray four-circle XCALIBUR Diffractometer, MoK  $\alpha$  radiation).

For electric measurements the Im-MAL crystallites were pressed (30MPa, RT) into the form of pellets, the surfaces of which were electroded with Hans Wolbring GmbH silver paste. Electric properties were carried out using impedance spectroscopy method, using Alpha-A High Performance Frequency Analyzer (Novocontrol GmbH) in frequency range  $1\text{Hz} \leq f \leq 10\text{MHz}$  and temperature range  $273\text{K} \leq T \leq 378\text{K}$ .

## RESULTS AND DISCUSSION

The Im-MAL crystal structure is of layer type and belongs to a triclinic system with P-1 space group. The unit cell contains two malonic acid groups and two imidazole rings. The Im-rings and one dicarboxylic acid molecule lie on the (-13 -7 -7) layers which are linked by chains of O-H...O bonded MAL groups.

One of the two heterocyclic molecules (Im-I) is ordered, whereas the second Im-II ring, located in the center of symmetry, can be considered as disordered since its atoms occupy two symmetrically equivalent position with the probability of 0.5. The structural motif of the crystal was found to be similar in the temperature range from 14K to 330K.

Impedance response in measured frequency and temperature range is composed of the two semicircles. The complex impedance  $Z^*$  can be described by connected in series two double RC parallel circuits, where one is connected with bulk material response

(which corresponds to  $\sigma_{gi}$  conductivity), whereas the other is connected to the grain boundaries parts of the sample ( $\sigma_{gb}$ ). Figure 1 presents Arrhenius plot of Im-Mal, where both contribution are presented as well as total conductivity of the sample.

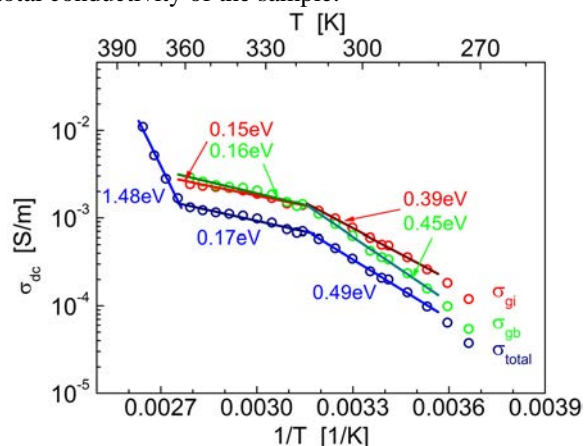


Fig. 1. Arrhenius plot of Im-Mal. In figure are presented values of activation energy of grain boundaries, bulk material (grain interiors) and total conductivity of the polycrystalline sample.

## CONCLUSIONS

In temperature range from 313K to 363K Im-MAL conductivity has low activation energy ( $E_A=0,17\text{eV}$ ), similar to the superprotonic conductors.

Considerable increases in the anisotropic thermal displacement parameters of the Im atoms is observed between 295K and 330K. These changes suggest that proton transport in the high conducting phase can be considered as phonon assisted proton diffusion.

Hydrogen bonds N-H...O between Im molecules and carboxyl group of the MAL changes between 295K and 330K. It appoints important role of such hydrogen bonds in proton conductivity.

## REFERENCES

1. P. Ławniczak, K. Pogorzelec-Glaser, C. Pawlaczyk, A. Pietraszko, L. Szcześniak *J. Phys. Condens. Matter* **21** (2009) 345403
2. K. Pogorzelec-Glaser, A. Rachocki, P. Ławniczak, A. Pietraszko, C. Pawlaczyk, B. Hilczer, M. Pugaczowa-Michalska *CrystEngComm* **15** (2013) 1950-1959
3. K. Pogorzelec-Glaser, J. Garbarczyk, Cz. Pawlaczyk, E. Markiewicz, *Mater. Sci. Poland*, **24** (2006) 245
4. S.K. Callear, M.B. Hursthouse, T.L. Threlfall, *CrystEngComm*, **12** (2010) 898-908

# STRUCTURAL, TRANSPORT AND ELECTROCHEMICAL PROPERTIES OF $\text{Li}_x(\text{Li}_y\text{Fe}_z\text{V}_{1-y-z})\text{O}_2$ – CATHODE MATERIALS FOR LI-ION BATTERIES

*B. Gedziorowski, M. Fuksa, J. Molenda*

Faculty of Energy and Fuels  
AGH University of Science and Technology, ul. al. A. Mickiewicza 30  
30-059 Krakow, Poland  
e-mail: gedzior@agh.edu.pl

Keywords: Li-ion batteries,  $\text{LiVO}_2$ , lithium vanadium oxide, cathode material

## INTRODUCTION

Layered  $\text{LiVO}_2$  and its deintercalated derivatives were studied due to their structural and magnetic properties [1]. Recently  $\text{Li}_{1+x}\text{V}_{1-x}\text{O}_2$  compounds were found as potential anode materials for lithium ion batteries [2]. However, there are only few papers roughly discussing properties of these materials in cathode region [3].

This work intends to fill this gap, presenting structural, transport and electrochemical properties of three groups of deintercalated compounds:  $\text{Li}_x\text{VO}_2$ ,  $\text{Li}_x(\text{Li}_{0.07}\text{V}_{0.93})\text{O}_2$  and  $\text{Li}_x(\text{Li}_{0.07}\text{Fe}_{0.1}\text{Fe}_{0.83})\text{O}_2$ .

## EXPERIMENTAL

$\text{LiVO}_2$ ,  $\text{Li}(\text{Li}_{0.07}\text{V}_{0.93})\text{O}_2$  and  $\text{Li}(\text{Li}_{0.07}\text{Fe}_{0.1}\text{Fe}_{0.83})\text{O}_2$  were prepared using high temperature solid state method with  $\text{Li}_2\text{CO}_3$ ,  $\text{V}_2\text{O}_3$  and  $\text{Fe}_2\text{O}_3$  taken as substrates. Stoichiometric amounts of substrates were ball-milled, pressed into pellets and followed by two steps of annealing: 10h at  $800^\circ\text{C}$  in argon atmosphere and 12h at  $1050^\circ\text{C}$  in mixture 5%  $\text{Ar}$ -95%  $\text{H}_2$  followed by quenching

Structural studies were performed in  $10$ - $110^\circ$  range with  $\text{CuK}\alpha$  radiation using Panalytical Empyrean diffractometer.

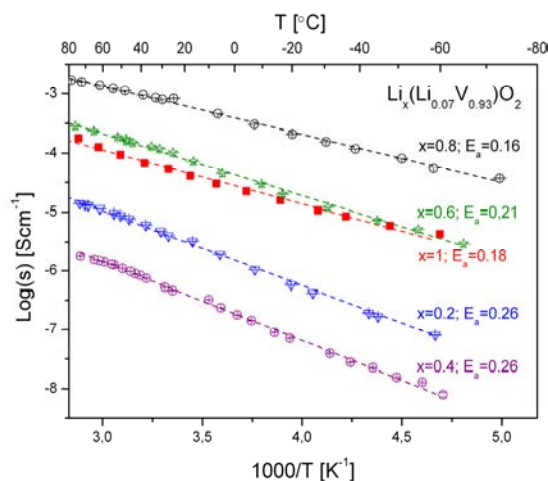
Electrochemical studies were performed by usage of ATLAS multichannel potentiostat/galvanostat.  $\text{Li}/\text{Li}^+/\text{Li}_x(\text{Li}_y\text{Fe}_z\text{V}_{1-y-z})\text{O}_{2-\delta}$  cells were constructed using Swagelok type containers. 1M solution of  $\text{LiPF}_6$  in EC/DEC (in 1:1 ratio) was used as the electrolyte. For the positive electrode, the active material was prepared in the form of a rectangular sample with a weight of approx. 35-50 mg.

Electrical conductivities of pristine and deintercalated samples were determined using frequency response analyzer Solartron 1260 with dielectric interface Solartron 1296.

## RESULTS AND DISCUSSION

XRD measurements showed all pristine materials to be single phase, exhibiting  $\alpha$ - $\text{NaFeO}_2$  type structure with R-3m symmetry. Deintercalated materials consisted of multiple phases with the same  $\alpha$ - $\text{NaFeO}_2$  type structure, varying the size of cell parameters. Relative reflection intensities are varying with decreasing lithium content, indicating partial displacement of vanadium ions from 8b (vanadium layer) sites to 8a sites (lithium layer).

Electrical conductivities measurements showed all studied materials to be semiconductors with energy



Rys. 1 Temperature dependence of electrical conductivity of  $\text{Li}_x(\text{Li}_{0.07}\text{V}_{0.93})\text{O}_2$  compounds.

activation below 0.4V. Room temperature electrical conductivities of deintercalated samples varies in wide range from  $\sim 10^{-3}$  to  $\sim 10^{-7}$   $\text{Scm}^{-1}$ . However, the values do not change linearly with decreasing lithium content (Fig. 1).

Open circuit voltage of tested cell was almost constant during deintercalation, most probably due to two phase mechanism.

## CONCLUSIONS

Properties of  $\text{LiVO}_2$ ,  $\text{Li}(\text{Li}_{0.07}\text{V}_{0.93})\text{O}_2$  and  $\text{Li}(\text{Li}_{0.07}\text{Fe}_{0.1}\text{Fe}_{0.83})\text{O}_2$  as cathode materials for lithium ion batteries were studied showing complex, two phase mechanism of lithium deintercalation.

## ACKNOWLEDGMENT

This work was supported by NCN grant no. NCN 2011 /02/A/ST5/00447.

## REFERENCES

1. T.A. Hewston, B.L Chamberland, J Solid State Chem **65** (1986) 100-110
2. A.R. Armstrong, C. Lyness, P.M. Panchmatia, M.S. Islam, P.G. Bruce, Nature Mater. **10** (2011) 223
3. A. J. B. Goodenough, G. Dutta, A. Manthiram, Phys Rev B. **43** (1991) 1170-1178

Polish Hydrogen and Fuel Cell Association is not responsible  
for the content of advertisements

## NOTES



# sartorius

## **Sartorius global innovative supplier of laboratory equipment.**

mgr BEATA GASIEWCZ – Sales Specialist SARTORIUS Poland

Sartorius is a leading international pharmaceutical and laboratory equipment supplier. As a global player with a corporate history dating back over 140 years, the Sartorius Group operates in dynamic markets. The customers it serves are from the biotech, pharma and food industries as well as from public research. Sartorius conducts its business operations in two divisions: Bioprocess Solutions and Lab Products & Services.

Bioprocess Solutions with its wide portfolio of products helps enable biotech medicines and vaccines to be manufactured safely and efficiently. Lab Products & Services with its premium laboratory instruments, high-quality consumables and excellent services focuses on laboratories for research and quality assurance at pharma and biopharma companies and on academic research institutes.

**The Sartorius Lab Products & Services Division** is a broad-based premium supplier of high-quality laboratory instruments, high-grade consumables and excellent services. Our customers are from research and quality assurance laboratories of the pharmaceutical, chemical and food industries as well as from the academic sector. The product portfolio of our division focuses on high-value laboratory instruments, such as lab balances, pipettes and laboratory water purification systems. Moreover, we offer the widest range of consumables, such as laboratory filters and pipette tips. In laboratory weighing technology, our company ranks as the world's second largest equipment supplier, and enjoys a strong position among the leading global suppliers for consumables, pipettes and laboratory water purification systems

### **Cubis - the best laboratory balance series**

The Cubis® was developed for users, who expect the best possible performance from a lab balance across the board but only want to invest in what is necessary. For this reason, Sartorius has gone far beyond simply further developing what already exists. The new Cubis® represents a groundbreaking new concept: Cubis® is the first lab balance of an entirely modular design which means that display and control units, weighing models, draft shield models, interfaces, and much more can be freely combined. Cubis balances adaptable to every application thanks to its modular design. Users can choose from thousands of options to configure their balance (from 2.7 g 0,1 µg to 0,1 g 70 kg) to suit their individual needs and obtain the optimal solution for integration into their process. This makes every Cubis® a unique and unrivaled balance because every Cubis® is tailored to an individual profile of specifications without compromising a thing.

Cubis® is the first lab balance that automatically checks, performs and documents its exact leveling. The Cubis® balance can be leveled with the push of a button or fully automatically when the isoCALfunction has been activated. Quick and safe leveling with a significantly reduced risk of contamination for the user. This eases the burden on the user and allows more time for the user's actual tasks, in addition to being safer.

At the touch of a button, the Q-Stat ionizer integrated into the DI draft shield can quickly dissipate electrostatic charges which would affect the weighing measurements on sample containers and substances. The effective principle of four ion jets achieves this without disruptive air streams. As a result, stable and accurate weighing results can be guaranteed regardless of external influences.



## NOTES



# LAB, PILOT & PROCESS

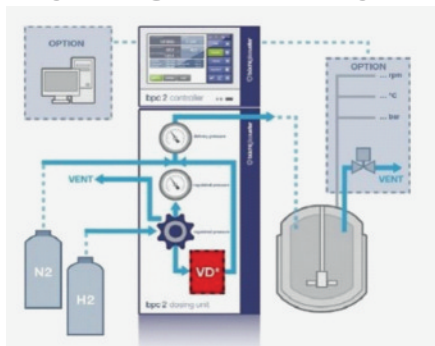
*we provide solutions*

## Pressure Reactors



High pressure ( up to 500 bar ), high temperature ( up to 500 C ), volume up to 5 liter, ATEX compliant, different materials ( SS 316L, C22, Ti, Zr, Ta)

## Hydrogenation system



Complete solution fulfilling highest safety standards for hydrogenations under low and high pressure

## Glass Reactors



Multipurpose reactor system up to 250 liters for chemical process development, scale up, process simulation, ATEX

## Planetary mixers



Mixing and deaeration at the same time, quick processing, high reproducibility

## NOTES

# FIRMA SYL & ANT INSTRUMENTS OFERUJE APARATURĘ:



## 3Flex

Surface Characterization

**3Flex CHEMI** jest w pełni automatycznym analizatorem, zaprojektowanym do przeprowadzania różnorodnych badań z najwyższą dokładnością, rozdzielczością i redukcją danych. Trzy-portowa budowa aparatu pozwala na długie analizy mezoporów/mikroporów. Analizy fizysoptyczne lub chemisorpcyjne mogą być przeprowadzane jednocześnie. Każdy port jest w stanie osiągnąć bardzo niskie ciśnienie bezwzględne, co wynika z budowy kolektora oraz jego połączenia do systemu super wysokiej próżni. Dzięki temu pomiary mikroporów w zakresie niskich ciśnień względnych są znacznie precyzyjniejsze od znanych do tej pory. Aparat może być również skonfigurowany pod analizę z użyciem kryptonu do pomiarów mały powierzchni.

## HPVA II

### High-Pressure Volumetric Analyzer



Seria analizatorów HPVA jest przeznaczona do wyznaczania izoterm adsorpcji takich gazów jak wodór, metan, dwutlenek węgla, tlenek węgla, argon, azot, tlen i innych w zakresie od ultra głębokiej próżni do 200 barów i w zakresie temperatur od -196°C do 500°C. Aparat pracuje w oparciu o technikę wolumetryczną. Analiza jest w pełni zautomatyzowana. Dołączone oprogramowanie do obróbki danych i grafiki zawiera bazę danych NIST RefProp 23. W zależności od opcji aparatu można analizować jednocześnie od 1 do 4 próbek. Zastosowania aparatu to badanie katalizatorów, zeolitów, węgla aktywnych i nanorurek dla procesów przechowywania wodoru, gazu naturalnego, produkcji ogniw i baterii, pochłaniaczy spalin czy też pułapek dla węglowodorów. Wbudowany zawór servo, pozwala uzyskać wysoce precyzyjne dawkowanie gazu. Wysoce precyzyjne przetworniki ciśnienia z odczytem z dokładnością do +/-0,04% pełnej skali ze stabilnością +/-0,01%. Oprogramowanie zawiera wbudowane makra do obróbki i przetwarzania danych i tworzenia wykresów. Dostępne są również 4 porty przygotowania próbek.



**Wysokociśnieniowe reaktory laboratoryjne, wraz z osprzętem.**

**W pełni automatyczne mikroreaktory PID wraz z osprzętem.**

**Autoclave Engineers**   
Division of Snap-tite, Inc.

**Parker**



Dostawca:

**SYL & ANT**  
**Instruments**

APARATURA NAUKOWO - BADAWCZA I KONTROLNO POMIAROWA  
NIEWIESZE/k GLIWIC tel 32 230 32 01  
ul. Pyskowska 12 fax 32 230 33 01  
99 44 - 172 PONISZOWICE e-mail: info@sylant.pl  
**WWW.SYLANT.PL**

## NOTES

## **Polish Hydrogen and Fuel Cell Association**

Polish Hydrogen and Fuel Cell Association was founded in 2004 as a non-profit organization to promote hydrogen as a sustainable energy carrier as well as modern technologies for energy conversion and storage. The Association is a rapidly growing organization, which gathered many scientists (to date 175 members, including 50 professors, 1 honorary member and 11 supporting members).

Members of the Association are employees of universities and research institutes, as well as directors of state-owned enterprises. Supporting members include universities and research institutes. Association collaborates closely with Polish Technological Platform of Hydrogen and Fuel Cells organizing meetings, schools and preparing national "hydrogen" research program. The Association is a member of EHA (European Hydrogen Association) and PATH (Partnership for Advancing the Transition to Hydrogen). Comparing the size and structure of the membership, the Polish Association is one of the largest in Europe, and has significant intellectual potential.

### **Mission**

- development of collaboration among universities, research institutes and industry,
- support of high-risk projects focused on basic studies of new materials for energy conversion and storage,
- stimulation of educational activities promoting modern technologies for energy conversion and storage.

### **Activity**

- Annual Bulletin,
- Every 2 years Association is organizing Forum dedicated to fuel cells, hydrogen production and storage, Li-ion batteries, supercapacitors, thermoelectrics, solar conversion,
- Every 2 years, interchangeably with Forum, Association is organizing Summer Schools on energy conversion and storage,
- Lectures at Technical Open University of AGH University of Science and Technology,



## Authorities of the Association

### **PRESIDENT**

**dr hab. inż. Konrad Świerczek, prof. AGH**

Faculty of Energy and Fuels  
AGH University of Science and Technology  
al. Mickiewicza 30, 30-059 Kraków



### **VICE-PRESIDENT**

**prof. dr hab. inż. Janina Molenda**

Faculty of Energy and Fuels  
AGH University of Science and Technology  
Al. Mickiewicza 30, 30-059 Kraków



### **VICE-PRESIDENT**

**dr hab. inż. Piotr Jasiński, prof. PG**

Faculty of Electronics, Telecommunications and Informatics  
Gdańsk University of Technology  
Gabriela Narutowicza 11/12, 80-233 Gdańsk



### **VICE-PRESIDENT**

**prof. dr hab. Henryk Figiel**

Faculty of Physics and Applied Computer Science  
AGH University of Science and Technology  
al. Mickiewicza 30, 30-059 Kraków



### **TREASURER**

**dr inż. Anna Milewska**

Faculty of Energy and Fuels  
AGH University of Science and Technology  
Al. Mickiewicza 30, 30-059 Kraków



### **SECRETARY**

**mgr inż. Dominika Baster**

Faculty of Energy and Fuels  
AGH University of Science and Technology  
Al. Mickiewicza 30, 30-059 Kraków



### **AUDITING COMMITTEE**

prof. dr hab. Leszek Czepirski

dr inż. Grzegorz Paściak

dr hab. Antoni Paja, prof. AGH

dr hab. Paweł Nowak, prof. IKiFP PAN

prof. dr hab. Czesław Pawlaczyk



